Abstracts Table of Contents

• b •

PRELIMINARY CONSTRAINTS ON VARIATIONS IN CRUSTAL COMPOSITION AND THICKNESS ACROSS THE BASIN AND RANGE-COLORADO PLATEAU TRANSITION ZONE IN WEST-CENTRAL ARIZONA USING RECEIVER FUNCTION ANALYSIS OF USARRAY DATA

Lon Abbott · Red Rocks Community College
Matt Fouch · Arizona State University

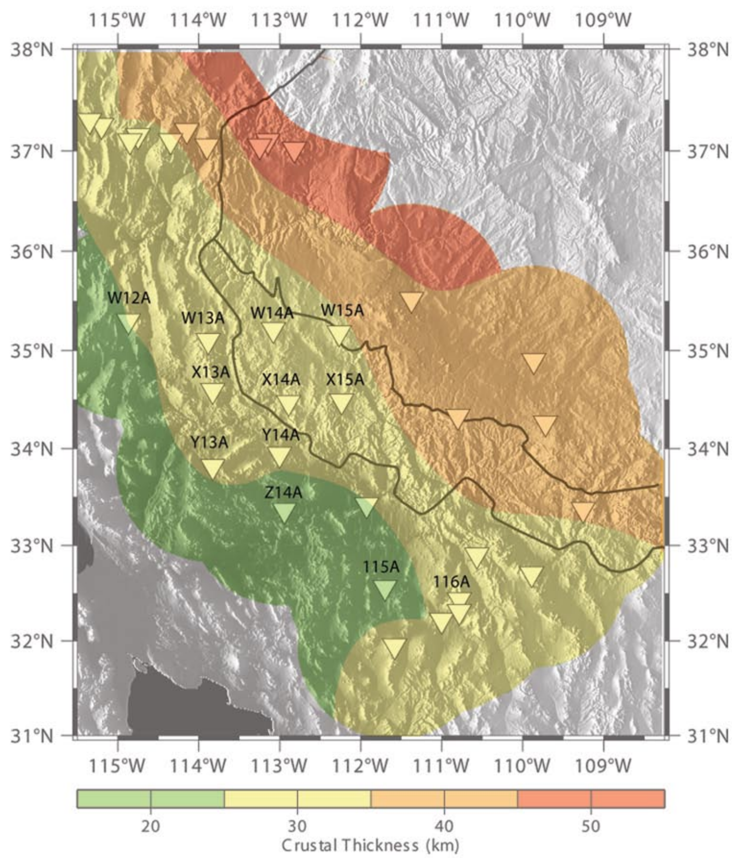

Preliminary crustal thickness map based on our study of USArray data (stations labeled), along with receiver function analyses of data from the COARSE array (Frassetto et al. 2006) and an array along the Arizona-Utah border (Zandt et al. 1995)

The juxtaposition of the highly extended Basin and Range (BR) and the minimally deformed Colorado Plateau (CP) provinces is a striking and poorly understood feature of Arizona. In some places the provinces are in direct contact with one another, whereas elsewhere they are separated by a narrow, topographically intermediate zone known as the Arizona Transition Zone (ATZ). Two fundamental questions, then, are: 1) why have the BR and CP responded to the changing plate boundary conditions of the last 80 m.y. in such dramatically different ways and 2) what is the tectonic significance of the ATZ?

A knowledge of the crustal composition and thickness of the BR, CP, and ATZ is integral to answering these questions. For example, several authors have suggested that the CP is composed of stronger, more mafic crust than the BR, thus enabling the CP to better resist deformation associated with the strong crustal compression and later extension that the region has endured since the late Mesozoic (e.g. Zandt et al. 1995). A related proposal is that the boundary between the CP and the BR is abrupt where Precambrian continental assembly processes juxtaposed strong, mafic crust with weaker, more felsic crust but a more gradual province boundary, marked by a transition zone of intermediate crustal thickness (the ATZ in Arizona), occurs in areas where both provinces share a similar crustal composition (e.g. Parsons et al. 1996).

Past active-source seismic investigations of the BR-CP transition in western Arizona have reached conflicting conclusions regarding both crustal composition and thickness (e.g. Wolf and Cipar 1993 and Parsons et al. 1996) and the almost total absence of broadband seismometers in the area has largely precluded the use of modern teleseismic techniques to probe these parameters. The deployment, during the spring of 2006, of 12 USArray stations that span the BR, the ATZ, and the CP in west-central Arizona has provided the first opportunity to study lithospheric variations across the region using teleseismic techniques. We have performed a preliminary receiver function study using 5 months of data to help constrain crustal thickness and composition under those 12 USArray stations.

Our preliminary results suggest that the crustal composition is intermediate to mafic throughout the study area (Vp/Vs values ranging between 1.76 and 1.96), with no systematic compositional differences between the BR, ATZ, and CP. This result is consistent with the hypothesis of Parsons et al. (1996) that where the ATZ exists there is no strong compositional difference between the BR and CP.

We find the crustal thickness of the BR in west-central Arizona to be 25-27 km, thickening only slightly to 28-30 km in the ATZ. A more dramatic thickening occurs across the ATZ-CP boundary. We obtained a thickness of 33 km for station W15A on the extreme western edge of the CP, while Frassetto et al. (2006) found the crust to be 41.5 km thick under station WUAZ, approximately 90 km farther into the CP. In contrast, Frassetto et al. (2006) found, across the BR-CP transition in southeastern Arizona, that the abrupt thickening occurred at the boundary between the ATZ and the BR rather than at the ATZ-CP boundary as in our study. From a crustal thickness perspective, the eastern ATZ is more similar to the CP, whereas the western ATZ appears to be more similar to the BR. This contrast in ATZ crustal thickness from east to west suggests that the transition zone is not simply a region of intermediate stretching, and hence intermediate topographic expression, between the highly stretched BR and the unstretched CP.

IMAGING SUBDUCTION, EPISODIC TREMOR AND SLIP IN THE PACIFIC NORTHWEST: CASCADIA ARRAYS FOR EARTHSCOPE (CAFE)

Geoffrey Abers, Zhu Zhang · Boston University
Tim Melbourne · Central Washington University
Stephane Rondenay · Massachusetts Institute of Technology
Bradley Hacker · University of California, Santa Barbara
Kenneth Creager, Steve Malone, Aaron Wech · University of Washington

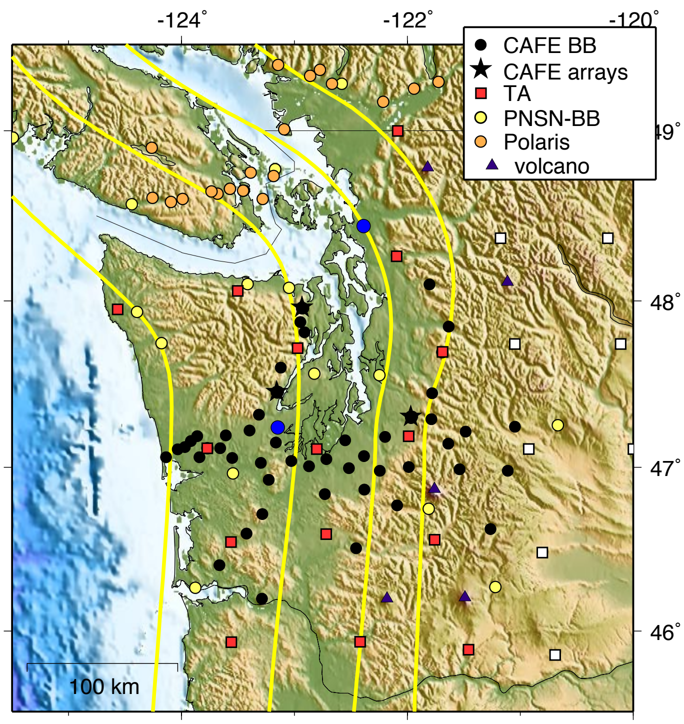

Subduction delivers fluids into the Earth's mantle by transport of hydrated crust downward on subducting plates. These fluids are released at depth and may be responsible for a wide variety of phenomena including weakened thrust faults, episodic tremor and slip (ETS), intraslab earthquakes, forearc serpentinization, and arc magmatism. These processes are fundamentally controlled by the thermal structure of the incoming plate. Cascadia is an important thermal endmember; it is the volcanic arc associated with the youngest subducting plate globally. In 2006 we launched a major EarthScope-supported project across the Cascadia margin, Cascadia Arrays For Earthscope (CAFE). CAFE explores these fluid processes using the tools of seismology, geodesy and petrology, and integrates these results with complementary constraints from geodynamics and geochemistry. Seismic imaging, the emphasis of this presentation, is employed to illuminate (i) the descending oceanic plate, from where fluids are expelled by metamorphism, and (ii) the mantle wedge, where fluids migrate to produce hydrous phases such as serpentine or, beneath the volcanic arc, primary magmas. The experiment traverses a section of the Cascadia system where earthquakes extend to nearly 100 km depth, thus permitting an investigation of the relationship between the release of fluids and the generation of Wadati-Benioff-zone earthquakes. The transport of fluids may also be a primary driver for ETS, a phenomenon for which Cascadia provides a primary natural laboratory, in particular beneath our study area.

The basic experiment has four components: (1) a 47-element broadband imaging array of Flexible Array instruments integrated with Bigfoot; (2) three small-aperture seismic arrays with 15 additional short-period instruments near known sources of ETS; (3) analysis of the PBO and PANGA GPS data sets to define the details of episodic slip events; and (4) integrative modeling. In July 2006, the seismographs were deployed in western Washington along a swath extending from the coastline (south of the Olympic Peninsula) to the back-arc across Mt. Rainier, with a spacing varying from 5 to 20 km. Most of these sites were constructed and deployed over a period of 3 weeks by a field crew of 12, including several interns, an activity that provided a good test of the USArray support facility. Here we present a first look at the experiment and the data collected to date. Initial data recovery has been excellent, with approximately 6 months of continuous data expected to be recovered and delivered to the IRIS DMC by the time of the EarthScope Meeting. This time window includes an ETS episode in Jan. 2007, discussed elsewhere. Given the success of this deployment, we expect to make good progress toward understanding the relationship between subduction, ETS, and fluid cycling.

CONVECTIVE INTERACTIONS IN THE MANTLE BENEATH THE PACIFIC NORTHWEST: THE FATE OF THE JUAN DE FUCA PLATE

Richard Allen, Mei Xue · University of California, Berkeley

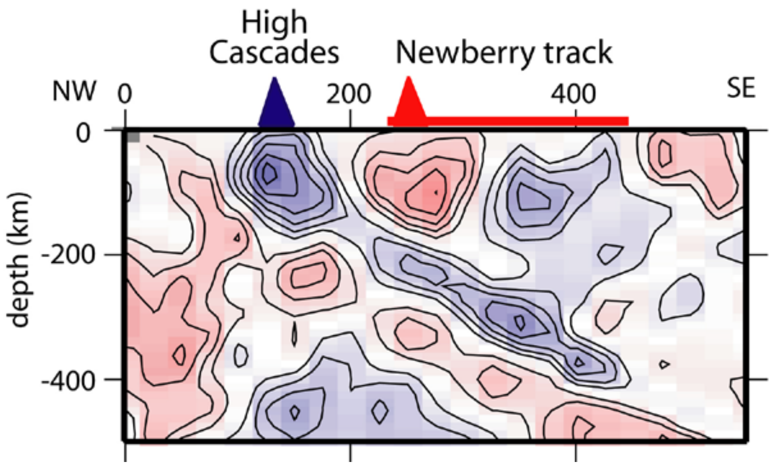

Vertical cross-section through the S-velocity model beneath Oregon.

Beneath the Pacific Northwest remanents of the Farallon plate continue to subduct beneath the North American continent. While the subducting slab has been imaged to the transition zone beneath British Columbia, previous studies suggest that the maximum imaged depth decreases to the south, reaching ~400 km beneath northern Washington, ~300km beneath southern Washington, and perhaps only ~150km beneath Oregon. To the east of the Cascadia subduction system lies the Yellowstone hotspot track. The origins of this track can be traced back to the voluminous basaltic outpourings of the Columbia River Basalts around 17 Ma. If the Columbia River Basalts are the result of a large melting anomaly rising through the mantle to the base of the North America continent, the anomaly would need to punch through the subducting Farallon slab.

We image the subducting Juan de Fuca slab beneath Oregon using teleseismic body-wave travel-time tomography and the stations of the OATS deployment across Oregon combined with data from regional seismic networks and the Earthscope Transportable Array. The 3D compressional and shear-velocity models show the high velocity slab extending to a depth of ~400km with a dip of ~50°, slightly shallower than the observed dip to the north which ranges from 60 to 65°. Resolution tests show that the dataset used would resolve the slab to greater depths if it was present in the mantle, suggesting that the slab ends abruptly at 400 km depth.

Global plate motion models constrain the convergence rate of the Juan de Fuca plate with respect to North America allowing us to trace the current location of the bottom edge of the imaged slab back to its location at 17 Ma when the source of the Columbia River Basalts reached the surface. We estimate that the bottom of the imaged slab would have been at the trench at 17 Ma. One explanation for the observed lower end of the slab is therefore that an upwelling responsible for the voluminous basaltic outpouring caused the Farallon slab to disintegrate around 17 Ma leaving no remanent of the slab deeper than the 400 km maximum depth extent that we observe today.

SIMILARITY OF PALEOSTRESS AND IN SITU STRESS AT SAFOD AND IMPLICATIONS FOR A WEAK SAN ANDREAS FAULT

Rafael Almeida, Judith Chester, Frederick Chester · Texas A&M University

In situ stress measurements along the San Andreas fault indicate a maximum principal compressive stress oriented at large angles to the fault surface and high differential stress consistent with a weak-fault-in-strong-crust model (Hickman and Zoback, 2004). Fracture fabrics in exhumed faults of the San Andreas system also are consistent with a weak San Andreas fault model (Chester & Logan, 1986; Chester et al., 1993) and further indicate that average paleostress directions were similar throughout much of the displacement history (Wilson et al., 2003). Borehole measurements and spot core recovered at the San Andreas Fault Observatory at Depth (SAFOD) permit a unique opportunity to compare the present-day stress (Hickman and Zoback, 2004; Boness and Zoback, 2006) and paleostress states at the same location and directly adjacent to seismogenic patches of the San Andreas fault.

Spot cores from two depth intervals (1.46 km and 3.06 km MD) were acquired during Phase 1 drilling of the main hole in 2004. The lower spot core is from the bottom of the deviated borehole (3055.6-3067.2 m MD), directly adjacent to a major drilling break interpreted as a significant fault, and possibly the Southwest Trace (see Rymer et al., 2006) of the San Andreas Fault (personal communication, S. Hickman, 2004). The lower spot core is composed of massive-bedded, pebble conglomerate to coarse-grained arkosic sandstone units and fine-grained, well-cemented arkosic sandstone that grades into a fine- to very fine-grained siltstone (Almeida et al., 2005). We prepared wrap-around tracings (1:1 maps) of the entire core surface. Although the spot cores were not oriented during drilling, we were able to orient the three contiguous sections of the core to each other by aligning fracture fabrics, and orient the core within the borehole by comparing bedding in the core with the bedding displayed in the image logs.

In the lower core the dominant brittle features include: a) numerous thin, dark colored natural shear fractures in the sandstone and pebble conglomerate that range up to several mm thick, b) thick (up to 20 mm thick) cataclastic shear zones oriented at high angles to the core axis, and c) thin, coring induced fractures. The fractures display kinematic indicators consistent with contraction subparallel to the core axis. Two of the thick cataclastic zones, including the 3067 m fault, juxtapose different rock types and likely have displacements of at least several meters. The majority of the shear fractures and cataclastic zones, including the 3067 m fault, are not parallel to the macroscopic orientation of the main trace or southwest trace of the San Andreas fault at SAFOD. The fracturing in the lower spot core likely reflects damage along the margin of the San Andreas fault. The orientation and kinematics of the natural fractures suggest that the principal paleostress directions at the time of their formation were nearly parallel and perpendicular to the main fault trace. The natural fractures and cataclastic zones define a conjugate pattern consistent with strike-slip faulting and a maximum principal compressive paleostress oriented at 80˚ to the fault plane. This is essentially parallel to the current in situ stress determined from analysis of borehole-breakout and shear-velocity-anisotropy data along the main borehole (Hickman and Zoback, 2004; Boness and Zoback, 2006). The similarity between the current state of stress and paleostress states supports the suggestion that the maximum principal compressive stress direction is, on average, at high angles to the San Andreas fault and that the fault has been weak on average over geologic time.

THE FLEXIBLE ARRAY COMPONENT OF USARRAY; INSTRUMENTS FOR FOCUSED STUDIES

Marcos Alvarez, Jim Fowler · IRIS
Eliana Arias, Noel Barstow · New Mexico Tech

The Flexible Array is a pool of seismic instruments available for Principal Investigator driven studies. These investigations are designed to augment the Transportable Array footprint in imaging key targets at higher resolution than other components of USArray . The Flexible Array program provides a standard shallow vault design for broadband seismic stations. The noise performance of these stations are compared with those of adjacent Transportable Array sites in Washington State using data from the CAFÉ Flexible Array deployment.

The current plan for the Flexible Array calls for 291 broadband seismic stations, 120 short period stations, and 1700 single channel active source stations. All or part of the pool can be used in multiple experiments of various size and duration. USArray personnel stationed at the Array Operations Facility (AOF) at New Mexico Tech in Socorro, New Mexico are responsible for equipment integration and maintenance, and provide technical assistance with the deployment and data collection. The primary responsibility for deployment and operation of the instruments, however, rests with the principal investigators of the individual research programs.

The flexible pool of instruments is scheduled to operate in a mode similar to the current PASSCAL operations. Investigators propose experiments via standard NSF grant procedures, to use the Flexible Array instruments in special high-resolution studies. The majority of experiments aim to enhance data gathering by the Transportable Array while it is located in a specific area. In this mode of operation, the PI furnishes the bulk of the crew of operation, as is done for the PASSCAL experiments. The AOF furnishes training, logistical support, and initial quality control and data formatting support. Many of the instruments are deployed with spread spectrum Ethernet radio telemetry. Data is archived at the DMC as quickly as possible with assistance from AOF staff.

THE PLATE BOUNDARY OBSERVATORY: DATA MANAGEMENT PROGRESS AND HIGHLIGHTS

Greg Anderson, PBO Data Management Team , Mike Jackson, Chuck Meertens · UNAVCO

The Plate Boundary Observatory (PBO), part of the NSF-funded EarthScope project, is designed to study the three-dimensional strain field resulting from deformation across the active boundary zone between the Pacific and North American plates in the western United States. To meet these goals, UNAVCO will install 880 continuous GPS stations, 103 borehole strainmeter stations, 28 tiltmeters, and five laser strainmeters, as well as manage data for 209 previously existing continuous GPS stations through the PBO Nucleus project and 11 GPS stations installed by the USArray segment of EarthScope.

As of 1 February 2007, 519 PBO GPS stations had been installed, of which 504 have returned data to Boulder, and PBO handled data flow for 153 PBO Nucleus stations and all USArray-installed GPS stations. Most of these stations return data to the UNAVCO Boulder Network Operations Center (NOC) on a daily basis, with 16 returning data on an hourly basis. Overall, the combined PBO and Nucleus networks have returned almost 220 GB of raw GPS data. These data are processed by the PBO GPS Analysis Centers, at Central Washington University and the New Mexico Institute of Mining and Technology, and the PBO GPS Analysis Center Coordinator at MIT. These groups create a range of GPS products, including station position time series, GPS velocity vectors, and related information. These centers typically process data from about 680 stations on a daily basis, with median RMS position uncertainties under 1.5 mm horizontally and 4 mm vertically. All PBO GPS data products are archived at and available from the UNAVCO Facility, with a second archive at the IRIS Data Management Center (DMC). All these products may be accessed via the PBO web page at http://pboweb.unavco.org/gps_data.

As part of PBO, UNAVCO will also install and operate the largest borehole seismic and strainmeter networks in North America, as well as tiltmeters and laser strainmeters. As of 1 February 2007, 27 PBO borehole stations had been installed and three laser strainmeter stations were operating, with a total of 60 borehole stations and 4 laser strainmeters expected by October 2007. Seismic data flow in real time to the Boulder NOC for initial quality checks, and thence to the IRIS DMC for final quality checks, archiving, and distribution; all PBO seismic data flow is via the Antelope software suite. Strainmeter data flow hourly and daily to the Boulder NOC and thence to the Borehole Strainmeter Analysis Center in Socorro, New Mexico, and the Laser Strainmeter Analysis Center at the University of California, San Diego. These groups transform the raw strainmeter observations into cleaned individual strain gauge components; time series of shear, areal, and linear strain; and related products. All strainmeter data products are archived at and available from the Northern California Earthquake Data Center and the IRIS DMC, in both the native raw formats and SEED format; all seismic data products are archived at and available from the IRIS DMC, in SEED format. As of 1 February 2007, the PBO seismic network had provided 105 GB of raw data, and the PBO strainmeter network had provided 45 GB of raw data. Please visit http://pboweb.unavco.org/strain_data for more information on data products from the PBO strainmeter and seismic networks.

TIME-DEPENDENT FINITE ELEMENT MODELING OF EFFUSIVE SILICIC ERUPTIONS

Kyle Anderson, Paul Segall · Stanford University

Geodetic source models used in volcanic environments are often highly simplistic, and do not consider deformation caused by viscous conduit drag, nonuniform conduit overpressure, or finite magma chambers of arbitrary shape. On the other hand, theoretical models of magma ascent are often extremely complex, including effects of magma compressibility, volatile exsolution and bubble growth, and crystallization. These models almost always assume a non-deformable conduit, and are difficult to constrain by field observations. Typically, the extruded mass flux as a function of time is the only observable that can be analyzed.

In this work we utilize the finite element method to combine these two approaches, such that geodetic data is used to better constrain magma properties in the conduit and chamber, while magma flow calculations are used as more realistic, physics-based deformation sources. A simple finite element model is used in which flow of a degassing magma from a chamber to the surface generates deformations in the surrounding medium. Use of the finite element method allows us to fully couple the highly nonuniform pressure and shear traction distributions caused by magma flow to the elastic medium. As a result, the total deformation field includes effects due to chamber evacuation, conduit overpressure, and the viscous drag of magma on the conduit walls. Also, by numerically coupling flow through the conduit with evacuation of the chamber in the elastic medium we are able to simulate the temporally-varying behavior of a long-term effusive eruption.

Temporal variations of effusion rate, and temporal and spatial variations in surface deformation can be matched to observations. As expected, temporal variations depend heavily on chamber volume, initial chamber overpressure, conduit properties, and magma compressibility. Deformation in the far field is dominated by pressure change associated with chamber evacuation, while the conduit may become a significant deformation source closer to the vent. While the model is general, applying it to the 2004-present eruption of Mount St. Helens, Washington, results in a reasonable fit to data given the simplifications inherent in the model.

NASA CONTRIBUTION TO THE EARTHSCOPE PROJECT

Victoria Andreatta · UNAVCO
Dave Stowers · JPL
Oivind Ruud, Steve Fisher · UNAVCO

NASA-JPL provides support for the GPS infrastructure through a network of permanent GPS stations called the Global GPS Network (GGN) which represent approximately 20% of the stations that make up the IGS permanent station global network. Data from these stations are used to produce highly accurate products that are essential for Earth Science research, multidisciplinary applications, and education. These products include GPS satellite ephemeredes, Earth rotation parameters, global tracking station coordinates, and velocities, GPS satellite and tracking station clock information, zenith tropospheric path delay estimates, and global ionospheric maps.

The UNAVCO Facility supports the operation and maintenance of these critical components of the NASA–GGN efforts through the daily monitoring of the GGN network, research application projects, special project support, and support to the IGS central bureau. The hourly monitoring support of the 75 permanent NASA GPS stations is performed in conjunction with personnel from JPL.

The NASA-GGN network helps to provide the highly accurate global GPS data products needed for accurate and timely processing of PBO station data, meeting the science goals set forth by Earthscope.

GPS AND PLATE TECTONICS: WHAT ARE WE MEASURING?

Edwin Apel, Roland Burgmann · University of California, Berkeley

Plate tectonics is the fundamental process that drives deformation and the earthquake cycle in the earth's crust. The plate tectonic paradigm has been parameterized in the past using rigid blocks and works quite well for first order interpretations of geodetic data. We explore this paradigm in three different areas of the world and the limitations and implications of modeling geodetic data using various assumptions. 1) We determine the statistical significance of independent micro-plate rotations in NE Asia. 2) We examine a scenario of an artificial rigid block geodetic signal produced by coeval contractional and extensional strain fields on the Aegean block in the Mediterranean. 3) We estimate rigid block model limitations within the Tibetan plateau and along Himalayan range front. In each case we couple the rigid plate assumption with near-boundary elastic strain effects to invert for poles of rotation in a formal inversion of the GPS velocities. Each of these areas provides a unique study that furthers our understanding and quantifies the limitations of our current plate tectonic paradigm.

GEOEARTHSCOPE AND RELATED TOPOGRAPHIC LIDAR DATASETS IN THE CLASSROOM: LESSONS ABOUT GEOMORPHOLOGY, DIGITAL ELEVATION MODELS, AND CYBERINFRASTRUCTURE

Ramon Arrowsmith · Arizona State University

High resolution topography and imagery provide a representation of the earth's surface at a level of detail high enough for students to "see" landforms at unprecedented scales. Such a view enables students to explore landscapes and develop ideas about the important processes that act to develop the topography. As part of GeoEarthscope, several high resolution topographic datasets along major fault systems in the western US are being collected using LiDAR mounted in an aircraft. These systems use a scanning laser coupled with GPS and inertial navigation to return point clouds measuring the earth's surface, including built structures and canopy. Typical shot densities are several per square meter. In collaboration with San Diego Supercomputer Center colleagues, we have built the GEON LiDAR Workflow (GLW) to facilitate internet-based access to LiDAR topography datasets. This example of cyberinfrastructure for the earth sciences permits users to select a subset of the billions of ground returns typical for a airborne LiDAR survey and to manipulate it, including producing digital elevation models at user-defined resolution. The points and derived products can be downloaded to the user's desktop and used in earth science investigations. We have built a number of free tools that are downloadable from our website and also encourage the use of Geographic Information Systems software for desktop processing. In the classroom, we contend that GeoEarthscope LiDAR data and its designated delivery system, the GLW, present a great opportunity to discuss several new technologies (LiDAR, GPS, inertial navigation, and Geographic Information Systems), the concepts of GRID computing and cyberinfrastructure, and to enable students to explore the geomorphology of the active fault systems of the western US, including the San Andreas Fault system.

SPATIAL AND PROCESS ONTOLOGIES FOR BRITTLE SHEAR ZONES: SAFOD PROJECT

Hassan Babaie · Georgia State University
Jafar Hadizadeh · University of Louisville

Shear zones evolve by changes in the state of material entities through processes that start and end by events. The deformation processes (e.g., slip) that change a rock and its minerals from one state (e.g., undeformed) to another (e.g., mylonitized) commonly include a set of subprocesses (e.g., recrystallization, recovery), each occurring within a time interval between the temporal boundaries of the main deformation. A set of fault rocks, each having its own initial properties, goes through different trajectories in its possible states during deformation. At each time, the actual state of a fault rock is a point in this 'state space'. The movement of the actual state along the state trajectory (i.e., history) over the life span of the shear zone is a function of the deformation process, material properties, and environmental conditions. The boundaries of the segments along the trajectory curve are defined by events that mark the beginning of the processes that change the state of entity x from s to s', or turn x into a new thing, y. The process that changes the state of the entity occurs in a 'process space', which is a set of possible processes and corresponding events. Some combination of events and processes is possible under a given environment and deformation conditions. For example, a fault may slip after it has already slipped, it may stick and then slip again, or it may remain stuck.

In a shear zone, continuants include objects such as mylonite, gouge, core, fault, and fracture. These entities occupy same or different spatial regions at different times, and acquire different properties by participating in processes such as cataclasis, weathering, and frictional sliding. These continuants are said to endure over time by maintaining their identity despite the changes that are realized through processes. For example, the San Andreas Fault remains the same fault even though it goes through continuous spatial and qualitative change, for example, in its thickness, length, and extent of its damage zone and seismicity. Geoscientists capture information about the continuants at different times and places (e.g., field, laboratory) while these entities are going through change. The perduring entities (i.e., occurrents) include processes such as cataclasis, frictional sliding, and creep, that unfold over time intervals that start and end with instantaneous, or relatively short-duration, events (e.g., slip event, seismic event). These entities involve one or more continuant entities (e.g., rock, grain) that display different properties under different ambient conditions (e.g., pressure, temperature). In this paper, we present an approach based on a perspective that combines both the continuants (i.e., spatial entities) and perdurants (i.e., processes) components of reality in brittle shear zones, and discuss a method to design dynamic ontologies to depict the processes in shear zones. The scope, purpose, and ontological commitment of our ontologies are limited to reflect those of the Earthscope's SAFOD project.

PROGRESS ON A NEW REGIONAL MODEL OF THE UPPER MANTLE S-VELOCITY STRUCTURE BENEATH THE NORTH AMERICAN CONTINENT

Heather Bedle, Suzan van der Lee · Northwestern University

Here we present our progress towards a new regional three-dimensional S-velocity model of the North American upper mantle. This new model was created by inverting both fundamental and higher mode waveforms for S-velocity structure, following the methodology of partitioned waveform inversion. The data used for this new model is completely independent of data used in previous regional models, such as NA04. We included waveforms from a variety of seismic networks, using eighty-eight events that occurred from January 2000 through September 2006. Among the seismic networks used were Earthscope's Transportable Array and Backbone stations, as well as data from IRIS PASSCAL experiments. In total, we interactively fit 5101 seismograms, which resulted in 47,450 velocity constraints on the upper mantle structure.

Based on 2-degree and 5-degree checkerboard resolution tests, this new model performs very well in the Western US, which is expected because of the inclusion of the relatively highly dense USArray Transportable Array stations. The Texas and Northern Mexico region is the best resolved region in the model due to the crosscutting nature of seismic rays running from Central America earthquakes to stations in the Western US, and raypaths of Baja and Mexican events recorded in the Eastern US. In this region we accurately reproduce the spatial results of checkerboard tests on a 2-deg (200km) scale in the upper mantle. The central Canadian and North-Central portion of the US remain the least resolved regions of the model, due to relative lack of seismic stations, and seismic activity in those areas.

We find that the large scale features of this new model are consistent with those of previous regional- and global-scale S-velocity models, such as the low velocities that underlie the tectonically active western margin of the continent, the relatively fast velocities of the North American craton, as well as fast velocities associated with the subducted Farallon slab. But, in addition to these features, this new model images additional smaller features, which are below the resolving threshold of global models. Among these are fast velocities that are possibly related to the subducted Juan de Fuca plate in the Pacific Northwest, as well as low velocities beneath the Reelfoot Rift, and low velocities in the transition zone beneath the US Eastern Seaboard.

The S-wave velocities of the North American craton are on average 4.65km/s, and it extends to depths of ~250 km. We image a significantly shallower and less fast Wyoming craton. Further to the south, the seismic craton extends almost to the eastern front of the Southern Rocky Mountains in Colorado. The seismic craton does not reach as far west as New Mexico. It does extend into central Texas, incorporating the regions of the Llano uplift and the Edwards Plateau. The western edge of the North American craton in Texas abuts the Central Basin Platform, an Ancestral Rockies uplift. This southern limit of the Texan portion of the craton coincides with the Cambrian Marathon-Ouachita Thrust Belt. This may suggest that central Texas was tectonically buffered from Mesozoic and Cenozoic tectonics to the south in the Gulf region by the zone of weakness along the Marathon-Ouachita front.

UPPER MANTLE SEISMIC VELOCITY STRUCTURE IN THE GREAT BASIN

Caroline Beghein, Matthew Fouch · Arizona State University
J. Arthur Snoke · Virginia Polytechnic Institute and State University

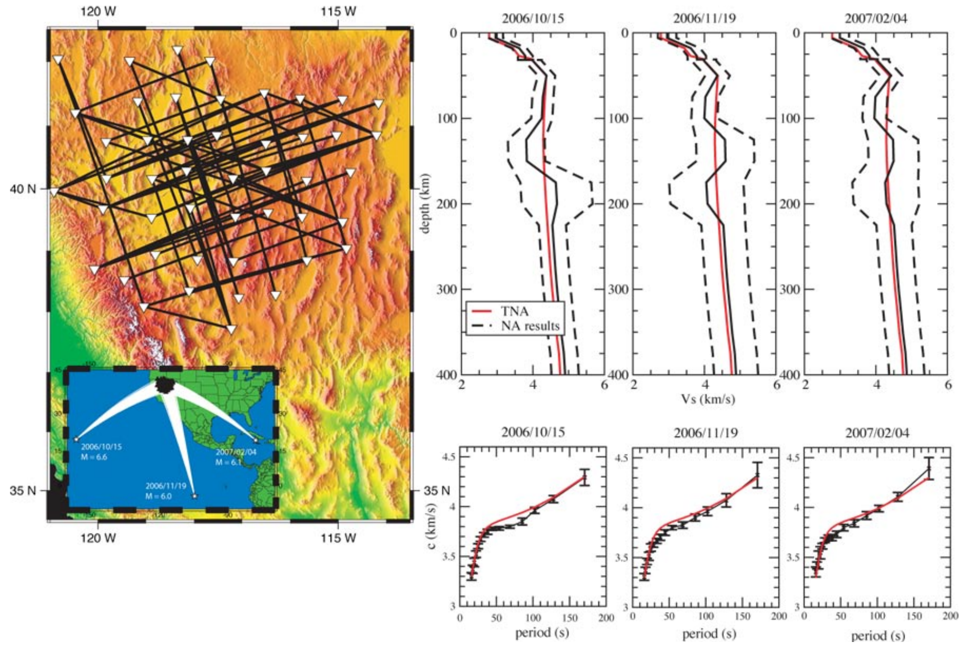

Left: Map showing the location of the USArray stations employed in this study (white triangles). The solid black lines correspond to the different station pairs for which phase velocity dispersion curves were determines. The location of the three events used is also shown.

Right: Shear-wave velocity profiles (top) obtained for each event using the measured phase velocity dispersion curves combined into an average dispersion curve (bottom). In the top figure, the red velocity profile corresponds to model TNA (Grand and Helmberger, 1984). The black solid line shows our most likely velocity profile and the dashed black lines correspond to one standard deviation. The bottom figure displays the dispersion curve predicted by model TNA (red line) and the measured phase velocities with associated uncertainties (black).

The relationship between lithospheric and asthenospheric processes is still poorly understood in the western United States, and fundamental questions remain concerning the influence of a subducting slab on the dynamics of upper mantle flow. Imaging upper mantle structure, detecting the presence of seismic anisotropy, and how it varies with depth in the mantle are key elements to answer these questions. We determine seismic velocity variations in the upper mantle beneath the Great Basin to improve our understanding of the interactions between lithosphere and asthenosphere.

In this study, we utilize surface wave dispersion data to image the upper mantle because of their good vertical sensitivity to bulk Earth structure. We employ a traditional two-station method (e.g., Larson et al., 2006) to generate Rayleigh wave dispersion curves between 20 and 170s using USArray seismic stations. The large number of broadband seismic stations from USArray enables excellent lateral and good azimuthal coverage of the region.

We apply the Neighbourhood Algorithm (NA) forward modeling approach to the measured dispersion curves in order to model shear-wave velocities in the upper mantle. This approach allows us to determine quantitative model uncertainties and parameter trade-offs, which are essential to interpret seismological results and they constitute an important improvement to previous studies of the region. In addition, the NA enables us to include a priori constraints on the Moho depth based on independent estimates from receiver functions that provide a mean Moho depth and a standard deviation. Three events occurring between 2006/10/15 and 2007/02/04 produced high quality Rayleigh wave dispersion curves for about 70 station pairs with interstation distances between 200 and 400km. For each event, the phase velocity dispersion curves were first combined into an average dispersion curve and a standard deviation was calculated. The dispersion curves obtained for paths aligned in the N-S and NW-SE directions are very similar and they differ from the data corresponding to SW-NE paths. We applied the NA to each average dispersion curve to obtain three shear-wave velocity profiles across the Great Basin. In our initial work, we choose a layered parameterization, including one layer in the crust and five layers below the Moho. We allow variations in the Moho depth and in shear-wave velocities within fixed boundaries. Our forward models show an increase in Vs in the crust compared to model TNA (Grand and Helmberger, 1984) for all three averaged datasets. Between 60 and 100km, we do not find any change in Vs with respect to model TNA. At greater depths, the results change with the azimuth. A well-resolved reduction in Vs (about 0.2km/s) with respect to model TNA is found between 60 and 100km depth for the NW-SE and N-S paths but not for SW-NE paths, which can be explained by model TNA at those depths. At larger depths (100-150km) SW-NE profiles clearly display shear-wave velocities lower than in model TNA by about 0.5km/s. The seismic wave velocities are less well constrained at those depths for other azimuths. Our results are consistent with a shear-wave velocity profile containing a small velocity jump across the Moho. Our models can be explained by the presence of a thin lithosphere down to about 60km with no well-defined azimuthal anisotropy, and an azimuthally anisotropic upper asthenosphere with a fast SW-NE direction between 60 and 100km depth. This result is consistent with recent results from shear-wave splitting analyses for the northern part of the Great Basin [West and Fouch, this meeting].

INSTANTANEOUS SLIP RATES FROM GEOLOGY AND GEODESY

Rick Bennett · University of Arizona

We develop a new method for analyzing fault slip rate data sets. The method converts long- and short-term rate estimates derived from geologic and geodetic data into estimates for temporally-localized rate-averages. These averages provide the closest approximation to the instantaneous slip rate history afforded by the given data. The method provides a means of quantitatively comparing and contrasting results obtained by different measurement techniques that fully accounts for the possibility of temporal variations in slip rate. We demonstrate the utility of the method using numerical simulations representing rate-variations over late Pleistocene, and Holocene time scales. We find that a typical slip rate data set comprising geodetic, paleoseismologic, geomorphologic, and/or structural geologic constraints allows for reconstruction of instantaneous slip rate history with resolution that decreases with time before present. Resolution for recent time-periods (≤100 ka) is fairly high. The method should be useful for studies of the earthquake cycle and earthquake recurrence, repartitioning of slip rates within broad plate boundary zone fault systems over long time-intervals, and related problems, and could also be useful for identifying possible discrepancies arising from invalid assumptions and other model errors associated with the estimation of slip rates from basic geologic and geodetic observables.

SCEC COMMUNICATION, EDUCATION, AND OUTREACH PROGRAM

Mark Benthien · Southern California Earthquake Center

The Southern California Earthquake Center (SCEC) is a community of over 500 scientists, students, and staff from over 50 academic institutions across the United States, in partnership with many other science, engineering, education, and government organizations worldwide. To develop applications of the knowledge and scientific products developed by this community, SCEC maintains a Communication, Education, and Outreach (CEO) program with four long-term goals:

- Coordinate productive interactions among a diverse community of SCEC scientists and with partners in science, engineering, risk management, government, business, and education.
- Increase earthquake knowledge and science literacy at all educational levels, including students and the general public.
- Improve earthquake hazard and risk assessments
- Promote earthquake preparedness, mitigation, and planning for response and recovery.

CEO is well integrated within the SCEC science planning process. This includes participation of CEO staff in the development of short-term research objectives and evaluation of proposals received each year in order to develop products and services needed by our various audiences. SCEC scientists in turn are involved in developing and fulfilling CEO short-term objectives, through activities organized within six CEO focus areas: research partnerships coordinated within the SCEC Seismic Hazard & Risk Analysis focus group; Knowledge Transfer activities with practicing professionals, government officials, scientists and engineers; Public Outreach activities and products for the general public, civic and preparedness groups, and the news media; K-12 and Informal Education programs and resources for students, educators, and learners of all ages; the Experiential Learning and Career Advancement office which coordinates undergraduate and graduate internships and support for early career scientists; and SCEC Community development activities and resources for SCEC scientists and students.

This poster will highlight major activities within these focus areas that may be of interest to EarthScope participants from other areas of the country seeking to develop similar products and programs.

GEO/THERMOCRHONOLOGY OF LOWER CRUSTAL XENOLITHS FROM MONTANA : IMPLICATIONS FOR THE STRUCTURE AND EVOLUTION OF NORTH AMERICAN LITHOSPHERE

Terrence Blackburn, Samuel Bowring, Frank Dudas, James Crowley · Massachusetts Institute of Technology

A goal of the Earthscope initiative is to produce a comprehensive 4-dimensional view of the United States beyond which any single discipline or technology can achieve. The present focus of the initiative is to image the lithosphere using seismic data. Essential to the interpretation of the seismic velocity structure is an understanding of the age, composition and thermal history of the North American lithosphere. The lower crust contains a rich record of heat and mass transfer from the mantle as well as deformation and metamorphism associated with lithopsheric assembly, maturation, and reactivation. Rocks formed in the lower crust are found preserved in exposed and exhumed orogenic belts and as xenoliths carried to the surface in kimberlites and related rocks. The Archean to Proterozoic evolution of Montana is known from isolated exposures although numerous xenolith bearing igneous intrusions (mostly Eocene) allow study of the long term thermal evolution of the lower crust beneath exposed Precambrian rocks. As an example of what can be learned from xenolith studies we have constrained the high to moderate temperature (800-400°C) history of several lower crustal granulite facies xenoliths sampled from the Bear Paw, Sweet Grass Hill and Robinson Ranch kimberlites in Montana. Specifically, high-precision U/Pb geochronology of zircon, rutile and titanite are used to place constraints on the thermal history of these lower crustal samples which in turn are essential for interpreting the seismic velocity structure of the North American lithosphere.

PLATE BOUNDARY OBSERVATORY ANALYSIS USING THE AMBIZAP GPS PROCESSING ALGORITHM

Geoffrey Blewitt · University of Nevada

In GPS positioning, resolution of the integer cycle ambiguity in the carrier phase data typically improves precision and accuracy significantly, typically by a factor of 2-3 in relative longitude [Blewitt et al., 1989]. Theoretical properties of ambiguity resolution are here exploited to derive a very rapid algorithm, which is then applied to GPS network solutions that have first been derived by precise point positioning (PPP).

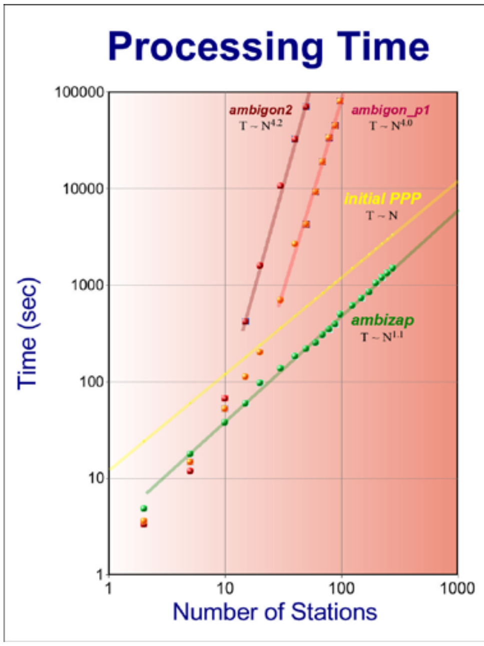

Figure 1. Processing time versus number of stations for currently used algorithms (red) and the new ambizap algorithm (green) described here. The current algorithms shows tends to 4th power behavior for large networks, whereas the new algorithm remains approximately linear with processing time. For comparison, PPP is also shown (yellow), which is a necessary preliminary step for all algorithms.

Since its invention by Zumberge et al. [1997], PPP has become popular for regional GPS network processing, because processing time scales linearly with the number of stations (unlike traditional processing models that scale to the power 4), and it closely reproduces the global solution (exactly for stations used for orbit determination). However, the processing time for ambiguity resolution generally scales to the power 4, thus the main practical advantage of PPP can be lost. Ad hoc ways around this have involved resolving biases in subnetworks which are then combined [Hurst, 2001], but even these methods are excruciatingly slow compared to PPP.

Motivating this study was the idea that theoretical properties of ambiguity resolution might point the way to schemes that scale linearly with network size. A reasonable condition for such schemes is that the differences between optimal and sub-optimal solutions should be statistically insignificant ("near-optimal").

A fixed point theorem was derived, which identifies linear combinations of network parameters that are theoretically invariant under ambiguity resolution. Specifically, under certain assumptions (which prove to be valid in practice): "Ambiguity resolution between previously resolved subnetworks only affects the relative positions between the centroids of the subnetworks, and does not affect the centroid of the entire network nor the internal geometry of any subnetwork." This theorem was used to assist the design and justification of a near-optimal network processing scheme (ambizap) that scales linearly with number of stations. As a corollary of the theorem (verified in practice): "The solution for any baseline within a network is entirely fixed by its own ambiguity resolution, and is not changed as other surrounding baselines are resolved."

Thus a complete network solution can be constructed by a two step procedure: (1) rigidly construct the vectors of N-1 linearly-independent baselines; and (2) translate the solution to align with the original PPP solution. Note this is different than the perhaps more intuitive but incorrect approach of "combining" least squares solutions from subnetworks (e.g., baselines), which turns out to be significantly sub-optimal both in accuracy and speed.

Tests show that a 98 station network is resolved on 1 cpu in 7 minutes versus the 22 hours it takes using the current GIPSY-OASIS II method – nearly a factor of *200* improvement in speed. The resulting station coordinates agree to 0.8 mm RMS, smaller than the daily repeatability (approx 3 mm for PPP), and so are "near-optimal." A block-diagonal covariance is also produced which closely approximates the rigorously formal variances of station and baseline coordinates, suitable for subsequent strain analysis.

In addition to reducing processing time, linear schemes readily lend themselves to parallel processor implementation. Thus real processing time can be reduced by several of orders of magnitude for extremely large networks. For example, on our 40 cpu cluster, the above 98 station network can be resolved in ~15 seconds, a factor ~5000 faster than the standard approach.

The ambizap algorithm allows for very rapid, multiple reanalysis of extremely large networks, and makes trivial the addition of extra stations or subnetworks to an existing solution. The method is also amenable to rigorous removal from the network solution of individual stations that have data problems.

Application of the ambizap algorithm will greatly assist analysis of crustal movement in regions such as the western North America, which have dense overlapping GPS networks. For example, a network solution from one day of the ~1000 station Plate Boundary Observatory can be produced from RINEX files in about 7 minutes on a 40-cpu cluster (4.5 min PPP + 2.5 min ambizap).

EARTHCHEM'S DEEP LITHOSPHERE DATASET: WEB-BASED ACCESS TO MANTLE XENOLITH GEOCHEMISTRY AND PETROLOGY

Karin Block, Kerstin Lehnert · Lamont-Doherty Earth Observatory
Mihai Ducea · University of Arizona

Understanding the evolution of the North American continent requires correlation between seismic and structural studies and physical conditions inferred from the composition of the underlying lower crust and mantle. Geochemical and petrological studies of xenoliths provide a crucial complement to geophysical endeavors currently underway through EarthScope science. The EarthChem project, an NSF-supported effort to advance access to geochemical data for the broad Earth Sciences, is developing the Deep Lithosphere Dataset, a compilation of geochemical and petrological data from upper mantle and lower crustal xenoliths, with an initial focus on localities in the western United States. The dataset can be accessed at the EarthChem web site (www.earthchem.org) via an interactive user interface that allows users to search the dataset and extract customized subsets of data. The database contains major oxide, trace element and isotopic compositional data, for minerals and rocks, and includes a wide range of supplementary information such as sample location, rock type, tectonic setting, analytical technique and data quality that can be used as search criteria. Analytical data values and modeled pressure, temperature and modal compositions reported in the publications are displayed in html tables where each value is linked to detailed information on analytical procedure, standards, and precision. Customized datasets and associated publication information can be viewed at various points in the query process and are downloadable in *.xls format. In the near future, query capability will be expanded to allow users to retrieve data by host rock, geobarometry and geothermometry. Addition of physical property data to the dataset will be guided by discussions with EarthScope scientists to insure that the database evolves to maximize its utility.

LAND USE PERMITTING OF THE PLATE BOUNDARY OBSERVATORY COMPONENT OF THE EARTHSCOPE PROJECT

Kyle Bohnenstiehl, Chelsea Jarvis, Keegan Fengler · UNAVCO

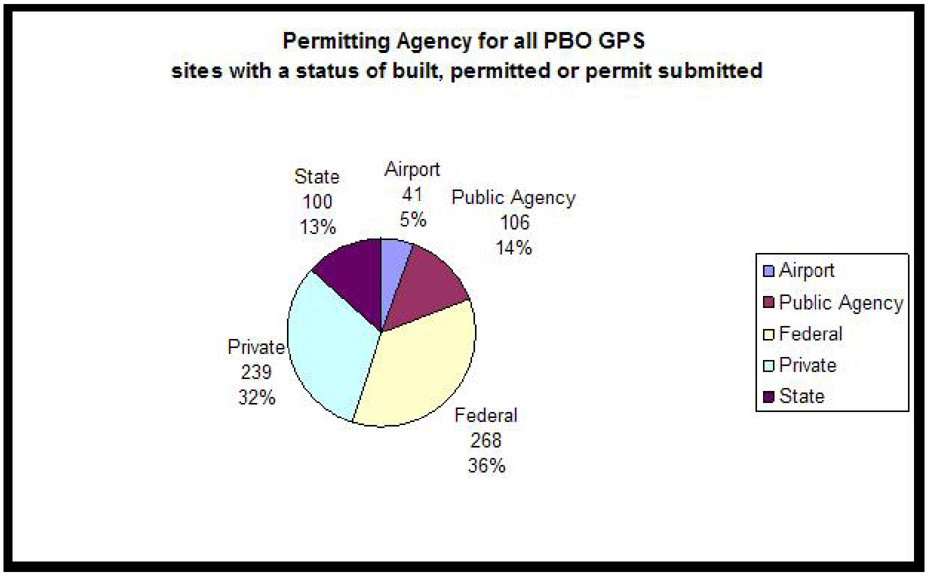

Given the geographic extent of the Plate Boundary in the 18 western states, it is inevitable that in the course of permitting the over 1200 PBO sites in the network, we would face some challenges and also learn some valuable lessons for other scientists working on distributed observatories. This poster provides information on the permitting progress to date, summaries of the experiences with different agencies to date, the costs of permitting, and 4 case studies of permitting challenges. As of March, 2007, we have permitted over 630 of the new GPS sites, 100 of the NUCLEUS transfers, and about 70 of the Borehole Strainmeters. For new GPS sites, we have permitted over 268 sites with federal agencies, 239 sites with private landowners, 100 sites on state lands, 106 with other public agencies, and 41 at airports. At 208 new GPS sites on private or other land where UNAVCO pays fees, the sites average $2932 per site for a long term lease. On the 24 GPS sites with annual rental, the fees average $200/year. We also present a case study of Mt. St. Helens Volcanic Monument (USFS) permitting, 2 examples of BLM permitting, and a look at permitting with the National Park Service. Overall the PBO project permitting remains ahead of schedule and under budget, however it has taken significant resources in terms of staff time to achieve these goals. Planned and future distributed observatories will need to devote considerable resources to land use permitting in order to be successful.

ANALYSES OF SIDEWALL CORES AND CUTTINGS FROM A DEEPER SECTION OF THE SAFOD BOREHOLE

Kelly Bradbury, James Evans, Sarah Draper · Utah State University
Corey Barton · Baker Hughes Inteq
John Solum · Sam Houston State Univsersity

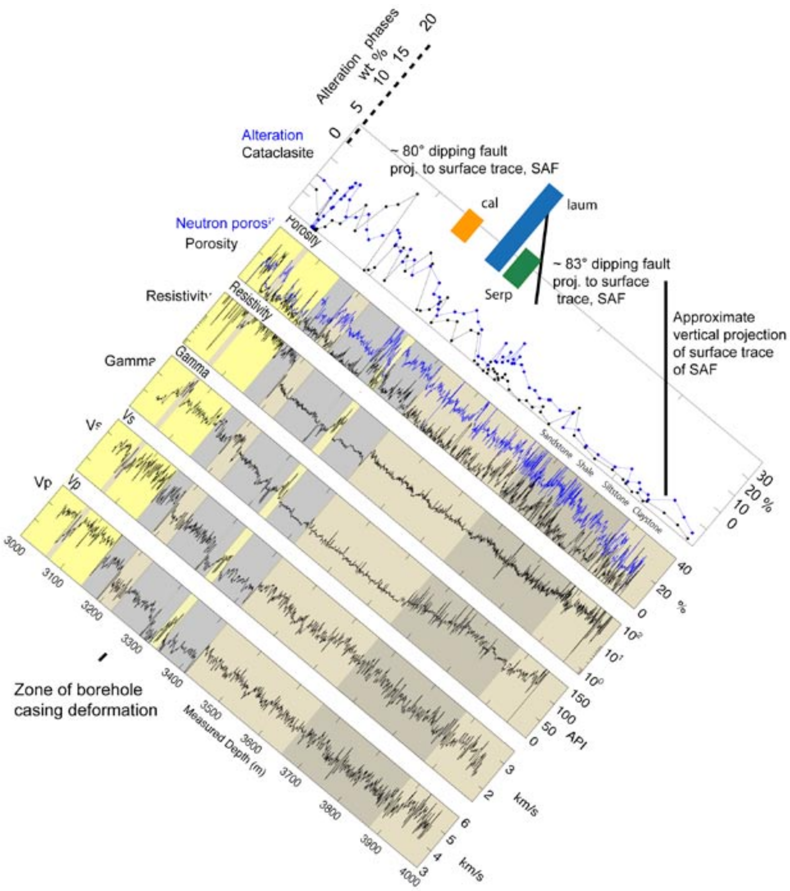

Examination of sidewall cores and cuttings from the San Andreas Fault Observatory at Depth (SAFOD) mainhole was conducted to characterize the lithology, structure, and alteration within this seismically active fault zone. We present work that focuses primarily on the area of sidewall core extraction extending from the depth interval between 3085 m to 3872 m. Our work, in combination with other whole-rock geochemical and X-Ray Diffraction studies (Solum et al., 2006; Kirschner et al., 2005), and borehole geophysical studies (Boness and Zoback, 2006), may provide further understanding of the physical and chemical processes associated with faulting and microearthquakes and may assist in the design and coring efforts planned for the summer of 2007.

Analyses from 19 of the thin-sectioned sidewall cores and correlated to data from the nearest available cuttings sample. Thin-section analyses of samples from fault zones allow for the quantitative measures of mineral abundance, degree of deformation, and alteration products associated with faulted sequences throughout the borehole. Identification of the abundance of cataclasite in the cuttings allows for the determination of the relative locations (m-scale range) of damage zone and fault core, and may correlate with previously identified shear zone locations using geophysical logs (Boness and Zoback, 2004l Boness et al., 2005). X-Ray Diffraction (XRD) analyses are also used to supplement the thin-section analyses is also used to supplement the thin-section analyses and to determine the primary mineral assemblages in several samples.

From the cuttings analyses, we identified arkosic and lithic arenites, interbedded with siltstone sequences from 1920 to ~ 3150 m MD, and a siltstone and shale sequence from 3150 m to 3987 m MD. Significant abundances of cataclasite are observed between 3000 and 3350 m MD with lesser amounts near 3300 m, 3400m, and 3650 m MD, and are interpreted to represent fault zones. Relatively little deformation is observed below 3600 m. Zones of alteration within this interval of study were chosen based on a combination of cuttings and X-Ray diffraction analyses and include: 2700 m –3000 m, 3050-3350 m, and 3500 m MD.

Deformation features observed in the grain mounts may indicate a complex array of slip surfaces with multiple slip events and/or episodic pulses of fluid migration within and adjacent to the main trace of the San Andreas Fault zone. The supporting evidence for this interpretation includes: 1) cross-cutting calcite veins; 2) numerous open to tight microfractures and slip surfaces; 3) halos of iron-oxide staining surrounding open fractures; 4) multi-layered zones of cataclasis; 5) at least two distinct types of cataclasis and 5) recrystallization of quartz.

Review of the sidewall cores suggest we may underestimate the intensity of deformation within the borehole and therefore limit our understanding of the processes associated with a particular style of deformation. For example, iron-oxide stained lithics are categorized simply as "lithics" during point-count analysis of the cuttings, however, examination of the sidewall cores suggest zones of abundant iron-oxide staining commonly penetrate the walls adjacent to open fracture systems. Also, calcite seen in cuttings analysis may appear as an individual grain, yet in the sidewall cores we see that calcite occurs in a complex array of veins. Therefore, correlation of the sidewall cores to the cuttings samples provides a more complete picture of the structural history within the borehole.

CONTRIBUTIONS OF EARTHSCOPE TO EARTHQUAKE HAZARD ASSESSMENT IN NORTHERN CALIFORNIA

Tom Brocher, Brad Aagaard, Bill Ellsworth, Steve Hickman, Diane Moore, Jessica Murray, Carol Prentice · U.S. Geological Survey
Arthur Rodgers · LLNL

We briefly describe some of the ways each of the three components of EarthScope (PBO, SAFOD, US Array) as well as GeoEarthScope contribute to earthquake hazard assessment in Northern California. First, SAFOD and US Array have directly contributed to the development and testing of regional 3D seismic velocity models for Northern California used to calculate strong ground motions for scenario earthquakes. Compressional- and shear-wave velocity logging of Salinian granitic rocks and sedimentary rocks in the SAFOD pilot and main boreholes provided important constraints on empirical Vp/Vs relations that were used to convert geology-based Vp models to Vs models. Arrival times between US Array stations in Northern California, determined from correlations of the ambient background noise, are being used to calibrate the accuracy of the regional 3D seismic velocity model for Northern California. Eventually, regional shear-wave velocity models developed from the US Array recordings of ambient noise may prove useful in calibrating regional geology-based velocity models outside of the Bay Area where the geology model is highly simplified. Second, identification of talc in cuttings from the SAFOD borehole, near the active trace of the San Andreas fault, suggests that its presence or absence may play an important role in the creeping and locking behavior of faults in the San Francisco Bay Area. Third, data from PBO continuous GPS sites are incorporated into our automated processing system as the stations come online. This station densification improves our ability to monitor deformation in Northern California. We are developing strategies for including PBO strainmeter data in routine monitoring as well. The continuous GPS data provide a strong framework of regional measurements which permit us to conduct focused survey-mode GPS observations in order to refine our understanding of Northern California deformation and fault slip rates, for example along the Bartlett Springs fault. Fourth, GeoEarthScope is acquiring 1400 square km of LIDAR data mainly along 1 km wide swaths centered on many of the major strike-slip faults in Northern California. As part of this effort, a consortium of other agencies and corporations will fund collection of an additional 220 sq. km of LIDAR data. These LIDAR swaths are designed to produce images of the fault zones that will help better locate and define active traces within these fault zones, identify new places suitable for paleoseismic excavations across fault strands, and provide baseline imagery prior to the next major earthquake with surface fault rupture.

A MOORED GEODETIC SEAFLOOR MONITORING SYSTEM (GEOCE)

Kevin Brown, David Chadwell, Uwe Send, Mike Tryon · Scripps Institution Of Oceanography

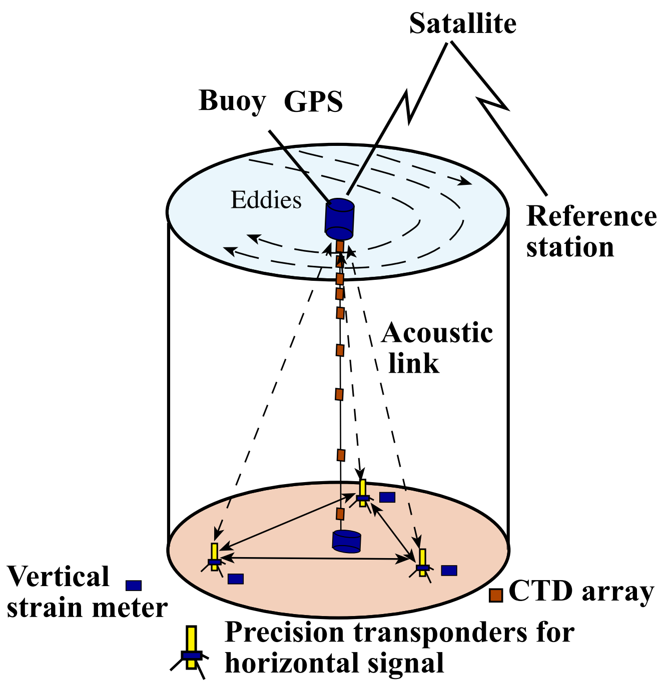

GEODETIC SEAFLOOR MONITORING SYSTEM (GEOCE)

We are currently constructing and will demonstrate in the next three years a novel capability to carry out geodetic seafloor motion measurements from oceanographic moorings and observatories. They are expected to be installed as part of the future Margin/ORION program in both coastal and open-ocean sites including a potential offshore Cascadia array. This array would be aimed at quantifying patterns of strain accumulation and release across the subduction complex. These marine geodetic measurements would naturally dovetail with any onshore Pacific Northwest geodetic network. The GEOCE system would integrate several components, most of which have been proven separately in different applications already. It consists of continuous raw-waveform differential GPS measurements on the surface buoy of the mooring, to determine the horizontal and vertical motion of the buoy with subcentimer accuracy. Horizontal seafloor motion is measured via acoustic transponder interrogations relative to the surface buoy, a variant of an existing ship-based approach. Vertical seafloor motion is determined via high-precision bottom pressure measurements, after removing sea surface height motion (using the GPS) and internal ocean density fluctuations (using water column CTD sensors in the mooring). The residual bottom pressure signal is seafloor motion or sensor drift. The accuracy of the sensors except for a long-term drift has been demonstrated in prior applications. Here an in-situ calibration system will be added to determine the drift. Irregular vertical motion or sudden events would be detectable even without this calibration system. Some of the data would be telemetered in real-time. The subsurface part of the system relies on existing and proven robust technologies, such as acoustic time-delay recovery of bottom pressure data, inductive communication with the CTD sensors in the mooring wire, while the transponders are interrogated with buoy-mounted transducers.

The ability to measure seafloor motion with subcentimeter accuracy on long timescales (months to years) in a continuous mode using moored installations would represent a significant advance over our current technological and scientific capabilities. It should also be very feasible to track geodetic response of large earthquake rupture propagation events (Mw 7+ to 9+) over sort time scales of seconds because the geodetic signals are very large (meters to 10s m) and arrays of GEOCE buoys can measure progressive deformation as the earthquakes in some cases propagate several 10s km to 1000+ km at Km/s. Even though based on existing elements, the integration of various geophysical and oceanographic methods into a stand-alone system is pushing all the elements to their limits and together results in novel tools for geophysics and physical oceanography. The oceanographic benefit of the system (thus the acronym “geophysical and oceanographic” observatory system) comes from the ability to perform bottom pressure observations without long-term drift, which until now has hampered the detection of long-period signals in bottom pressure, important for interannual, interdecadal and climatic changes in ocean circulation.

The proposed system is a step towards making mutual use of ocean observatory hardware between disciplines, towards merging expertises and technologies, and towards implementing multi-use ocean moorings in sites of common interest between geophysics and oceanography (such as those identified in ORION planning letters and conceptual proposals). It demonstrates how existing or planned water column observatories can be easily upgraded to serve more scientific objectives. In addition, the real-time aspect of the system allows for monitoring of events, such as seafloor motions, which often proceed major, quake or slip events. Thus the system could contribute to early warning strategies for undersea earthquakes and tsunamis.

TRAVEL TIME TOMOGRAPHY WITH USARRAY DATA

S. Burdick, C. Li, R.D. van der Hilst · Massachusetts Institute of Technology
V. Martynov, T. Cox, J. Eakins, L. Astiz, F.L. Vernon · University of California, San Diego

The increasing availability of broad band waveform data from USArray and regional networks offers unique opportunities for multi-scale seismic imaging. Constraining structures on a range of length scales and their physical and chemical causes is a prerequisite for understanding the relationship between near surface and deeper mantle processes. As a first step we aim to produce a 3-D model of P-wavespeed variations in the mantle from the inversion of travel time picks from station networks in the western states, the USArray stations as installed so far, and the global data base maintained by Engdahl and co-workers (BSSA, 1998). We expect that such a model will be of tremendous interest in its own right, but in the future we also intend to use it as a starting model for future high-resolution transmission and reflection waveform tomography studies (e.g., De Hoop, Van der Hilst, GJI, 2006). Phase arrivals in the USArray records are determined routinely using automated procedures, with data quality control by analysts, and association with the preliminary epicenter determinations by the U.S. Geological Survey produces the data used in the tomography. (In the future these data will be incorporated in and processed along with the EHB data, but that is not yet done at this early stage of processing.) For the tomography we use code developed for multi-scale inversion for upper mantle structure beneath Tibet from regional network data and PASSCAL arrays (Li et al, PEPI, 2006). We perform a global inversion but a variable parameterization was used in order to reveal smaller scale structure in the western United States where data coverage was much higher. We will present our tomographic approach and present preliminary images of mantle structure beneath western North America.

INTEGRATING EARTHSCOPE WITH REGIONAL GEOLOGY AND GEOLOGIC HAZARDS: LESSONS LEARNED FROM TEACHERS ON THE LEADING EDGE

Robert Butler · University of Portland
Bonnie Magura · Jackson Middle School
Charles Ault Jr. · Lewis and Clark College
Roger Groom · Mt. Tabor Middle School
Chris Hedeen · Oregon City High School
Jenda Johnson · USArray consultant

The Pacific Northwest provides opportunities to connect EarthScope science to actual geologic features that many K-12 teachers and students have visited or viewed but rarely examined in classroom activities. To engage K-12 teachers and their students in EarthScope, we must build educational programs that: (1) invite novice learners of Earth Science to geophysical studies of earthquakes, volcanoes, and tectonics; (2) provide access to EarthScope's seismology, geodesy, and remote sensing observations in an understandable fashion; and (3) demonstrate the significance of EarthScope science to society. Teachers on the Leading Edge (TOTLE) is a teacher professional development program featuring field study of active continental margin geology in the Pacific Northwest, its past and present plate tectonic processes, and the societal implications of this geologic heritage. Program themes include: (1) convergent margin processes from great earthquakes and tsunamis to continent building through volcanism and terrane accretion; (2) geophysical studies that illuminate the geology beneath the tree-covered landscape and provide an introduction to USArray and PBO; and (3) geologic hazards as incredible but not mysterious aspects of living on the "leading edge" of our continent. Two examples of successful transfer of science content learning to classroom teaching are: (1) The Grand Cross Section. Connecting regional geologic features with plate tectonic processes is repeatedly addressed and leads to teachers drawing cross sections from the Juan de Fuca Ridge across the active continental margin to the accreted terranes of northeast Oregon. Several TOTLE teachers have transferred this activity to their classrooms by having student teams relate earthquakes and volcanoes to plate tectonics through artistic renderings of The Grand Cross Section. Analysis of PBO observations emphasizes how the continental margin is "locked and loading" as it stores elastic energy that will be released in the next Cascadia megathrust earthquake. (2) Great Earthquakes and Tsunamis. Working with Brian Atwater (U.S. Geological Survey, Seattle), we are developing classroom activities that feature Cascadia tsunami geology and the Orphan Tsunami of 1700 as a focus for studies of earthquake seismology and tsunamis. TOTLE teachers have successfully used tsunami geology as a launch point for classroom studies of tsunamis, earthquakes, and active continental margin geology. These experiences make frontier geophysical research, like GPS observations of slow earthquakes and seismic tomography of the subducting Juan de Fuca Plate, accessible to K-12 teachers and useful in their teaching of plate tectonics and earthquake seismology. These lessons and strategies may be valuable to other Geoscience educators seeking to prepare K-12 teachers to convey the discoveries of EarthScope's USArray and Plate Boundary Observatory experiments to their students.

EARS AND THE BULK CRUSTAL PROPERTIES OF THE SIERRA NEVADA

Katrina Byerly, Thomas J. Owens, Philip Crotwell · University of South Carolina
Hersh Gilbert · Purdue University
George Zandt · University of Arizona
Craig Jones · University of Colorado

The Sierra Nevada Earthscope Project (SNEP) seeks to advance our understanding of the ongoing foundering of mantle lithosphere beneath the Sierra Nevada. SNEP is a temporary broadband deployment within the broader USArray Transportable Array (TA) network. The SNEP deployment consists of two phases and a network totaling ~75 broadband stations. The network extends from the western foothills to eastern Nevada between roughly 37°N to 40.5°N with an average station spacing of 25km. Using the automated receiver function technique implemented by EARS (The EarthScope Automated Receiver Survey), we are calculating the bulk crustal property estimates (thickness and Vp/Vs ratio) for SNEP stations and surrounding USArray TA stations. Through the study of areas of suspected transitions in crustal properties and comparison of EARS results to other SNEP results, we will be able to evaluate the value of the EARS approach as an interpretational aid to portable PASSCAL and USArray/FlexArray experiments. The resulting determination of the lateral variations in the bulk properties of the Sierra Nevada crust will provide baseline observations in the search for the existence and extent of foundered crust/upper mantle within the SNEP footprint and serve as a starting point for more advanced analysis of receiver functions within the SNEP footprint.

OFFSET OF A BRIGHT, SHALLOW MOHO ACROSS THE COAST SHEAR ZONE IN THE COAST MOUNTAINS BATHOLITH, 52°-56° N

Josh Calkins, George Zandt · University of Arizona
Ken Dueker · University of Wyoming

Common conversion point stacks of receiver functions from the passive seismic component of the Batholiths Continental Dynamics project reveal a ~7 km offset in the Moho discontinuity in the vicinity of the Coast Shear Zone (CSZ) in western British Columbia. Cross sections from the southern transect, near 52° North, reveal a bright, nearly flat Moho at 33 km east of the CSZ and at 26 km west of the CSZ. Analysis of well-recorded crustal multiples reveals a change in the Vp/Vs ratio coincident with the change in crustal thickness. The high Vp/Vs (~1.88) to the west of the CSZ indicates the average crustal composition is more mafic than that to the east, where Vp/Vs averages 1.76. A similar, if somewhat less distinct change in Moho depth and Vp/Vs is observed near the CSZ on the northern line, between 53.5° and 55.5° North, indicating that the CSZ is a crustal scale structural feature in the study area. The high amplitude of the Moho converted phase throughout the Batholiths project area indicates a sharp velocity contrast between the lower crust and upper mantle, suggesting that a residual ultramafic root is not currently present beneath the Coast Mountains Batholith.

INTERPRETATION OF SEISMIC STRUCTURE FROM MANTLE XENOLITHS: CIMA VOLCANIC FIELD - WALKER LANE (CA), SAN CARLOS VOLCANIC FIELD - BASIN AND RANGE (AZ), POTRILLO VOLCANIC FIELD - RIO GRANDE RIFT (NM), AND KNIPPA QUARRY - BALCONES IGNEOUS PROVINCE (TX)

Keith Cardon, Elizabeth Anthony, Minghua Ren · University of Texas at El Paso
Randy Keller · The University of Oklahoma
Robert Stern, Urmidola Raye · University of Texas at Dallas

Xenoliths will be used in EarthScope science to constrain interpretations of seismic velocity data. Examples of the promise held by the integration of xenolith and geophysical data are described here. Textures, compositions, and thermometry have been determined for peridotites (Anthony, Andronicos, Ren, unpublished data) and pyroxenites (this study) from Kilbourne Hole in the Potrillo Volcanic Field (PVF), New Mexico. Temperatures for the peridotites range from approx. 1000° C to 1184° C, and more cpx-rich lherzolite is interpreted to overlie ol-rich harzburgite and dunite. Os isotope ages, which reflect lithospheric stabilization, are Paleoproterozoic. Pyroxenites are compositionally distinct from peridotite, and we interpret them to have formed from melt/fluid interaction with peridotite, including perhaps interaction with slab-derived fluids from the Farallon plate. North of the PVF, the LA RISTRA teleseismic profile shows strong seismic wave attenuation centered under the Rio Grande Rift and extending approximately 100 km west and 200 km east at a depth of 200 to 250 km. The observed seismic velocities can be explained by a combination of high sub-Moho temperatures and cpx-rich lithologies. The pyroxenites are an important consideration because velocity contrasts within peridotite are limited. However, pyroxenites, which are up to 90% cpx, may provide sufficient velocity contrasts with the peridotites to explain mantle reflectors found under the Cima field and PVF regions. We have established that peridotite xenoliths from two other Quaternary volcanic fields, the Cima field in the Walker Lane and the San Carlos field, which lies within the COARSE teleseismic array, also have temperatures of 1000° C and greater. All three fields lie in the portion of western US characterized by slow mantle seismic velocities. At least for the Cima field, these temperatures may represent ambient conditions immediately below the Moho, because the samples contain spinel reacting to plagioclase. These temperatures are not unusual for the Basin and Range, and place constraints on the conductive geotherm. A question to be addressed by the 3-D nature of USArray is whether the geotherm will be as steep in areas distant from active volcanic fields.

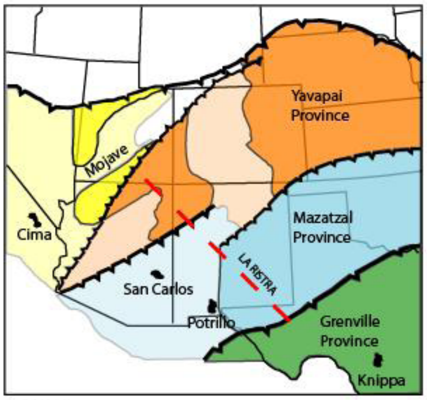

Figure 1a.
Adapted from Karlstrom et al. (2001). Dark colors represent cool upper mantle with fast seismic velocities. Light colors represent hot mantle with slow S-wave velocities. The red line refers to LA RISTRA teleseismic array.

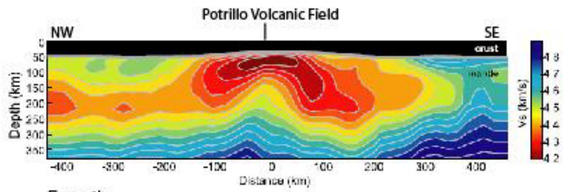

Figure 1b.
From West et al. (2004). LA RISTRA teleseismic profile centered over Rio Grande Rift north of PVF. Profile indicated in figure 1a.

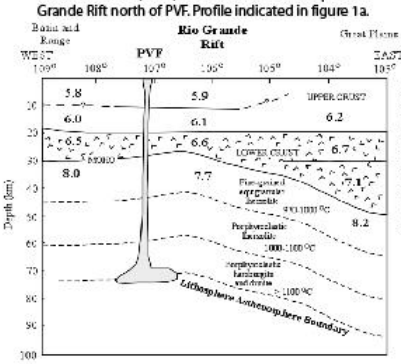

Figure 1c.
Integrated seismic and petrologic profile at PVF. Numbers are P-wave velocities in km/s. Tentative depth to the lithosphere - asthenosphere boundary established by teleseismic studies.

EARLY INSIGHTS INTO THE MECHANICAL BEHAVIOR OF MATERIALS INTHE 3D SAFOD VOLUME

Brett Carpenter, Andrew Rathbun, Demian Saffer, Chris Marone · Pennsylvania State University

A central problem in evaluating the relationship between fault zone properties and earthquake physics is a lack of detailed laboratory data for fault zone materials recovered from hypocentral depths. Gaining a better understanding of the strength and stability of the San Andreas Fault is important for assessment of earthquake hazards and linking observations of fault behaviors to physical processes. We report on experiments designed to explore the mechanical behavior of rocks in the 3D SAFOD volume. Experiments were conducted on fault zone materials recovered from SAFOD phase 1 drilling and surface samples of rock formations within the 3D volume containing the SAFOD drill hole, selected using recent detailed cross sections. Samples from San Andreas Drilling range in depth from 1.4 km to 3.1 km and surface samples include country rock, wall rock, and fault rock.

Experiments were conducted in a servo-controlled, double-direct shear apparatus at room temperature and humidity. Layers of pulverized fault and surface rock were sheared at constant normal stress between rough rigid forcing blocks. Normal stress and shear velocity ranged from 5 to 100 MPa and 1-300 micron/s, respectively. Permeability of surficial host rock outcrops was determined by flow-through measurements under uniaxial compression at stresses up to 90 MPa.

Normal stress was stepped to define the Coulomb failure envelope and friction constitutive properties at a range of fault stresses. These data show consistent values of the coefficient of sliding friction (we assume zero cohesion for the granulated layers) ranging from 0.52 to 0.63. At each normal stress, samples recovered from greater depth exhibit slightly lower friction values compared to the granite from 1.4 km. Preliminary flow-through measurements on fine-grained cemented sandstone from the SAFOD pilot hole indicated a permeability of 1.74 x 10-17 m2 and 6.78 x 10-18 m2 at 5 MPa and 9 MPa, respectively.

Velocity stepping tests indicate that steady-state friction values were reached and that the fault rocks exhibit slip-rate and history-dependent friction behavior similar to that documented for simulated fault gouge. A sudden increase in load point velocity results in an immediate increase in friction followed by a displacement-dependent decay to a new steady-state level. Measurements of steady-state friction as a function of slip velocity show velocity-weakening frictional behavior for some SAFOD materials at low normal stress.

These early experiments aim to begin populating a database used to constrain fault mechanical and hydrologic models as well as to explore the controls of strength and stability of SAF rocks. Future work will be aimed at determining the effects of temperature and pore/confining fluids on the strength and second-order frictional characteristics of fault zone materials. Additionally, the evolution of permeability across the fault zone will be studied on characteristic samples colleted from Phase 1 Drilling and surface outcrops.

ACCELERATED UPLIFT OF THE YELLOWSTONE CALDERA, 2004-2006, FROM GPS AND INSAR OBSERVATIONS

Wu-Lung Chang Chang, Robert Smith, Jamie Farrell, Christine Puskas · University of Utah
Chuck Wicks · U.S. Geological Survey

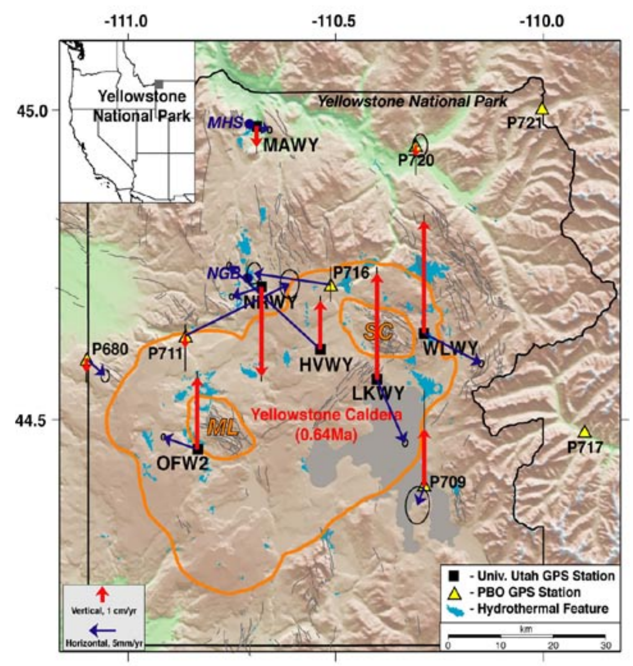

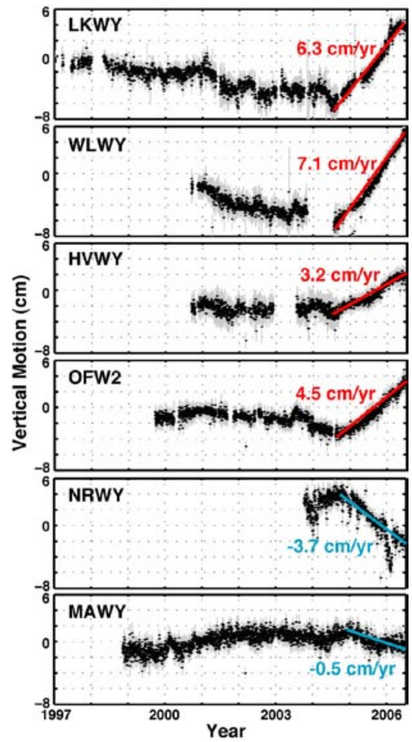

Geodetic techniques have been employed to monitor crustal motion of Yellowstone beginning with precise leveling of benchmarks installed in 1923. Since 1997, the University of Utah has installed six permanent GPS stations inside Yellowstone National Park for continuously monitoring of ground deformation associated with seismic, volcanic, and hydrothermal activities. Starting in mid-2004, the GPS network recorded an episode of unprecedented uplift of the Yellowstone caldera concomitant with subsidence of the northeast caldera area including Norris Geyser Basin. The deformation continues into 2007, with nearly constant inflation rates of ~6 cm/yr and 4 cm/yr at the Sour Creek and Mallard Lake resurgent domes, respectively (Fig. 1). These rates are up to three times faster than preceding caldera uplift rate from 1923 and 1984. The horizontal velocities, in addition, are 7 to 21 mm/yr outward from both domes. Meanwhile, Norris Geyser Basin experienced subsidence at ~4 cm/yr that is two times higher than the 1996-2002 uplift rate.

Incorporating GPS data from the University of Utah and five new PBO stations, we evaluated source models by inverting the GPS and InSAR data for the geometry and expansion (contraction) of dislocations in an elastic half-space. Results show two horizontal sill-like structures ~8 km beneath the caldera with a total volumetric expansion rate of 0.11 km3/yr, and a NW-dipping tabular body 16 km beneath the Norris Geyser Basin with a volumetric contraction rate of 0.018 km3/yr. Incorporating seismic, hydrothermal, and geochemical evidence, we propose that a new intrusion of magma into the mid-crustal or pressurization of a deep hydrothermal system likely caused the uplift within the Yellowstone caldera. The Norris subsidence, in contrast, may be induced by the crystallization and contraction of crustal magmatic bodies and the associated loss of dissolved fluid and gas to shallow fault and hydrothermal systems.

INFLUENCES ON THE TOPOGRAPHIC CHARACTER OF THE WESTERN U.S.: SPECULATIONS ON THE ROLE OF INHERITED STRUCTURES, PLATE MOTION, AND UPPER MANTLE PROPERTIES

David Coblentz, Jolante van Wijk · Los Alamos National Laboratory
Karl Karlstrom · Universiy of New Mexico

The relationship between topography and tectonics is complex and is controlled by many factors. In the Western U.S. these factors include tectonic forces due to Pacific-North American interactions, sub-lithospheric buoyancy, and the geometry of inherited tectonic features in the lithosphere such as paleo-sutures.

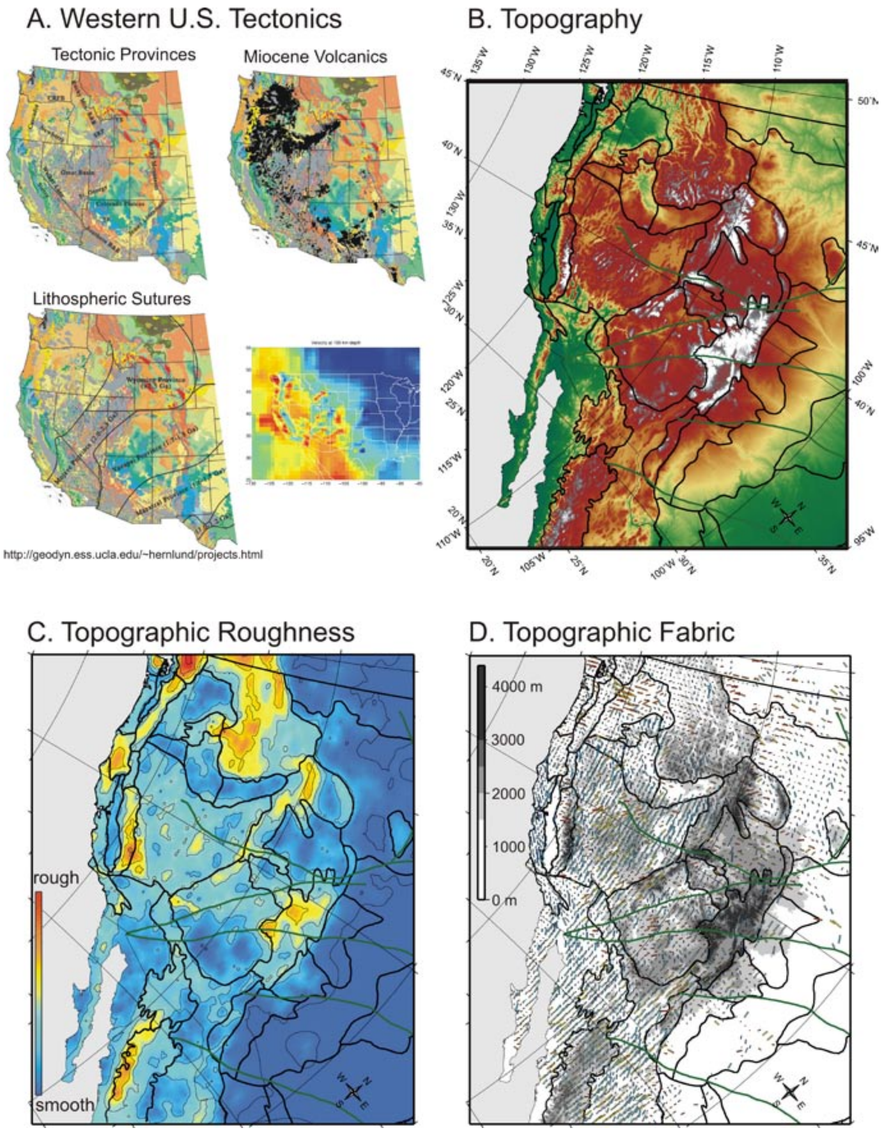

Here we present results from a quantitative topographic analysis of the Western U.S., motivated by the hypothesis that inherited tectonic features from the evolution of the Cordillera have been preserved in regional topography and can be evaluated through an analysis of the geomorphometric characteristic such as roughness and topographic grain orientation. A number of recent studies have explored ways to extract tectonic information from topography and propose several provocative interpretations to explain Western U.S. landscapes, including:

1) A systematic decrease in topographic spectral power with increasing tectonic age of underlying crust,

2) Variation in local relief, mean elevation, and thermochronologically-determined exhumation history across major Paleozoic accretionary boundaries,

3) A relationship linking Neogene and ongoing rock- and surface-uplift with the creation of mantle buoyancy;

4) A strong correlation between topography and lithospheric features such as mantle velocity structure, crustal thickness, and Precambrian crustal provinces.

We explore and expand these correlations through an evaluation of topographic fabric and the geography of the terranes, tectonic provinces and recent maps of the upper mantle velocity anomalies (Figure 1A).

Because the influence of Pacific-North American plate interaction can be expected to have a profound influence on the topographic character of the Western U.S. (many of the tectonic province boundaries are based on topography) we use an oblique Mercator projection about the PAC-NAM rotation pole to help the visual interpretation of plots of topographic roughness and fabric orientation (note that the vertical direction in Figure 1B-D corresponds to the current Pacific-North American relative plate motion.) In the context of the EarthScope project, we plan to refine this approach and further quantify the influence of the crustal and upper mantle structures imaged through the USArray component and on the topographic character of the Western U.S.

SEISMIC EVIDENCE FOR A WIDE DAMAGE ZONE AT THE CALICO FAULT, CALIFORNIA

Elizabeth Cochran · University of California, Riverside
Peter Shearer, Yuri Fialko · IGPP, Scripps
YongGang Li · University of Southern California
John Vidale · University of Washington

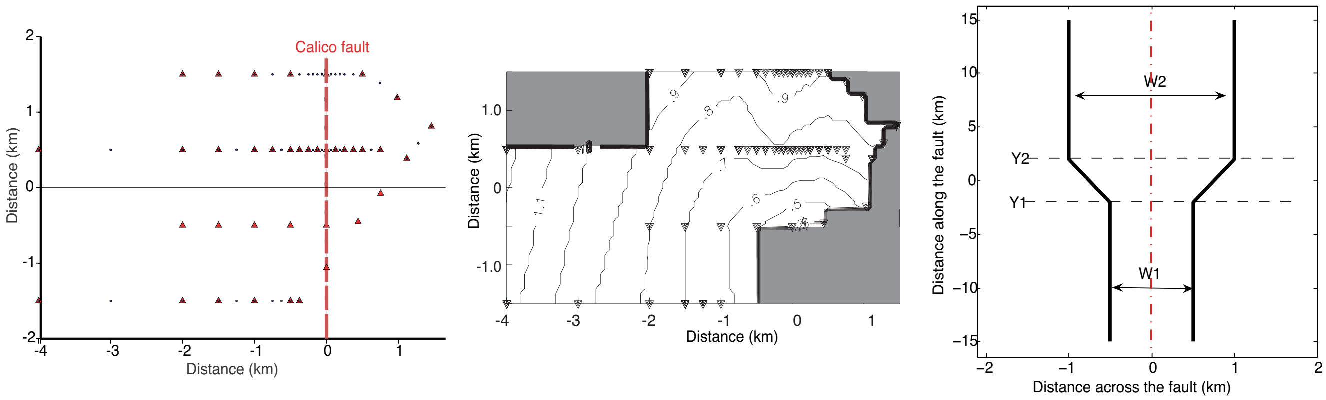

Figure 1: (a) Array layout near the Calico fault in a local coordinate system with the Calico surface trace located at x=0 km. Triangles and dots represent intermediate and short period stations, respectively. (b) Travel time contours for the shot located at x = 0, y = -1.0 km showing reduced velocities in the fault. (c) Preliminary interpretation of compliant zone width variations along strike as determined from forward modeling.

One of the primary targets of EarthScope is the network of faults that scar the western United States, and one of the most pressing mysteries is the nested cycles of tectonic deformation. The eastern California shear zone, home to the 1992 Landers and 1999 Hector Mine earthquakes, is an ideal natural laboratory to attack these questions owing to its recent activity and the abundance of available seismic and geodetic data. Recent InSAR observations provide the first large-scale maps of the three-dimensional response of a fault network to an applied stress. We investigate in detail the seismic structure of one of these compliant fault zones, the Calico fault.

A dense array of 100 seismometers deployed near the Calico Fault recorded explosions and seismicity between June and December 2006. Seismic velocity reductions associated with the fault damage zone are mapped in detail along and across strike; in addition, the depth extent of the velocity reduction is investigated. Our measurements are in accord with InSAR observations showing that the Calico fault suffered twice the strain of the surrounding bedrock during the Hector Mine and Landers earthquakes, confirming a zone of reduced shear modulus around the fault.

We use arrivals from 3 active-source explosions as well as local, regional, and teleseismic earthquake body waves to measure the width of the low-velocity zone and investigate variations in that width along strike and with depth. In our forward modeling we start with the SCEC velocity model and then perturb the velocities in a finite zone along the Calico fault to find a match to the observed travel times. Preliminary results suggest a 1 to 2 km wide low-velocity zone, in good agreement with the InSAR-derived compliant zone. These findings indicate that faults can affect rock properties at significant distances from the primary fault slip surfaces, a result with implications for the portion of energy expended during rupture to drive the cracking and yielding of rock.

GPS INSTALLATION PROGRESS IN THE NORTHERN CALIFORNIA REGION OF THE PLATE BOUNDARY OBSERVATORY

Brian Coyle, Andre Basset, Todd Williams, Doerte Mann, Adam Woolace, Karl Feaux · UNAVCO-PBO

The Plate Boundary Observatory (PBO) is the geodetic component of the NSF funded EarthScope project. The final PBO GPS network will comprise 852 continuously operating GPS stations installed throughout the Western US and Alaska. There are 435 stations planned for California, with 229 of these in Northern California (NCA). This poster presents a progress report and highlights of GPS installations in NCA over the past year.

At the end of the second year of the project (10/2005), PBO NCA had installed 68 GPS stations. In the third year of the project (2006), we installed 56 stations for a total of 124. In year four, we have installed 12 stations so far, for a total of 136. This total comprises 65% of the proposed sites along the active transform margin, 20% of the sites on volcanoes and calderas, and 44% of the sites covering the extensional regime of the Basin and Range. We have submitted permit applications for all but 24 of the remaining stations proposed for NCA and expect to have these completed in the next few months.

A particularly important metric for planning our schedules is the time lag between reconnaissance and permit accepted. Over the past three years this time lag has varied from 1 day to over a year. Our average to date is 199 days from reconnaissance to installation.

Other highlights include completing station installations along the Maacama Fault Zone and onshore of the Mendocino Triple Junction. Data from these stations are available from the UNAVCO archive (http://pboweb.unavco.org/?pageid=88). As part of our operations and maintenance activities we are also developing a catalog of the effects of fences, trees and other near-field objects on GPS data quality.

We plan to have 190 stations built by the end of Sept 2007. In order to accomplish this goal, we are working to finalize our reconnaissance and permitting activities for stations located in National Forests and National Parks; installations we expect to complete by September 2007. We expect to be finished with all reconnaissance activities by spring 2007, after which crews will focus on installations, maintenance of the 130+ station network, and the transition to full time operations and maintenance mode after 9/2008.

LOCATING CASCADIA DEEP TREMOR USING ENVELOPE CROSS CORRELATION

Kenneth Creager, Aaron Wech, Stephen Malone · University of Washington
Geoffrey Abers, Zhu Zhang · Boston University
Tim Melbourne · Central Washington University
Stephane Rondenay · Massachusetts Institute of Technology
Bradley Hacker · University of California, Santa Barbara

We have developed a new method for locating deep non-volcanic tremor events. First we identify a 5-20 minute time window containing strong tremor bursts, band-pass filter from 2-6 Hz, calculate an envelope function and low-pass filter to 0.1 Hz. All pairs of envelope functions are cross correlated. For each point in a spatial grid the differential S-wave travel time for each station pair is calculated. The cross-correlation values at those differential times are determined and summed over all the station pairs. The tremor source is estimated to be at the location that provides the best weighted sum of cross correlations. Using this method we have located about 150 tremor bursts, approximately evenly spaced in time, for the September 2005 and January 2007 ETS events in northern Washington and southern Vancouver Island. The locations of tremor for these two episodes are quite similar, although the migration pattern is very different. The 2005 sequence initiated just south of the San Juan Islands, migrated 50 km to the SW towards Port Angeles, then bifurcated heading simultaneously NW and SE. On the other hand, the 2007 episode started in the southern Puget Sound region and headed linearly NW at about 10 km/day ending at southern Vancouver Island. This method locates epicenters of typical earthquakes to within a few km, but errors in depths can be 10 or more km. Similarly, the tremor appears to be robustly located in epicenter, but not in depth. Data from the PNSN and the EarthScope Transportable Array are used in the locations. Data from the Flexible Array CAFE experiment are still in the field, but may be available for a quick look a few days before the EarthScope Workshop.

THE GEON LIDAR WORKFLOW AS A DISTRIBUTION PATHWAY FOR FORTHCOMING GEOEARTHSCOPE LIDAR DATASETS

Christopher Crosby, Ramon Arrowsmith, Newton Alex · Arizona State University
Han Kim, Efrat Frank, Viswanath Nandigm, Ashraf Memon, Chaitan Baru · University of California, San Diego

The forthcoming GeoEarthScope LiDAR topography acquisition offers an unprecedented opportunity to examine the strain field adjacent to major active faults in the western United States at time scales greater than those provided by the Plate Boundary Observatory geodetic instrumentation. Modeled after the recent B4 data acquisition, the GeoEarthScope LiDAR data is expected to provide digital elevation models (DEMs) of one meter or better spatial resolution with scientific-grade geodetic accuracy. These datasets will be exceptionally valuable for geologic slip rate studies, paleoseismic research, and as a pre-earthquake representation of the landscape should an event occur in the near future. These datasets will be utilized extensively. They must be available to the EarthScope community as quickly and as easily as possible.

Traditionally, access to community LiDAR datasets is difficult because of the massive volumes of data generated by LiDAR technology. For example, the recently acquired B4 dataset covers nearly 1000 kilometers of the southern San Andreas and San Jacinto faults and contains approximately 35 billion individual LiDAR returns. With the B4 dataset as a model, the tremendous volume of data generated by the forthcoming GeoEarthScope LiDAR acquisition effort could potentially be a significant barrier for user community access and processing of these data.

In order to address the challenges posed by the distribution and processing of community LiDAR datasets, we have applied a geoinformatics approach that capitalizes on cyberinfrastructure developed by the GEON project (http://www.geongrid.org). The internet-based resource we have developed, the GEON LiDAR Workflow (GLW), is designed to democratize access to these challenging datasets and provides tools to enable users to perform basic processing (e.g. DEM generation) of the data. As a proof of concept, we have made four community LiDAR datasets, including the B4 data, available via the GLW. Our approach utilizes a comprehensive workflow-based solution which begins with user-defined selection of a subset of point data and ends with download and visualization of DEMs and derived products. In this workflow, users perform point cloud data selection, interactive DEM generation and analysis, and product visualization all from an internet-based portal. This approach allows users to carry out computationally intensive LiDAR data processing without having appropriate resources locally.

With the expectation of GeoEarthScope LiDAR datasets being delivered via the GLW, we are currently in the process of migrating the system from its current proof of concept implementation to a fully robust, production level, community data portal. As part of this migration, we are improving system stability, documentation and portal usability, adding processing capacity, and providing new job monitoring and job archiving capability.

The distribution of GeoEarthScope LiDAR topography via the GLW represents an excellent example of utilization of cyberinfrastructure to facilitate access to computationally challenging community datasets.

SEISMIC ARRAY PROCESSING WITH HIGH RATE GPS DATA

James Davis, Robert Smalley · University of Memphis

Array analysis of kinematic 1-second High Rate GPS data from the Great Sumatra-Andaman Mw=9.0 earthquake is used to estimate a Love wave phase velocity dispersion curve using seismic FK beamforming. HRGPS data recorded by 30 CORS sites in Michigan and one GPS Array for Mid-America site in Missouri are used to produce 30 differential displacement time series. An estimate for the absolute displacement time series of the fixed site, which is common to all the differential kinematic time series, is found by averaging the differential sites. Subtracting the fixed site estimate from each of the differential sites, we obtain estimates of the absolute displacement time series for the kinematic sites. The absolute displacement estimates are filtered using zero-phase bandpass filters to attenuate multipath and noise outside the frequency range of interest. F-K beamforming is then used to suppress both noise and multipath to determine the slowness of seismic waves crossing the array. We find both Love and Rayleigh waves, which are naturally polarized on the E-W and N-S components respectively, that have the correct back-azimuth to the Sumatra earthquake and appropriate slownesses. Dispersion curves are obtained by repeating the analysis using a series of narrow-bandpass filters. There is also evidence that surface waves of 300+ second periods are observable by HRGPS which is beyond the long period range of all but the best broad band seismometers. Application of similar array processing techniques to the dense PBO network and other open networks will complement seismic studies of both strong and weak motion but large amplitude seismic waves.

A HIGH RESOLUTION SEISMIC CHIRP INVESTIGATION OF ACTIVE FAULTING ACROSS LAKE TAHOE, AT THE WESTERN EDGE OF THE WALKER LANE.

Jeffrey Dingler, Graham Kent, Neal Driscoll, Jeff Babcock, Alistar Harding · Scripps Institution of Oceanography
Gordon Seitz · San Diego State University
Charles Goldman · University of California, Davis
Bob Karlin · University of Neveda

Extension rates across the Lake Tahoe basin have been estimated for the last 60 ka based on analysis of offset marker surfaces across the three major active fault strands beneath Lake Tahoe. Seismic CHIRP imaging with sub-meter accuracy, together with detailed multi-beam and LIDAR derived bathymetry were used to measure fault offset, earthquake derived colluvial wedges, wave-cut paleo-terraces, and other geomorphic features. Analysis of these features provides updated extension rates, as well as new information on Holocene faulting and places the Tahoe deformation into the larger context of Walker Lane tectonics. Measured offset marker surfaces include the submerged wave-cut paleo-terraces of Tioga age (19.2 ± 1.8 ka), McKinney Bay debris slide (? ~60 ka), and a winnowed boulder transgressive surface of Tahoe age (~62 ka). Vertical offsets across submerged geomorphic surfaces are 0.35 – 0.60 mm/yr for the Stateline – North Tahoe Fault, 0.12 – 0.30 mm/yr for the Incline Village Fault, and 0.44 – 1.09 mm/yr for the West Tahoe Fault. The combined east-west extension rate across Lake Tahoe Basin, assuming 60° fault geometry, translates to 0.53 – 1.15 mm/yr. This updated result, when combined with the Genoa fault slip rate, yields an extension rate consistent with the magnitude of the extension deficit across the Carson Valley and Lake Tahoe basin derived from GPS velocities. The Stateline – North Tahoe Fault, Incline Village Fault, and West Tahoe fault all show evidence for large 2+ m Holocene rupture events. Faulting in Lake Tahoe is on the scale of Basin and Range style faulting observed to the west in the Walker Lane, and suggests that the Lake Tahoe Basin should be considered the western edge of the actively deforming Walker Lane.

CHANGES IN TIDAL RESPONSE OF PORE PRESSURE DATA OF PBO BOREHOLES

Mai Linh Doan, Emily Brodsky · University of California, Santa Cruz

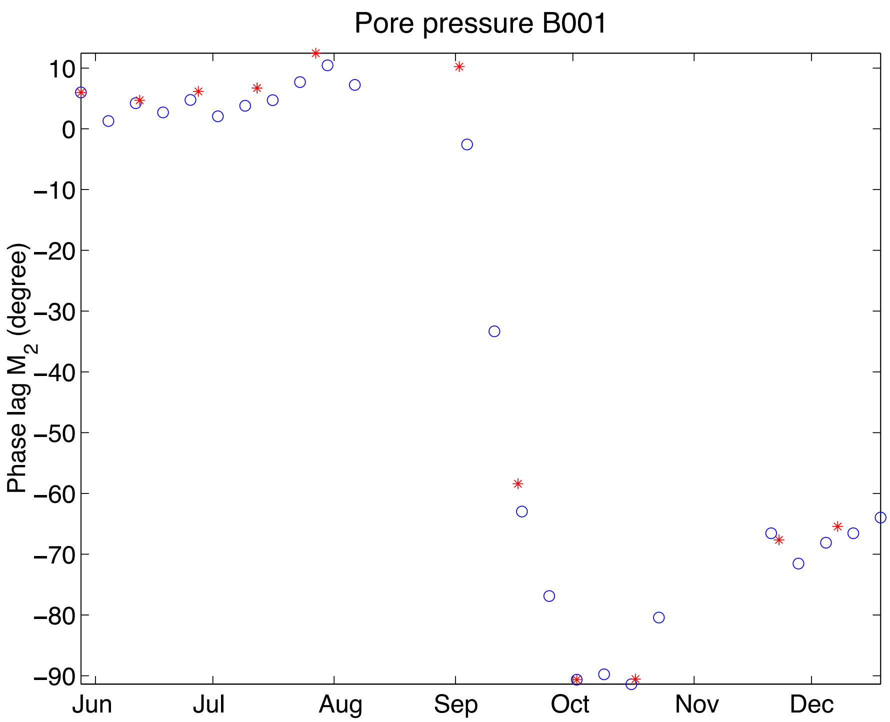

Change in phase lag of tidal response of the pore pressure of well B001 relative to the theoretical compressive strain, computed over time spans of 7 and 15 days during year 2006.

Seismic waves increased permeability in the Pinyon Flat Observatory (Elkhoury,2006). This was observed thanks to the large changes in tidal response. In the case of the open wells of Pinyon Flat, the low permeability limited the amplitude of the tidal oscillation and induced a large phase lag.

The pore pressure of the Plate Boundary Observatory are acquired in small sand packed section of the observation borehole. The pore pressure data should then reflect directly the poroelastic properties of the formation around. Yet, preliminary studies on pore pressure data of the Plate Boundary Observatory show tidal changes with time.

SITE RECONNAISSANCE AND OUTREACH ACTIVITIES FOR THE TRANSPORTABLE ARRAY

Perle Dorr, Robert Busby, John Taber · IRIS
Matt Mercurio · IAGT

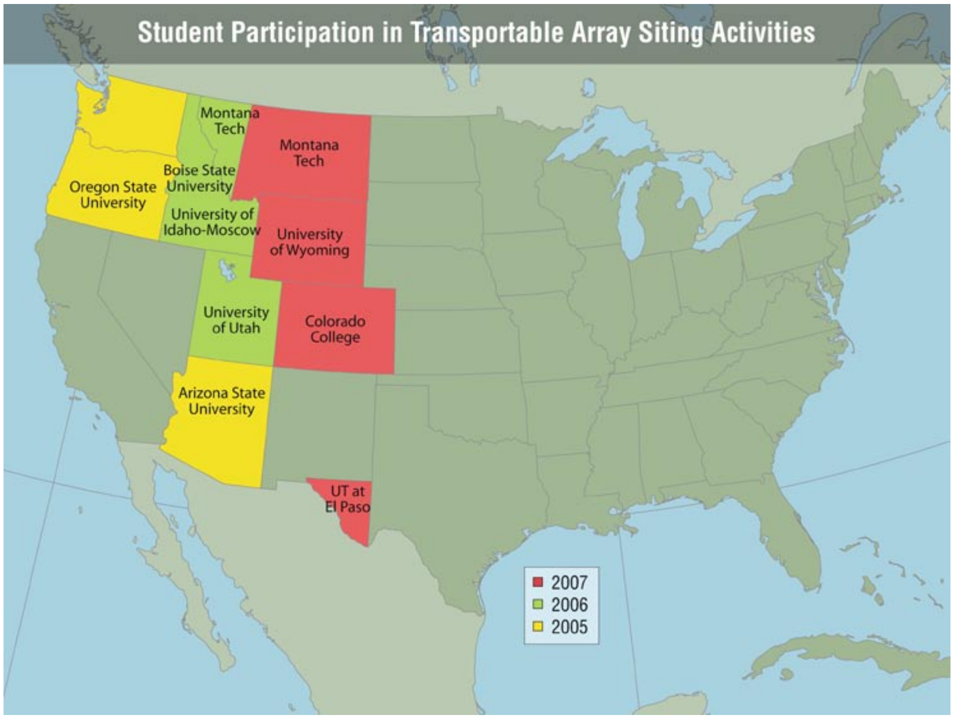

One of the goals of EarthScope is to actively engage students who will become the next generation of Earth scientists. Over the last two years, the Transportable Array has supported this goal by employing university students to conduct site reconnaissance for future seismic stations in six western states.

Multi-day workshops were held at Oregon State University in 2005 and at the University of Utah in 2006 to introduce selected students and their faculty sponsors to EarthScope and USArray and to review seismic station requirements and a variety of mapping tools. The workshops also included a day in the field to provide students an opportunity to evaluate actual sites and to gain experience using GPS units, cameras, cell phones, etc.

Once assigned a geographic working area, the students applied GIS-based suitability analysis techniques to identify locations for further investigation and then traveled to these sites to determine the best location for the seismic station. An important aspect of the students' task involved interacting with landowners. The students prepared detailed reconnaissance reports to document their findings which were later verified onsite by USArray recon staff.

This program has proven to be an efficient and cost-effective way to locate a large number of sites for Transportable Array stations. It also provides an exciting learning opportunity for students and involves participation of universities within the region. In 2005, more than 50 sites in Oregon as well as about 25 sites in Washington and Arizona were identified by 10 students. Last summer, 12 students and their sponsors conducted site reconnaissance for more than 100 sites in Utah, Idaho, and western Montana. Plans are well underway for this summer's siting effort in central and eastern Montana, Wyoming, Colorado, and in the Big Bend area of Texas where more than 200 sites will be located by university students and secondary school Earth science teachers.

USArray and PBO are also collaborating on the production of a newsletter, EarthScope onSite. Initiated in early 2006 and published quarterly, the newsletter informs station hosts and the general public about the status of EarthScope. The first issue was a general introduction to EarthScope, with subsequent issues alternating in focus between the Transportable Array and the Plate Boundary Observatory. The newsletter provides a brief update on the EarthScope facilities and features articles on how the station the landowners are hosting contributes to expanding our knowledge of the North American continent. More than 400 copies of each issue are mailed to current and potential hosts of Transportable Array stations.

PETROLOGIC AND TECTONIC ANALYSES OF EOCENE [?] ROCKS WEST OF THE SAN ANDREAS FAULT, SAFOD

Sarah Draper · Utah State University
David Kirschner · Saint Louis University
Jon Garver · Union College
James Evans, Kelly Bradbury, Laird Thompson · Utah State University

A sequence of well-indurated, high Vp arkosic sedimentary rocks lies southwest of the San Andreas fault [SAF], as determined from analyses of cuttings and wireline log data from the San Andreas Fault Observatory at Depth (SAFOD) main borehole. These rocks apparently underly the Miocene and younger sedimentary rocks of the Salinian block. The presence of these rocks poses intriguing tectonic questions regarding the SAF system and tectonic history in this area. We characterize this sequence of rocks with microscopy of cuttings and core, image log analysis, and integration of borehole-based geophysical data in order to determine their depositional, diagenetic and deformational history. We also used zircon fission-track analyses of grains from the sequence to constrain their history. Our analysis shows that the arkosic section is a deformed fault-bound block between the modern strand of the San Andreas fault to the northeast and the Buzzard Canyon fault to the southwest with at least 10 intraformational faults and 2 major block-bounding faults identified over a horizontal distance of ~ 500 m. The arkosic section is composed of three lithologic units: an upper arkose at1920-2530 meters measured depth (mmd), a clay-rich zone, 2530-2680 mmd, and a lower arkose, 2680-3150 mmd. The upper arkose is a 156 – 381 m thick feldspathic unit rich in iron-oxides composed of five distinct structural blocks with different bedding orientations. We infer intraformational faults separating different dip domains within the upper arkose. The clay-rich zone is 28.7 m -121.3 m thick, composed of three structural blocks, has a high abundance of clay-sized particles and clay minerals, and is characterized by low Vp and poor borehole stability. The lower arkose is 224 m -331 m thick, composed of three structural blocks with different bedding orientations, and is finer grained than the upper arkose with more clay minerals and less feldspar. Feldspars are altered with near complete replacement by muscovite in the lower arkose than the upper arkose, indicating that diagenesis in the lower arkose has taken place under higher temperatures with different fluid compositions, perhaps as a result of fluid compartmentalization. Zircon fission-track [ZFT] cooling age analysis are tightly bracketed at 70-64 Mya and show a unimodal cooling history for the grains. This indicates either a] the source terrain was exhumed through the ZFT cooling temperature at that time, or b] the entire rock package was exhumed then. In either case, we have a maximum age of earliest Paleocene for the arkoses, and other work on the cooling history of the region [Barbeau et al., 2005] are consistent with the source terrain being exhumed at ~70 Ma. We suggest, based on the cooling history, petrography, and geophysical properties that these rocks are equivlent to a sequence of Eocene rocks derived from a fan complex shed off the Salinian block in the Paleocene-Eocene [Nilsen and Clarke, 1975; Nilsen, 1984, 1987] and that the SAF has most of the slip in the area. Possibly equivalent rocks encountered in exploration wells 30 km to the northwest that lie on the Salinian block may suggest a small fraction of strike slip motion on the Buzzard canyon and related western strands of the SAF system.

STRUCTURAL ANALYSIS OF THE SAN ANDREAS FAULT ZONE IN THE SAFOD BOREHOLE

Sarah Draper, Kelly Bradbury, James Evans · Utah State University

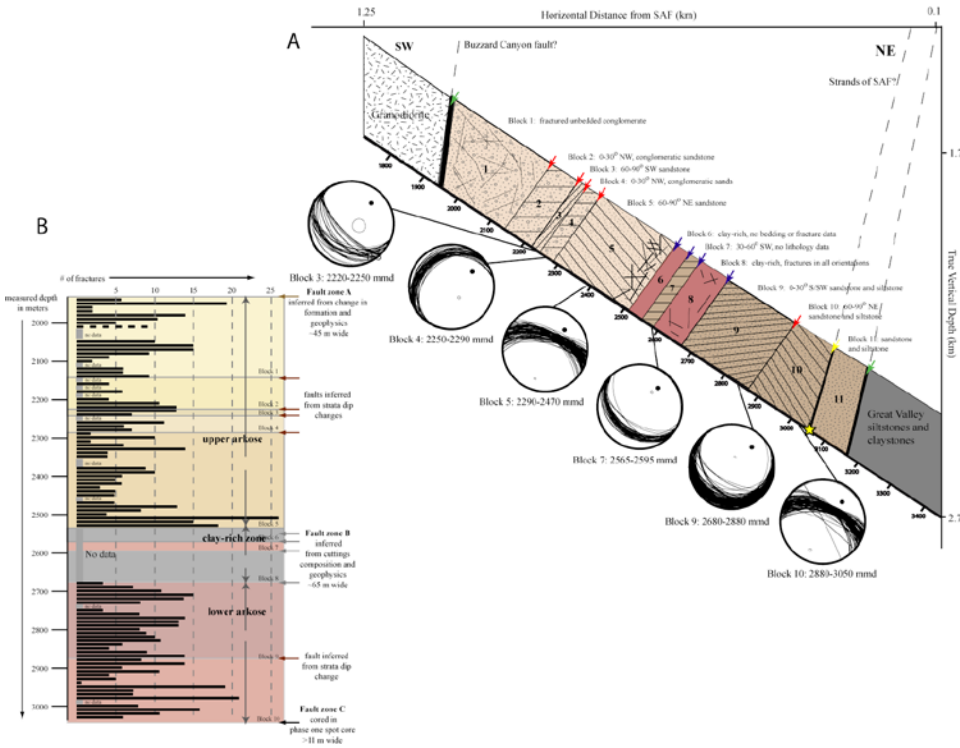

A. Southwest to northeast cross section of the arkosic section in the SAFOD borehole, with individual structural blocks labeled.
B. Fracture densities for entire arkosic section beginning at 1920 mmd.

We characterize the physical properties, microstructures, and composition of the faulted rocks and three of the major fault zones out of 12 total identified in an arkosic section of rocks 500-100 meters west of the San Andreas fault encountered in the SAFOD borehole. We use a combination of petrography of cuttings, detailed analysis of electic image log data, borehole geophysical data, and previos XRD work [Solum et al., 2006] to constrain the structure of the faulted rocks at depth. The westernmost fault is the largest fault encountered and correlates to the Buzzard Canyon fault [Rymer et al], and was drilled at 1920 meters measured depth (mmd). It is approximately 45 m wide, separates Salinian granodiorite on the southwest from the arkosic section on the northeast and contains fine-grained quartzofeldspathic cataclasites and abundant calcite. The middle fault zone lies at 2530 mmd, is localized in a clay-rich sedimentary unit between the upper and lower arkoses and is a diffuse >65 mmd wide low-velocity, high gamma, clay-rich fault zone with numerous sheared clay-filled veinlets. Fault zone B may correlate to a fault mapped at the surface by Thayer and Arrowsmith (2005) on the west flank of Middle Mountain with a dip of 70°SW, parallel to the Buzzard Canyon and San Andreas faults. The deepest fault juxtaposes arkosic rocks and fine-grained sedimentary rocks, and was cored during phase one drilling at 3067 mmd. It is brittly damaged with little textural or mineralogic evidence of fluid driven alteration and is an intraformational fault, and may be a small fault within the active San Andreas fault zone. Each fault zone is marked by an increased abundance of altered and cataclastically deformed grains as seen in cuttings. Analysis of image logs indicates the presence of 11 structural blocks that have distinctly different bedding orientations, and fracture distributions throughout the section roughly correlate with the presence of faults. In detail the seismic vevlocities, which appear to depend at least in part on the presence of fracture zones and faults, are highly variable. Each of the three larger faults zones have different characteristics. The Buzzard Canyon fault at depth contains abundant calcite and iron-oxide alteration; and fault zone B has numerous clay-filled veins, features consistent with extensive subsurface fluid flow. The deepest fault does not show evidence of alteration resulting from extensive fluid flow. The deepest fault is potentially updip from the hypocenters of the small earthquakes that appear to occur below the borehole. The entire zone between the Buzzard Canyon and San Andreas [senso stricto] faults at depth appear to contain a series of southwest-dipping faults and damage zones that bound blocks with a variety of bedding and fracture orientations.

KINEMATIC MODELING OF THE SAFOD TARGET EVENTS

Douglas Dreger, Robert Nadeau, Angela Morrish · University of California, Berkeley

We have investigated the rupture kinematics of the SAFOD target repeating events by inverting seismic moment rate functions obtained from empirical Green's function deconvolution. With this method it is assumed that if a suitable empirical Green's function (eGf) can be found, a collocated smaller event with the same radiation as the targeted larger event, the shared propagation, attenuation and site effects can be removed by deconvolution of the smaller signal from the larger one leaving the moment rate function of the target event. As shown by Mori and Hartzell (1990) and Dreger (1994) the obtained moment rate functions may then be inverted for the spatial distribution of moment release, the rupture speed and possibly the slip velocity. In this study we present inversions for the Mw2.1 repeating sequence using a M0.0 event located 10m from the larger event as the eGf. The deconvolution process recovers stable seismic moment rate functions with excellent signal to noise. The functions display azimuthal variability which may be due to directivity. Our results indicate that the repeating events have a rupture velocity consistent with what is typically reported for larger events (approximately 80% of the local shear-wave velocity). We find that rupture area is extremely compact (radius of 20m), with a peak slip of 6.3cm, corresponding to a static stress drop of approximately 1000 bars. Using the method of Ripperger and Mai (2004) for the estimation of non-uniform static stress change on the fault we find correspondingly high values of stress drop. These values are consistent with stress drop inferred for repeating earthquakes using the tectonic loading asperity model of Nadeau and Johnson (1998).

UPPER MANTLE VELOCITY DISCONTINUITY STRUCTURE BENEATH THE PACIFIC NORTHWEST, UNITED STATES FROM PS CONVERTED PHASES

Kevin Eagar, Matthew Fouch · Arizona State University

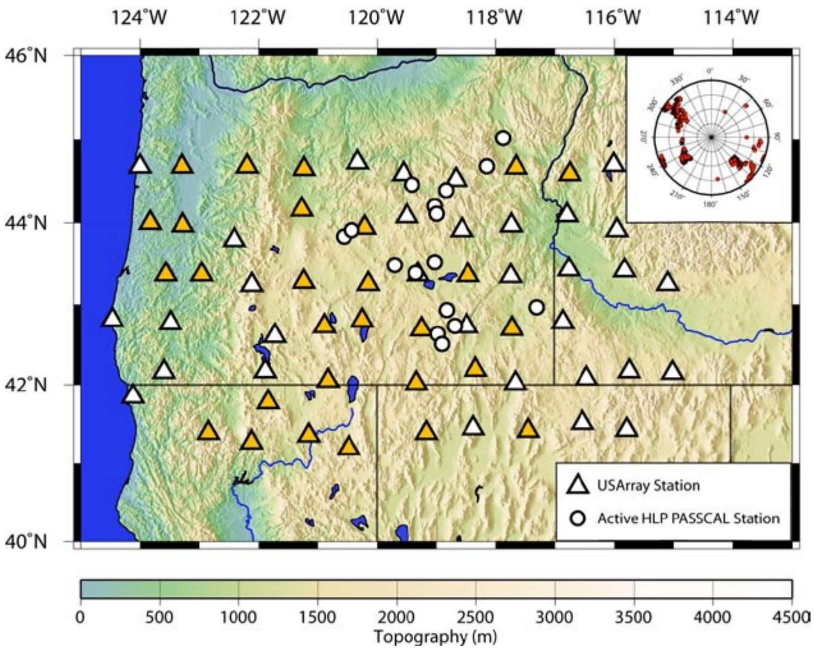

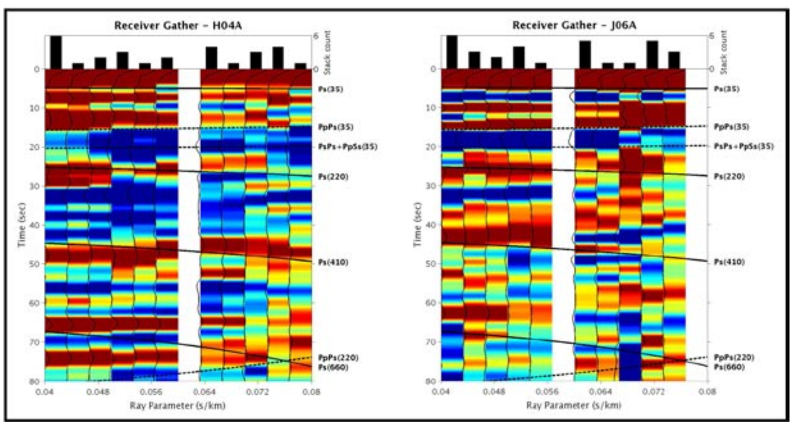

Figure 1. Receiver function stations in the Pacific Northwest used in this study. USArray sites (triangles) represent the majority of the data for this study. Stations with robust radial receiver function results are indicated in yellow. Currently installed stations from the High Lava Plains Broadband Seismic Experiment (circles) in eastern and central Oregon will be used to supplement preliminary results. An additional 80 stations will be installed in summer 2007 and will provide much more detail of regional structure. Upper right inset shows arrivals used for analysis in backazimuth - ray parameter space. Ray parameters are displayed as the radial circles with a range from 0.08 s/km at the edge to 0 s/km in the middle, and incremented by 0.02 s/km.

Figure 2. Two common receiver gathers (H04A and K06A) for radial receiver functions binned and stacked from all contributing sources using a bin width of ~0.0033 s/km.

Since the late Cenozoic, the Pacific Northwest has developed through a complex interaction of tectonic processes, including subduction of the Juan de Fuca plate under North America, extension in the Basin and Range province, and wide-spread magmatism in much of the back-arc region and Basin and Range. Variations in tectonic regime suggest a complex upper mantle thermal and compositional structure throughout the study area. The goal of this study is to examine mantle velocity discontinuities beneath the region to elucidate the role of the mantle in these processes.

We present results from analysis of P-to-S converted phases to investigate the upper mantle under Cascadia, the High Lava Plains, and the Basin and Range. Data for this study come from USArray Transportable Array stations, providing excellent coverage by which to image lateral variations in upper mantle discontinuity structure. Waveforms were high passed at 0.02 Hz before applying an iterative time-domain deconvolution procedure to calculate radial P receiver functions. We used a Gaussian width of 0.6 to lowpass the receiver functions at ~0.3 Hz. Primary features of our preliminary results include: (1) clear arrivals from crustal conversions and multiples; (2) coherent arrivals near predicted P220s at most stations; (3) a strong positive arrival followed by a negative arrival between 30-40 seconds at stations just east of the Cascade range; (4) very few stations that follow predicted P410s moveout; (5) negative arrivals between predicted P410s and P660s at several stations; and (6) negative arrivals prior to predicted P410s that show flipped polarity at varying ray parameter and/or backazimuth at some stations.

Our observations of weak arrivals at predicted P410s and P660s and deviations from normal moveout, indicate an influence of complex upper mantle structure and/or azimuthal dependence on conversion points. Discontinuous arrivals and polarity reversals observed at some stations suggest an azimuthal sampling bias for epicentral distances. Probable causes of these observations are the complex nature of the subducting slab in this region, strong lateral variations near the mantle wedge, and likely seismic anisotropy in the region. We are currently carrying out efforts to improve imaging using, among other things, common conversion point stacks to map depths of conversions from P to S waves and azimuthal binning to explore anisotropy in the upper mantle.

THE EARTHSCOPE USARRAY ARRAY NETWORK FACILITY (ANF): METADATA, NETWORK AND DATA MONITORING, AND QUALITY ASSURANCE

Jennifer Eakins, Frank Vernon, Vladik Martynov, Luciana Astiz, Robert Newman, Trilby Cox · University of California, San Diego

As we begin our fourth year of operations, the Array Network Facility (ANF) for the EarthScope USArray Transportable Array seismic network has continued the timely delivery of metadata and waveform data from the growing number of Transportable Array stations. The network has increased in size to 308 stations with 244 out of the 400 new TA sites installed (as of February 2007). Starting in Fall 2007, equipment will start to roll from current stations to new locations to the east of the current footprint.

Use of the Antelope software package has allowed us to maintain and operate such a dynamic network configuration, facilitating the collection and transfer of data, the generation and merging of the metadata as well as the real-time monitoring of state of health of TA station data-loggers and their command and control. Four regional networks (Anza, BDSN, SCSN, and UNR) as well as the USNSN contribute data to the Transportable Array in real-time. Although the real-time data flow to the IRIS DMC has been consistently above 90% in the last year, the ANF has strived to recover the remaining 10% of data to the DMC by connecting to a data storage device (Baler) at each station to generate day long seed files: automation of this process is ongoing.

Operation of the USArray at the ANF has benefited by the real-time interface with the ORB and the Datascope database using PHP for display on the ANF website (http://anf.ucsd.edu). A recent feature in the website is round-robin database (rrd) plotsallowing for scoping of individual and grouped state of health parameters. Information available for all stations includes: location, maps, photographs, equipment deployed, communications, distribution of events recorded by each station, and displays of daily, weekly, and monthly station noise spectra as generated by the DMC.

Analyst review of automatic locations for the USArray network is being done at the ANF to monitor data quality. All events are associated with the U.S. Geological Survey and regional network bulletins. As of February 2007, around 13,000 weekly picks are being fully reviewed by analysts at the ANF and over 19,000 events have been recorded. We find a small percentage (<10%) Vlaof events that cannot be associated with existing bulletins. This information is used by the regional network operators to help them determine which stations may be beneficial to permanently add to their seismic networks.

BROADBAND SEISMOLOGY AT THE BLUE END OF THE SPECTRUM: OPPORTUNITIES AND CHALLENGES FOR EARTHSCOPE SCIENCE *(Speaker)*

William Ellsworth · U. S. Geological Survey

The term “broadband” in seismology commonly refers to that part of the seismic spectrum lying between the lowest eigenfrequencies of the Earth (~0.3 mHz) and the highest frequencies normally observed at local and regional distances (~30 Hz). The upper frequency is not a physical limit, but rather a practical one created by the attenuation of seismic waves when we observe them at the Earth’s surface. As a central goal of seismology is to understand the physics of the earthquake source, we need observations that are truly broadband with respect to source process time scales. For example, the high frequency limit in the seismogram directly controls the spatial scale at which we can resolve the breakdown zone at the crack tip in a dynamically propagating rupture. With 30 Hz data we can resolve scales no smaller than about 100 m, which is far below even the corner frequency of the smallest earthquakes. From this perspective, the requirement for “broadband” data means bandwidth sufficient to record the shortest pulse produced by the physical system (a delta function being the ultimate broadband signal). The deployment of seismic sensors in the PBO and SAFOD boreholes of the EarthScope, as well as in other boreholes and in deep mines around the world, have extended the observed frequency range to 1 KHz or higher, allowing us to probe deeper into the nature of the seismic source process. In this talk, I will review some of the recent developments and explore some of the challenges that lie ahead.

AN ONGOING PROJECT TO TRANSLATE EARTHSCOPE EDUCATION AND OUTREACH MATERIALS TO SPANISH

Charley Faria · University of New Hampshire
John DeLaughter · EarthScope Education & Outreach Program
Carlos Rios · Oregon State University - Universidad de Antioquia

The U.S. Latino/Hispanic minority has increased 58% between 1990 and 2000 (Natalicio, 2003) and now represents 14.4% of the total population (U.S. Census Bureau, 2006). This growth in the Latino/Hispanic community, however, is not mirrored in it's representation in academics. According to the Los Angeles Unified School District, 71.9% of its students are Latino/Hispanic (LAUSD, 2005), however, Latino/Hispanic students are just as likely to drop out of high school as they are to complete it (Lopez et. al., 2005).This under representation continues as Latino/Hispanics enter institutions of higher education. In 2004, the University of Texas at El Paso ranked first nationwide for the highest number of PhD degrees awarded to Latino/Hispanics in the field of computer engineering, with one such degree (Natalicio, 2003). In recent years many research programs have started to breach the bilingual barrier by making their websites easily accessible to the Latino/Hispanic community. Organizations such as NOAA, NASA, ODP, and the NSF's EarthScope project, have portions of their web materials available in Spanish (Lopez et. al, 2005). Currently, the EarthScope Education and Outreach Program has 100% of its website and many teaching resources translated to Spanish (http://www.earthscope.org/education/espanol/). The success of these efforts can be seen when "Ferias Científicas" (Science Fairs) is entered into Google, where EarthScope is ranked second (Lopez, et al, 2005). These efforts are surely, but slowly, chipping away at the barriers that impede members of the Latino/Hispanic community from furthering themselves in the sciences.

TEMPORAL STRESS VARIATIONS OF THE YELLOWSTONE VOLCANIC SYSTEM: SEISMIC AND MAGMATIC CONTRIBUTIONS

Jamie Farrell, Robert Smith · University of Utah
Greg Waite · U.S. Geological Survey

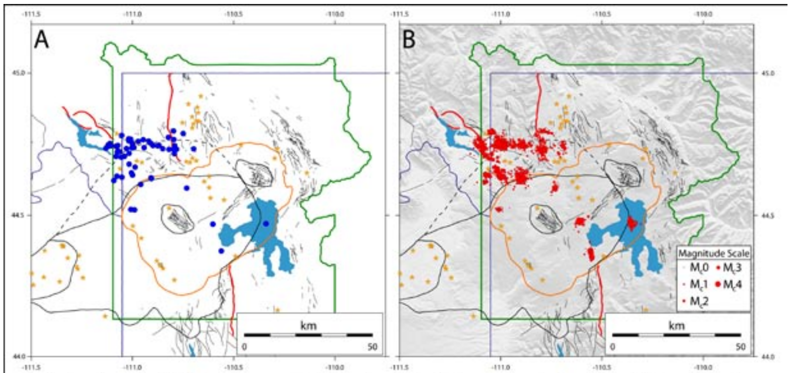

Earthquake epicenters for all 57 Yellowstone swarms. (a) shows mean locations for the 57 swarms shown by blue circles and (b) shows all events from the 57 swarms shown in red circles. Post-caldera volcanic vents are shown as orange stars. The 0.64 Ma caldera is outlined in orange and the 1.2 Ma as well as the 2.0 Ma caldera boundaries are outlined in black with the possible northern extent of the 2.0 Ma caldera shown with a dashed black line. Quaternary faults mapped by Christiansen [2001] are shown as thin black lines. Major Quaternary faults are shown as thick red lines.

Temporal Stress Variations of the Yellowstone Volcanic System: Seismic and Magmatic Contributions

Yellowstone seismicity is characterized by small generally shallow earthquakes that occur in swarms associated both with tectonic and magmatic features. Fifty-seven independent swarms have been identified in Yellowstone for the period 1984-2003. The swarms reflect 40% of the total number of earthquakes and account for 38% of the total seismic moment during this period. Focal mechanisms of the larger swarms including those of June of 1995 (439 earthquakes), June, 1997 (363 earthquakes), June, 1999 (722 earthquakes), July, 1999 (586 earthquakes), November, 2001 (480 earthquakes), and December, 2002 (331 earthquakes) were determined and were analyzed for stress field directions. Composite stress fields will be determined and compared to the regional stress field determined by GPS and InSAR measurements. Stress field directions will also be compared between individual swarms within the dominantly magmatic environment of the Yellowstone caldera and swarms occurring on normal-fault zones outside the caldera. Temporal variations in swarm characteristics are also examined and compared with the decadal changes in the vertical and horizontal motions of the caldera of up to 6 cm/yr.

VARIABLE FAULT STRENGTH AND CRUSTAL BLOCK INTERACTIONS IN THE WESTERN UNITED STATES: INSIGHTS FROM DYNAMIC MODELING OF THE SIERRA NEVADA BLOCK

Noah Fay · University of Arizona
Gene Humphreys · University of Oregon

Deformation of the western United States lithosphere is generally attributed to a number of superimposed processes, most notably shear owing to relative motion of the Pacific plate and gravitational collapse of the high-standing continental interior (e.g., Flesch et al., 2000). We attempt to quantify the importance of these deformation "drivers" at the Pacific-North American plate boundary by numerically modeling the state of lithospheric stress in and around the Sierra Nevada block (SNB) in California. Our dynamic (finite element method) models compare the predicted stress field from a given set of loads acting on the block to the available stress observations (Reinecker et al., 2005; Provost and Houston, 2003). The three most relevant results of this research are as follows. 1. Vertically integrated shear stress changes by as much as an order of magnitude along the length of the San Andreas fault system, from ~2.6 TN/m (Mendocino Triple Junction to San Francisco Bay), to ~0.3 TN/m (~San Juan Bautista to the San Emigdio bend). This indicates that plate interaction stress can by quite variable in space, and therefore also in time as the plate boundary evolves. Because much of this along-strike change in shear stress is related to frictional evolution and organization of the San Andreas fault system, fault strength is variable in time and space. 2. We resolve a relatively large (≤ ~3 TN/m) ~N-S oriented compressional load on the northern end of the SNB. This is a result of ~N-S compression of the rigid SNB and Oregon Coast Block (e.g., Wells et al., 1998), suggesting the dominantly N-S orientation of compressional stress in the Pacific Northwest can be explained by impingement of the SNB from the south. 3. Shear stress owing to relative motion of the Pacific plate is largely responsible for transport of the SNB and this stress penetrates into the Basin and Range (BR) province slightly beyond the actively shearing Walker Lane Belt. In a more regional sense, we conclude that Pacific-related shear stress penetrates a limited distance into the continent and this load is supported in part by compression of the Pacific Northwest and Canadian lithosphere.

PBO FACILITY CONSTRUCTION: GPS NETWORK STATUS

Karl Feaux, Mike Jackson, Dave Mencin, Ben Pauk, Katrin Hafner, Brian Coyle, Chris Walls, Barrett Friesen · UNAVCO

The Plate Boundary Observatory (PBO), part of the larger NSF-funded EarthScope project, will study the three-dimensional strain field resulting from active plate boundary deformation across the Western United States. PBO is a large construction project involving the reconnaissance, permitting, installation, documentation, and maintenance of 875 permanent GPS stations in five years. PBO has a demanding 5-year project installation schedule, for both GPS and strainmeter installations.

Some of the GPS construction highlights from the project include the San Simeon earthquake response, Mount Saint Helens volcano emergency response, the Magnitude 6.0 Parkfield earthquake emergency response, the GPS installations on Augustine and Akutan volcanoes in Alaska, and the reconnaissance on Unimak Island. GPS operations also prioritized permitting activity and installations in response to the Magnitude 5.2 Southern California earthquake and the Magnitude 6.7 Northern California earthquake in June, 2005. To date, the GPS operations of PBO have installed 545+ GPS stations, and are ahead of schedule in the earned value method of project management. In addition to network construction, the GPS operations stepped up its maintenance, which will continue to accelerate over the course of the project.

SPACE GEODETIC IMAGING OF DEFORMATION DUE TO ACTIVE FAULTS THROUGHOUT THE EARTHQUAKE CYCLE *(Speaker)*

Yuri Fialko · University of California, San Diego

Precise measurements of surface strain due to co-, post-, and inter-seismic deformation allow robust inferences about the mechanical behavior of the seismogenic crust and the underlying ductile substrate. The observed coseismic deformation patterns due to large shallow earthquakes are well explained by a classic elastic-brittle model of the upper crust. Analysis of small-scale features of the coseismic displacement field from several major earthquakes, including the 1992 Landers, 1999 Hector Mine (California), and 1999 Izmit (Turkey) earthquakes reveals the presence of kilometer-wide low rigidity zones that presumably manifest highly fractured and damaged rocks around active crustal faults. The inferred reduction in the effective shear modulus within the damage zones varies between 40 and 60%. In the framework of the damage mechanics, such variations in the effective elastic modulus imply that the average crack density within the fault zone exceeds the crack density in the ambient crust by a factor of 5 to 7. Geodetic inferences about the presence of wide low rigidity zones were recently verified using seismic tomography. Preliminary results form the Calico fault zone experiment (collaboration among UCSD, UCLA, and USC) reveal a low velocity structure that coincides with a compliant fault zone inferred from earlier InSAR work. The presence of wide damage zones is also sugested by observations of near-field postseismic deformation. In particular, data from the Hector Mine (California) and Bam (Iran) earthquakes show centimeter-scale subsidence and contraction of kilometer-wide zones centered on the earthquake rupture trace. This deformation can be explained in terms of postseismic healing and microcrack closure, presumably reversing the effects of coseismic dilatancy. On a larger scale, measurements of deformation following large earthquakes are increasingly used to discriminate among several commonly assumed mechanisms of postseismic relaxation, such as visco-elastic flow, poro-elastic rebound, and localized afterslip. Ultimately these measurements may help resolve a long-standing debate about the effective thickness, strength, and rheology of the continental lithosphere.

HIGH RESOLUTION POTENTIAL OF THE EARTHSCOPE FLEXIBLE ARRAY: AN IMAGE OF CONTINENTAL DELAMINATION IN THE ROMANIAN EASTERN CARPATHIANS

Melvin Fillerup, James Knapp, Camelia Knapp · University of South Carolina

The 1200 single-component Texan seismometers of the EarthScope flexible array, when deployed in an active source experiment, represent the potential to image key lithospheric-scale targets with greater resolution than transportable and permanent arrays. Data collection of this type is economically feasible but requires careful planning of experimental design and field operations. Two lithosphere-scale, explosive-source seismic reflection profiles (DRACULA I and DACIA PLAN) from Romania, collected with Texan seismometers, image the Transylvanian hinterland and foreland (respectively) of the Eastern Carpathians, and illustrate the scientific potential of the EarthScope flexible array. These data provide new evidence for the geodynamic origin of the Vrancea Seismogenic Zone (VSZ), a concentrated 30x70x200-km volume of intermediate-depth seismicity originating under the Eastern Carpathian bend zone. Data collected to evaluate existing subduction-related and delamination geodynamic models proposed to explain the intermediate depth seismicity associated with the Vrancea zone, show evidence of continental crust extending continuously above the VSZ from the Carpathian foreland well into the Transylvanian hinterland. Crustal thicknesses inferred from these data based on reflectivity show a 38-45 km crust below the Transylvanian basin abruptly shallowing to ~32 km for ~120 km beneath the fold and thrust belt of the main Carpathian orogen and thickening again to 38-42 km crust in the foreland. This thinned crust, directly underlying the topographic edifice of the Eastern Carpathians, outlines an apparent lower-crustal sub-orogenic cavity that is overlain by a relatively subhorizontal reflective fabric absent of significant dipping reflectivity. The northwest dipping Vrancea seismogenic body is located on the southeastern flank of the apparently thinned crust beneath the Carpathian orogen. Rotation of the VSZ about a hinge beneath the foreland basin at a depth of ~50 km restores to fill the lower-crustal cavity under the orogen, suggesting the VSZ represents a portion of brittle lower crust removed during continental lithospheric delamination. The lack of through-going, dipping crustal-scale boundaries along this composite lithospheric transect would appear to preclude subduction as an explanation for seismicity in the VSZ, consistent with abundant surface geologic data. These seismic data advocate lower crustal continental lithospheric delamination as a mechanism for generating intermediate depth seismicity in the absence of a plate boundary. The image provided by the DRACULA I and DACIA PLAN reflection profiles in conjunction with published refraction, tomography, and seismic attenuation studies shows the potential to collect economical, high-resolution, lithosphere-scale CMP data over regions of interest previously identified by lower resolution geophysical studies. While experiment cost is a significant factor in funding active-source seismic reflection experiments under the current EarthScope budget the 1200 instrument flexible array will remain unused until a provision is made to capitalize on this highly effective imaging resource.

PROBABILISTIC MODELING OF EARTHQUAKE OCCURRENCE: FIRST EXAMPLES OF DATA INTEGRATION WITHIN A BAYESIAN FRAMEWORK.

Delphine Fitzenz · Institut de Physique du Globe, Strasbourg, France
Chris Spiers · HPT lab, Utrecht University, The Netherlands
Andre Jalobeanu · LSIIT, Strasbourg, France
Stephen Hickman · U.S. Geological Survey

Building upon our recent experience in the analysis and integration of isotropic creep experiments into numerical models of interseismic fault processes, we study creep under deviatoric stresses, and then perform time-forward simulations of interseismic fault behaviour. Given a shear loading rate and a rupture criterion, our model provides probability density functions for the time to failure and fault zone physical properties at the onset of failure. The first step in the forward modeling is the point-source model, in which we evaluate the robustness of the modeling results in response to uncertainties in the input parameters and alternative models for the creep law.

Our modeling framework addresses two big issues in seismic hazard assessment: the evaluation of the aleatory uncertainties and the reduction of the epistemic uncertainties (via model selection).

Current efforts also include extending the approach to study the relative influence of more complex simulations (with 2D to 3D faults), to provide a modular probabilistic “synthetic earthquake simulator”. This will allow us to test the impact of different sources of heterogeneity in fault zone physical properties and loading conditions on the statistics of time to failure.

DRIVING FORCES OF THE WESTERN NORTH AMERICAN PLATE BOUNDARY ZONE *(Speaker)*

Lucy Flesch · Purdue University
William Holt · Stony Brook University
John Haines · University of Cambridge

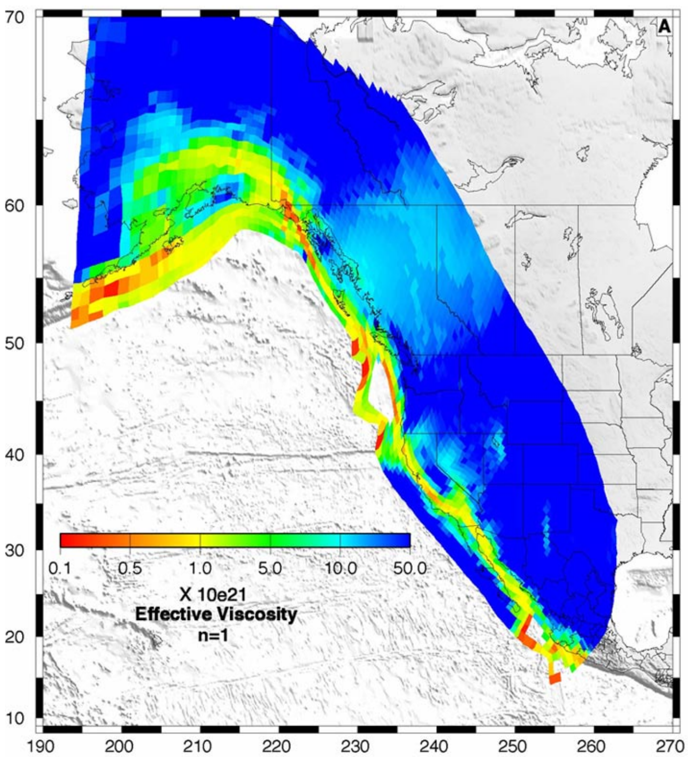

Figure 1. The vertically averaged effective viscosity field for the western North American plate boundary zone determined from estimates of deviatoric stress, and strain rates inferred from GPS and geologic data.

Understanding the forces and factors responsible for deforming and driving the continental lithosphere remains a fundamental question in geophysics. Over the past 15 year there has been an explosion of GPS measurements in the western United States, where the long-term surface motions and strain rates over the North American plate boundary zone have been quantified by several authors. Recently, two studies have used these deformation indicators to directly quantify the relative importance of lithospheric buoyancy forces, relative plate motions and basal tractions in driving deformation in western North America plate boundary zone. Both found that gravitational potential energy (GPE) variations and plate interactions were the main deformational components. Quantification of the deviatoric stress and strain rate fields allows for the investigation of the lateral variation in lithospheric strength, which can vary over two orders of magnitude (Figure 1).

The knowledge of a vertically averaged effective viscosity field (Figure 1) allows for the investigation of the role that lithospheric strength plays in driving deformation. We present a series of dynamic forward models determined from the lateral distribution of GPE and the effective viscosity with velocity boundary conditions (determined from the kinematic studies) for a given power-law rheology for western North America. The resulting stress, strain rate and velocity fields can then be directly compared with observations. Additionally, these models incorporate anisotropic (stress/strain rate) behavior along the San Andreas and Queen Charlotte fault zones and we investigate variations in fault strength along strike. These results will be compared with other recent models for the San Andreas fault to address questions relating to fault strength, fault slip rate, and how far east shear associated with the Pacific plate is transmitted. The dynamic model velocity field is able to match the recent PBO solution in the western United States. However, it does not reproduce the clockwise rotation of the GPS in the Pacific Northwest associated with the elastic locking of the Juan de Fuca plate. Instead we argue that the dynamic model velocities there represent long-term motion and are similar to long-term geologic estimates. An interesting feature of the dynamic velocity field is 1-2 mm/yr eastward motion around the Rio Grande rift, where small motions have been measured in the recent PBO data and also by other investigators. The dynamic model does not incorporate any GPS data in that region: the modeled velocities are a result of the GPE variations and plate interactions that produce this eastward motion.

ASTHENOSPHERIC DYNAMICS OF THE PACIFIC NORTHWESTERN UNITED STATES

Matthew Fouch · Arizona State University

The goal of this study is to provide a better understanding of subduction system processes in the mantle, with a focus on the dynamics of a slab system in the final stages of subduction. A particularly interesting example is the Pacific Northwest, which has experienced a rich recent history of flat slab subduction, slab breakup, and rapid trench retreat. Massive tectonomagatism over the past 50 My in this region is manifested by the Columbia River Basalt system, the High Lava Plains, and active arc volcanism in the Cascades. Extension in the northern Great Basin is relatively limited compared (on the order of 50%) relative to extension in the remainder of the Basin and Range.

In this study, I provide new constraints on the dynamics of the Pacific Northwest region of the United States using shear wave splitting measurements as a proxy for deformation. Data for this study come from broadband seismic stations of the USArray Transportable Array, regional arrays, and two temporary broadband arrays (CASC and High Lava Plains). I measured SKS phases from events between 85 and 130 epicentral degrees with body wave magnitudes of at least 5.8. The current dataset is comprised of over 450 new shear wave splitting measurements with well-constrained splitting parameters.

Regional similarities are evident across the entire study region (Figure 1). Fast polarization directions exhibit a limited range from E-W to NE-SW with few exceptions. Isolated regions of less consistent splitting measurements tend to be limited to regions of the accreted terranes and active of the Cascades. In the south, some stations also exhibit complexity and are likely the result of complex structure near the edge of the subducting Farallon slab as represented by the Mendocino Triple Junction in that region. Splitting times are variable across the region (Figure 2) and are largest near the southern Cascades and across the High Lava Plains.

Assuming that flow is parallel to the observed splitting parameters, regional correlations of fast directions and splitting times over hundreds of km strongly suggests that the asthenosphere beneath the region is the dominant source of the anisotropy. Flow in the asthenosphere along the fast directions could be generated by the subducting Juan de Fuca slab, mantle wedge flow due to rapid back-arc spreading to the west, or a combination of both. The thin (70 km or perhaps less) lithosphere of the overriding plate is likely not a primary influence on the splitting, though the E-W extension direction from very recent and rapid back-arc spreading would enhance the splitting signal generated by asthenospheric flow. Results from the CASC array (the linear array near 44.4 deg N in Figure 1) show well-resolved small-scale variations that are likely due to local differences in crust and/or uppermost mantle structure. These results are not consistent with the notion of plume-driven flow or other regional upwelling as the primary cause of anisotropy in the region.

EARTH SCIENCE COMMUNITY IT RESOURCES THROUGH A UNIFIED DATA AND ANALYSIS PORTAL *(Speaker)*

Kedar Sharon, Dong Danan, Newport Brian · JPL
Bock Yehuda, Jamason Paul, Chang Reuy-juin, Fang Peng · SIO

We are in the process of merging the capabilities of three NASA-funded projects under the umbrella of the NASA Access Project, ”Modeling and On-the-fly Solutions for Solid Earth Sciences (MOSES)” to facilitate data mining and modeling of rapidly expanding multi-disciplinary geoscience data sets. (1) The SCIGN- REASoN project is focused on the combination, validation, archive, and delivery of high-level data products and data mining capabilities from space geodetic measurements, in particular from over 600 CGPS stations in Western North America; (2) The QuakeSim project is developing linked Web service environments for supporting high performance models of crustal deformation from a variety of geophysical sensors, including GPS and seismic instruments; (3) The SENH-Applications GPS/Seismic integration project has developed a prototype real-time GPS/seismic displacement meter for seismic hazard mitigation and monitoring of critical infrastructure. The focus of the MOSES project is to enable direct interaction between modelers and data/data-product providers using Web services, within a unified portal architecture. Modeling applications include, for example, time series analysis of continuous and real-time data (e.g., RDAHMM and st_filter programs) and fault dislocation modeling (e.g., Simplex program). Community resources include access to extensive infrastructure and distributed data archive holdings, an on-line map server/client linked to a GIS database, a ”GPS Explorer” data portal that is extensible to heterogeneous data sets, and ”Geophysical Resource Web Services.” We present the current capabilities of the unified data and analysis portal, and provide a few examples of combinations of independent geophysical measurements.

SEISMIC ANISOTROPY OF THE LOWER CRUST IN THE CENTRAL SIERRA NEVADA

Andy Frassetto, George Zandt, Owen Hurd · University of Arizona
Hersh Gilbert · Purdue University
Craig Jones · University of Colorado
Ian Bastow, Tom Owens · University of South Carolina

The Sierra Nevada Earthscope Project (SNEP) is an Earthscope-funded broadband seismic deployment in the central and northern Sierra Nevada with the objective of investigating the processes of lithospheric foundering and corresponding uplift and deformation of the crust. We use teleseismic receiver functions to characterize crustal seismic anisotropy using a ray-theoretical forward modeling technique (Frederiksen and Bostock, 2000). Our preliminary models require a 5-km thick zone of 15% slow-axis anisotropy above the crust-mantle boundary [Fig. 1], which we interpret to result from a C-S fabric striking southwesterly, consistent with the inferred direction of removal of an eclogitic, negatively buoyant granitoid residue. Current efforts are focusing on refinement of the forward model and performing a neighborhood inversion of these receiver functions to constrain the trade-off between anisotropy parameters and thickness throughout the central Sierra Nevada.

These observations also correspond to a region beneath the western foothills of the Sierra which lacks a coherent P-S converted phase from the crust-mantle boundary and contains several clusters of anomalously deep seismicity [Fig. 2]. We believe that the absent Moho signature on receiver functions, combined with the presence of deep crustal seismicity, identifies a zone of actively foundering lithosphere. Our new observations of seismic anisotropy match well with modeled orientation of crustal shear induced by the delamination of a dense ultra-mafic root from beneath the eastern Sierra Nevada (Le Pourhiet et al., 2006)

PBO FACILITY CONSTRUCTION: BASIN AND RANGE AND ROCKY MOUNTAIN REGIONS STATUS

Barrett Friesen, Fred Jenkins, David Kasmer, Karl Feaux · UNAVCO

The Plate Boundary Observatory (PBO), part of the larger NSF-funded EarthScope project, will study the three-dimensional strain field resulting from active plate boundary deformation across the Western United States. PBO is a large construction project involving the reconnaissance, permitting, installation, documentation, and maintenance of 875 permanent GPS stations in five years. 163 of these stations lie within the Basin and Range and Rocky Mountain Regions consisting of the states of Montana, Idaho, Nevada, Utah, Wyoming, Colorado, New Mexico, and Arizona.

During the third year of the project, the Basin and Range and Rocky Mountain regions of PBO accelerated production goals in reconnaissance, permitting, and installation activities. The summer and fall of 2006 saw the completion of nearly all of the reconnaissance field work for the regions, with permits submitted to landholders for 92% of the total number of stations. A major milestone in the permitting phase of the construction project was the approval of 33 GPS stations located on Bureau of Land Management controlled public lands in Nevada. This transect is located along Highway 50 and will profile the extension of the Basin and Range province. Construction of these stations began during the fall of 2006, and will be completed in spring 2007. The focus for construction efforts in year 3 was in the state of Montana, where many of the backbone and Yellowstone cluster stations were completed. To date, construction is complete for 106 of 163 GPS stations.

THE SAN ANDREAS FAULT IN SOUTHERN CALIFORNIA IS ALMOST NOWHERE VERTICAL—IMPLICATIONS FOR TECTONICS, SHAKING HAZARDS, AND GEODETIC MODELING

Gary Fuis, Victoria Langenheim, Daniel Scheirer · U.S. Geological Survey
Monica Kohler · University of California, Los Angeles

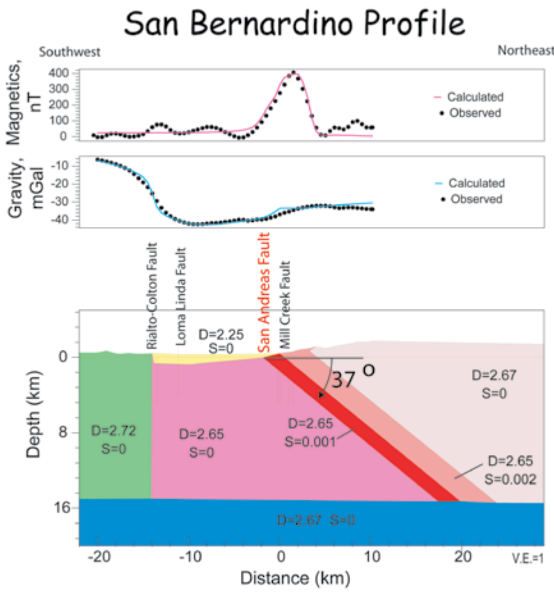

Figure 1

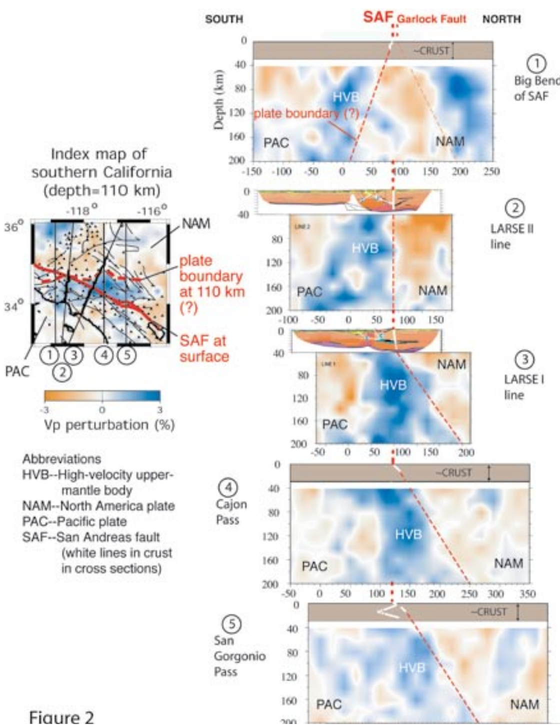

Figure 1. An example of new information on the dip of the San Andreas fault in southern California. This gravity and magnetic model is from San Bernardino.

Figure 2. Five cross sections across the San Andreas plate boundary in southern California. Tomographic images of mantle velocities along these sections suggest that the plate boundary extends into the mantle with a dip similar to that within the crust. Mantle velocities south of this interpreted plate boundary, on the Pacific plate, are relatively high and form the famous upper-mantle high-velocity body (HVB) of the Transverse Ranges.

The San Andreas Fault (SAF) in southern California is almost nowhere vertical, based on seismic-imaging, potential-field, and earthquake-aftershock studies of the upper crust. The southern SAF typically has dips of 55 deg-75 deg, although dips may be as shallow as 15 deg. From northwest to southeast, the estimated dips of the SAF, along with the data sources and depth ranges, are:

a) 55 deg. SW, Mt. Pinos (20 km northwest of junction of SAF and Garlock fault); gravity data; 0-5 km

b) 75 deg SW, Three Points (30 km southeast of junction of SAF and Garlock fault); magnetic data; 0-8 km

c) 90 deg., Lake Hughes (45 km southeast of junction of SAF and Garlock fault); seismic-imaging data (LARSE line 2); 0-35 km

d) 85 deg. NE, Jackson Lake (10 km northwest of Wrightwood); seismic-imaging data (LARSE line 1); 0-20 km. 90 deg., same location; gravity data; 0-15 km

e) 37 deg. NE, central San Bernardino; magnetic data; 0-15 km

f) 15 deg. N, San Gorgonio Pass (Banning branch); gravity data; 0-2 km

g) 45-50 deg. NE, North Palm Springs (Banning or Garnet Hill branch); main shock and aftershocks of MW 6.1 1986 North Palm Springs earthquake; 5-14 km

h) 60-70 deg. NE, Desert Hot Springs (Banning branch); relocated main shock and aftershocks of the ML 6.3 1948 Desert Hot Springs earthquake; 0(?)-12 km

i) 70 deg. NE, Indio; gravity and magnetic data; 0-6 km

The allowable variances in most of the dips above is of the order of 5-10 deg. In its switch from a southwesterly dip in the northwest to a northeasterly dip along the majority of its trace, the SAF has the crude geometry of a propeller.

Tomographic images of mantle velocities beneath the above-noted locations suggest that the plate boundary extends into the mantle with a dip similar to that within the crust. Mantle velocities south of this interpreted plate boundary, on the Pacific plate, are relatively high and form the famous upper-mantle high-velocity body of the Transverse Ranges. A somewhat similar relationship between the Alpine fault of New Zealand and underlying mantle is also seen. In one interpretation, Pacific-plate lithospheric mantle is downwelling along the plate boundary in both southern California and New Zealand. The mechanism by which lithospheric mass (crust and mantle) moves obliquely along this propeller-shaped plate boundary is the subject of continuing research. Calculation of shaking potential for scenario major earthquakes on the southern SAF and calculation of geodetic deformation from buried slip in the SAF may be inaccurate unless the non-vertical dip of the fault is taken into account.

BAYESIAN GEODETIC INVERSION FOR FAULT SLIP DISTRIBUTION

Junichi Fukuda, Kaj Johnson · Indiana University

As a first step towards understanding the dynamics of fault slip, it is important to estimate the location and magnitude of slip on faults using geodetic and seismic data. It is well known that inversions of geodetic and seismic data for fault slip are nonunique and unstable. A common approach for stabilizing the inversion is to introduce prior information on the slip distribution such as spatial smoothness. A weighting parameter specifies the relative weight placed on the prior information and the fit to the data. While objective criteria for selecting a weighting parameter exist (e.g., maximum likelihood, ABIC, and cross validation), subjective criteria such as trade-off curves are commonly employed. In each of these methods a single weighting parameter is selected and therefore uncertainty in the weighting parameter is not reflected in the uncertainty of the estimated slip distribution. We develop a new geodetic inversion method to simultaneously estimate fault slip distribution and weighting parameter. The method utilizes a Bayesian approach in which spatial smoothing regularization is incorporated as a prior Gaussian probability distribution. In the Bayesian formulation, the solution of the inverse problem is the joint posterior probability distribution of slip and the weighting parameter.

Using the definition of conditional probability, the joint posterior distribution can be expressed as the product of posterior distributions of the weighting parameter and slip given the weighting parameter.

The former distribution is non-Gaussian and cannot be estimated analytically, whereas the latter is Gaussian and can be estimated by least squares.

The inversion algorithm involves the following:

1) Generate samples of the posterior distribution of the weighting parameter by a Markov chain Monte Carlo method.

2) Estimate the posterior distribution of slip by least squares.

3) Marginalize the joint posterior probability distribution over the weighting parameter.

By marginalizing the weighting parameter, the slip distribution estimate is not dependent on a single choice of weighting parameter. That is, the uncertainty in slip estimate reflects the uncertainty in the weighting parameter.

Tests of this inversion method on synthetic data sets validate the method. We will present comparisons of results using this new method with results using conventional methods.

THE EFFECT OF THERMAL REFRACTION ON HEAT FLOW SCATTER NEAR THE SAN ANDREAS FAULT, PARKFIELD, CA

Patrick Fulton, Demian Saffer · Pennsylvania State University

Heat flow data from the California Coast Ranges are noteworthy in that they do not show evidence of a near-fault thermal anomaly as expected from frictional heating on the San Andreas Fault (SAF), and that they exhibit considerable spatial scatter – as a much as 15 mW/m2 variation over distances of 5-10 km. Previous work has shown that in the area around the SAFOD site near Parkfield, CA, some of the scatter can be explained by 3-D terrain effects but the remaining unexplained patterns are unlikely a result of frictional heating on the SAF and/or substantial redistribution of heat by topographically-driven groundwater flow.

Here, we evaluate the potential role of thermal refraction caused by differences in thermal conductivity of rock units in the subsurface. We use numerical simulations of heat transport along a transect perpendicular to the SAF near Parkfield to assess the heat flow patterns resulting from geologic structure and reasonable values of thermal conductivity. Thermal conductivity is partially constrained by measurements on core samples and chips, and is assigned for general geologic units: sediment cover, Salinian granite, Franciscan mélange, and serpentinite. Regional scale geologic structure is constrained by published geophysical interpretations of cross sections coincident with our model transect. Models are prescribed atmospheric conditions at the surface and a basal heat flux of 78 mW/m2 representing the regional average heat flow.

Results show that with only the gross-scale heterogeneity in our models, considerable spatial scatter in heat flow is generated at 100-200 m depth, with magnitudes and wavenumbers similar to observations. In addition, simulated heat flow along our transect exhibits long wavelength trends that are remarkably similar to the corresponding data. Sensitivity analysis reveals that resulting heat flow patterns are most sensitive to the ratio in thermal conductivity between sediments and underlying units, and to the geometry of the geologic contact. The observed heat flow patterns are consistent with a plausible thermal conductivity ratio of bedrock/sediments = ~1.5, and are robust even with fine-scale adjustments to the geologic model. Our results suggest that thermal refraction may be a significant source of heat flow scatter in this region. However, our results suggest that it is unlikely that subsurface refraction conceals a frictional heating anomaly from a strong fault.

INVESTIGATING FAULT CREEP PHENOMENA IN THE SAN FRANCISCO BAY AREA USING PS-INSAR AND GPS

Gareth Funning · University of California, Berkeley
Alessandro Ferretti, Fabrizio Novali · Tele-Rilevamento Europa
Roland Burgmann · University of California, Berkeley

Several of the major faults of the San Francisco Bay Area (e.g. the Hayward, Calaveras and Concord-Green Valley faults) are known to creep at the surface. Such interseismic creep may reduce the seismic potential of a fault, compared to the case when it is fully locked. An understanding of the distribution of creep with depth is therefore essential for the estimation of the hazard posed by a fault to nearby populations, and also poses interesting scientific questions about the stress state and frictional regime that it operates under. To image subsurface creep, surface velocity measurements at a range of distances from the fault are required, as motion on the deeper portions of a fault will create a deformation signal tens of kilometers across.

Space geodetic observations provide, therefore, an excellent body of data for our investigation of creep in the area. A dense spatial set of over 300,000 surface velocity measurements is obtained by processing PS-InSAR data from three satellite tracks covering the major creeping faults. Complementary viewing geometries for these data allow us to distinguish between horizontal and vertical motions in many cases. In addition, we use over 200 horizontal velocities from campaign and continuous GPS sites to provide a strong constraint on the regional pattern of strike-slip faulting.

We find that the Hayward fault is creeping at rates between 3 and 8 mm/yr, and is apparently locked in at least two regions at depths greater than 6 km. These may be considered as asperities for future earthquakes. We investigate further the mechanical behavior of the fault using boundary element stress models; preliminary indications show that the highest creep rates (located in the city of Fremont) are difficult to accommodate with instantaneous frictionless slip on a partially locked structure, suggesting either a structural linkage to another fault, or that the fault may demonstrate some episodic behavior. In addition, we are able to resolve a creep rate of 5.5 +/- 1.5 mm/yr for the Rodgers Creek fault north of Santa Rosa, a fault previously considered fully locked along its length. There is clear potential for extending this analysis further northward, particularly as several PBO continuous GPS stations are due to be installed in this region in the next few years.

MAPPING UPPER-MANTLE ANISOTROPY BENEATH THE WESTERN US: TOWARD A COUPLED SEISMIC AND GEODYNAMIC ANALYSIS OF CRUST-MANTLE COUPLING

James Gaherty · Lamont-Doherty Earth Observatory
Li Zhao · Academica Sinica, Taiwan
Po Chen, Arthur Lerner-Lam · Lamont-Doherty Earth Observatory
Joya Tétreault, Mousumi Roy · University of New Mexico

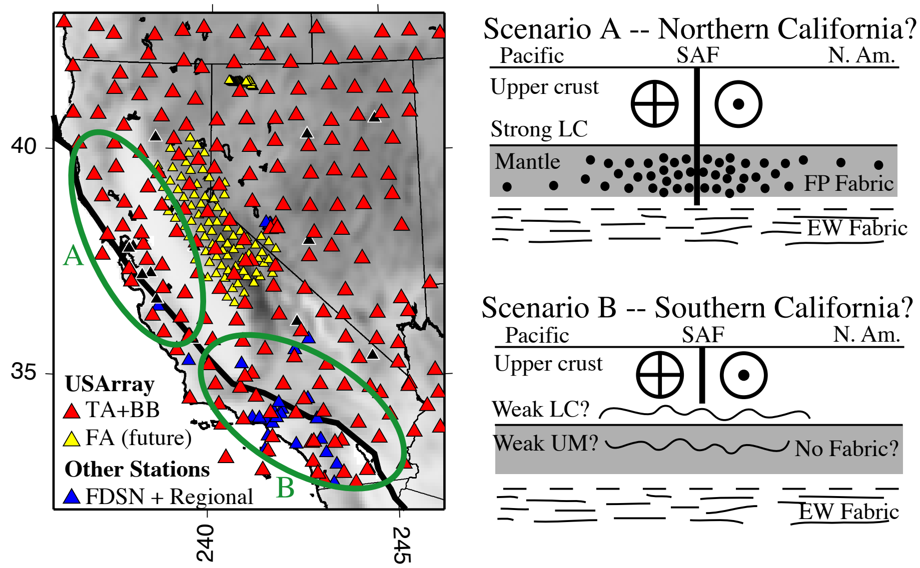

Figure 1. (left) Map of study region. We employ all available Transportable Array (TA) and Backbone (BB) stations, as well as other permanent stations. Future analysis will include broadband Flexible Array (FA) data as they become available. Circled regions indicate areas for joint seismic-geodynamic modeling of competing deformation scenarios suggested by shear-wave splitting observations, as depicted in cartoons on right. (right top) Scenario A contains localized plate-boundary-oriented shear extending into the upper mantle, and is suggested by data from northern California. (right bottom) Scenario B is based on observations from southern California that imply dominantly east-west flow unrelated to the San Andreas. This suggests a zone of decoupling beneath the plate boundary within the lower crust and/or upper mantle.

Surface deformation and plate-boundary evolution in the western US are likely driven by upper-mantle dynamics. The character of the tectonism is dependent not only on the forces driving the deformation, but also on the strength of the crust and mantle lithosphere that transmit those forces. Previous analyses of seismic anisotropy in the region imply that Pacific-North America plate boundary deformation penetrates into the mantle in northern California, while the crust and mantle are largely decoupled across the plate boundary in southern California (Figure 1). In this project, an integrated seismic-geodynamic analysis is being developed and applied to better quantify the coupling between crust and mantle across the plate boundary, and the implications for plate boundary evolution. Our seismic modeling is focused on building a regional scale 3D model of general upper-mantle anisotropy beneath the western US, including isotropic heterogeneity and radial and azimuthal anisotropic variations. The models are derived from frequency-dependent phase delays and amplitudes of long-period surface and body waves recorded at USArray stations. The 3D banana-doughnut Fréchet kernels of these measurements are computed by coupled normal-mode summations for isotropic and anisotropic velocity perturbations as well as the lateral variations on the Moho and transition-zone discontinuities. Work to date has focused on implementing the kernel algorithms, and collecting phase and amplitude measurements using large regional and near-teleseismic events. We will invert these data for upper-mantle models using constraints provided by numerical models of upper mantle flow and fabric development across the Pacific-NA plate boundary. Currently, we are constructing numerical models that simulate upper-mantle flow beneath the plate boundary using a viscous fluid subject to surface and basal kinematic boundary conditions, testing a variety of viscosity structures and rheologies (Newtonian vs. non-Newtonian). While the models are simple representations of the plate-boundary environment, the boundary conditions that drive them are derived from surface geologic and kinematic data, including surface deformation data from the Plate Boundary Observatory. Using the Kaminski and Ribe methodology, these kinematic flow models can be mapped into expected olivine LPO and hence anisotropy structure across the plate boundary. We will merge the expected flow-fabric-anisotropy from numerical models into the seismic inversions using a Gaussian-Bayesian formalism. This will allow us to explicitly assess the degree to which particular deformation scenarios are acceptable to the seismic data. This is a three-year project initiated in Spring 2006, and is supported by grants from the NSF EarthScope program to CU and UNM.

LOCAL STRESS CONCENTRATION DUE TO FAULT INTERSECTIONS: A POSSIBLE CAUSE OF INTRAPLATE SEISMICITY IN NEW MADRID AND MIDDLETON PLACE SUMMERVILLE SEISMIC ZONES

Abhijit Gangopadhyay · University of Texas at Austin
Pradeep Talwani · University of South Carolina

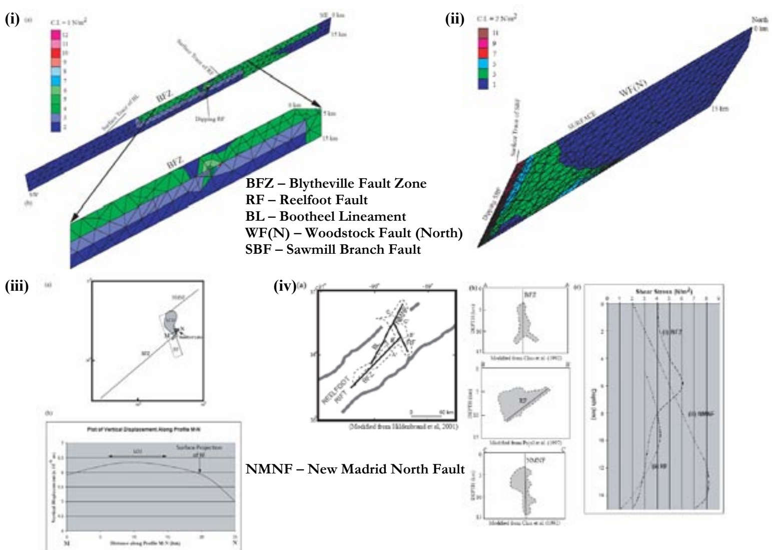

Figure 1: (i) (a) Cross-sectional view of variation of shear stresses along BFZ. NE-Northeast, SW-Southwest. The region around the intersection of BFZ and RF is enlarged in (b). (ii) Cross-sectional view of variation of shear stresses along WF(N). (iii) (a) Schematic representation of the three main faults in NMSZ and location of Lake County Uplift (LCU) and Reelfoot lake (Modified from Gomberg and Ellis (1994)). The boundaries of RF shown by dashed lines implies those in the subsurface. (b) Plot of vertical displacement from results of modeling along profile M-N ~perpendicular to the strike of RF. (iv) Schematic diagram of NMSZ showing the main faults and seismicity-depth cross-section profiles (dotted lines). The instrumental seismicity in the region is bounded by the dotted line and is adapted from the CERI catalog 1974-2005. (b) Seismicity-Depth cross-section profiles along AA', for BFZ, BB' for RF, and CC' for NMNF. The shaded area bounded by the dotted line on each profile represents the seismogenic depth. (c) Shear stress plots along dip for (i) BFZ, (ii) RF, and (iii) NMNF along the shown profiles in (a).

We investigate the causal association of stress concentration at fault intersections, with current intraplate seismicity in New Madrid and Middleton Place Summerville Seismic Zones (NMSZ and MPSSZ). We show that intersecting faults, optimally oriented with respect to the direction of SHmax in these two regions, are associated with anomalous stress concentrations and observed seismicity. We develop simple, three-dimensional mechanical models of these regions using a Distinct Element Method implemented by a commercially available code called "3DEC". Our models include the structural geometry and major seismogenic faults in each region. We assign realistic mechanical properties to these models based on known geology, and load them tectonically along the direction of SHmax. At the end of a specified loading period, we obtain the spatial distribution of shear stresses and sense of motion along the faults, and vertical displacements along specific profiles within the models. The modeled locations of anomalous relative values of shear stress and vertical displacement agree well with the observed locations of epicentral and hypocentral distributions, and uplift (Figure 1 (i)-(iv)). The obtained shear stresses that are relatively large, concentrate at and near the fault intersections. As examples, Figure 1 (i) and (ii) show the distributions of shear stresses obtained from the modeling results along Blytheville Fault Zone (BFZ) in NMSZ and Woodstock Fault (North) in MPSSZ respectively. Our modeling results also duplicate right-lateral strike-slip movement along the NNE-SSW trending faults in response to ENE loading direction, and successfully mimic uplift in the left-stepover regions, both in NMSZ (Figure 1 (iii)) and MPSSZ. We therefore demonstrate that fault intersections within a pre-existing weak crust can concentrate stresses when subjected to background plate tectonic forces, and then become local areas of ongoing seismic activity in otherwise stable regions.

RELATIONSHIPS BETWEEN VOLCANIC CINDER CONE ANGLE AND AGES: A POTENTIAL DIAGNOSTIC TOOL FOR ESTIMATING QUATERNARY ERUPTION AGES AND VOLCANIC HAZARDS

Miriam E. Garcia, Elizabeth Y. Anthony, Jose M. Jr. Hurtado, Joseph G. Miller · University of Texas at El Paso

The Potrillo Volcanic Field (PVF), located in southern Doña Ana County, New Mexico, consists of maars, fissure flows, shield volcanoes, and over 150 cinder cones (Figure 1). The volcanic activity ranges in age from 916 +/- 67 ka to 20 +/- 4 ka (Anthony and Poths, 1992; Williams, 1999). Our study focuses on the correlation between cinder cone slope angle and age. In this arid climate, cone degradation is a product of mechanical weathering, and may be quantitatively modeled by diffusion equations, similar to an approach suggested for fault scarp retreat (Nash, 2005).

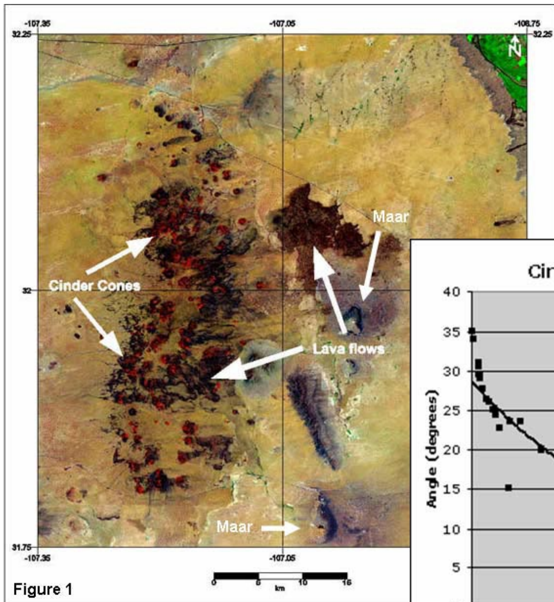

Figure 1

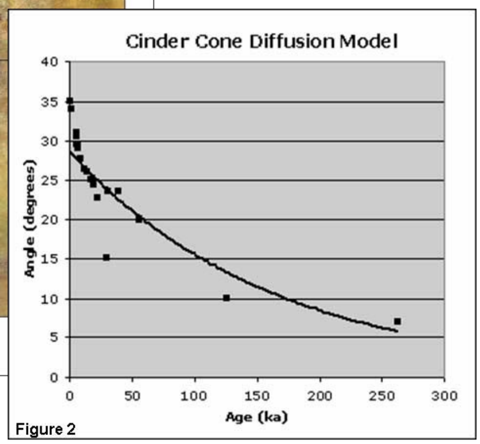

Figure 2

Data were obtained by overlaying U.S. Geological Survey digital topographic maps, U.S. Geological Survey digital elevation models (DEMs), and a Landsat image using Global Mapper software. The average radius and the height were determined for each cinder cone. The expression theta = tan-1(h/r) was used to obtain the angle, where r is the radius and h is the height. A total of 128 (76% of the cones in the field) cinder cone angles were calculated, 95% of which have slope angles between 4 and 15 degrees.

The range of angles (4-15 degrees) is limited, and none are as steep as the angle of repose (35 degrees) expected for very young cinder cones. An example of such a young cone morphology is that of the Paricutin cone that last erupted in 1952 (Luhr and Carmichael, 1981). The places in PVF where we correlate 3He surface exposure and 40Ar/39Ar dates with cone angles represent volcanic activity from 350 ka to 100 ka (Williams, 1999). Other slope angle-age studies in arid to semi-arid climates include work at Capulin, New Mexico (Stroud, 1997), the Chichináutzin Group, Mexico (Bloomfield, 1975), and the Colima Volcanic Complex, Mexico (Luhr and Carmichael, 1981). Each of these fields contributes to the analysis because their slope angle-age relationships reflect distinct time periods: Capulin has been dated with 40Ar/39Ar at 55 ka (Stroud, 1997), the Chichináutzin Group dated with 14C ranges from 38.59 +/- 3.21 to 8.44 +/- 0.07 ka (Bloomfield, 1975), and the Colima Complex dated with 14C from 16.5 to 1.5 ka (Luhr and Carmichael, 1981). Combining the data from these fields with ours results in angle vs. age plot (Figure 2).

Future work will focus on utilizing data from other cinder cone fields where slope angle-age data exist (including Cima volcanic field) to test the validity of our degradational model. Once well-calibrated, this can be used as a chronologic tool for cinder cone fields that lack age constraints. A space-time analysis will also be considered for the Potrillo Volcanic Field, using the cones with the smallest analytical uncertainties.

DECONVOLUTION EXPERIMENTS WITH USARRAY DATA BRING DEEP EARTH STRUCTURE INTO GREATER FOCUS

Ed Garnero, Wolfgang Stefan, Rosemary Renaut · Arizona State University
Thorne Lay · University of California, Santa Cruz

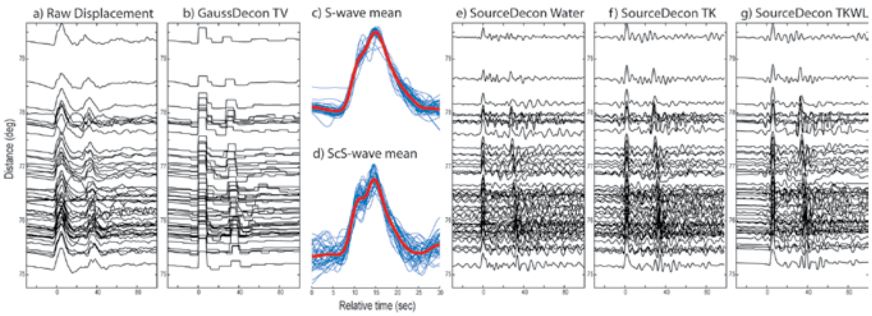

The density, uniform spacing, and spatial aperture of the current USArray station configuration makes possible stacking, source, and receiver structure deconvolution experiments that permit finer Earth structure determination than previously possible. Here we present results of algorithms containing various levels of automation in seismic wave picking, aligning, empirical source time function determination, and source deconvolution. The figure below shows transverse component data from a deep focus Fiji earthquake. Panel (a) displays the raw broadband instrument deconvolved SH displacement data of S (first pulse) and ScS (second pulse). The character of the earthquake source is clearly visible in these traces. These traces were automatically deconvolved by a Gaussian pulse to give the signals in panel (b), which were used in an edge detection algorithm to automatically align S and ScS waves, correcting any flipped polarities. This alignment was used for an initial stack of S and ScS, whereby S and ScS amplitude scaling, DC offset, and time shifting were iteratively inverted for to update the stack while minimizing the misfit of each record with the stack. The resulting average S and ScS waves are shown in panels (c) and (d), and while done automatically, this step allows for a variety of types of user input (e.g., individual record signal to noise ratio criteria). Below we show the example of using the ScS source as the empirical earthquake source, and deconvolved that with a standard water level deconvolution in panel (e), a Tihkonov regularization for the ScS source deconvolution in panel (f), and the same with a wavelet-based denoising algorithm that strips high frequency oscillatory noise from the signal, panel (g).

We will present stacking experiments based on the deconvolved data that highlight structure at the base of the mantle beneath the Pacific Ocean. This study region is significant as it has been proposed to contain a thermochemically distinct D” region, with possible structural elements including a post-perovskite lens, an ultra-low velocity layer right at the core-mantle boundary (CMB), seismic wave speed anisotropy, and possible connection to deep mantle plume genesis resulting in hot spot volcanism responsible for the Hawaiian volcanic chain. These data permit a variety of stacking and wavefield migration experiments aimed at utilization of the narrower S and ScS pulse widths after deconvolution. For example, reflections from a positive velocity jump 200-300 km above the CMB arise in a reflection (Scd) that closely follows the direct S wave in time, typically broadening the S wave relative to ScS. These types of deconvolution experiments, however, enable direct access to Scd arrivals.

BRINGING RESEARCH AND DISCOVERY INTO EARTH SCIENCE CLASSROOMS WITH 3D VISUALIZATION OF GEOPHYSICAL DATA

Ed Garnero, Marvin Simkin · Arizona State University

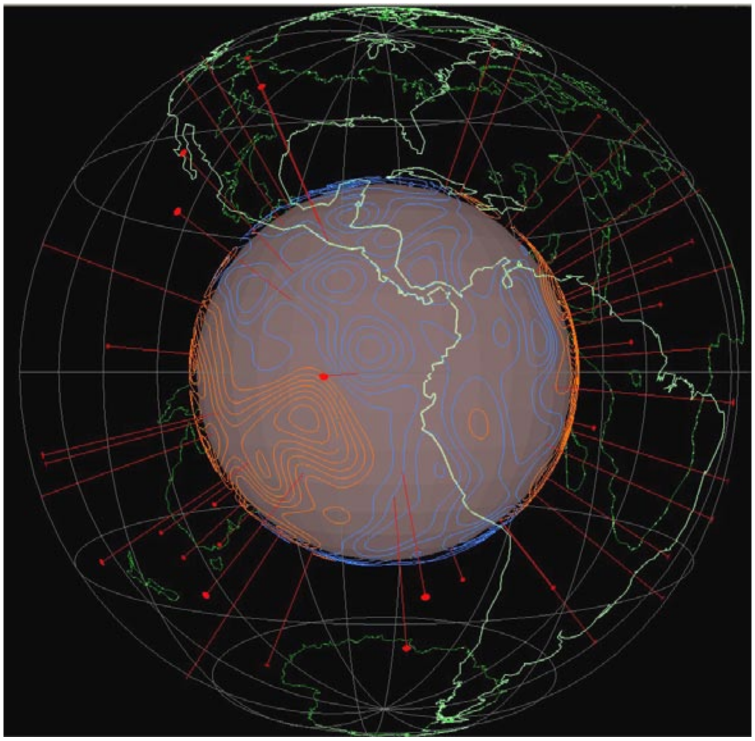

Figure Caption. This image was created using GMT commands for generating a coastline (green lines), contouring (orange contour lines are low seismic wave speeds in the D” layer, blue contour lines are high seismic wave speeds in the D” layer), and drawing lines (red lines connect hotspot locations to the core-mantle boundary). The output of the GMT commands was directed to HoloDraw programs which rendered the spherical geometry image, as well as gridlines and the core-mantle boundary surface. The resulting image can be interactively rotated or enlarged in a web browser or on the GeoWall.

Geophysical data are often spatially based and thus well suited for 3D visualization. Distributions of earthquakes and volcanoes, for example, can be plotted by latitude, longitude and depth together with surface topography. Estimates of regional and global variations in Earth’s gravity field, heat flow and seismic velocities are also candidates for 3D visualization, as well as, for example, numerically derived mantle convection velocities and temperatures.

3D visualization, in turn, is well suited for student and researcher exploration and discovery. Many researchers have pioneered a number of software and hardware applications for the purpose of visualizing such data in 3D; for example, the 3D projection system GeoWall[1] has become increasingly common in Earth science classrooms. The freeware application HoloDraw[2] permits straightforward porting of output from 2D graphics packages common in the geophysics community[3] into either the GeoWall, or into a computer web browser via a freeware VRML plugin[4]. Thus, simple script programming coupled with GMT and Holodraw result in striking 3D images of geophysical data.

These tools are powerful for conveying often complicated comparisons between volume data, e.g., seismic velocities derived from global tomography, and other phenomena, e.g., global hot spot distribution. The figure below shows a screen capture of hot spots compared to D” shear wave velocities. This approach is also well-suited for displaying seismic ray paths from earthquakes to USArray stations in 3D [figure?], along with other information of potential interest, e.g., seismic wave speeds, or other geologic phenomena. This presentation will show several examples using this method, and provide all scripts and data for reproducing images.

Students in a one-semester upper division undergraduate course entitled “Computers in Geology”, in the School of Earth and Space Exploration at ASU, following a simple template[5] after only one class session, were able to create GeoWall images of several types of data, including distributions of earthquakes and volcanoes, as well as 3D xyz plots of geochemical data. Some student examples will also be included.

[1] http://geowall.org

[2] http://holodraw.org

[3] e.g., Generic Mapping Tools, GMT, http://gmt.soest.hawaii.edu

[4] e.g. http://www.parallelgraphics.com/products/cortona

[5] http://simkin.asu.edu/2004_7_glg410/holomake.html

THE SIERRA NEVADA: EVIDENCE OF THE IMPORTANCE OF MANTLE LITHOSPHERE IN CONTINENTAL DEFORMATION

Hersh Gilbert · Purdue University
George Zandt · University of Arizona
Criag Jones · University of Colorado
Tom Owens · University of South Carolina

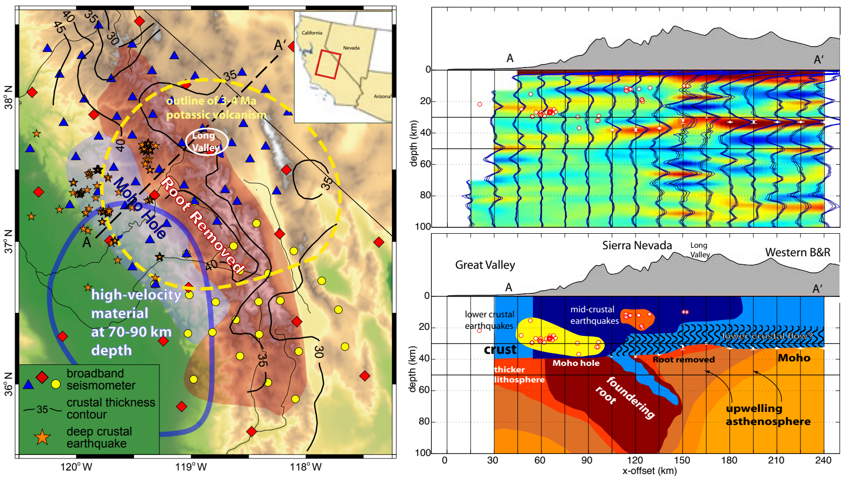

(left) The Sierra Nevada region showing locations of seismic stations, crustal thickness contours (labeled in km), regions where lithosphere has been removed. The outline of potassic volcanism and locations earthquakes, both possibly associated with removal, are also noted. Southwest-northeast oriented receiver function cross-section across the Sierra Nevada (top) with interpretations (bottom).

Evidence for the far-reaching influence of the mantle lithosphere in continental deformation can be found in the consequences of its removal. Modes of deformation that have been attributed to lithospheric removal include surface uplift, mountain building, volcanism, and magmatic intrusions. Features observed in disparate regions including the Mediterranean, the Central Andes, Tibet, the Southern Alps in New Zealand, and several locales across western North America have been suggested to result from the removal of the mantle lithosphere. Still, the mechanisms by which the dense mafic and ultramafic portions of the lithosphere are removed are not well constrained. In order to better understand this crucial facet of continental deformation the Sierra Nevada EarthScope Project (SNEP) has configured the FlexArray component of the USArray across the Sierra Navada batholith in eastern California. Evidence from xenoliths that erupted in the Sierra indicates that the eclogitic and peridotitic mantle lithosphere, which was present during the Mesozoic, had been removed from the southern Sierra by ~3.5 Ma. The recent occurrence of this event makes it an ideal region to investigate the development of lithospheric removal. Although the SNEP array is still deployed, the initial data already provide new insights into the structure of the Sierran lithosphere. The crustal thickness appears to be asymmetric with thin crust to the east and thicker crust to the west, where elevations decrease. Changes in the sharpness of the curst-mantle boundary accompany these crustal thickness variations. A diminished Moho signal characterizes the thicker crust and indicates a smaller, or more gradual, impedance contrast at the base of the crust. Results to date from the southern Sierra, which is the region of the batholith with highest elevations, appear consistent with models of east-to-west detachment of the lower crust. The central Sierra may represent a less evolved stage of lithospheric removal if the larger area characterized by no Moho in the central Sierra marks where the lithosphere there remains connected to the overlying batholith in the west. Additional analysis of SNEP data similarly indicates differences between the eastern and western Sierra Nevada. Combining these data with results from geologic studies to be conducted in the region will improve our understanding of the evolution of the Sierra Nevada and the process and effects of lithospheric removal.

FRICTIONAL PROPERTIES OF SERPENTINE AT HIGH SLIDING VELOCITY

David Goldsby · Brown University
Greg Hirth · Woods Hole Oceanographic Institute

We have conducted experiments to investigate the frictional properties of antigorite serpentine rocks at sliding velocities approaching seismic slip rates. Previous laboratory experiments on the frictional behavior of serpentine exhibit velocity strengthening behavior at low sliding velocities (<0.03 microns/s), providing a possible explanation for the modest seismicity rate in serpentinized regions (e.g., Reinen et al., 1994; Moore et al., 1997; Boettcher and Jordan, 2004). Experiments on serpentinite also show a transition from velocity strengthening to velocity weakening at higher sliding velocities in the range 0.03 to 10 micron/s (Reinen et al., 1994), suggesting that ruptures that propagate into serpentinized regions could trigger seismicity. However, these sliding velocities are orders of magnitude lower than experienced during earthquakes. Our experiments were conducted in a 1-atm rotary-shear apparatus at a fixed normal stress of 3 MPa. Two types of test - one in which samples were subjected to repeated reciprocating oscillations of the sliding direction over ~4 m of cumulative slip, and another in which samples were slid in only one direction over ~40 mm of slip - were conducted. Reciprocating slip tests were begun by sliding at 10 microns/s for several mm of slip, then at V up to 100 mm/s over the remaining 4.5 m of slip. Unidirectional slip tests were begun by sliding at 10 microns/s for several mm of slip, then at V up to 360 mm/s over the remaining 40 mm of slip. Reciprocating tests, over the V range 10 microns/s to 30 mm/s, yield a value of the friction coefficient of ~0.83, whereas at 100 mm/s a value of ~0.6 is observed. Unidirectional slip experiments reveal a 1/V decrease in friction coefficient with increasing V over the range 50 to 100 mm/s, to a value of 0.4 at 200 mm/s, and a 1/V increase in friction with velocity for V > 200 mm/s. In both types of test, friction is nearly independent of slip, i.e., is nearly a pure function of V, above V=50 mm/s. The results suggest that macroscopic friction of serpentine is controlled by flash heating of microscopic asperities on the fault surface at relatively high slip velocities. In the highest V regime, the 1/V increase in friction with V may reflect dehydration reactions which may occur at flash heated asperities. Our results suggest that ruptures which propagate into serpentinized regions - such as hypothesized for some regions of the San Andreas Fault, transform faults in the oceanic lithosphere, and altered lithosphere along the slab-wedge interface of subduction zones - may trigger seismicity, but only if sliding velocities are relatively low. Furthermore, propagation may be limited or terminated at velocities higher than the transition velocity to velocity strengthening behavior for serpentine.

INSAR AS A TOOL TO STUDY CONTINENTAL SCALE DEFORMATION *(Speaker)*

Noel Gourmelen, Falk Amelung · University of Miami
Mariarosaria Manzo, Francesco Casu, Riccardo Lanari · IREA-CNR

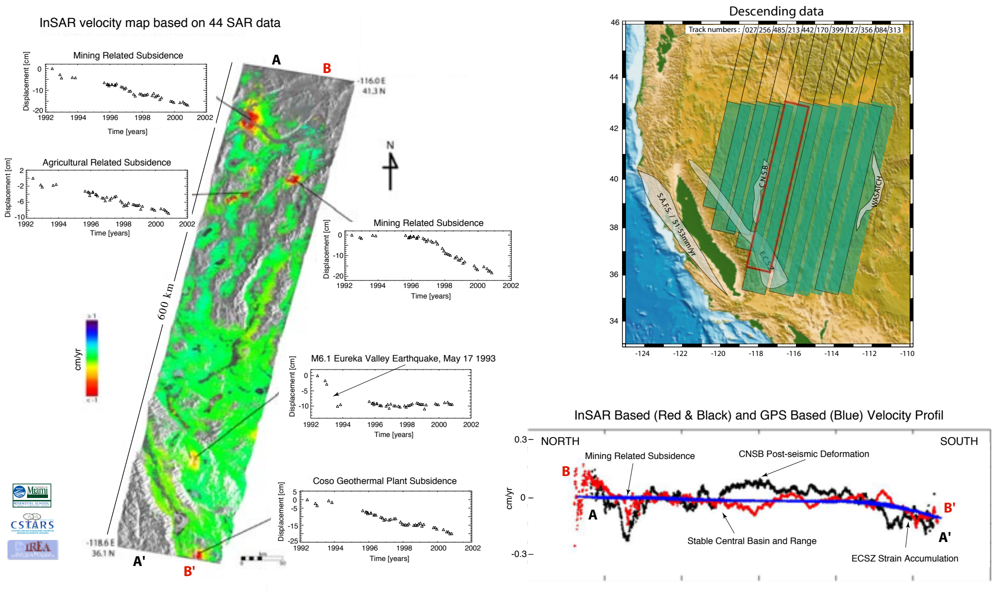

Left : InSAR mean velocity map (color scale) and time series of deformation for an area in central Nevada, USA, extending about 600 x 100 km. The presented map, superimposed to a SAR amplitude image (grey scale) of the zone, has been obtained by combining data relevant to 6 contiguous standard ERS SAR frames (track: 442, frames: 2781-2871) and by subsequently applying the SBAS-InSAR algorithm to the overall dataset composed by 264 frames (44 dataset for each frame). The investigated time period spans the 1992-2000 interval and the spatial resolution of the InSAR products is of about 200 x 200 m. Right : Up – map of planned InSAR based measurement with highlighted in red the current result. Down - Profile along track (~north-south) of the eastern (Red – location on left figure) and western (Black - idem) InSAR velocity map showing stable Basin and Range and post-seismic deformation within the nearby Central Nevada Seismic Belt (C.N.S.B) as well as the interseismic strain accumulation across the Eastern California Shear Zone (E.C.S.Z.). The comparison with a GPS based model (Kreemer et al. 2004) suggests that no significant vertical deformation is associated with the regional scale deformation.

We produced a time series of deformation by processing multiple Synthetic Aperture Radar Interferograms using a time-series analysis algorithm (Small Baseline Subset, SBAS) algorithm for a large-scale dataset. We obtain a detailed picture of the deformation field with high measurement density and sensitivity to vertical deformation. When studying fault zone deformation with InSAR, the challenge is to discriminate between what is error (orbital, atmospheric) and what is signal. Processing interferograms over a large area allows to minimize the uncertainty due to orbital errors because the wavelength of deformation is likely to be smaller than the wavelength of orbital error, because often stable areas are present, and because a set of permanent GPS velocities are available that can be used as tie points.

We present time series and mean deformation measurements for an area 500 x 100 km within Nevada and California, encompassing the stable Basin and Range with a few subsidence areas, post seismic deformation along the Central Nevada Seismic Belt, The M6.1 Eureka Valley earthquake, the Coso geothermal field and the interseismic strain accumulation across the Eastern California Shear Zone.

GEOMETRICAL EFFECTS OF FAULT BENDS ON FAULT DEFORMATION AND STICK SLIP BEHAVIOR: INSIGHTS FROM DISTINCT ELEMENT SIMULATIONS

Yonggui Guo, Julia Morgan · Rice University

Fault surfaces are seldom perfectly planar and often consist of nonlinear segments, i.e., restraining bends and releasing bends that have significant impacts on stress pattern, strain accumulation, slip rate, and therefore the variation of seismicity along these faults. In order to study the geometrical effects of nonlinear faults on fault deformation and stick slip behavior, we simulate the rupture process of faults with bends using the Distinct Element Method (DEM) in 2-dimensions. Breakable elastic bonds were added between adjacent, closely packed circular particles to generate fault blocks. A nonlinear fault surface, with symmetrically distributed restraining bend and releasing bend, was defined in the middle of the fault blocks. Deformation was introduced by pulling a spring attached to one of the fault blocks at a constant velocity while keeping another block fixed. This configuration produces compression and contraction along the restraining bend, and tension and dilation along the releasing bend.

Deformation of our simulated non-linear fault during the stick phase is characterized by the development of secondary faults that preferentially initiate at locations where the master fault changes orientation. Foreshocks correlate either to the rupture of the secondary faults under tension, or to pronounced changes in volume strain rate. In contrast, deformation during the slip phase is characterized by rapid, non-uniform slip along the master fault and the development of damage around the restraining bend. In general, an increase in bend angle leads to an increase in the duration of the stick phase and a decrease in the duration of the slip phase. The intensity of fracture under tension during the stick phase does not show a systematic variation with bend angle, while the intensity of fracture under shear during the slip phase tends to increase with increasing bend angle. These results confirm the importance of geometrical effects of fault bends on the characteristics of earthquake and associated deformation.

INTERFEROMETRIC SAR INVESTIGATION OF THE SLOW RATE OF SURFACE DEFORMATION IN THE EASTERN SNAKE RIVER PLAIN, IDAHO, USA *(Speaker)*

Mohamed H. Aly, David W. Rodgers, Glenn D. Thackray, Christopher D. Kemp · Idaho State University

The Eastern Snake River Plain (ESRP) is a northeast-trending volcanic basin that marks the former track of the Yellowstone hotspot. The ESRP is ~350 km long and ~80 km wide, is bounded north and south by the Basin and Range province, and has no significant faults along its margins. Previous geologic studies reported the ESRP experienced ~6 km of rock subsidence during the past 10-15 Ma, and ~0.9 km of surface subsidence since ~6 Ma. To test whether the ESRP is experiencing annual to decadal vertical movements, such as regional subsidence relative to the adjacent Basin and Range or local differential movements, various Interferometric Synthetic Aperture Radar (InSAR) techniques have been considered. The conventional Differential InSAR (DInSAR) approach has been applied to identify areas of regional deformation using InSAR data acquired at the C-band by the European Radar Satellites (ERS-1/2) during 1992-2006. The short wavelength of the C-band (5.66 cm) is appropriate for detecting slow rates of surface movements. To reduce the potential geometric and temporal decorrelations, the analysis has been limited to ERS pairs of short perpendicular baselines (<50 m) spanning ~1-5 yr. Preliminary results from the two-pass interferometric technique indicate no regionally consistent deformation occurred in the Line-Of-Sight (LOS) over a large area (~100x100 km) during periods of observations. However, local surface deformation of 1-3 cm magnitude over short time periods (~2-4 yr) has been detected north of Howe, Idaho (Lat: 43˚ 51` N, Long: 113˚ 7` W). This deformation is not attributed to long-term deformation of the ESRP, but instead to local tectonic or groundwater processes. The Permanent Scatterer interferometric technique will be applied next to overcome conventional DInSAR limitations and to improve the capability of the analysis to detect and measure potential surface movements in the ESRP over a longer time period (~15 yr). This interferometric investigation will help to better understand the geodynamics of crustal deformation in the ESRP.

WHAT IS THE ROLE OF MINOR GOUGE ZONES IN THE DAMAGE ZONE OF THE SAF SYSTEM?

Jafar Hadizadeh · University of Louisville
Hassan Babaie · Georgia State University
Karen Mair · University of Oslo
Giulio Di Toro · University of Padova

We describe a 7mm thick hard gouge zone (340°, 35°SW) intersected by SAFOD drillhole at a measured depth of 1465m. The zone has a sharp contact with fractured and veined granodiorite protolith and appears to have been developed entirely by brittle deformation as indicated by grain-scale deformation features. Elemental and oxide analyses suggest that sericite, laumontite, and chlorite are present in the gouge as alteration products. Highly twinned and brecciated vein calcite as well as µm-aperture fractures with calcite-lining are common throughout the gouge zone. A left-lateral sense of shear could be recognized via the disposition of the Riedel shears in the gouge zone. An SPO (shape preferred orientation) foliation is well-developed in the Y-orientation and is partly defined by the apparent flow of alteration products and highly comminuted mineral fragments around relict feldspar and quartz particles. An interesting microstructural feature is high variability of thickness of the foliated gouge over mm distances in the plane of shearing. SEM imaging shows that the zone includes lenses of gouge at different stages of comminution with most of the alteration phyllosilicates concentrated in and around the foliated gouge.

The microstructures of the gouge are compared to previously studied simulated and exhumed gouges, in which the development of similar microstructures had required only few tens of mm of shear displacement. The studied gouge represents one of several shear zones with similar features that have been characterized or investigated by others in the SAFOD core samples to a measured depth of 3100m. The combined observations suggest that the studied gouge zone might have developed along preexisting suitably-oriented and alteration-softened fracture surfaces. This model is consistent with previous findings that suggest mesoscale fracture systems in fault damage zones act as fluid flow pathways and therefore are affected most by mineral alterations. Thus, in addition to a network of fractures, a system of gouge zones with highly variable thickness and limited lateral extent might exist within the flower structure of the SAF at shallow depths giving the entire damage zone a beanbag-like deformability. We present evidence of repeated displacements along the studied gouge zone and discuss the mechanical implications of the proposed model for the damage zone of mature faults such as the SAF system.

UPDATE ON PLATE BOUNDARY OBSERVATORY GPS INSTALLATIONS IN THE PACFIC NORTHWEST

Katrin Hafner, Ken Austin, Sarah Doelger, Keegan Fengler, Karl Feaux · UNAVCO

The Plate Boundary Observatory (PBO), which is part of the larger NSF-funded EarthScope project, is 5 months into year 4 of the installation phase of 852 continuously operating GPS stations in the Western United States. The Pacific Northwest (PNW) region will install 134 continuous GPS stations by the end of September 2008. The sites are distributed along the fore and back-arc of the Cascadia Subduction Zone and at Mt. St. Helens. The end of year 3 installation goal was 75 stations. As of February 13th, 2007, the PNW region has installed 79 GPS monuments. The scientific priority during this past year was to complete the installations on Mt. St. Helens, and to continue to increase the density of the GPS network along the fore-arc regions of Washington and Oregon.

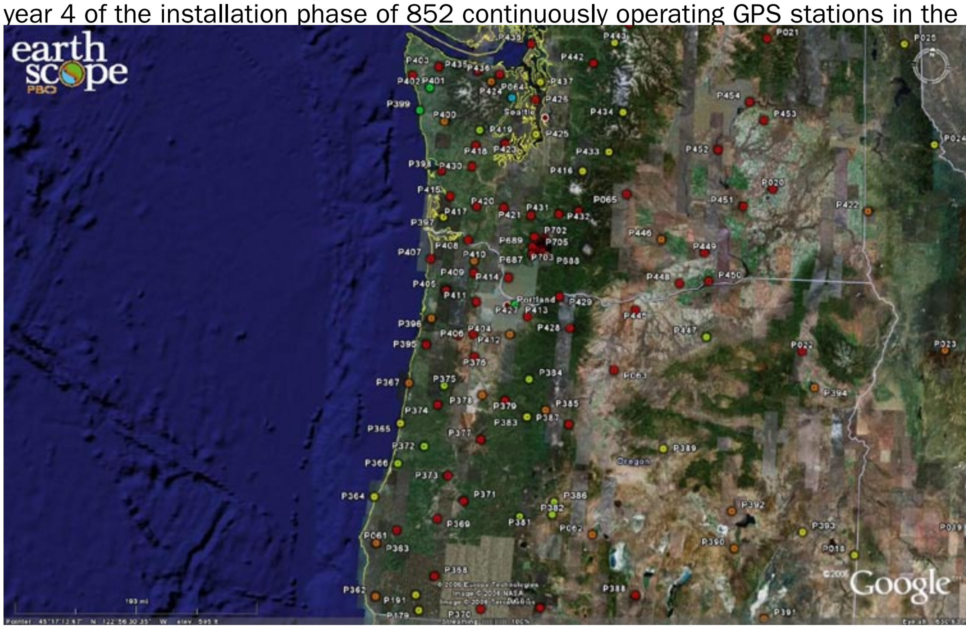

Distribution of GPS stations in the Pacific Northwest Region

PBO installed 7 additional GPS and 4 tiltmeter stations on Mt. St. Helens in September of 2006. Data analysis from GPS stations installed in 2004 and 2005 indicate an inward and downward deflation of the volcano of several centimeters out to distances of 5 to 10km from the crater. GPS stations installed high on the mountain were subjected to severe winter weather and heavy rime ice accumulations over the last year. The build up of ice on the GPS antennas caused cm-level pseudo-displacements that mask the ground movements associated with the eruption.

The PNW region of PBO will install 34 new continuous GPS stations in year 4, concentrated in the back arc regions of Oregon, the Idaho panhandle, and the Southwest Oregon fore arc region. For those 14 stations where locations could not be found within the original buffer, additional reconnaissance work is continuing in conjunction with suggestions from the scientific community.

STRENGTH AND DEFORMABILITY OF GRANODIORITE CORE FROM SAFOD DRILLHOLE UNDER TRUE TRIAXIAL STRESS CONDITIONS

Bezalel Haimson, HiKweon Lee · University of Wisconsin

A limited amount of core from the 1462-1470m segment of the SAFOD (San Andreas Fault Observatory at Depth) drillhole, near Parkfield, California, was made available to us for mechanical testing under true triaxial stress conditions. The objective of this project is to derive critical mechanical properties, analyze brittle fracture characteristics, and establish the strength criterion of the local Salinian granodiorite, as well as assist in the estimation of the in situ stress conditions adjacent to the Fault. The core received was intact but traversed by numerous fractures, a fact that reduced the number of rectangular prismatic specimens (19×19×38 mm3) produced. Nevertheless, a series of true triaxial tests in which σ1 was monotonically raised to failure while holding constant σ2 and independently σ3, revealed some important mechanical characteristics. Five sets of tests in which σ3 was kept constant (20, 40, 80, 120, 160 MPa) and σ2 was varied from test to test, consistently showed that the granodiorite compressive strength increases not only with σ3, but also with σ2 for constant σ3, contrary to the commonly accepted Mohr criterion assumption. Depending on the magnitude of σ2 the true triaxial strength can reach levels of up to 60% higher than those predicted based on conventional triaxial tests (where σ2 = σ3). Plotting all test results in the domain of octahedral shear stress at failure σoct as a function of the mean stress acting on the plain of failure, as proposed by Mogi (JGR, 1971), yielded a well constrained true triaxial strength criterion in the form of a power function: σoct = 2.39[(σ1 + σ3)/2]0.78 (r = 0.99). Failure plane was always steeply dipping in the σ3 direction, with the dip angle increasing with σ2 for constant σ3. Volumetric strain for constant σ3 indicated a rise in the dilatancy onset as the intermediate principal stress was raised above the least principal stress. For example for σ3 = 80 MPa, dilatancy onset rose from 31% of σ1(at failure) at σ2 = 160 MPa, to 48% of σ1(at failure) at σ2 = 320 MPa. SEM inspection of tested specimens reveals that the brittle fracture process involves microcrack localization, culminating in a through-going inclined shear fracture that follows a tortuous path and in places develops an en-echelon pattern. Microcracks are largely aligned with the σ1 - σ2 plane, as previously observed in other crystalline rocks tested under similar conditions (Haimson, PAGEOPH, 2006).

AN INTERACTIVE MAP TOOL FOR EARTHSCOPE EDUCATION AND OUTREACH

Michael Hamburger, Anne Hereford · Indiana University
Marianne Weingroff · DLESE-UCAR
William Holt · Stony Brook University
Lou Estey, Chuck Meertens, Susan Eriksson, Stuart Wier · UNAVCO

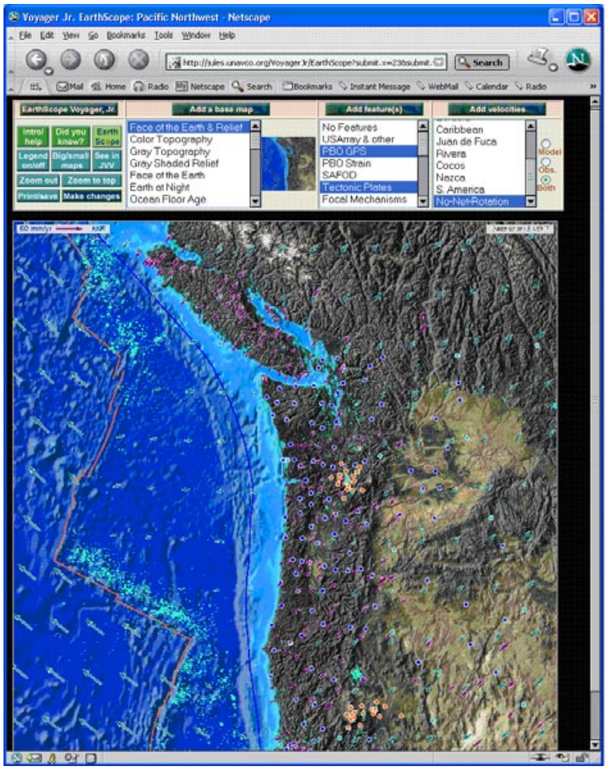

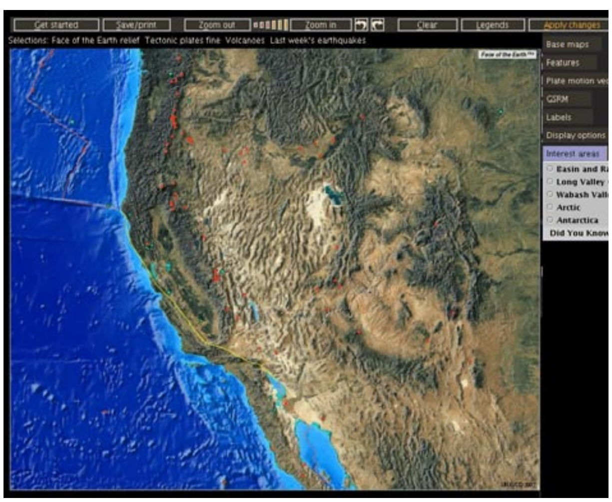

Image created using the EarthScope Voyager, Jr. map tool, showing proposed PBO sites (blue and orange circles for backbone and magmatic cluster sites, respectively), observed and modeled geodetic velocities (purple and blue vectors, respectively), seismicity and plate boundary locations, superimposed on a base map showing Face of the Earth imagery that combines satellite reflectance data with high resolution topographic and bathymetric data.

Image created using the new Jules Verne Voyager map interface, showing menu-based selection system and high resolution satellite image of the western U.S., with volcano locations superimposed.

We have created a new, interactive, web-based map utility that can make EarthScope-related scientific results accessible to a large number and variety of users. The tool provides a user-friendly interface that allows users to access a variety of maps, satellite images, and geophysical data at a range of spatial scales. The EarthScope Voyager map tool allows users to interactively create a variety of geographic, geologic, and geodynamic maps of the EarthScope study area. The utility is built on the “Jules Verne Voyager” suite of map tools, developed by UNAVCO for the study of global-scale geodynamic processes. Users can choose from a variety of base maps (including satellite imagery, global topography, geoid, sea-floor age, strain rate and seismic hazard maps, and others), add a number of geographic and geophysical overlays (coastlines, political boundaries, rivers and lakes, earthquake and volcano locations, stress axes, etc.), and superimpose both observed and model velocity vectors representing a compilation of 5170 geodetic measurements from around the world. Users can select from 26 frames of reference, allowing a visual representation of both ‘absolute’ plate motion (in a no-net rotation reference frame) and relative motion along all of the world’s plate boundaries. For the EarthScope Voyager, we include maps of proposed USArray and Plate Boundary Observatory sites and “Did You Know” educational modules, which provide examples of EarthScope-related scientific results linked to EarthScope study areas. Two versions of the tool are available: (1) a Java-based map tool “EarthScope Voyager”, a server-based map creation system which allows users complete control over base maps, overlays, and map scale; and (2) “EarthScope Voyager, Jr”, an HTML-based system that uses pre-constructed GIF maps and overlays, allowing the system to rapidly create and display maps to a large number of users simultaneously. The tool allows users to zoom among at least four map scales. In addition, we have developed companion educational materials, on the “Exploring our Dynamic Planet” website, a Javascript-based interface that incorporates explanatory material for the map tool and curricular activities that encourage users to explore Earth processes using the Voyager map tools. We have also created an entirely new user interface for the “Jules Verne Voyager” suite, which allows users to make ‘maps on demand’ using a new user-friendly menu interface. The map tool and associated educational materials can be viewed through the Jules Verne map portal http://jules.unavco.org. This work was supported by NSF grant EAR-0346180.

ACTIVE CRUSTAL DEFORMATION IN THE SOUTHERN ILLINOIS BASIN

Michael Hamburger, Gary Pavlis, Qizhi Chen · Indiana University
Kevin Eagar · Arizona State University

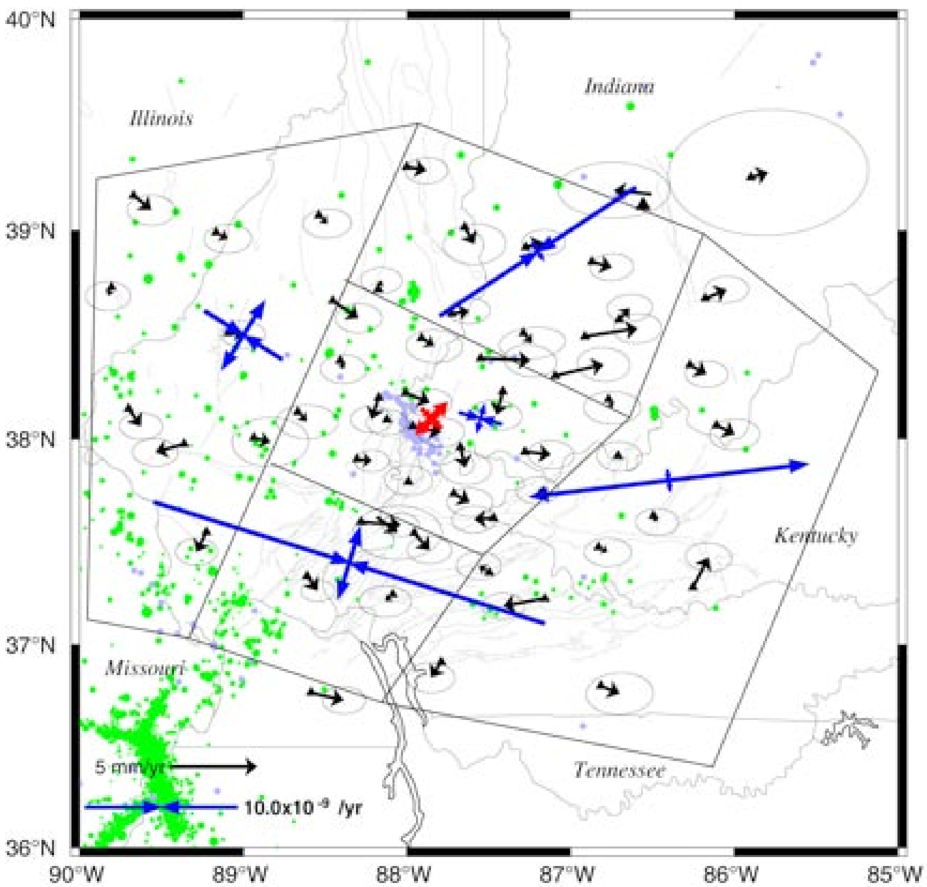

Evidence of present-day deformation in the Wabash Valley seismic zone. Green dots show instrumentally recorded earthquakes, 1974-1995, recorded by the Central Mississippi Valley Seismograph Network, symbol size proportional to magnitude. Light blue dots show events recorded by the Wabash Valley seismic array experiment, 1995-96. Triangles indicate locations of campaign GPS sites; vectors with 95% confidence ellipses show inferred velocities, 1997-2002. Blue and red vectors indicate orientation and magnitude of principal components of horizontal strain inferred from GPS velocities for local subareas surrounding the WVSZ and entire network, respectively.

We examine a broad suite of geophysical data to constrain upper crustal deformation associated with the Wabash Valley Seismic Zone (WVSZ) of southern Indiana and Illinois. Regional seismic and potential field data indicate that a sequence of highly Precambrian basement rocks underlie the relatively undeformed Paleozoic sediments of the Illinois Basin. Detailed seismic reflection and potential field data in the vicinity of the WVSZ indicate that the Wabash Valley Fault System is rooted in a series of basement-penetrating, high-angle transtensional faults that define a narrow, elongate graben extending beneath the fault system. We used data from a regional educational seismograph network, combined with a temporary seismic array deployed in the WVSZ in 1995-1996 to examine present-day seismicity associated with the fault system. A detailed examination of the regional network data produced only two local earthquakes, 18 regional events, and many thousands of local blasts, during a six-month period of intensive observation. In contrast, the temporary array experiment, which included a continuously recording, small-aperture phased array, with ten regional stations deployed at 20-30 km intervals, recorded approximately 100 events that we identified as earthquakes and for which we could obtain reliable magnitude estimates, ranging from 0.7 - 2.2. The events show a concentration of activity in and around the Wabash Valley Fault System. The magnitude-frequency relation of these events shows a distinct excess of smaller events relative to that predicted from a linear extrapolation of previous data. Based on refined locations of these events, we interpret them as shallow-level, induced earthquakes associated with oil production in the Illinois Basin. Finally, in order to measure present-day crustal deformation rates and assess possible relationships with defined structures within the WVSZ, we have installed and measured a new GPS geodetic network in the southern Illinois Basin. The network consists of 56 high-stability benchmarks distributed across a 100,000 km2 area in southern Indiana and Illinois and western Kentucky at an average spacing of 25 km. Comparison of data from five GPS campaigns from the period 1997-2002 provide little evidence for statistically significant velocities for individual sites in the southern Illinois Basin. Average strains for the entire network, however, show marginally significant strains, with an orientation consistent with the overall direction of intraplate stress in the U.S. mid-continent. In this tectonic context, the recent June 2002 Darmstadt, Indiana earthquake provides evidence for reactivation of basement faults associated with the Wabash Valley fault system.

THE WALKER LANE: HOW COMPLEX IS IT? GEODETIC AND GEOLOGIC STRAIN IN THE WESTERN BASIN AND RANGE USING ENHANCED BLOCK MODELING ALGORITHMS

William Hammond, Corné Kreemer, Geoff Blewitt · University of Nevada

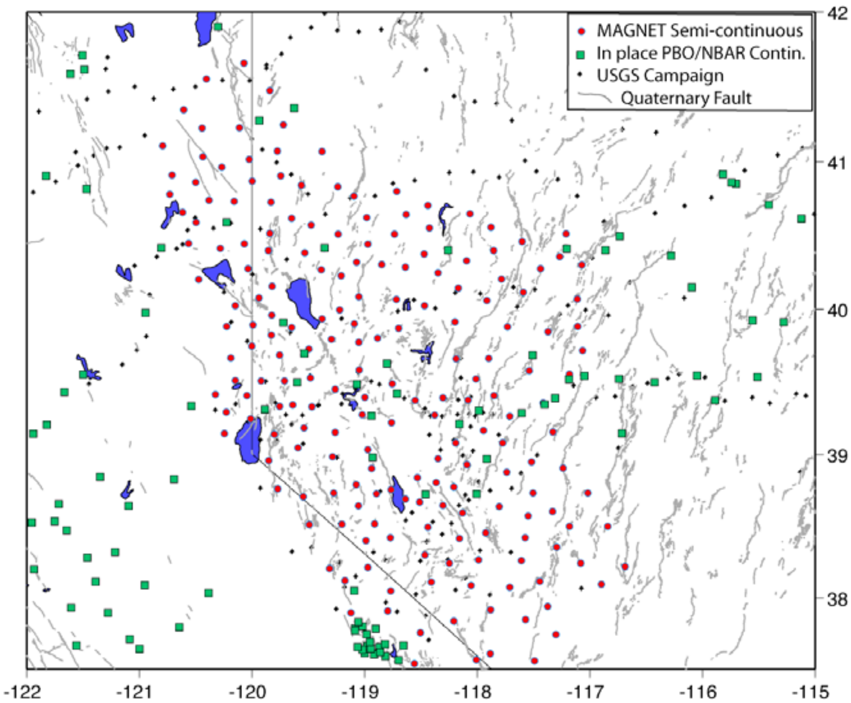

Northern Walker Lane regional faulting and GPS sites.

Crustal deformation in the northern Walker Lane accommodates roughly 25% of the Pacific/North America relative motion. In contrast to other parts of this plate boundary system, the regional patterns of faulting are complex, and are not completely described. For example, the role and importance of crustal block rotations, fault system step-overs, and off-fault deformation are not well understood. Furthermore, given the present state of knowledge there is a large discrepancy between geologically and geodetically observed moment rates, which suggests a fundamental gap in knowledge and/or understanding of this important part of the plate boundary.

Geodetic velocities along with fault trace geometries and seismicity patterns are often used to create and constrain analytical block models of crustal deformation. However, drawing the block boundaries sometimes requires a certain degree of assumptions and subjective judgment as to how individual fault segments are connected to form through-going fault systems and prevent kinematic inconsistencies. Furthermore, other assumptions are implicitly applied such as that all the deformation is accommodated on well-defined faults, implying that strain accommodated on other types of structures such as folds, dike intrusions, and distributed strain are not important for accommodating long-term motions. In many localities where fault systems are relatively simple, this approach may work well. However in the northern Walker Lane the complexity of the system and the gaps in our knowledge may suggest that we can improve our understanding if we 1) take an integrative approach that incorporates geologic and geodetic data, 2) allow for structures that we have not imagined, and 3) allow for the possibility that incongruous geodetic and geologic data may be reconciled by fault slip rates that vary over time. Evaluating the characteristic size of blocks that are needed to explain the data is an important step in determining the limiting size scale to which intracontinental deformation is block-like or continuum-like.

In our presentation we will go over preliminary results obtained from implementing innovations in block modeling strategy, including iterative non-linear algorithms that refine estimates of fault dip and select block boundaries that best fit the geodetic and geologic data. As constraints we will use northern Walker Lane/western Basin and Range GPS velocities from our own MAGNET network of 132 sites with a roughly 20 km station spacing. This study will serve as an evaluation of the performance of this network with respect to crustal deformation models of various levels of complexity.

ACCRETION AND CRUSTAL IMBRICATION: EXAMPLES FROM WYOMING AND BRITISH COLUMBIA IRIS-PASSCAL TELESEISMIC EXPERIMENTS

Steven Hansen, Jeannette Peck, Ken Dueker · University of Wyoming

First-order receiver function images and teleseismic tomography velocity images from the IRIS-PASSCAL Laramie and BATHOLITH broad-band deployments are presented. These new images constrain the style of continental accretion in Wyoming and British Columbia and subsequent felsification of the crust via granite distillation events.

The Laramie array was a 10 month deployment of 30 broad-band seismometers with a two kilometer station spacing. The 60 km line array traversed the Archean-Proterozoic Cheyenne suture in SW Wyoming that formed via an arc-continent collision between a juvenile Proterozoic block and the Archean Wyoming craton. Previous seismic imaging from the CDROM experiment imaged a north dipping high velocity body named the “Cheyenne Slab” (Yuan and Dueker, 2003). The Cheyenne Slab is interpreted to be a fragment of oceanic lithosphere that was trapped against the Wyoming lithospheric margin during accretion. Several slab emplacement mechanisms have been suggested: e.g., a subduction polarity reversal as the arc collided with the Archean crust. Receiver function images show that the moho beneath the Proterozoic aged crust is imbricated beneath the Archean moho. This new seismic structural observations supports the hypothesis that a subduction polarity switch did occur during the ancient accretion event.

The BATHOLITH array ran for 15 months and consisted of 44 seismometers deployed in two line arrays with a nominal 14 km spacing. The lines were located along the coast of British Columbia and traverse several terrane boundaries, in particular the enigmatic coast shear zone (CSZ) which defines the western extent of the Eocene granitic flare-up event that formed the Coast Mountain batholith (CMB). An important question with respect to the evolution of the CMB, is whether the CSZ accommodated a large thrust component during late Cretaceous shortening. Receiver function images from the teleseismic lines show a sharp moho that is depressed by 5-10 km beneath the CMB. The south line image reveals a crustal-scale east dipping ’reflector’ that projects towards the surface location of the CSZ. New geochemical results from the Coast Mountain batholith suggest distillation from a primitive source with anomalously high 180 values (Wetmore et. al., in press). From this data, it is hypothesized that the outboard Wrangellia terrane was thrust beneath the inboard Stakina terrane and subsequently partially melted to create the CMB. If this is the case, and the batholith was distilled below 35 km, the resitic root would be gravitationally unstable. The P-wave tomographic images show 4% lateral P-wave velocity variations perhaps consistent with a post-CMB formation foundering event.

ACCRETION AND CRUSTAL IMBRICATION: EXAMPLES FROM WYOMING AND IRIS-PASSCAL TELESEISMIC EXPERIMENTS

Steven Hansen, Jeannette Peck, Ken Dueker · University of Wyoming

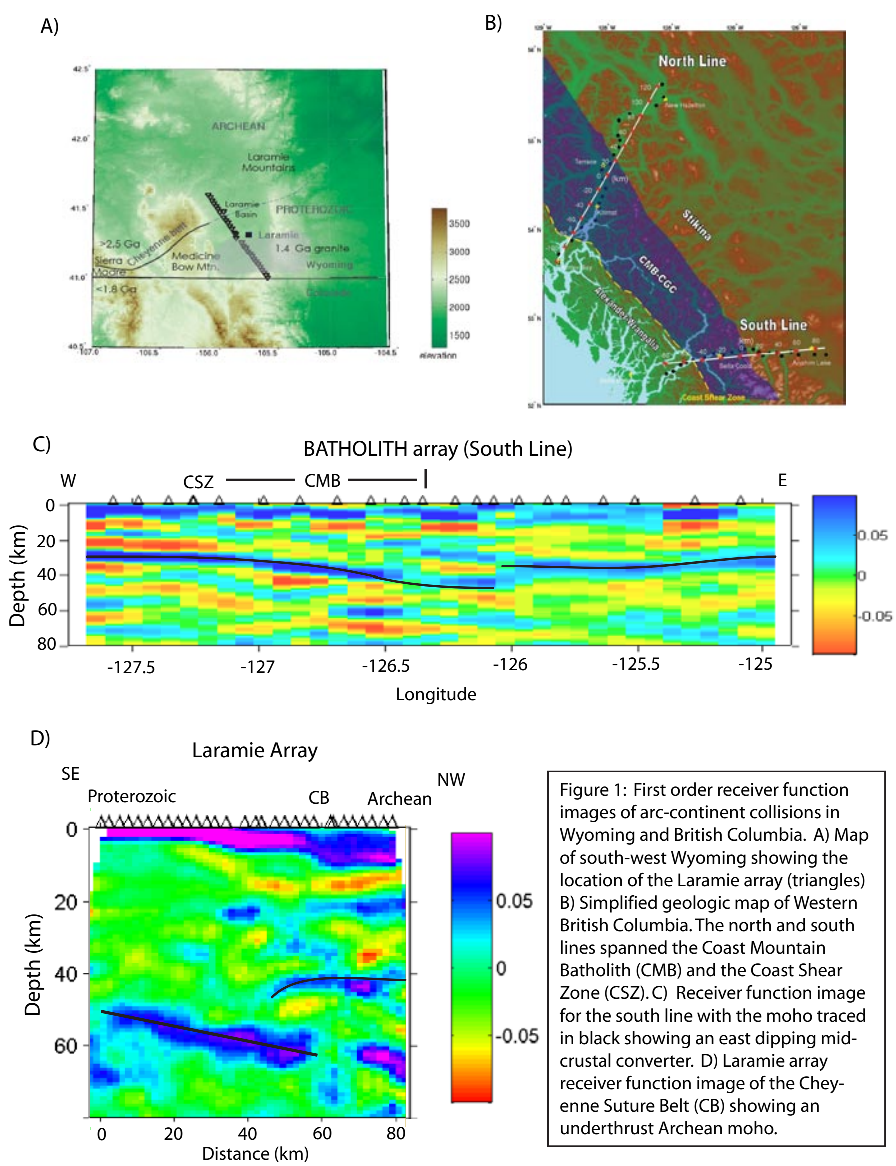

Figure 1: First order receiver function images of arc-continent collisions in Wyoming and British Columbia. A) Map of south-west Wyoming showing the location of the Laramie array (triangles) B) Simplified geologic map of Western British Columbia. The north and south lines spanned the Coast Mountain Batholith (CMB) and the Coast Shear Zone (CSZ). C) Receiver function image for the south line with the moho traced in black showing an east dipping mid-crustal converter. D) Laramie array receiver function image of the Cheyenne Suture Belt (CB) showing an underthrust Archean moho.

First-order receiver function images and teleseismic tomography velocity images from the IRIS-PASSCAL Laramie and BATHOLITH broad-band deployments are presented. These new images constrain the style of continental accretion in Wyoming and British Columbia and subsequent felsification of the crust via granite distillation events.

The Laramie array was a 10 month deployment of 30 broad-band seismometers with a two kilometer station spacing. The 60 km line array traversed the Archean-Proterozoic Cheyenne suture in SW Wyoming that formed via an arc-continent collision between a juvenile Proterozoic block and the Archean Wyoming craton. Previous seismic imaging from the CDROM experiment imaged a north dipping high velocity body named the “Cheyenne Slab” (Yuan and Dueker, 2003). The Cheyenne Slab is interpreted to be a fragment of oceanic lithosphere that was trapped against the Wyoming lithospheric margin during accretion. Several slab emplacement mechanisms have been suggested: e.g., a subduction polarity reversal as the arc collided with the Archean crust. Receiver function images show that the moho beneath the Proterozoic aged crust is imbricated beneath the Archean moho. This new seismic structural observations supports the hypothesis that a subduction polarity switch did occur during the ancient accretion event.

The BATHOLITH array ran for 15 months and consisted of 44 seismometers deployed in two line arrays with a nominal 14 km spacing. The lines were located along the coast of British Columbia and traverse several terrane boundaries, in particular the enigmatic coast shear zone (CSZ) which defines the western extent of the Eocene granitic flare-up event that formed the Coast Mountain batholith (CMB). An important question with respect to the evolution of the CMB, is whether the CSZ accommodated a large thrust component during late Cretaceous shortening. Receiver function images from the teleseismic lines show a sharp moho that is depressed by 5-10 km beneath the CMB. The south line image reveals a crustal-scale east dipping ’reflector’ that projects towards the surface location of the CSZ. New geochemical results from the Coast Mountain batholith suggest distillation from a primitive source with anomalously high 180 values (Wetmore et. al., in press). From this data, it is hypothesized that the outboard Wrangellia terrane was thrust beneath the inboard Stakina terrane and subsequently partially melted to create the CMB. If this is the case, and the batholith was distilled below 35 km, the resitic root would be gravitationally unstable. The P-wave tomographic images show 4% lateral P-wave velocity variations perhaps consistent with a post-CMB formation foundering event.

TECTONIC IMPLICATIONS OF HEAT FLOW DETERMINATIONS IN PBO STRAINMETER BOREHOLES

Robert N. Harris · Oregon State University
Colin F. Williams, Frederick V. Grubb · U.S. Geological Survey
David S. Chapman · University of Utah

The overarching goal of EarthScope is to enhance our understanding of the dynamics and evolution of the North American continent. To reach this goal, focused studies of the continental seismic structure, the strength of the lithosphere and modes of deformation, the patterns of stresses and strain and the manner in which the lithosphere responds to earthquakes are all a high priority. The common factor linking these EarthScope objectives is the thermal state of the lithosphere. Given the relevance of subsurface thermal conditions to the physical processes governing the spatial and temporal variations of lithospheric deformation, a greater knowledge of the subsurface thermal regime will contribute greatly to the overall objectives of EarthScope generally, and the Plate Boundary Observatory (PBO) experiment specifically. Heat flow determinations provide the strongest observational constraint on the thermal state of the lithosphere. We are adding to the existing heat flow coverage in the western United States by obtaining temperature-depth profiles, thermal conductivity measurements, and heat production values in PBO boreholes drilled for strainmeter emplacement. To date, we have obtained thermal data along the San Andreas Fault System (SAFS) in the San Francisco Bay Area, Parkfield, and Anza, California.

We have logged 13 boreholes that vary in depth from 140 to 250 meters and have made more than 300 thermal conductivity measurements on chip and core samples from 10 of these boreholes. Raw temperature data are corrected for three-dimensional terrain effects that include heat transfer due to topography and variable solar insolation due to the angle and azimuth of terrain slopes. Reliable heat flow values have been acquired at the majority of sites, which fill significant gaps in existing heat flow coverage. These new values together with existing values provide a better characterization of crustal thermal conditions that influence the spatial and temporal pattern of deformation within this plate boundary zone.

GEOTHERMS, FLUIDS AND LITHOSPHERIC STRUCTURE OF THE GREAT BASIN–COLORADO PLATEAU TRANSITION ZONE, 38.5N LATITUDE

Derrick Hasterok, David S. Chapman · University of Utah
Phillip E. Wannamaker · Energy and Geoscience Insititute
William Doerner · Quantech Geoscience

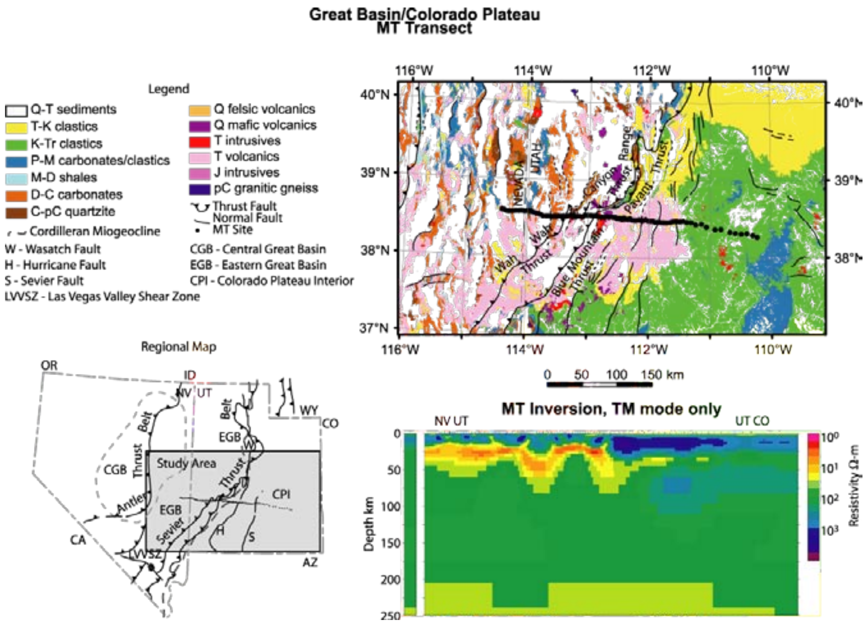

Surface geology and electrical structure of the Great Basin-Colorado Plateau.

The Colorado Plateau-Great Basin transition zone (TZ) in central Utah is a presently extending lithospheric block composed of previously stable Proterozoic lithosphere. TZ extension may be driven by high topography resulting from overthickening during the Laramide Orogeny and passive plate boundary forces similar to the Great Basin. However, high TZ topography may also indicate dynamic mantle upwelling and active processes acting within the TZ. We have collected 56 new broadband and 9 long-period MT sites to merge two existing MT lines for a combined length of 400 km (124 sites) covering the eastern Great Basin into the Colorado Plateau at a latitude of 38.5N. MT data show a highly conductive body that is semi-contiguous in the middle crust of the eastern Great Basin that rises to a shallow depth of <20 km beneath the TZ. This conductive layer appears to be connected to the surface by a series of symmetric rift related normal faults mapped at the surface. These normal faults may be acting as pathways for large scale fluid connection between the upper and lower crust. Using over 300 new heat production measurements made across the southwest, combined with existing heat flow data and MT measurements, we estimate the thermal structure and lithospheric thickness of the mantle along the MT profile. Temperatures within the

asthenosphere appear to be near the current average mantle adiabat. Lithospheric thicknesses estimated from the thermal structure suggest a thick, 150 km, lithosphere beneath the resistive core of the Colorado Plateau and thin, 60 km, in the Great Basin. Geodynamic modeling using the new thermal constraints may reveal insight into the active/passive nature of the rift. Data collected by EarthScope will help provide a regional framework to constrain the 3-dimensional extent of the processes acting within the TZ.

COMPOSITIONAL AND THERMAL CONTRIBUTIONS TO NORTH AMERICAN ELEVATION

Derrick Hasterok, David Chapman · University of Utah

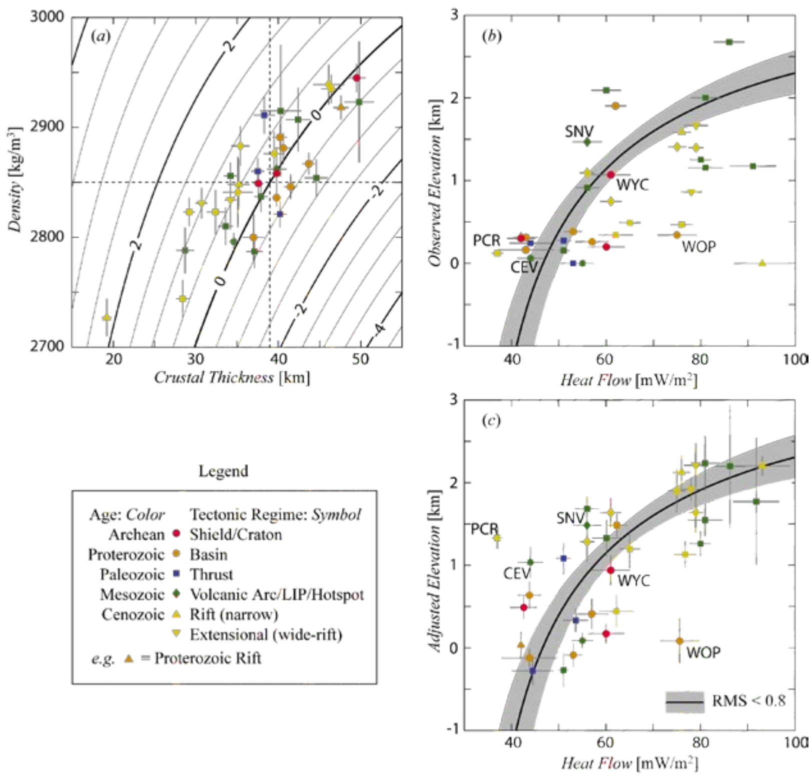

(a) Compositional elevation adjustments computed for the tectonic provinces of North America. The intersection of the dashed lines represent the areally weighted average crustal thickness and density of the North American crust and the crustal standard used in this study (39 km and 2850 kg/m3). (b) Observed elevations of the provinces. (c) Elevations of the provinces adjusted for crustal composition. The black curve in (b) and (c) shows the best-fitting model and the grey patch outlines the region with RMS values <0.8.

Elevation results from a combination of compositional and thermal buoyancy and geodynamic processes. Because geodynamic effects on elevation are typically small (<1 km), the potentially larger (~3 km) effects of compositional and thermal buoyancy must be accurately removed before geodynamic processes may be examined. Thirty-six North American tectonic provinces have been analyzed to separate the compositional and thermal components to elevation. Predicted thermal elevation relative to a computed thermal isostatic model parametric in surface heat flow still contains considerable scatter. In some regions, this scatter can be attributed to variations in crustal radiogenic heat production whereby the actual geotherm for an observed heat flow deviates significantly from the standard geotherm. For example, heat production effects on elevation of the Proterozoic Wopmay region of Canada may be as large as 2 km. Thus, it appears that radiogenic heat production must also be assessed prior to determination of geodynamic effects. Heat production distribution within the lithosphere is unfortunately one of the least documented physical parameters and can only be determined by direct measurement as it may differ by an order of magnitude within a single rock type. We have collected >300 new gamma ray spectra from rocks within the Basin and Range, Colorado Plateau and Southern Rocky Mountains. Preliminary estimates of heat production yield 0.8 μW/m3 for Colorado Plateau sediments, 4.3 μW/m3 for volcanics within the Marysville Volcanic Field, and 1 μW/m3 for miogeoclinal sedimentary rocks in the eastern Basin and Range. Proterozoic crystalline rocks within the Arizona Transition Zone and Southern Rocky Mountains yield heat production values of 2.2 and 2.7 μW/m3, respectively. Preliminary models of crustal heat production in the southwestern United States suggests a radiogenic contribution of ~100-200 m to the observed elevation. Using these data, we hope to improve our estimates of the thermal state of the lithosphere in the southwestern United States, thereby reducing the scatter in thermal component of elevation.

THE PBO BOREHOLE STRAINMETER/SEISMIC NETWORK

Michael Hasting, David Mencin, Wade Johnson, Tim Dittmann · UNAVCO

Lowering the first strainmeter at B004 Hoko Falls Washington

The Plate Boundary Observatory (PBO), part of the larger NSF-funded EarthScope project, will record the three-dimensional strain field resulting from active plate boundary deformation across the Western United States. PBO is a large construction project involving the reconnaissance, permitting, installation, documentation, and maintenance of GPS, Borehole Strainmeter (BSM) and Laser Strainmeter stations over a five year period which began in late 2003. PBO has a demanding installation schedule for the BSM network for FY07 with over 35 BSM stations planned for installation. Currently over 25 station have already been completed and are sending data to Boulder for processing. When completed the end of FY08 the network will comprise over 100 BSM stations.

BSM sensors are installed at depths of between 200 and 250 meters and data are sent to Boulder several times per day where it is processed and raw level 1 data are put online within 24 to 48hrs of being recorded. Three data streams are currently being recorded by the BSM's data logger; 20Hz, 1Hz and 600 second. Currently only level 2 data is being processed on the 1Hz and 600 second data with future plans to include the 20Hz data into level 2 processing. Environmental and state of health data are also recorded by the BSM data logger and forwarded on to Boulder.

Borehole seismic data are forwarded to Boulder in near real-time and are recorded at the site on a Q330 at both 1Hz and 100Hz sampling rates. Data is forwarded to Boulder where it is recorded using Antelope and then forwarded to the IRIS DMC for archiving. We use passive 2Hz, 3 component sensors that are cemented into the borehole above the strainmeter and provides high signal to noise environment for these sensors.

Paroscientific Digiquartz Depth Sensors are used to record pore pressure data. These sensors have a range of 60m and a resolution of 0.001mbar or hPa. The sensors are installed inside the 2 inch PVC to depths of 2 to 4 meters below the static water level at 10 second intervals. The sensors are pack off using an inflatable packer to seal the PVC from the atmosphere and provide actual pore pressure rather than water level reading.

Uphole equipment is enclosed in a fiberglass enclosure and houses the various electronic, power and communications systems. Most sites are power using A/C power but in some cases this is not possible. In those cases Photovoltaic (PV) power systems are used and/or Thermal Electric Generators (TEG). Several 12V 100amp-hr batteries provide backup power at all sites. Primary communications is provided through VSAT systems, but we have also used local IP connections and DSL lines when possible.

EARTHSCOPE IN 'FLY-OVER' COUNTRY . . . EXPLORING THE STRUCTURE AND GEOLOGICAL EVOLUTION OF THE CRUST AND LITHOSPHERE OF THE CONTINENTAL INTERIOR

Ernest Hauser · Wright State University

EarthScope and USArray will soon roll into and across the U.S. continental interior – that wide expanse of the continent between the Rocky Mountains and the Appalachians. A region covered to a major extent by Phanerozoic platform strata, the Midcontinent is presently largely known/mapped through potential field data, some seismic refraction and reflection profiles, scattered drill holes, and local basement inliers with outcrops mostly on the periphery. Locally there are seismic zones associated with reactivated basement structres. However, beneath the Midcontinent lies the evidence of the assemblage of the North American continent where it is little disturbed by the younger tectonism of the Rockies and Appalachians. The Penokean and Trans-Hudson Orogens beneath parts of the Midcontinent have bound together the ancient Archean continental cores. The Central Plains Orogen, representing the accretion of significant new crust to the margin of the growing North American continent is sliced and diced by the Laramide structures of the Rockies; however, it is likely better preserved beneath the continental interior than in the Rockies. The broader region of the Central Plains Orogen also experienced substantial crustal remobilization manifest as the Grantie-Rhyolite Province, which begs the question of how the lower crust and Moho of this region reflects (or, rather, does NOT reflect) the likely associated processes of mafic magma underplating. The Midcontinent Geophysical Anomaly that became associated with the broader Keweenawan rift system is a type locality for an aborted (or still-born) rift, perhaps stunted by the smothering embrace of the Grenville Orogen; but, what is the expression of this rift in the lithosphere beneath, and does it have a more substantial eastern arm than currently appreciated? In the eastern Midcontinent (Ohio, Indiana, Kentucky) reddish brown lithic arenites underlie significant regions and are thought to be either associated with an eastern arm of the Keweenawan rift or perhaps a remnant of a Grenville foreland basin, or both. In addition, is there a common driving mechanism for the major Phanerozoic intracontinental basins that have formed in the U.S. Midcontinent? Each apparently overlies very different crustal/lithospheric structures of very different ages. These and may other major questions still remain regarding the structure and evolution of the crust/lithosphere of the U.S. continental interior, or 'Fly-Over' country, and geophysicists AND geologists must find creative ways to use the opportunity afforded by EarthScope and USArray to address these and similar questions, perhaps guided along major transects, to make significant strides in understanding the evolution of our continent.

QUANTIFYING REGIONAL VELOCITY RATIO IN CALIFORNIA: USING SEISMIC DATA TO MAP SHALLOW STRUCTURE

Gavin Hayes, Kevin Furlong · Pennsylvania State University

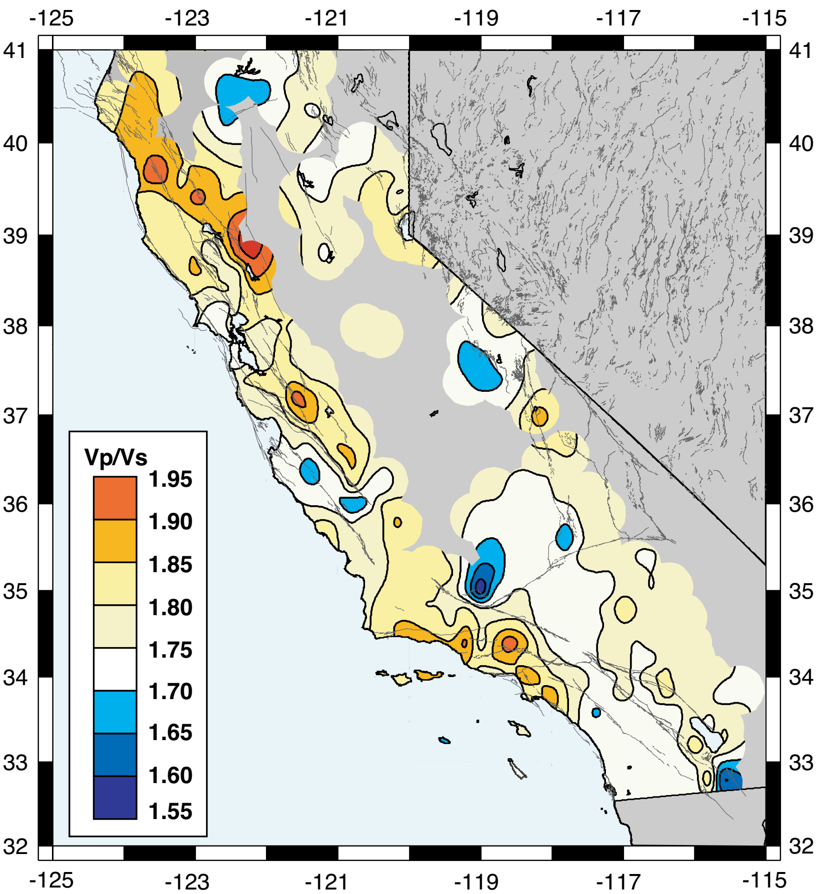

Velocity ratio map of California

For several decades, seismologists have used a variety of different methods to model the P-wave velocity structure of the Earth, and in particular, the Earth's crust. Modeling of the S-wave velocity field has been (and remains) more difficult, and as a result S-wave velocity structure is often directly related to P-wave models through empirical measurements of the velocity ratio in rocks. These velocity models are subsequently used in many different types of analyses, such as the calculation of strong ground motions in regional hazard maps, earthquake locations, and the inference of subsurface geology. In all cases, better estimates of S-wave velocity models lead to more accurate models of the parameters they are used to describe. This is of particular importance for estimates of shallow S-wave velocity structure, where we need improved models to aid in any predictive hazard analysis.

Here, we develop a straightforward technique for computing apparent velocity ratio of both the bulk seismogenic crust and shallow crust throughout California based on P- and S-wave travel-times from earthquakes to the dense network of broadband and short-period stations across the state, significantly improved since the implementation of the EarthScope project. As the seismogenic zone is constrained to the shallow, brittlely deforming part of the crust, we can use these earthquake travel-times to estimate the apparent velocity ratio of that crust. Using this approach, we produce regional maps of Vp/Vs for all California, where station coverage is dense enough and rates of seismicity high enough to allow this type of analysis. We can also isolate the very shallow (generally aseismic) crustal section to construct a velocity ratio map of the near surface.

This method, which we call the Local Velocity Ratio Calculation (LVRC), provides a simple yet powerful way to analyze the velocity ratio of the crust on a regional basis. The model compares favorably to the SCEC three-dimensional velocity model, giving confidence in the robustness of the approach. Results may be related to geologic structure, used to infer parameters such as ground shaking susceptibility, and also to calibrate geology-based three-dimensional velocity models such as the U.S. Geological Survey 3D model of northern California.

REGIONAL MOMENT TENSORS IN NORTHERN CALIFORNIA: ADDING DATA FROM USARRAY STATIONS

Margaret Hellweg, Douglas Dreger, Barbara Romanowicz · University of California, Berkekey

Since 1994 the Berkeley Seismological Laboratory (BSL) has been calculating moment tensor (MT) solutions for Northern California earthquakes with ML > 3.5 using data from the broadband stations of the Berkeley Digitial Seismograph Network (BDSN). The deployment of additional USArray (TA) stations in Northern California began in 2005. Since then, we have been incorporating data from these temporary stations in routine MT analysis and review. TA stations have been used for 12 of the 52 MTs calculated for the Berkeley moment tensor catalog between January 2005 and January 2007. They have improved solutions particularly for events near the Long Valley caldera and eastern Sierra Nevada, along the central California coast, and along the northern California coast. The Figure shows events with magnitudes greater than 2.0, with all moment tensors from that period. The contributions of the TA stations depend on their noise levels, as well as the size of the event and the station's proximity. The BSL MT catalog is available on the web at http://seismo.berkeley.edu/~dreger/mtindex.html

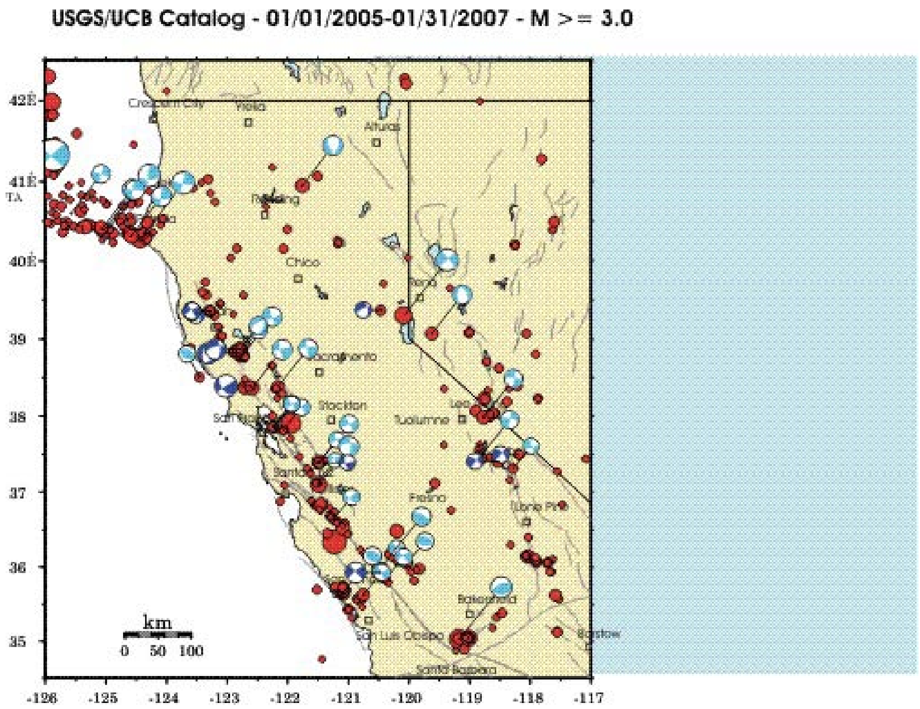

Figure 1. Events from Northern California between January 1, 2005 and January 31, 2007 with magnitudes greater than 2.0 (red). Moment tensors in dark blue are calculated using data from US Array stations in addition to BDSN broadband stations

REFINING THE CHARACTERIZATION OF A STRAIN RATE TRANSIENT ALONG THE SAN ANDREAS AND SAN JACINTO FAULTS FOLLOWING THE OCTOBER 1999 HECTOR MINE EARTHQUAKE.

Daniel Hernandez, William E. Holt · Stony Brook University
Richard A. Bennett · University of Arizona
A. John Haines · University of Cambridge

We are developing and refining a prospecting tool for recognizing strain rate transients, as well as for quantifying the magnitude and style of their temporal and spatial variations, inferred from continuous GPS time series. The present study uses the continuous SGIGN network between the periods of late 1999 to 2004 (post-Hector Mine). We first interpolate the continuous time series with smooth functions. Fourth-order polynomials have proven stable and capable of capturing first-order temporal variations within the time series. Annual and semi-annual signals are removed. We use Monte-Carlo simulations to estimate the model uncertainties in the time-dependent velocities inferred from the continuous GPS time series. Once model continuous velocity estimates are inferred for all stations, we investigate the spatial and temporal coherence of strain rate changes by interpolating velocity estimates within a 0.1° x 0.1° finite element grid in southern California. That is, a self-consistent model velocity gradient tensor field solution is determined for each epoch by interpolation of the GPS velocity vectors using bi-cubic Bessel interpolation [Beavan and Haines, 2001]. Using this method we estimate model dilatation strain rates, shear (pure strike slip component) strain rates, and the rotation rates for each epoch. Optimal smoothing of strain rate estimates is obtained by adjusting the a priori strain rate variances. These variances represent the expected magnitude of strain rate departure, associated with the strain rate transients that are embedded in the GPS time series, from the secular deformation field. This value is adjusted until we obtain a reduced Chi-Squared misfit between observed and model time-dependent GPS velocities of 1.0. Epoch solutions are compiled into movies to view the model strain rates over time (see http://rock.geo.sunysb.edu/~holt/EarthScope/). Plotted in each epoch solutions (or frame in the movie) are velocity difference vectors between the model epoch velocity estimate and the time-averaged estimate for the four years of data (95% confidence). In the region surrounding the 1999 Hector Mine earthquake, particularly the Anza segment of the San Jacinto fault, we observe several noteworthy time-dependent changes. There is a corridor of shear strain rate that extends from the southern part of the ECSZ, through the Pinto Mt. Fault, and into the San Andreas Fault, adjacent to the Salton Trough that immediately follows the Hector Mine earthquake. At the same time, shear strain rates along the Anza segment of the San Jacinto are very low (5-15 nanostrain per year), which increase over the next 6 months to a steady-state value of 35 – 50 nanostrain per year. The shear strain rate anomaly in the Anza segment occurs concomitant with a positive dilatation strain rate anomaly of more than 40 nanostrain per year. Hence, the strain rate anomalies along the Anza segment are consistent with a significant unloading of the San Jacinto fault directly following the Hector Mine event. The strain rate anomalies appear to be robust, as there is a strong temporal and spatial coherence of the GPS velocity difference vectors following the earthquake. Significant transients also appear within the LA Basin region during the time period, but interpretation remains difficult due to the possible influence of anthropogenic forcings [e.g., Argus et al., 2005]. Even though our analysis is comprised mainly of SCIGN network stations, future solutions involving post-2004 time series analysis will involve the increased spatial coverage provided by the Plate Boundary Observatory of EarthScope.

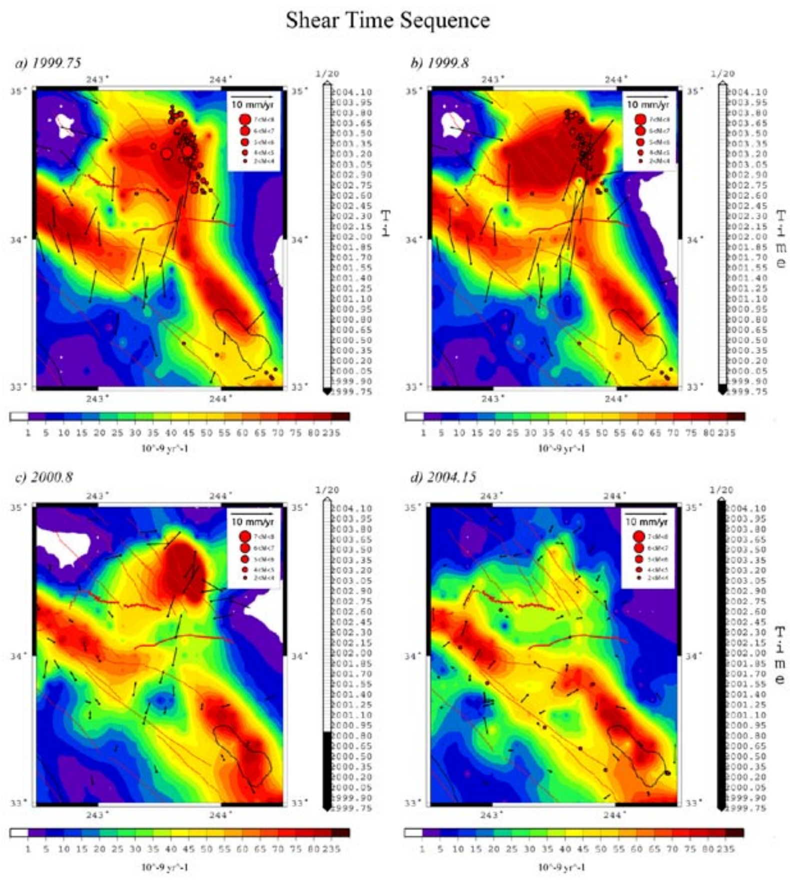

RECONCILING DEFORMATION AND RHEOLOGY USING EARTHSCOPE DATA *(Speaker)*

Thomas Herring · Massachusetts Institute of Technology

Earthscope is installing new instrumentation and taking advantage of previously installed instrumentation in a variety of tectonic settings in the North American plate boundary area. GPS receivers and strainmeters are being installed in extensional, strike-slip, subduction zone and volcanic provinces. In these areas a wide variety of tectonic deformation signals are being measured including episodic tremor and slip events, co- and post-seismic signals from strike-slip and thrust earthquakes, and steady strain accumulation at various times in the earthquake cycle including late in the cycle in some cases. These deformation measurements are sometimes complicated by non-tectonic signals such as the effects of water in the environment and systematic effects of snow and vegetation. In this talk, we examine the progress being made using Earthscope data in developing rheologies and force models that are consistent with the range of deformation and structural signals being observed in the plate boundary.

THE PLATE BOUNDARY OBSERVATORY BOREHOLE STRAINMETER PROGRAM: DATA ANALYSIS AND PRODUCTS

Kathleen Hodgkinson, Greg Anderson, Mike Hasting, Brent Henderson, Mike Jackson, Wade Johnson, Dave Mencin, PBO-DMIT Group · UNAVCO

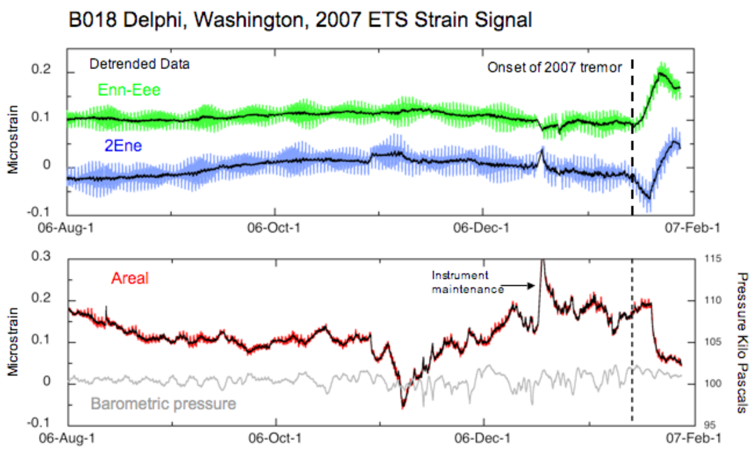

2007 ETS strain signal, PBO strainmeter B018, Washington

The Plate Boundary Observatory (PBO) is designed to measure deformation across the Pacific and North American Plate Boundary, the data being collected will give an insight to plate boundary crustal deformation processes. Borehole strainmeters are included in the PBO network because their stability over periods of hours to months means they bridge the gap between seismology and GPS. The strainmeters sites are multi-instrumented installations with seismic, pore pressure, atmospheric pressure, rainfall and temperature data being measured at almost all locations. On completion, the PBO strainmeter network will consist of 103 strainmeters. As of February 1, 2007 the network consists of 27 strainmeters: 15 in the Pacific Northwest, 7 in Anza and 5 in Parkfield, California. Regions targeted for installation include, Yellowstone, Long Valley, San Juan Bautista, the Mendocino triple junction and the San Francisco Bay Area.

PBO strainmeters record data at 20-sps, 1-sps and 10-minute interval and are downloaded hourly. The strain data are transferred to the archives, the IRIS DMC and NCEDC, via SEEDLink and LDM and are available within minutes of being retrieved from the logger. Both the raw data in the logger's format, bottle form, and the SEED data are being archived. PBO's Borehole Strainmeter Analysis Center (BSMAC) in Socorro, New Mexico, monitors data quality and produces processed strain data every 10 to 14 days. The processed data are stored in XML format containing time series corrections for the atmospheric pressure, the Earth tides and borehole effects. Every 3 months the data are reviewed and the borehole trends and tidal signal are re-estimated to form the best possible processed data set.

The UNAVCO strainmeter web pages (http://pboweb.unavco.org/strain_data) provide links to the raw and processed data and are a source of information on data formats, software and instrument documentation. A homepage has been developed for each strainmeter where plots of strain, state-of-health data and metadata can be viewed. A station notes file for each strainmeter provides a history of firmware upgrades and details anything that might affect data quality. UNAVCO will hold a short course at the EarthScope National Meeting, 2007, showing users what strainmeter data products are available and how to access them, http://www.unavco.org/cws/PBO_Data_Course .

LITHOSPHERE COUPLING WITH MANTLE CIRCULATION IN WESTERN NORTH AMERICA, CENTRAL ASIA, AND THE REST OF THE WORLD *(Speaker)*

William Holt, Attreyee Ghosh, Lianxing Wen · Stony Brook University
John Haines · University of Cambridge

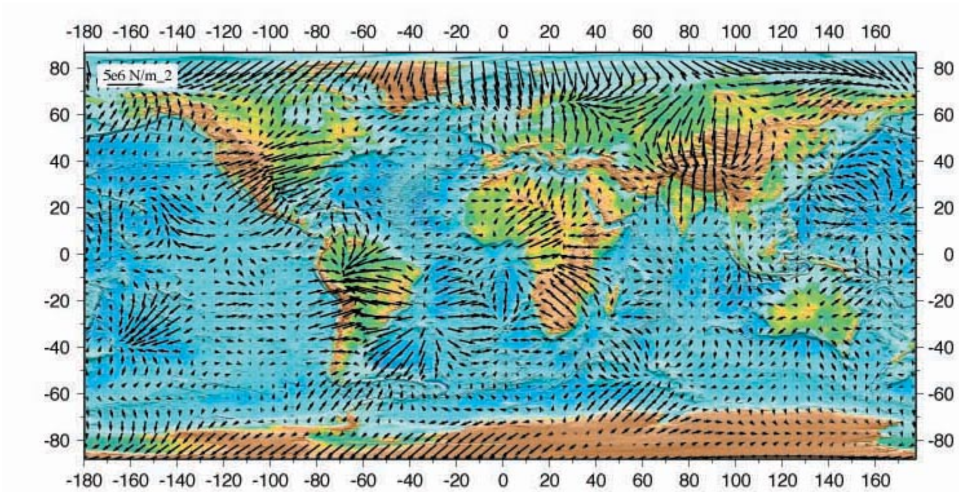

Figure 1. Distribution of basal tractions obtained from inversion. The best-fit traction solution is obtained by expanding potentials in spherical harmonics with truncation at l=m=9, solving force-balance for each input distribution of potential to obtain the stress field basis functions, and then finding the coefficients for all basis functions that minimize the misfit function between total deviatoric stress field and observed deformation indicators. The deviatoric stress field associated with the best-fit distribution of basal tractions is added to the deviatoric stress field associated with lithospheric gravitational potential energy differences. The total deviatoric stress field is scored with the Global Strain Rate Map.

The influence of mantle circulation on continental deformation has remained a controversial topic in geophysics. Tractions associated with density buoyancy driven mantle circulation can couple to the base of the lithosphere. These basal tractions can thus have a profound influence on the state of stress and strain within the continental lithosphere. Nevertheless, a wide range of models exist, ranging from basal tractions being unimportant as a driving mechanism for continental deformation to basal tractions playing a dominant role in continental deformation. Seismic tomography models continue to improve in resolution and provide constraints for making inferences on density buoyancy variations at a variety of depths and length-scales, thereby enabling the quantification of mantle circulation patterns, basal traction distributions, and lithospheric deviatoric stress and strain rate patterns. Moreover, structural variations in the lithosphere itself, including crustal thickness variations, and the geometry and density distribution of continental keels, are also vitally important for understanding the lithosphere deviatoric stress field because these define lithospheric gravity potential energy differences. Seismic anisotropy patterns also yield constraints on the nature of coupling between mantle circulation and the continental lithosphere beneath regions such as western North America and central Asia. In this paper we will review existing models for coupling in western North America, as well as for some other regions of continental deformation. We will present results from global dynamic models that address mantle circulation and the detailed lithosphere deviatoric stress field response to both basal tractions and to lithospheric gravity potential energy differences. The total deviatoric stress field response is scored with deformation indicators, consisting of the strain rate tensor components from the World Strain Rate Map. Models to date show that basal tractions, of order 2-3 MPa, most likely associated with mantle circulation set up by subducted density buoyancies (Farallon Slab) beneath North America, have a significant influence on the deviatoric stress field there. Likewise, beneath central Asia there appears to be a need for downwelling mantle zones, also most-likely associated with old subducted lithosphere. Results show north-directed tractions beneath the Indian subcontinent and southern Tibet, south-directed tractions beneath north-central Asia, and a convergence of these tractions beneath northern Tibet (1-2 MPa; Figure 1). These tractions likely play a major role in driving India into the Eurasian continent. The important role of basal tractions associated with mantle circulation must be reconciled with the obvious problem of a possible weak lower crust and uppermost mantle beneath some zones of continental deformation. Such a weak crust beneath the seismogenic zone, for example, may decouple deformation there from deeper zones of deformation in the mantle. It should be emphasized that basal tractions associated with mantle flow act over very long length-scales, and that for the purpose of regional modeling the influence of these tractions may be equivalently approximated using either stress or velocity boundary conditions.

CALREF, A STABLE REFERENCE FRAME FOR THE NORTHERN CALIFORNIA

Nicolas Houlié, Barbara Romanowicz · University of California, Berkeley

The San Francisco Bay area (SFBA) is one of the most actively deformed areas in California. A large part of the deformation (75 %) between the north American plate and the Pacific plate is accommodated along faults lying in a land stripe of about 50 km width. At least two major events (Mw>6.5) are expected along two major faults: the San Andreas and the Hayward fault. Possible triggering between the two events is not excluded. Since 1994, the Berkeley Seismological Laboratory has been involved in collecting and processing data from the cooperative regional BARD network of permanent GPS receivers (Bay Area Regional Deformation network, reference: Murray et al., 1998).The Berkeley Seismological Laboratory (BSL) currently maintains 30 BARD sites and is in the process of upgrading its infrastructure so that it better responds to the needs of earthquake hazards related research, and in particular the use of GPS data in real-time. Most of the BARD stations operated by BSL are collocated with seismic instruments (broadband seismometers or geophones) or strain-meters. We present here for the first time the BARD GPS sites velocities computed in the ITRF2000 (Altamimi et al, 2002) from the data collected from 1994 to present. The velocity field highlights the deformation across the two main active faults in the SFBA. We have compared our results with the velocity field obtained from previous studies and obtained good agreement. In particular the ITRF2000 and the BAVU (d'Alessio et al., 2005) velocities will be discussed. Additionally, we discuss the velocities of sites belonging to the recently installed "mini-PBO" network which contribute to constraining the extent of the locked section on the northern part of the Hayward fault.

IRIS UNDERGRADUATE INTERNSHIP PROGRAM AND ORIENTATION ENTERS ITS SECOND YEAR

Michael Hubenthal · IRIS
Rick Aster · New Mexico Tech

The 2006 IRIS undergraduate internship class, representing ten different US institutions, participated in the first intensive orientation from May 28th to June 3rd, 2006 at New Mexico Tech in Socorro, New Mexico.

This orientation, hosted by the NMT Geophysics Program and the IRIS PASSCAL Instrument Center, was a new addition to an existing internship program supported by the National Science Foundation (EAR-0453427).

Through this funding the IRIS Education and Outreach program is developing a novel approach to internships that blends the spirit of traditional Research Experience for Undergraduates (REU) programs, which traditionally host participants in a single location, with IRIS's successful experiences

hosting undergrad students at widely separated institutions where they work closely with individual researchers (Hubenthal /et al.,/ 2004). This blending is being achieved through the development of a diverse week long group orientation experience, the use of web-based communications technology,

and other enhancements based on the program's ongoing evaluation and assessment efforts. Key features of this new model of undergraduate intern education are:

- One-on-one mentoring by researchers at IRIS institutions
- Developing a learning community among interns through both face-to-face and virtual interactions,
- Developing interns' abilities to self-evaluate and work independently, through carefully designed web-based tools,
- Increasing interns' awareness of the IRIS community and its activities,
- Introduction to professional career opportunities in Earth science.

Thus, beginning with the 2006 and 2007 internship classes, IRIS seeks to evolve a refined internship program for students that features the desirable characteristics of a traditional REU program, enhanced through both individual mentoring and remote peer collaboration

that closely represents the intensive computer and networking culture of modern scientific research.

BACK-PROJECTION IMAGING THE RUPTURES OF THE NOVEMBER 15, 2006 AND JANUARY 13, 2007 KURIL EARTHQUAKES

Alexander Hutko · UCSC
Thorne Lay ·

Back-projection of energy to grid points assumed to act like point sources at different times allows us to image the direction and propagation of recent Mw 8.1 and Mw 8.3 earthquakes in the Kuril Islands. We use high frequency P-waves recorded by USArray and other arrays across the globe with sufficient aperture to track the rupture front where high frequencies originate. While energy from the rupture front away from the hypocenter arrives buried in the coda of the first arrival, its moveout in time is unique and back-projects to a narrow region. Nth root stacking is used to raise these weak but coherent arrivals above the noise level. Travel time corrections specific to each station for both events are calculated by picking first arrivals for the January event. First arrivals for the November event are very emergent and difficult to pick. These corrections eliminate artifacts introduced by receiver side structure and using the same corrections for these similarly located earthquakes allows us to confidently image the November event. Some of our results for the November event are consistent with coseismic triggering on the outer rise where many aftershocks have been located. Results using USArray data for the January event show rupture propagating towards North America, presumably along strike. Results using ORFEUS data show secondary features originating ~30 seconds after the main rupture initiation, but offset by at least 100 km to the Northwest. Given its large offset from the hypocenter, it is difficult to reconcile this as part of the main rupture and may be evidence for triggering of smaller earthquakes downdip.

LITHOSPHERE TEMPERATURE, STRENGTH, AND DEFORMATION IN W. NORTH AMERICA & EARTHSCOPE

Roy Hyndman, Stephane Mazzotti · Geological Survey Canada
Claire Currie · Dalhousie University

Deformation of the lithosphere, mountain building, and earthquakes are controlled by the combination of driving forces mainly transferred from plate boundaries, and variations in lithosphere strength. Driving forces may be obtained from forces generated by different types of plate boundaries and maps of gravitational potential. Plate Boundary Observatory GPS stations have greatly increased the spatial resolution of current deformation in Western North America. Strain maps based on western North America GPS and other current deformation data may then be compared to maps of driving forces and of lithosphere strength estimators.

The primary control of lithosphere strength and thickness appears to be temperature. Variations in composition and other factors have second order influence. Therefore, mapped temperature indicators or proxies should be at least qualitatively correlated with the distribution of deformation rates. There are a number of deep temperature constraints; the most familiar is surface heat flow. However, heat flow data irregularly distributed, are subject to many disturbing effects, and deep lithosphere temperatures derived from heat flow data are strongly influenced by upper crustal radioactive heat generation which affects the surface heat flow but makes a limited contribution to deep temperature. Other semi-quantitative constraints on lithosphere thermal structure come from the occurrence of basaltic mantle-derived volcanism that suggests temperatures near the solidus at shallow depth, surface elevation and crustal thickness data in isostasy, maximum depth of seismicity, depth to Curie temperature, and P-T estimates of upper mantle xenoliths. Xenoliths provide quantitative temperature-depth estimates in cratons but the lack of garnets in the western North America Cordillera and other high temperature regions means that depths of origin (pressure) are poorly constrained.

We examine the pattern of the two best temperature indicators with regional coverage, temperature-dependent mantle velocities (Vs and Vp), and lithosphere effective elastic thickness (Te). EarthScope is providing much improved constraints on Vs and Vp. Temperature appears to be the dominant control of upper mantle velocity; the effects of composition, partial melt, and anisotropy, etc., usually are much smaller. Temperatures just below the Moho can be estimated from Moho head wave velocities (Pn). The high temperature Cordillera generally has Pn velocities of less than 7.9 km/s in contrast to over 8.1 for stable cratonic areas. This parameter has the limitations of highly variable data density, sampling the sometimes heterogeneous mantle just below the Moho, and common seismic anisotropy. More spatially uniform although low resolution sampling of upper mantle Vs is available from surface wave seismic tomography, which gives velocities and inferred temperatures as a function of depth. The other useful temperature-related parameter is lithosphere effective elastic thickness obtained by the coherence of 2D gravity and topography data. The elastic thickness of continental lithosphere is primarily controlled by temperature, and it is also closely related to the lithosphere total strength and therefore to its susceptibility to tectonic deformation and earthquakes.

Both the Vs and Te distributions are strongly bimodal. As previously found globally, Te is less than 20 km for the high temperature Cordillera and over 100 km for the adjacent cold stable North American Craton. Only intermediate thermal regimes have intermediate Te that suggests a weak layer in the lower crust over a stronger upper mantle. We have compared the Vs tomography with the Te data to examine the consistency of these two temperature proxies. There is excellent general agreement, although there are important local differences. Strength envelopes based on the temperatures from Vs tomography and rheologies from laboratory data correspond to the observed Te for thermal regimes with temperatures at the Moho of 800-900C for the Cordillera and 400-500C for the Shield. From the total estimated lithosphere strengths, it is clear that the Cordillera (and other continental backarcs) is weak enough to be deformed by plate boundary forces, whereas cratons are generally much too strong. The temperature-strength boundary is close to the Rocky Mountain front. In the Cordillera, the upper mantle is too hot for brittle failure and earthquakes occur only in the upper 10-15 km of the crust. In the cool craton, earthquakes occur rarely if at all in the upper mantle because the total lithosphere strength is too great for significant deformation by plate tectonic forces.

Important previous estimates have been made of the correlation between the distribution of driving forces and the pattern of deformation in western North America. The temperature proxy data from tomography Vs (and Vp), and effective elastic thickness Te, now allows us to estimate the second control on deformation, the spatial distribution of lithosphere strength.

EARTHSCOPE MAGNETOTELLURICS - WHAT NEXT?

Shane Ingate · IRIS

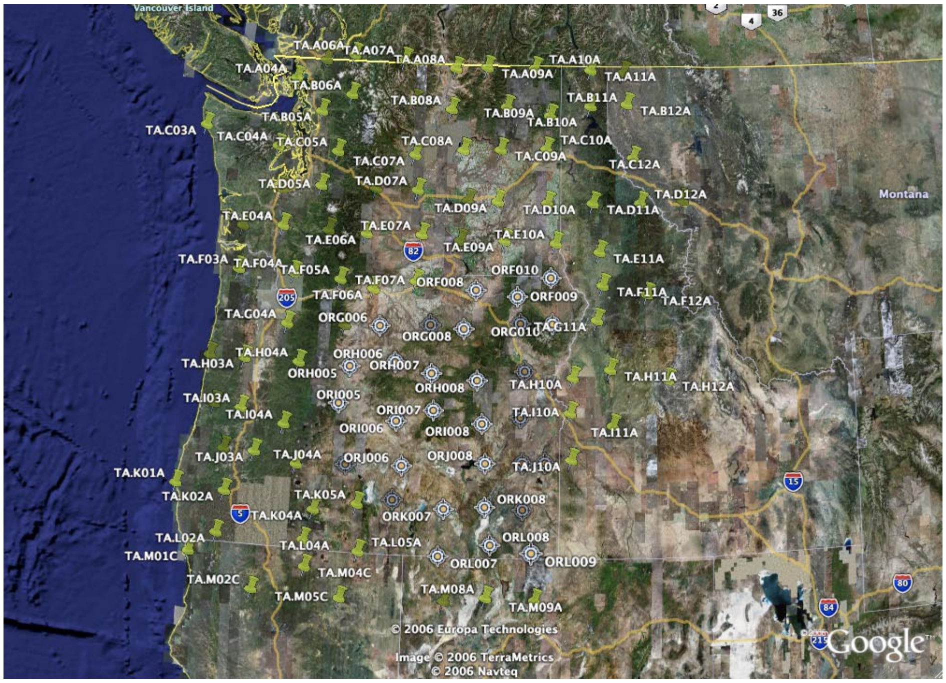

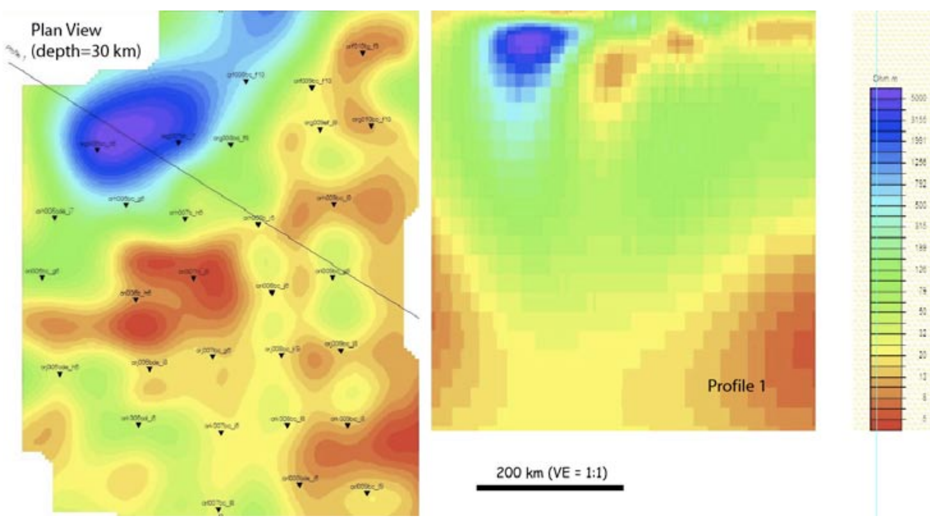

Map showing 2006 MT campaign sites (stars), and proposed 2007 campaign sites (push-pins)

Preliminary 3-D inversion of the 2006 MT data shows a plan view at a depth of 30 km, along with a profile from NW to SE.

The IRIS consortium (http://www.iris.edu), in conjunction with the ElectroMagnetic Studies of the Continents (EMSOC) consortium (http://emsoc.ucr.edu/emsoc/) is installing 7 permanent magnetotelluric (MT) stations across the contiguous US as part of EarthScope/USArray. In addition, IRIS will conduct a campaign of installing temporary MT sites on a 70 km grid in regions of scientific interest throughout the EarthScope Project.

During the Summer of 2006, IRIS, University of California Riverside, University of Oregon, Oregon State University and GSY-USA deployed 10 MT systems at 30 sites uniformly distributed throughout Oregon east of the Cascades, coincident with the High Lava Plains and Wallowa temporary seismic experiments. In 2007, this experiment will be continued with coverage extending west of the Cascades, Washington state, and trending east towards Yellowstone.

This poster discusses opportunities for transportable MT campaigns during 2008-2013, notably within the context of

(OVER) HALFWAY THERE: A PLATE BOUNDARY OBSERVATORY PROGRESS REPORT

Mike Jackson, Greg Anderson, Karl Feaux, David Mencin, Brian Coyle, Barrett Friesen, Katrin Hafner, Michael Hasting, Wade Johnson, Ben Pauk, Chris Walls, Chuck Meertens · UNAVCO

The Plate Boundary Observatory (PBO), part of the NSF-funded EarthScope project, is designed to study the three-dimensional strain field resulting from deformation across the active boundary zone between the Pacific and North American plates in the western United States. To meet these goals, UNAVCO will install 880 continuous GPS stations, 103 borehole strainmeter stations, 28 tiltmeters, and five laser strainmeters by October 2008, as well as manage data for 209 previously existing continuous GPS stations through the PBO Nucleus project and 11 GPS stations installed by the USArray segment of EarthScope.

As of February 2007, UNAVCO had completed 519 PBO GPS stations and had upgraded 73% of the planned PBO Nucleus stations. Highlights of the past year's work include the expansion of the Alaska subnetwork to nearly 70 continuously-operating stations, including coverage of Akutan and Augustine volcanoes and reconnaissance for future installations on Unimak Island; the installation of nine new stations on Mt. St. Helens; and the arrival of 33 permits for station installations on BLM land in Nevada. The Augustine network provided critical data on magmatic and volcanic processes associated with the 2005-2006 volcanic crisis, and has expanded to a total of 11 stations. Please visit http://pboweb.unavco.org/?pageid=3 for further information on PBO GPS network construction activities.

UNAVCO is also installing and operating the largest borehole seismic/strainmeter network in North America, as well as tiltmeters and laser strainmeters. As of February 2007, 27 PBO borehole stations had been installed and three laser strainmeter stations were operating, with a total of 60 borehole stations and 4 laser strainmeters expected by October 2007. In response to direction from the EarthScope community, UNAVCO installed a dense network of six stations along the San Jacinto Fault near Anza, California, and has densified coverage of the Parkfield area. During Fall 2006, the first PBO borehole tiltmeters were installed on Mt. St. Helens, and in Spring 2007, they will be joined by the first PBO volcanic borehole strainmeter stations. Please visit http://pboweb.unavco.org/?pageid=8 for more information on PBO strainmeter network construction progress.

The combined PBO/Nucleus GPS network has now provided almost 220 GB of raw data, with special downloads of more than 130 GB of high-rate GPS data following large earthquakes in Russia and the Tonga Islands, as well as for community requests. The standard-rate GPS data are processed routinely to generate data products including station position time series, velocity vectors, and related information, and all data products are available from the UNAVCO Facility archive. The PBO seismic network seismic network has provided 105 GB of raw data, which are available from the IRIS Data Management Center (DMC). The PBO strainmeter network has provided 45 GB of raw data, available in both raw native format and SEED format from the Northern California Earthquake Data Center and the IRIS DMC, along with higher-level products such as cleaned strain time series and related information. Please visit http://pboweb.unavco.org/gps_data and http://pboweb.unavco.org/strain_data for more information on PBO GPS and strainmeter/seismic data products, respectively.

FUTURE DEVELOPMENTS IN THE GEON WORKFLOW-BASED TOOL FOR LIDAR PROCESSING AND ANALYSIS

Efrat Jaeger-Frank, Viswanath Nandigam, Ashraf Memon, Ilkay Altintas, Chaitan Baru · San Diego Supercomputer Center
Christopher J Crosby, J Ramon Arrowsmith · Arizona State University

The Geosciences Network (GEON) is an NSF-funded large Information Technology Research (ITR) project to facilitate collaborative, inter-disciplinary science efforts in the earth sciences. One of the challenging tasks that GEON has focused on is the distribution, processing and analysis of LiDAR (Light Distance And Ranging) point cloud datasets. The massive volume of data associated with LiDAR makes internet-based access to these community datasets difficult and pushes the computational limits of typical data distribution and processing systems. Over the past two years, we have developed a three-tier architecture–called the GEON LiDAR Workflow (GLW)–to facilitate community access to LiDAR datasets. The GLW uses the GEON portal, a workflow system based on the Kepler scientific workflow environment, and a set of services for coordinating distributed resources using emerging Grid technologies and the GEONGrid clusters. GLW is available to the community via the GEON portal and is already in active use as an efficient and reliable LiDAR data analysis tool.

The increasing popularity of the GLW has imposed new requirements on the system for better load balancing, increased robustness of the system, and more system monitoring information. For example, users are interested in tracking the execution state of their LiDAR processing job in real time. A number of new features are being added to GLW to address these requirements. We use the Kepler "provenance" capability, which collects job provenance data, to enhance GLW's job monitoring interface to provide users with live job status monitoring. The data provenance is also useful when publishing results and sharing GLW products among scientists. In addition, we are working on replicating the processing services originally deployed on a GEON cluster at Arizona State University, to additional clusters for system load balancing and failover. This includes deployment of a similar cluster both at the San Diego Supercomputer Center and at UNAVCO in Boulder, CO. With multiple processing clusters we plan to utilize a Grid scheduler to map jobs onto the Grid clusters by taking into account the availability of the corresponding compute, storage, and networking resources. With these enhancements we expect to make GLW more robust and useful to a wide range of earth science users.

GLW currently has 117 registered users who have submitted a total of 1245 LiDAR processing requests which result in a total of over 500 Gigabytes of data.

UBIQUITOUS LOW-VELOCITY LAYER ATOP THE 410-KM DISCONTINUITY IN THE NORTHERN ROCKY MOUNTAINS

John Jasbinsek, Ken Dueker · University of Wyoming

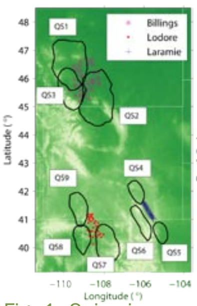

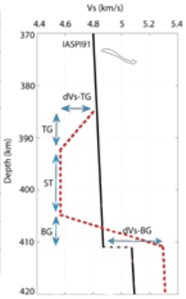

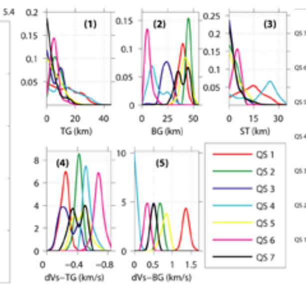

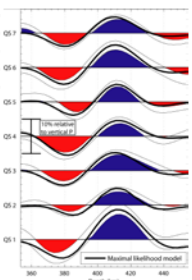

Fig. 1. Seismic arrays, sampling of 410 km discontinuity region, and topography. Black lines contour the piercing points of the P-S conversions at 410 km depth for the three well-sampled back-azimuth quadrants (NW, SW, and SE) for each of the three seismic arrays denoted in the legend. Labels correspond to the quadrant stack (QS) numbers labeled in Figure 2. Each array consisted of 30 broad-band seismic stations operating for 10 months.

Fig. 2. Double gradient slab (DGS) model parameterization. The IASPI91 velocity model is indicated by the solid black line with a DGS velocity model indicated by the dashed red line. The five model parameters are: TG, top gradient thickness (km); ST, constant velocity slab thickness (km); BG, bottom gradient thickness (km); dVs-TG, shear wave velocity decrease for top gradient (km/s); dVs-BG, shear wave velocity increase for bottom gradient (km/s). The value of dVs-BG is the velocity increase with respect to the IASPI91 model value immediately above the 410 km velocity step. The DGS model space consists of 116,160 parameter states: TG = [0:5:45] km; ST = [0:5:35] km; BG = [0:5:55] km; dVs-TG = [-0.84:0.084:0] km/s; dVs-BG = [0:0.168:1.68] km/s.

Fig. 3. Overlay of best fitting waveforms and observed waveforms. The modeled QS 1-7 are lined up on the mean 410 km discontinuity depth (415 km). Significant variation in the 410-LVL is observed. The maximum likelihood model fits the peaks and troughs in each case. However, broader 410 arrival pulses are less well fit (QS 2, 3 and 7) reflecting the fact that the simple DGS models can not capture second-order velocity features of the 410-LVL.

Fig. 4. 1-D marginal probability distributions for QS 1-7. For each model parameter subplot, the seven 1-D marginal probability distributions are overlain. Model parameters display a range of values in the best fits of each QS. However, significant overlay is seen in subplots (1) and (4).

Receiver functions (RF) from three 30-station IRIS-PASSCAL small aperture arrays (2-15 km station spacing) operated for ten months each in the northern Rocky Mountains show a ubiquitous negative polarity P to S arrival (NPA) just preceding the 410-km discontinuity arrival. Data from each of the three arrays was divided into NW, SE and SW backazimuths and stacked to form nine well sampled quadrant stacks (QS). Remarkably, the NPA is apparent in 8 of the 9 QS, with 7 of the 8 displaying a similar dipole shape (paired negative and positive swings). Each QS contains well resolved P to S arrivals from the 410- and 660-km discontinuities. All these arrivals display the correct moveout.

To model the NPA, a "double gradient slab" model consisting of five parameters is used: top gradient thickness and shear wave velocity drop; a constant velocity layer; bottom gradient thickness and shear wave velocity increase. Model misfit is assessed via a grid search over the model space using a reflectivity code to calculate synthetic seismograms. Assessment of model likelihood is done by calculating 1 and 2-D marginal probability density functions (PDF). Model parameters for each QS are generally well resolved with modest correlations observed between the top and bottom velocity gradients and slab thicknesses. Although the 1-D marginals display a range of peak values, the 1-D PDFs show significant overlap in the top gradient thickness and velocity decrement. Multiplying the 1-D PDF together to form an average distribution reveals that at 90% probability: the top gradient thickness is <6.4 km with a shear velocity decrease of 8.9%. The effective width of the low velocity layer atop the 410 (herein called the 410-LVL) is characterized as the layer thickness plus half the two gradient widths. Thus, the 410-LVL is found to have a mean thickness of 22.5 km and a mean shear wave velocity decrement of 8.9% (corresponding to a 4.0% melt porosity assuming the uppermost mantle melt-velocity scaling of Kreutzmann et al., 2004).

Physical explanations for the origin of this 410-LVL suggest that temperature and/or compositional effects are unlikely causes. The positive Claypeyron slope associated with the 410 km discontinuity is expected to enhance thermal convection; thus, no thermal boundary layer or ponding of chemical heterogeneity is expected (as opposed to the 660). While a layer of oceanic crust could produce a low velocity anomaly, again the 410 km discontinuity is not expected to trap chemical heterogeneity; thus, ascribing the ubiquitous 410-LVL to oceanic crust would be serendipitous. Dipping layers or anisotropic velocity contrasts are unlikely to cause the observed velocity contrasts because the tangential QS are quiet.

Therefore, in conjunction with a growing body of similar observations [Revenaugh and Sipkin, 1994; Vinnik & Farra, 2002; Vinnik et al., 2003; Song et al., 2004; Gao et al., 2007 in press] we suggest our results are most consistent with the "water-filter" model [Bercovici and Karato, 2003] which predicts a layer of partial melt atop the 410 resulting from the melting of hydrous wadsleyite as it upwells across the 410. Finally, preliminary data analysis from the linear, long aperture (~ 900 km) RISTRA array displays similar 410-LVL arrivals. The 410-LVL is observed intermittently along the length of the array in approximately 200-km intervals, further supporting a pervasive albeit heterogeneous expression of the "water-filter" induced by a 410 melt-layer beneath the western U.S.

A 3D EARTHQUAKE CYCLE MODEL FOR THE SAN FRANCISCO BAY AREA

Kaj Johnson, Junichi Fukuda · Indiana University
Paul Segall · Stanford University

We use geodetic data and 3D earthquake cycle models to estimate the distribution of slip on strike-slip and reverse faults in the San Francisco Bay Area. Current GPS velocities and calculations of strain following the 1906 earthquake from triangulation data are inverted for fault slip using a new 3D viscoelastic earthquake cycle model consisting of elastic blocks bounded by faults in an elastic lithosphere overlying a viscoelastic asthenosphere. The model is similar to 3D elastic block models in that a “steady-state” deformation field is assumed to exist in the absence of fault locking and interseismic deformation is modeled as a perturbation to the steady-state field due to back slip on locked portions of faults and viscous flow in the asthenosphere in response to past earthquakes. A fundamental difference between this model and previously developed block models is that the steady-state deformation field includes vertical motion due to slip on dipping faults and accumulation of strain within the blocks near the bounding faults due to non-planar fault geometry. In addition to fault slip, we estimate earthquake recurrence times, times since the last earthquake, asthenosphere viscosity, and elastic lithosphere thickness. We formulate the inverse problem in a Bayesian framework incorporating geologic estimates of fault slip and recurrence times of earthquakes as Gaussian prior distributions. We use a Monte Carlo Metropolis algorithm to sample the posterior distributions of the target parameters. We find the timing of past earthquakes is not well resolved. The inversion refines estimates of slip rates on major strike-slip faults; the standard deviations of posterior slip rate distributions are significantly smaller than prior estimates from geology. If prior information from geology is not used in the inversion, estimated slip rates are significantly lower than geologic estimates, indicating the importance of incorporating prior information. Dip-slip rates of 0-10 mm/yr are possible on reverse faults in the Santa Cruz Mountains, southern Hayward fault region, and the Peninsula region.

THE BOSTON COLLEGE EDUCATIONAL SEISMOLOGY PROJECT: INVITING STUDENTS INTO THE WORLD OF SCIENCE RESEARCH

Alan Kafka, Anastasia Macherides-Moulis, Leslie Campbell, Barbara Sheffels, Michael Barnett, John Ebel, Dina Smith · Boston College
Stephen Swift · Woods Hole Oceanographic Institution

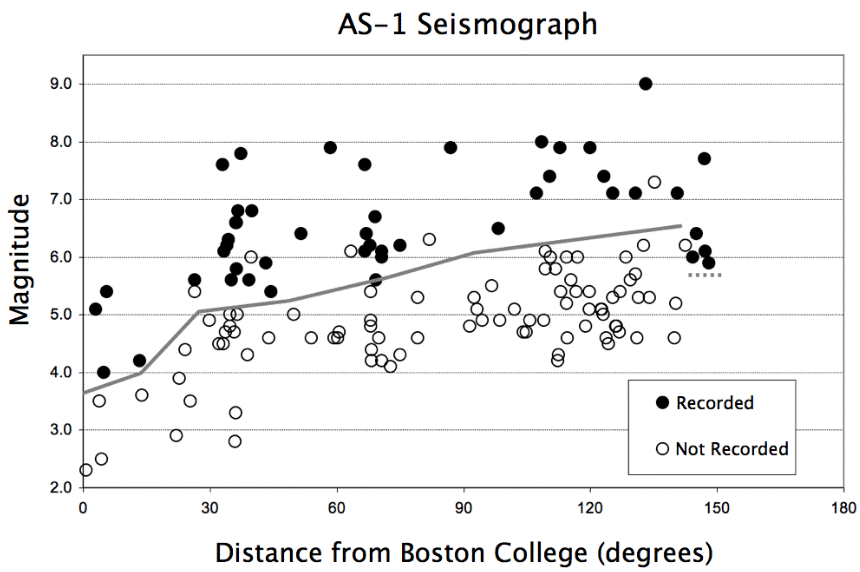

Plot of earthquakes recorded (closed circles) versus not recorded (open circles) by the AS1 seismograph operating at Boston College. The grey curve is an estimate of the threshold for how big an earthquake must be at a given distance in order for the AS1 to record it at this site.

The Boston College Educational Seismology Project (BC-ESP) operates an educational seismic network in Massachusetts, consisting of AS1 seismographs located at eighteen K-12 schools, as well as at the Boston College campus, Weston Observatory, and Smith College. This project uses seismology as a medium for inviting students into the world of science research by inquiry-based learning through investigation of earthquakes recorded by seismographs in their classrooms. Seismology is an interdisciplinary science that requires understanding a wide range of scientific concepts, and seismology also teaches students how the natural environment impacts society. Thus, the BC-ESP offers numerous possibilities for introducing students to the nature of scientific inquiry and to the importance of science in their everyday lives. Having their own seismograph in the classroom gives students a way of collecting real-world data and making measurements that directly relate to the internal structure of the Earth and to processes by which the Earth changes. The BC-ESP provides curriculum resources and research experiences for K-12 and undergraduate students, and encourages a culture of scientific inquiry in K-12 schools and college classrooms.

THE SPADE SEARCHABLE PRODUCT ARCHIVE

Linus Kamb, Rob Casey, Tim Ahern · IRIS

The IRIS Data Management Center (DMC) is expanding the services it provides to the geoscience community. Traditionally a permanent archive of seismic data and other timeseries-oriented data, the DMC is leveraging its experience and facilities to provide a community-oriented permanent data product archive. The Searchable Product Archive and Discovery Engine (SPADE) will support a broad variety of derived data products from many different disciplines. The development of SPADE was motivated by IRIS' involvement in the USArray component of EarthScope. Leveraging XML technologies, the SPADE product archive allows arbitrary products to be defined, submitted, and then queried for, by both common fields and arbitrary product-specific metadata fields through a single uniform interface. The common metadata fields are defined to support queries across all product types by standard geographic-, time-, and publishing-oriented attributes. The product-specific query interface allows a researcher to precisely filter result sets by criteria that are possibly relevant only to the particular product. The archive also supports metadata-only submissions that link to external resources, providing the same product- specific query interface for external resource discovery. Researchers will be able to discover a myriad of data sources as well as dig deeply and specifically into a particular resource archive through a single interface. SPADE provides both a browser-based interactive interface as well as a web services-based programmatic interface. In this way, it can easily act as a component within other systems, including the recent GeoWS integrated discovery tool and upcoming service-oriented development efforts at the IRIS DMC.

COLORADO ROCKIES EXPERIMENT AND SEISMIC TRANSECTS (CREST): CENOZOIC UPLIFT, MAGMATISM, AND MANTLE TO SURFACE FLUID INTERCONNECTIONS ASSOCIATED WITH THE ASPEN ANOMALY

Karl Karlstrom, Laura Crossey, Cristina Takacs-Vesbach · University of New Mexico
Rick Aster, Jon MacCarthy, Matt Heizler · New Mexico Tech
David Hilton · Scripps
Ken Dueker · University of Wyoming

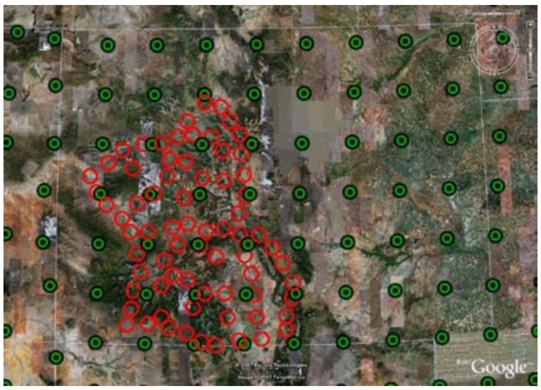

Figure 1. Location of planned IRIS PASSCAL broadband stations for the 2008-2009 CREST experiment (red circles) superimposed on the nominal 70-km-spacing of the USArray stations in Colorado. Through close coordination with the USArray component of EarthScope, approximately 10 of the USArray stations will be located at the nearest CREST sites to compose an array of ~ 70 stations for 3-D imaging of the Aspen Anomaly.

Three independent surface wave images suggest that the upper mantle beneath the Colorado Rocky Mountains has an overall low seismic velocity < 4.2 km/s: consistent with a temperature that is at or near the dry solidus of peridotite. At higher resolution, vintage body wave tomographic images suggest that central Colorado is underlain by an enigmatic low velocity mantle that we refer to as the Aspen Anomaly. This anomaly is similar in spatial scale (though not as low a velocity) to the Yellowstone anomaly. It is characterized by very sharp velocity transitions and is a key element for understanding the heterogeneous ~100-km-scale mantle velocity variations of the Rocky Mountain region and the western U.S. The geometry and tectonic history of the Aspen Anomaly are being evaluated through an integrated experiment involving: 1) 3-D passive IRIS PASSCAL-supported imaging (60 stations), with data collection planned for 2008-2009 across the Aspen anomaly and San Juan volcanic field; this is being closely integrated with USArray stations (10 stations; Fig. 1); 2) geologic and thermochronologic studies of the uplift history of the highest elevation region of the Colorado Rockies, which generally overlies the anomaly; and 3) studies of mantle to surface interconnections via mantle degassing, hydrochemistry, and neotectonics. Present seismic data suggest that the lowest mantle velocities may coincide with the intersection of the NE-trending Proterozoic Colorado mineral belt and the NNW-trending extension of the Rio Grande rift (Fig. 2). This geometry aligns the Aspen anomaly with both a dipping Proterozoic paleosuture zone in the lithosphere and with the Cenozoic San Juan volcanic field and/or the northern tip of the Rio Grande rift system. This suggests a geodynamic process in which Cenozoic and still-active asthenospheric upwelling is focused by ancient compositional heterogeneity in the lithosphere, implying important feedbacks between Cenozoic asthenospheric small-scale convection and ancient lithospheric composition and rheology.

These provocative time-space correlations between Cenozoic rock uplift and denudation patterns, magmatism, modern hydrothermal systems, and the modern day mantle anomaly indicate that the Aspen anomaly may have been an active tectonic feature of the southern Rockies throughout the Cenozoic. Magmatism in central Colorado has been episodic, and includes Laramide volcanism of the Colorado mineral belt, Yellowstone-sized volumes of Oligocene volcanics centered on the anomaly (San Juan volcanic field) and post-10 Ma basaltic magmatism at the edges of the anomaly. The highest peaks of the Colorado Rockies are located above the mantle anomaly and major drainage is radial away from the anomaly suggesting broad mantle-driven epeirogenic surface uplift above the anomaly. Quaternary faults in Colorado follow both rift- related NNW trends and NE trends suggesting that epeirogenic uplift may be expressed in the crust as block movements in a segmented lithosphere above the buoyant mantle domain. Mantle degassing and high heat flow through hot springs and CO_2 springs indicate continued mantle devolatilization. Highest 3He/4He values are up to 2.17 Ra (~0.25 of MORB) at Poncha Pass at the north end of the Rio Grande rift, and mantle 3He/4He values ranging between 0.1 to 2.17 Ra are detected in almost all the hot springs in Colorado, indicating active mantle degassing. Gas compositions are dominated by CO_2 (up to 99 %); hydrogen and reduced sulfur are also present. CO_2/3He ranges from 107 to 1012, and 13C values range from -2 to -10‰. Aqueous geochemical modeling indicates that considerable external carbon is present (up to 0.02 mol/L) and that these springs represent a flux of deeply-sourced carbon to the atmosphere (at 1800 l/s, Glenwood Springs emits 109 mol C/yr). High CO_2 abundance, hydrogen, and a suite of redox-sensitive trace components offer a chemically-rich setting for a diverse microbial community. These springs are geochemically analogous to the chemolithotrophic microbial ecosystems associated with mid-ocean ridges, hence we refer to them as “continental smokers”. Analysis of microbial community small sub-unit ribosomal RNA genes by DNA sequencing is underway to test for differences among the sites and the presence of microorganisms utilizing similar metabolic pathways to those found in oceanic hydrothermal settings and Yellowstone. The emerging data and the ongoing experiment offer rich potential for understanding ongoing and dynamic mantle to surface interconnections and feedbacks between (from the bottom up): mantle dynamics, lithospheric heterogeneity and reactivation, Cenozoic orogenesis and magmatism, microseismicty, tectonic geomorphology, microbiology of extreme life forms, hydrothermal systems, and groundwater quality.

REGIONAL GEOPHYSICAL ANALYSES TO PATCH TOGETHER THE PIECES OF THE GEOSWATH

Randy Keller, Benjamin Drenth, Mai Ha, Evan Hamilton, Maxwell Okure, Jessica Pardo, Roderick Perez, Angelo Sipuikinene · University of Oklahoma

The GeoSwath concept is to create an integrated analysis of the structure and evolution of the lithosphere within a coherent swath that extends from coast to coast. A major goal of this effort is to provide links between mapped geologic features, major structures in the upper crust, and deeper structures and thus provide an improved understanding of the structure and evolution of North America. Databases of gravity and magnetic data have recently been complied for the U.S., and their analysis provides one way to attain an initial look at the major structures in the upper crust across the continent. We have created a series of gravity and magnetic maps of the areas that together constitute the GeoSwath. When viewed together, these maps display many correlations with mapped geologic features that provide indications of the magnitude and lateral extent of these features. They also reveal relationships between known geologic features and anomalies whose geologic interpretation is not clear. In the latter case, these maps suggest areas and features worthy of further attention during the life of EarthScope.

IMMERSIVE VIRTUAL REALITY FOR INTERACTION AND VISUALIZATION OF 3D GEOPHYSICAL DATA

Louise Kellogg, Magali Billen, Eric Cowgill, Bernd Hamann, Oliver Kreylos, Margarete Jadamec · University of California, Davis
Gerald Bawden · U.S. Geological Survey

The large quantities of data generated by EarthScope create a challenge for scientists to process, manipulate, and interpret data. We are developing and using interactive visualization software to view, interact with, and manipulate geophysical and geologic data and associated geodynamics simulations. The innovation of our approach is highly effective use of human interaction in immersive 3D virtual reality (VR) environments. We tailor our visualization approach to the specific scientific problems to build on each visualization method's strengths, using both 3D perception and interaction with data and simulations, to take advantage of the skills and training of geoscientists exploring their data in the VR environment. In the process, we are developing a suite of tools that are adaptable to a range of scientific problems. We will demonstrate our approach on several geophysical datasets, including geodetic data and earthquake hypocenters. Virtual mapping tools allow virtual "field studies" in regions that are inaccessible to human geologists. A LiDAR viewer allows the user to be fully immersed in ground-based and airborne point cloud data to assess data quality and to analyze complex targets that lack detail in 2D non-VR visualizations. Visualizing 3D data enables us to construct and identify features in a flexible, intuitive environment. Interactive tools allow us to manipulate shapes, while feature extraction tools support quantitative measurement of structures that emerge from the data. Our software, Visualizer, runs in a range of 3D VR environments (e.g., GeoWall, ImmersaDesk, CAVE), and it has been demonstrated to provide advantages over other commonly used methods. Additional information about our work can be found at www.keckcaves.org.

RESULTS OF ELEMENTAL, STABLE ISOTOPE, ORGANIC MATTER, AND FISSION-TRACK ANALYSES OF SAFOD DRILL-HOLE CUTTINGS AND CORE MATERIAL

David Kirschner · Saint Louis University
John Solum · Sam Houston State University
Judith Chester, Fred Chester · Texas A&M University
Stephen Hickman, Diane Moore · U.S. Geological Survey
John Garver · Union College
Jim Evans · Utah State University

Geochemical analyses of cuttings and core material from the SAFOD drill hole provide important information on the subsurface geology and the fluid-rock interactions that have occurred in and adjacent to the fault zone. We have obtained an integrated geochemical data set from the main drill hole that includes elemental data (exceeding 120 samples), stable isotope data for 100 vein and breccia samples, organic maturity data for 30 samples, and zircon fission-track data for 6 samples. In the elemental data set, there are 6 breaks/transitions in the abundance of individual elements: at 3197 m (potentially corresponding to the western fault-bounded margin of the SAF damage zone); at 1926 m (a granite-sandstone fault contact); at 3319 m (perhaps the most important fault contact within the core of the SAF zone); at 2570 (core of clay-rich shear zone?); at 3481 (near faulted contact between folded and non-folded sediments); and at 3078m (near clay-rich fault zone that was encountered at end of phase 1 coring). In the stable isotope data, the carbon isotope values of the carbonate veins and cement vary significantly from +8 to negative 20 per mil; the oxygen isotope values vary from +26 to +12 per mil. The data can be separated into two groups, both of which are present on either side of the inferred SAF. The group with low carbon isotope values are consistent with the carbon having been derived from, or exchanged with, either 1) biogenically derived methane, 2) thermogenic methane at temperature greater than 180C rather than at their current down hole temperature of approximately 120C, or 3) dissolved carbon in groundwater that had been produced in the root zone of C3 plants. The latter hypothesis would be consistent with the carbon isotope data of soil gas in the Parkfield area (Lewicki et al., 2002). In contrast, the other group of veins and breccias are in oxygen isotope equilibrium with the silicate-buffered formation water obtained from the drill hole and close to carbon isotope equilibrium with the thermogenic methane sampled in the drill hole. The total organic content (TOC) of the cuttings are below 1 percent by weight. The kerogen is considered to be "gas prone" on the basis of the TOC and Rock-Eval pyrolysis, hydrogen index, and oxygen index values. The vitrinite reflectance of 23 samples increase with depth from 0.70 at 3230 m to 0.95 at 3960 m. This increase in reflectance values is consistent with increasing temperature and organic maturation with depth. Although the data is limited, there is no significant offset in organic maturity across the inferred SAF zone. Six zircon fission-track dates range from 64 to 70 Ma, which are interpreted as cooling ages of the sediments' source terranes. There is no discernable difference in dates across the inferred SAF zone. Zircons from approximately 15 other samples are in the process of being analyzed at this time. [Please note this is the same abstract submitted to AGU Fall 2006 meeting, but not presented].

FRICTIONAL BEHAVIOR OF SAFOD FAULT-ROCKS AND PUNCHBOWL ULTRACATACLASITE SHEARED AT SEISMIC SLIP RATES

Hiroko Kitajima, Judith Chester, Frederick Chester · Texas A&M University
Toshihiko Shimamoto · Kyoto University

Several dynamic weakening mechanisms have been proposed to explain the reduction in frictional strength during coseismic slip, including flash heating (e.g., Rice , 1999), thermal pore-fluid pressurization (Lachenbruch, 1980), silica-gel formation (Di Toro et al., 2004) and moisture-drained weakening (Mizoguchi et al., 2006). In order to characterize the frictional behavior at seismic slip rates, document conditions under which dynamic weakening occurs, and identify the dynamic weakening mechanisms, we have conducted friction tests at seismic slip rates on fault rocks from the San Andreas fault zone at SAFOD and on natural ultracataclasite from the exhumed Punchbowl fault. Disaggregated samples (<106 micrometer diameter) of four distinct fault rocks from the 3067 m MD fault in Phase 1 spot core recovered from SAFOD, and of two ultracataclasite samples from the Punchbowl fault, were sheared between sawcut cylinders of gabbro or granite in a high-velocity rotary shear apparatus at Kyoto University. The SAFOD samples included a fractured arkosic sandstone (B23-F1), fractured siltstone (B23-F6), dark-brown fault gouge (B23-F2), and red-brown fault gouge (B23-F5).

The SAFOD samples were sheared at 1.3 m/s sliding velocity and normal stresses of 0.3, 0.6, and 1.3 MPa in order to determine the magnitude of dynamic weakening and the influence of fault-rock type on frictional behavior. Coefficient of sliding friction is 0.5 to 0.6 initially, but gradually decreases to 0.05 to 0.1 by tens of meters of displacement. The friction coefficient at steady state is similar overall, but the transient weakening behavior is variable, which is interpreted to reflect initial microstructural state and mineralogy of the fault-rocks.

For Punchbowl ultracataclasite samples, three types of shear experiments have been conducted: constant velocity, constant acceleration, and slip-hold-slip experiments. In the constant velocity experiments, samples were sheared at 0.1 to 1.3 m/s under normal stresses of 0.3 to 1.3 MPa, and to total displacements of 1.5 to 80 m, to investigate the role of frictional heating and localization. Significant dynamic weakening occurs at the highest slip rates tested, 0.7 m/s and 1.3 m/s, under all normal stress conditions. Less dramatic dynamic weakening also is apparent for sliding velocities between 0.2 m/s and 0.7 m/s. The velocities at which weakening occurs are comparable to the critical sliding velocity determined for the onset of thermal weakening due to flash heating assuming an average asperity temperature of 20 oC (Rice 2006). The constant acceleration experiments show that sliding friction coefficient decreases with increasing velocity and recovers with decreasing velocity. Of particular interest is that the friction strength drops quickly on water-dampened samples regardless of acceleration magnitude; a behavior not noted for dry samples. This observation is consistent with thermal pressurization and water-drainage (water removal) mechanisms. Friction strength recovers more completely in dry samples and the slip-hold-slip tests demonstrate that weakening and recovery strongly depend on temperature.

All results indicate that frictional strength is strongly related to friction heating. Further microscopy work is directed at testing the hypothesis that initial friction behavior relates to the initial particle size, and subsequent behavior to the degree of slip localization as a function of displacement and temperature.

GEOLOGICAL INTERPRETATION OF MULTI-DIMENSIONAL GEOPHYSICAL MONITORING DATA BASED ON SELF-ORGANIZING MAPS

Christian Klose · Columbia University

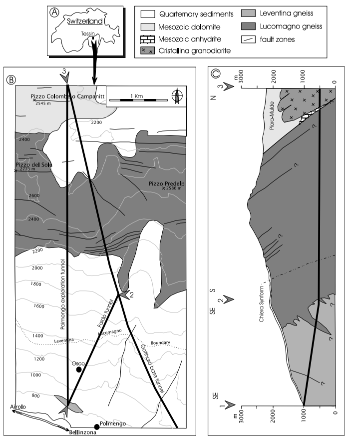

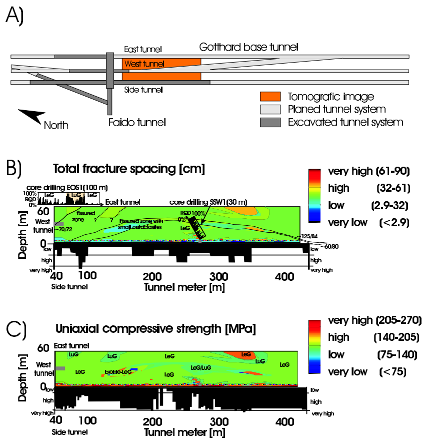

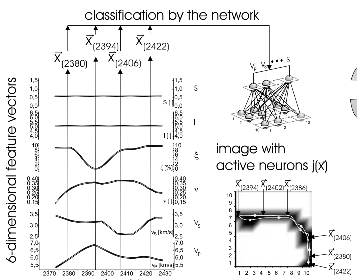

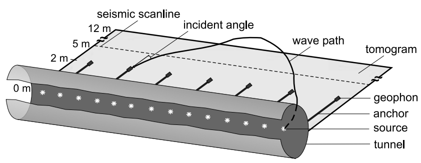

Geographical and geological overview of the Faido tunnel in southern Switzerland. A) Location of the observed region. B) Schematic geological map and picture. C) Cross section along the Faido adit (profile 12) and along a part of the Gotthard base tunnel (profile 23).

Interpretation results of a tomographic image (400x60 m2) in the Gotthard base tunnel (A). A SOM-network, trained with seismic data from the Faido adit (Figure 2), was applied to a new seismic data set in the Gotthard base tunnel. The total fracture spacing (B) and the uniaxial compressive strength (C) were predicted as class labels (Intervals!). The labels (i.e., LeG and LuG) within the images show the predicted gneiss varieties similar to data along the Faido tunnel. The added black lines describe significant boundaries based on the classification/prediction results. The predicted spatial distribution of the geological parameters are in agreement with both independent geological mapping results along the side tunnel and borehole results (petrographical data and RQD-values) of the drill cores (EOS1, SSW1). The excavation damage zone (EDZ, approximately 5 m deep) can be observed along the side tunnel.

Classification scheme of a SOM neural network. 6-dimensional seismic feature vectors x were drawn along a seismic profile (here: profile 2360 - 2433 m). Several tunnel locations can be seen: 2380 m, (2386 m), 2394 m, (2402 m), 2406 m and 2422 m. Every x is presented to the SOM neural network. The classification is done, when a neuron in the Kohonen lattice is stimulated. This neuron is active (black) and can be imaged in the lattice. All active neurons can be seen that are related to every x. The white trace in the black region shows schematically which neurons get active along the sampling path of the seismic profile.

Schematic illustration of the installed geophysical measurement units (sources, receivers, and anchors) and of the tomographic imaging within the tunnel. A generated acoustic wave propagates in the interior of the rock and reaches a receiver with an incident angle that is only a few degrees. The incident angle is the angle between the idealized wave path plane and the tomogram plane.

Since geoscientific initiatives like EarthScope have been increasing with a number of monitoring projects, the amount of geophysical data is continuously accumulating over time. Thus, geoscientists are challenged to interpret large amounts of different geophysical parameters and many times simultaneously. Interpretation difficulties occur especially, when data, that need to be interpreted, are of arbitrary dimension. In tandem, interpretations (e.g., correlations) are very often based on single parameters that lead to ambiguous interpretation results.

This presentation describes the application of a statistical method, called Self-Organizing Maps (SOM), to classify and interpret multi-dimensional, non-linear, and highly noised geophysical data for prediction purposes of mechanically unstable geological regions and brittle deformation areas. Results of SOM-classifications can be represented as 2-dimensional images, called feature maps. These maps illustrate the complexity and demonstrate inter-relations between single parameters or clusters of the entire parameter space. SOM-images can be visually described and easily interpreted.

An application example is shown, based on a six geophysical parameters (Figure 1). Geophysical data were acquired from scanlines within tomographic images and seismograms as result from active seismic monitoring measurements in the 60 km long and up to 2000 m deep Gotthard base tunnel (Figures 2 and 3). The measurements were conducted by the GFZ Potsdam and ETH Zurich.

The results demonstrate that it is possible to characterize geological rock mass properties from interpretations of multi-dimensional geophysical (seismic) in-situ data, when all seismic features are simultaneously used. Complicated distributions of parameters within the SOM-maps exemplify the complexity and non-linearity of the multi-dimensional parameter spaces. Hence, the overview of all features and all relationships can be retained for each interpretation. Visual interpretation results can be discussed among scientists and non-scientist as well as experts and non-experts. SOM-classifications are helpful for on-line predictions of unstable geological conditions in undiscovered rock mass regions (Figure 4). In conclusion, it is suggested that this interpretation method could be helpful for EarthScope monitoring projects, e.g., for the San Andreas Fault and Earth's upper mantel. (Reference: Klose, C.D. (2006) Self-Organising Maps for Geoscientific Data Analysis: Geological Interpretation of Multi-dimensional Geophysical Data, Computational Geosciences, 10(3), 1-13)

LITHOSPHERIC STRUCTURE OF NORTH AFRICA AND WESTERN EURASIA *(Speaker)*

Minoo Kosarian, Charles Ammon · Pennsylvania State University

Although much progress has been made over the last few decades towards understanding the structure of the Earth, many questions regarding the details of Earth's lithospheric structure remain unanswered. The primary goal of this study was to gain a better understanding of upper and lower continental crustal composition and structure. To contribute this goal, we focused on the estimation of first order seismic structure using receiver functions and tomography-based surface-wave dispersion estimates, and constructed a library of shear-velocity structures in the vicinity of seismic stations across western Eurasia and north Africa.

One hundred and seventy one stations recording a total of about 6,000 teleseismic events producing more than 100,000 seismograms have been investigated. The distribution includes 78 stations in the Middle East and Asia, 57 stations in Europe, and 36 stations in central and north Africa. We have examined receiver functions for 119 stations with the best data for the period of 1990-2004 and applied the receiver function stacking procedure of Zhu & Kanamori (2000, JGR) to estimate bulk crustal Poisson's ratio (s) and crustal thickness (H). The research area is divided to five tectonic environments, explicitly shields, platform, Paleozoic orogenic belts, Mesozoic-Cenozoic orogenic belts, and rift zones based on Condie's (1989) simplified classifications. The results show a slightly lower value of Poisson's ratio s = 0.25 for shields compared to the orogenic-belts with s = 0.26. Crustal thickness, H, ranges from 32-47 km with an average of 38 km and standard deviation of 3 km for the shields. The less well sampled platforms show a wider distribution of crustal thickness, ranging from 30-58 km with an average 42 km and a standard deviation of 9 km. Orogenic regions also show a wide variation of crustal thickness, with thickness values from 20 to 55 km and standard deviations in the range of 8-10 km.

Since the ultimate goal of this study was to provide an improved imaged of global continental structure and composition, we combined observations obtained in this study with receiver functions results from other published analysis. In total, we have integrated observations from 606 stations located in different geologic settings. The compiled results show a value of s = 0.26 for Poisson's ratio and H = 39 km for crustal thickness in shields and platforms, and s = 0.26-0.27 with H = 35-37 km for the orogenic belts.

CONTINUOUS GPS VELOCITIES IN THE INTERMOUNTAIN-WEST : NEW CONSTRAINTS ON THE MOTION OF THE COLORADO PLATEAU

Corné Kreemer · University of Nevada

Except for the Basin and Range Province, the present-day kinematics and deformation pattern for most of the North America's Intermountain-West has, until recently, been ill-quantified. This situation is changing rapidly with the deployment of the backbone of the Plate Boundary Observatory (PBO). We analyze data for PBO sites (with occupation over ~1 year) and CORS sites (with stable monumentation) from northern Mexico to Montana. In this area the expected velocities relative to stable North America are very small and we would commonly need long time-series to infer significant motions. The two main sources of uncertainty in the rates inferred from short time-series are common-mode errors and seasonal signals. Here we deploy a new regional filtering technique that aims at reducing those errors. We create a regional-filter for each site by using residuals of all sites within 500 km of that site (except the site itself). Those residuals are the result of fitting a linear rate and annual and semi-annual term to the unfiltered time-series. In a region that does not have many stations with long-series, our procedure makes optimal use of the availability of short-running stations to create robust regional filters while preserving seasonal signals. The ITRF2000 velocities are transformed into the SNARF reference frame by using ~30 velocities across the North American continent common with those in the SNARF solution. The use of this reference frame is consistent with, for instance, the Rio Grande Rift clearly separating stable North America to the east from the moving Colorado plateau to the west.

We focus here on the Colorado Plateau region. A consistent pattern is emerging with sites on the CP moving ~1 mm/yr towards the northwest, implying that the block is to first-order rigid and that the extension rate across the Rio Grande Rift is ~1 mm/yr. The result also implies ~1-2 mm/yr of motion across the Hurricane Fault system between the Colorado Plateau and the Basin and Range. Anomalies to the observed velocity pattern exist near large urban areas (e.g., Phoenix, Tucson, Las Vegas) or along the Colorado River. The anomalous velocities are probably due to loading effects from local ground-water variations.

NOISE IN GPS MEASUREMENTS FROM SOUTHERN CALIFORNIA AND SOUTHERN NEVADA

John Langbein · U.S. Geological Survey

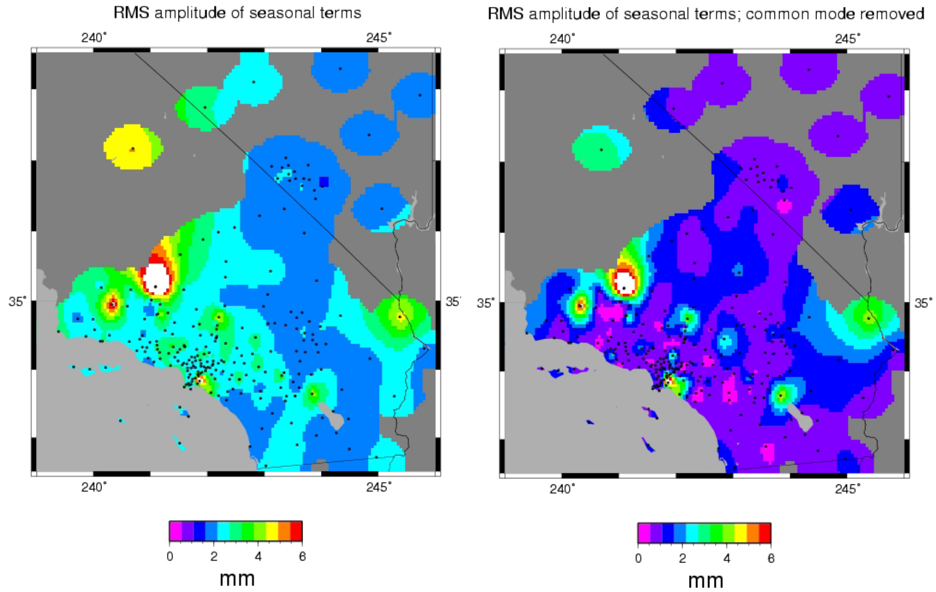

Estimate of RMS amplitude of seasonal noise from continuous GPS in Southern California and Nevada. Note that minimum amplitude is more than 1 mm. Dots show locations of GPS sites.

Estimate of residual RMS amplitude of seasonal noise from continuous GPS in Southern California and Nevada after removing common mode terms. Highest residual amplitudes are, in general, associated with anthropogenic sources.

Time series of position changes estimated from data from continuous GPS receivers spanning Southern California and Southern Nevada are evaluated for noise models that characterize their temporal correlations. This paper extends the analysis of Williams et al (2004) by using the methods of Langbein (2004). The time series range between 3.5 and 10 years in length. After adjusting these data for postseismic deformation, offsets, and annual and semi-annual periodicities, I find that no single type of noise model best represents these observations. Instead, about one-half of the time series have temporal correlations that are categorized as either flicker or random-walk noise. The remaining time series can be best categorized either a combination of flicker and random-walk, power-law noise, first-order Gauss-Markov plus random-walk noise, or power law plus broad-band, seasonal noise. A variety of geodetic monuments are used Southern California and Nevada which include deep-braced designs, cement pier, pins drilled in outcrop, and buildings. When I evaluate the noise for each time-series in terms of estimating the standard error in velocity, I find that those sites located in Nevada having deep-braced monuments have the lowest noise. And, for those sites that are located within regions of active pumping, both for ground water and oil, those time-series had the largest standard errors in velocity. Comparison of monument stability as measured by standard error in rate with nearby average, annual rainfall indicates a marginally significant correlation. In addition, even though regional filtering removed much of the common-mode signals in these time-series, there still remained a common-mode seasonal signal.

TIDAL CALIBRATION OF PBO STRAINMETERS LOCATED IN THE PACIFIC NORTHWEST

John Langbein · U.S. Geological Survey

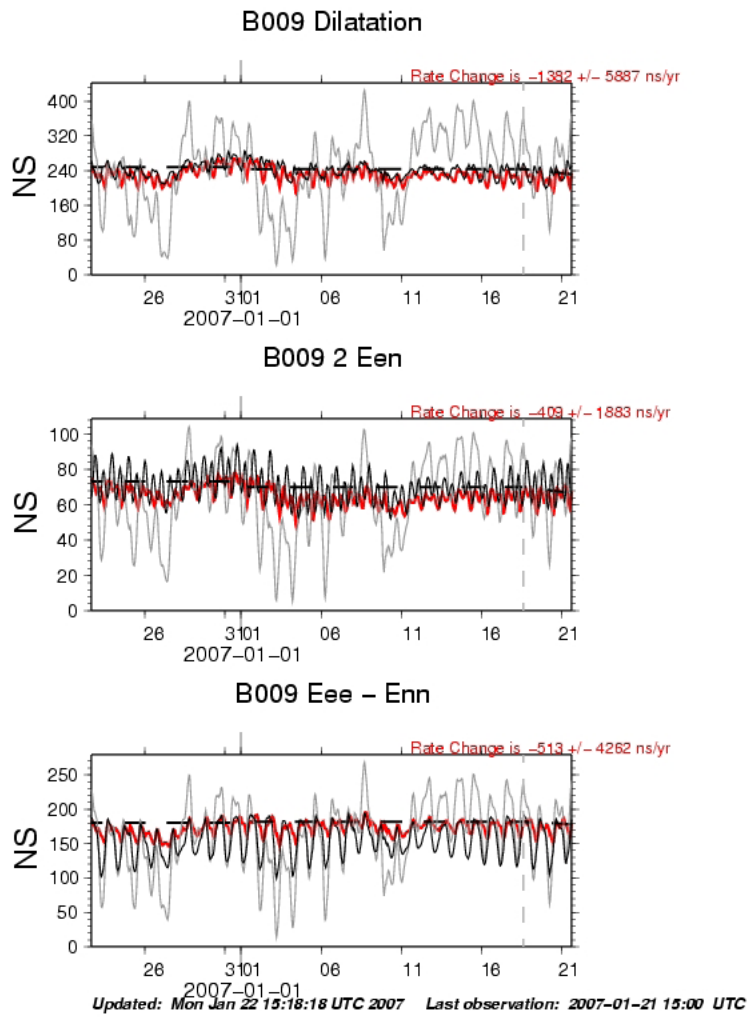

Example of reduction of borehole strainmeter data for site B009 located on Vancouver Island adjacent to Patricia Bay where the tidal range is 3.8 meters. The gray line is the raw data after the transforming the extensometer data into tensor quantities using tidal calibration. The black curve shows the data after adjusting for changes in atmospheric pressure and changes in the water level in Patricia Bay. Red represents the residual strain after removing the solid Earth tide and Ocean-load. The dashed line is a fit for a linear trend over the 30 day interval and its rate change over the last 3 days; the rate change with its standard error is posted over each plot.

The Plate Boundary Observatory (PBO) has installed a dozen Gladwin Tensor strainmeters in the coastal region between Vancouver Island and Oregon with the goal of measuring strain changes resulting from “episodic tremor and slip” (ETS) events in the Cascadia subduction zone. My primary goal is to process these data automatically to be able to detect significant strain changes that can be attributed to tectonic activity. I have selected six of the PBO strainmeters to calibrate and to estimate their background noise so that rate-changes in tensor strain can be measured and tested for their statistical significance. Each instrument consists of four extensometers. For each extensometer, the expected tidal amplitudes and atmospheric pressure response are estimated simultaneously. At two sites located adjacent to inlets, the sensitivity of each extensometer to changes in ocean height resulting from the ocean tide is evaluated along with the standard tidal analysis; This is complicated because the local height change data must be filtered into two frequency bands; less than 18 hours and greater than 18 hours. Each band effects the instrument differently. Finally, the amplitude and phase of the M2 and O1 tidal constituents at each extensometer are compared to the theoretical tides including ocean loading (Agnew, 1999) that is computed for each of the tensor strain components. I use the method suggested by Hart el al. (1996) (their equation 13) where the theoretical tides are fit to the observed tides using standard least-squares. This is a “black-box” approach where no assumptions are made concerning isotropic borehole deformation or topographic effects.
After removing the effects of the grout curing, the background noise level of each tensor component is evaluated in terms of a covariance matrix representing a power-law noise-model so that rate changes can be estimated together with realistic estimates of their significance using the methods of Langbein (2004). More more information, go to: http://quake.wr.U.S. Geological Survey.gov/research/deformation/twocolor/PBO_strain/

WAVE GRADIOMETRY FOR EARTHSCOPE

Charles Langston · University of Memphis

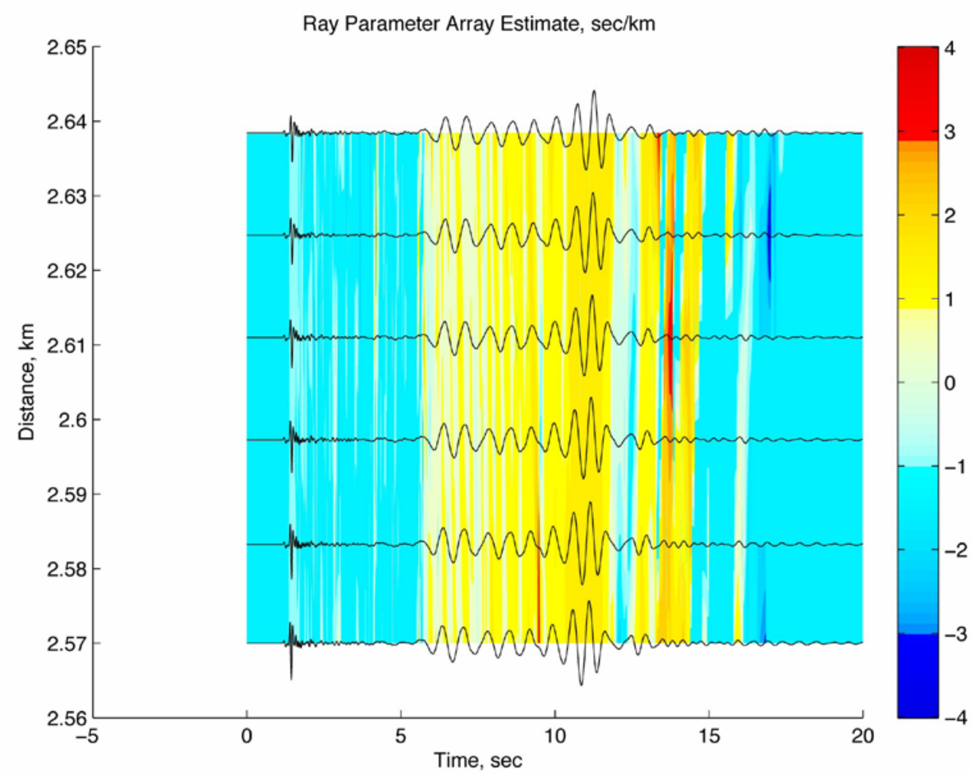

An example of mapping horizontal slowness as a function of time and space along a linear seismic gradiometer 105m in length. The source was a large explosion 2.5km distant. P and multimode Rayleigh waves are seen that propagate slowly across the array.

EarthScope facilities offer several opportunities for applying a new seismic technique, wave gradiometry, to the analysis of long-period waveforms recorded by USArray and PBO strain meter observatories. The spatial gradient of wave fields as a function of time and space over a gradiometer array gives information on horizontal slowness, geometrical spreading changes, azimuth, and radiation pattern changes of the wave field that, in principle, can be used to map heterogeneity in the lithosphere and mantle under North America. With an average station spacing of 70km, broadband stations of USArray can serve as gradiometer elements for the analysis of 100 s and longer period surface waves propagating across the continent and shorter period, but higher horizontal velocity teleseismic body wave phases. Maps of horizontal phase velocity, azimuth, and amplitude perturbations may yield empirical information on the location of major heterogeneity within the continent and provide a unique dataset for more detailed modeling of velocity structure. PBO strain meter observations in conjunction with a co-located broadband seismometer may also be used as a point "array" for analyzing the wave propagation of local, regional, and teleseismic events to yield additional constraints on event location and wave scattering. Such strain/seismic gradiometers may be useful in understanding the source of volcanic and deep fault tremor.

THE UPLIFT OF THE SOUTHERN SIERRA NEVADA, THE ISABELLA SEISMIC ANOMALY AND DEATH VALLEY EXTENSION: A SINGLE GEODYNAMIC PROCESS?

Laetitia Le Pourhiet · Laboratoire de Tectonique, Univ. Paris VI
Michael Gurnis, Jason Saleeby · Caltech

Within the last decade, a variety of evidence for the recent removal of a relatively high-density garnet pyroxenite root of the Cretaceous Sierra Nevada batholith has been inferred from both geochemical analysis of mantle xenoliths and geophysical imaging of the upper mantle and Moho. As the density associated with this mineralogical assemblage (3500 kg m-3) is larger than the density of the surrounding mantle peridotite (3300 kg m-3) gravitational instability is believed to have triggered its foundering. Simple models exist to describe gravitational instabilities (including linear or non linear Rayleigh Taylor (RT) instabilities. However, for reasonable geothermal constraints and creep parameters, RT models poorly explain: 1) the long stability of the root (~90 Myr) 2) its rapid removal (1-3 Myr), and 3) the magnitude of associated uplift.

In order to establish new mechanical models that allow gravitational instabilities to develop slowly and then be rapidly removed within the critical timescale fixed by the simultaneity of uplift and onset of Plio-Quaternary volcanism in the southern Sierra at 3 Ma, we carried out a systematic study of the influence of the strength of the lower crust on the mode of the instability by means of thermo-mechanical models that allow thermo-chemical convection and plastic softening. Using a thermo-mechanical code based on the FLAC method, we modeled realistic topography, visco-elasto-plastic thermo-dependant rheologies, and the temperature and compositional dependent density.

We found that models with a strong crust remain stable as predicted by RT. However, we found models which did destabilize and can explain: The short timescale of the removal, the formation of the Sierra Nevada micro-plate at ca. 10 Ma, and the extension in the Death Valley area at ca. 15 Ma within the framework of one single mantle instability. Those models also explain the current seismic structure of Isabella Anomaly and its apparent dip towards the south east.

REFLECTION IMAGING THE 35°-DIPPING NORMAL FAULT THAT BOUNDS THE BASIN & RANGE PROVINCE

Derek Lerch · Feather River College
Simon Klemperer, Anne Egger · Stanford University
Joseph Colgan · U.S. Geological Survey

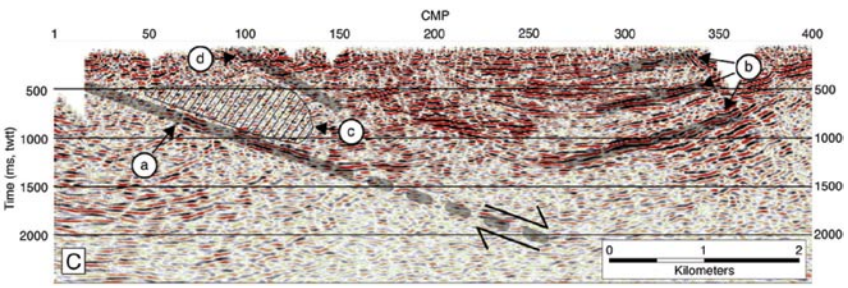

Migrated image of the Surprise Valley basin, with no vertical exaggeration based on basin-fill Vp=2 km/s. CMP spacing is 20 m. The SVF (a) forms a continuous, moderate–amplitude east-dipping reflection that bounds the western side of the basin. Prominent west-dipping reflections (b) on the eastern edge of Surprise Valley correspond to late Miocene to Pliocene (8–3Ma) volcanic strata. The reflection-free region (c) immediately above the SVF is interpreted as alluvium deposited along the range-front during footwall exhumation. West–dipping reflections near CDP100 appear to be truncated by a fault splay (d) above the SVF.

Surprise Valley, straddling the NV-CA-OR borders, is bounded to the west by the Warner Mountains forming the westernmost classic basin-range pair of the eponymous extensional province. The Surprise Valley fault (SVF) is an east-dipping, large-offset normal fault that developed isolated from other significant Basin-and-Range faulting by the essentially unfaulted Sheldon volcanic plateau to the south and east (and the Modoc Plateau to the west). Seemingly correlative Mio-Pliocene basalt flows and tuffaceous sediments east and west of Surprise Valley/Warner Range suggest continuous Pliocene basalt flows may have pre-dated significant faulting, so that up to 5 km of offset (3 km strata exposed in the Warner Range, 2 km imaged by us) may have occurred on the SVF in 3 to 5 Myr (time-averaged slip-rate of 1-2 mm/yr). Large-magnitude Holocene rupture, modern seismicity, local geothermal activity and overpressured basin strata are all consistent with a high present-day slip rate.

Our September 2004 EARTHSCOPE-supported seismic experiment across the northwestern margin of the Basin-and-Range province included a relatively high-resolution vibrator-source profile (20-m CMP spacing) from the surface trace of the SVF for 16 km east across Surprise Valley; a 300-km explosive-source seismic refraction survey including an 1100-kg shot-point on the east side of Surprise Valley recorded at 300-m spacing across the SVF, and complementary teleseismic recordings.

Our explosive-source recording shows a reverse-moveout reflection projecting to the surface trace of the SVF that can best be modeled as from a fault plane dipping 30 to 45° east (dip depends on assumptions about near-surface velocities, 2±0.2 km/s) to a depth >7 km.

The most significant reflector on our high-resolution reflection profile (figure) truncates intra-basin stratigraphic reflections, and has a migrated dip of 20°±2°. Because our experimental use of the 64,000-lb Network for Earthquake Engineering Simulation (NEES) T-Rex vibrator limited our work to unpaved roads, our west-east 2-D profile has an oblique intersection with the strike of the SVF, but appropriate geometric correction for this obliquity steepens the true dip of the fault plane to only 35°±3°. We image a separate fault-splay above the main fault with a true dip of 30°±5°. Cenozoic volcanic strata uplifted in the Warner Range dip 20° to the west, documenting footwall-block rotation during the development of the SVF. Restoring this rotation, the orientation of the SVF at its formation becomes 55°±3°, compatible with normal fault geometries observed in laboratory experiments.

However, trenching for paleoseismic studies constrains the near-surface dip of the active SVF to be ~65°, too steep to be the fault-plane geometry that produced the ~20°-dipping Cenozoic stratigraphy in the Warner Range. This active fault trace of the SVF is likely an extremely young feature in the Surprise Valley-Warner Range evolution, though it is not yet known whether it soles into, or cuts and offsets the less-favorable, now-shallow geometry (30°-35°) of the main SVF. Surprise Valley may provide the chance to study the process of abandonment of a major active low-angle fault in favor of a new high-angle fault; the developing EARTHSCOPE FlexArray facility, now with triple the recording capability available to our 2004 experiment, offers the means to do so.

CLUSTERING AND SCATTERING OF INTRAPLATE EARTHQUAKES: PRELIMINARY RESULTS FROM GEODYNAMIC MODELING

Qingsong Li · Lunar and Planetary Institute
Mian Liu · University of Missouri

The spatiotemporal pattern of intraplate seismicity varies in different continents. Earthquakes in Australia seem to occur randomly over the continent; seismicity in central and eastern US is concentrated along a few finite seismic zones; and earthquakes in North China migrated from the Shanxi-graben to the North China plain in the past 200 years. The causes of the clustering and scattering of intraplate earthquakes remain unclear. For the New Madrid Seismic Zone and others where earthquakes have clustered in recently geological history, would future earthquakes continue to cluster there, or will they migrate to other places? We have explored answers to these questions with a conceptual finite element model that simulates occurrence of intraplate earthquakes. The results show that in a homogeneous intraplate region, seismicity may appear spatially clustered in “seismic zones” over a short period, but earthquakes migrate over time and they eventually become randomly scattered over long time. Conversely, mechanical weak zones in the upper crust can cause persistent clustering of earthquakes that migrate along zones extending from the mechanical weak zones. Over long time earthquakes may extend far beyond the finite mechanical weak zones. Thus recent seismic clustering in the NMSZ may reflect a short-term feature of scattered seismicity in long-term or transient activity of earthquakes along a much longer seismic belt. In either case, future earthquakes are unlikely to be limited to the presently active NMSZ.

SPACE/TIME PROPERTY VARIATIONS ON THE PARKFIELD SAN ANDREAS FROM FAULT GUIDED WAVES

Yong-Gang Li · University of Southern California
Peter Malin · Duke University

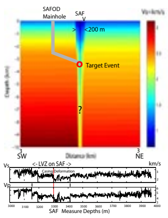

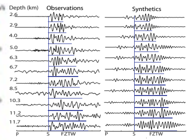

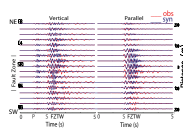

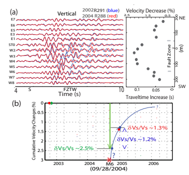

Fig. 1 (a) Fault-normal depth section showing the S-wave velocity model for the SAFOD site. The velocities within the 100-200-m wide waveguide and surrounding rocks were found by 3-D finite-difference fits to FZTW waveforms and traveltimes generated by explosions and earthquakes at different depths. The model suggest that, on average, a fault zone consists of two sub-vertical layers, a 30 m-wide fault core and a surrounding 100-200 m wide damage zone. S velocities within the damage zone are reduced by 25-35% from wall-rock velocities. The maximum reduction occurs in the fault core and can be as large as 50%. The arrow indicates the

Fig. 3 Left: Vertical-component seismograms at station ST0 on the SAF for 11 on-fault events occurring near the station at different depths. The lengths of the fault guided wavetrains (marked by the bars after the S-arrivals) increase with event depths for on-fault events, suggesting that a continuous low-velocity waveguide on the SAF extends across seismological depths. The S-arrivals for these events are aligned. Right: Synthetic seismograms computed for these events using the model in Fig. 1.

Fig. 2 Observed and 3-D finite-difference synthetic seismograms using the velocity model in Fig. 1. The seismograms are as seen at depth similar to the SAFOD drilling target event, as shown in Fig. 1. The seismograms have been <8 Hz filtered and are plotted using a fixed amplitude scale for all traces.

Fig. 4 (a) Left: Seismograms from 2002 and 2004 at the same stations of the cross-fault array for two repeated earthquakes before and after the 2004 M6 Parkfield earthquake. The P-wave arrivals are aligned and seismograms have been <5 Hz filtered. Right: The maximum S-traveltime increases of seismic waves in the 2-10s window measured by waveform cross-correlations between the 2002 and 2004 events recorded at stations of the cross-fault array. (b) S-wave velocity changes within the rupture zone of the M6 earthquake on September 28, 2004. The S velocity decreased by ~2.5% in the time period between the repeat events and shots in 2002 and 2004 (red circles are shots; green circle is the microearthquake on R291 in 2002; blue circles are its repeat aftershocks; red star is the M6 mainshock on September 28, 2004). The reduction is most likely due to co-seismic rock damage during the mainshock. Measurements for repeated aftershocks show that the S velocity within the rupture zone increased by ~1.2% in the following 3 months. This increase suggests that the fault healed recovering part of its rigidity in this time period.

Highly damaged fault rocks along the San Andreas Fault at Parkfield create a low velocity zone that can trap seismic waves from both earthquakes and explosions (Fig. 1). We have modeled these types of fault-zone trapped waves (FZTWs) waves using finite difference methods (Fig. 2). The models suggest that, on average, a fault zone cross section consist of a composite of two subvertical layers, one a 30 m-wide fault core, the other a surrounding 100-200 m wide damage zone. The damage zone velocities range between 65-75% of the fault zone wall rocks, while those of the core are even less, going as low as 50% of the intact rock [Li et al., 2004]. Down-hole seismographs emplaced in the SAFOD Main Hole at ~3 km depths also register prominent Fg waves from deeper events. The width and velocity reduction of the damage zone at this depth as delineated by fault-zone trapped waves has been verified by the SAFOD drilling and logging studies. These studies show that a ~200 m-wide zone of high porosity, multiple slip planes, and average velocity reductions of ~30-35% is present at these depths (Fig. 1). Thus this is the minimum depth to which the low velocity layers extend. Observations and models of FZTWs generated by microearthquakes at different focal depths suggest that this type of fault structure reaches to depths of 6-to-7 km or more (Fig. 3). In fact, while the velocity contrasts and layer thickness appear to become smaller with increasing depth, it is likely that a low velocity fault guided "channel" extend across the entire seismogenic depth at Parkfield. The damage zone of the SAF is not laterally symmetric. Instead, it appears to extend farther into the SW side of the fault. This could be due to rocks already weakened from previous faulting. It could also be due to greater damage in the extensional quadrant near the propagating crack tip of Parkfield earthquakes. We interpret the low-velocity waveguide as being a zone of accumulated damage from recurrent major earthquakes, including the 2004 M6 earthquake. This type of damage varies with depth and also along the strike, and may relate to the on- and near-fault variations in stress and slip distribution during earthquake rupture.

We have conducted several active and passive seismic experiments near the SAFOD site before and after the 2004 M6 Parkfield earthquake [Li et al., 2006a, b]. These experiments indicate that the Parkfield low-velocity zone weakened co-seismically, and then healed back toward its pre-earthquake state over a period of several months to several years (Fig. 4). Waveform cross-correlation measurements from repeated explosions and microearthquakes suggest that a peak decrease of ~2.5% in velocity occurred coseismically within the fault zone at seismogenic depths. Measurements from repeating aftershocks show that a ~1.2% velocity increase occurred within the fault zone in the first 3-4 months after the mainshock. The healing rate appears to be approximately logarithmic, with the largest rate in the earliest stage of post-mainshock period. The magnitude of fault damage and healing varies along the rupture zone, but it is most prominent above ~7 km. Its distribution also appears to roughly correlate with the slip distribution of the 2004 earthquake. The observed ratio between the P and S wave velocity changes is consistent with the opening of new fluid filled cracks at or near the time of the main shock. Yet our data were too infrequent and coarse to completely resolve these matters. Instead, with the successful drilling and instrumenting of the SAFOD Main Hole, new information on this process should be forthcoming in the next cycle of the Parkfield earthquake engine.

ROCK DAMAGE AND HEAL ON THE SAN ANDREAS FAULT INVOLVED IN THE 2004 M6 PARKFIELD EARTHQUAKE

Yong-Gang Li · University of Southern California
Po Chen · Lamont-Doherty Earth Observatory
Elizabeth S. Cochran · University of California at Riverside
John E. Vidale · University of Washington

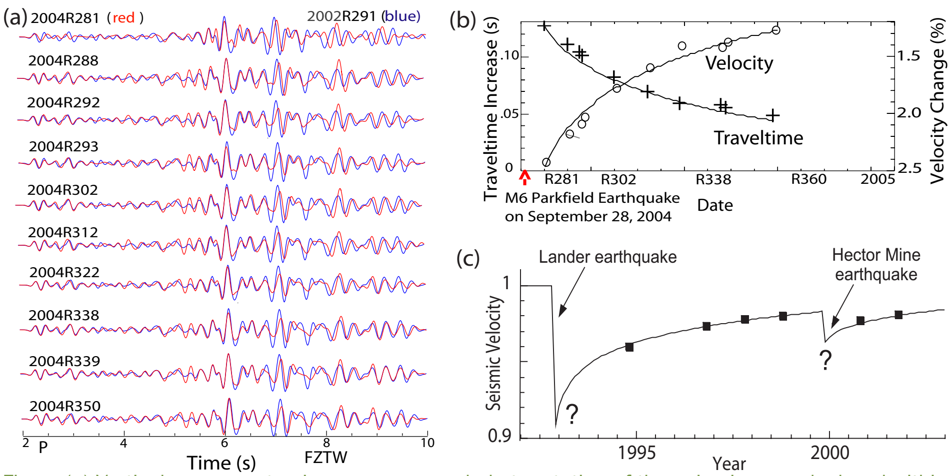

Figure (a) Vertical-component seismograms recorded at a station of the seismic array deployed within the fault zone for the microearthquake in 2002 (blue line) and its repeated events in 2004 (red lines), showing that waves traveled slower in 2004 with the largest time delay between the event in 2002 and the aftershock in the earliest stage of the 2004 M6 Parkfield earthquake. Seismograms have been <5 Hz filtered. The first P-arrivals are aligned. (b) The maximum traveltime and shear velocity variations in percentage measured by moving-window cross-correlation of waveforms recorded at this station between the event in 2002 and its repeated events in 2004, showing the largest velocity reduction for the earliest repeated event and a increasing trend with dates after the mainshock.. The curve is the logarithmic fit to measurements of traveltime changes with a constant of velocity change 0.012 /day in logarithm. The velocity reduction is most likely due to co-seismic rock damag e during the mainshock. The post-mainshock velocity increase suggests that the fault healed recovering part of its rigidity with time. (c) The observed fault zone rock damage and healing on the SAF caused by the 2004 M6 Parkfield earthquake is consistent with the model of velocity changes as a function of time owing to combination of damage and healing at rupture zones of the 1992 M7.4 Landers and 1999 M7.1 Hector Mine earthquakes [Vidale and Li, 2003], shows healing as a logarithm of time.

The M6 Parkfield earthquake that occurred on 28 September 2004 provides us a rare opportunity to examine the possible variations in the volume and magnitude of the low-velocity anomalies on the San Andreas Fault (SAF) over the earthquake cycle. After this earthquake, we deployed a dense seismic array at the same sites as used in our experiment in the fall of 2002. The data recorded for repeated explosions and microearthquakes before and after this M6 event show a few percentage variations in seismic velocity within a 200-m-wide highly damaged fault zone. The measurements using moving-window cross-correlation of waveforms for the repeated microearthquakes recorded at our arrays in 2002 and 2004 show a decrease in shear velocity of at least ~2.5% owing to co-seismic damage of fault-zone rocks caused by dynamic rupture of this M6 earthquake. The width (~200 m) of the damage zone characterized by larger velocity changes is consistent with the low-velocity waveguide model on the SAF near Parkfield derived from fault-zone trapped waves. The estimated ratio between the P and S wave traveltime changes is 0.57 within the rupture zone and ~0.65 in the surrounding rocks, indicating wetter cracks within the damaged fault zone, probably due to the ground water percolating into the cracks opened in the mainshock. The measurements of traveltime changes for repeated aftershocks in 21 clusters located at different depths along the rupture of the 2004 earthquake and found that the maximum shear velocity increased by ~1.2% within the fault zone in 3.5 months starting a week after the mainshock, indicating that the fault heals by rigidity recovery of damaged rocks in the post-seismic stage due to the closure of cracks. The healing rate is logarithmically decreasing through time with greater healing rate in the earlier stage of the inter-seismic period. The magnitude of fault damage and healing varies along the rupture zone, but is most prominent at depths above ~7 km and roughly correlating with the slip distribution on the SAF in the 2004 M6 Parkfield earthquake. Our observations of fault zone damage and healing associated with this M6 event illuminate the faulting-healing progression on an active fault in the major earthquake, in general consistent with the model of velocity evolution owing to damage and healing for Lander and Hector Mine earthquakes [Vidale and Li, 2003]. However, the magnitude of damage and healing observed near Parkfield on the SAF is smaller than those on the Landers and Hector Mine rupture zones, probably related to the smaller magnitude mainshock, and smaller slip, and possibly differences in stress drop, pore-pressure, and rock type.

HIGH RESOLUTION GROUP VELOCITY MODEL FOR EASTERN NORTH AMERICA BASED ON AMBIENT NOISE TOMOGRAPHY

Chuntao Liang, Charles Langston · University of Memphis

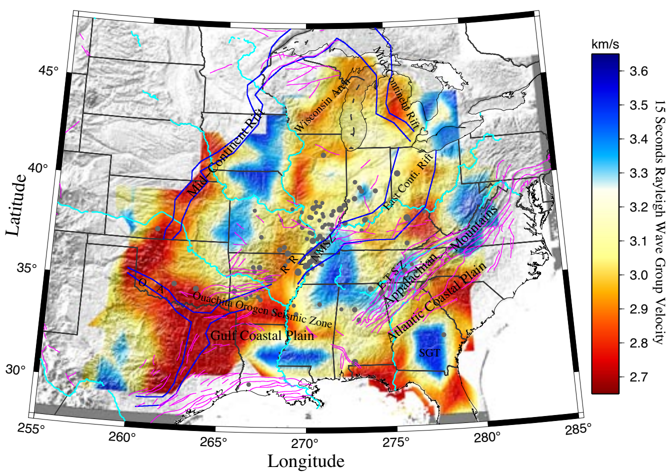

15 second group velocity (color) overprinted on topography (relief). Black dots and magenta lines are seismicity and faults, respectively. The thick blue lines associated with the Mid-continental rift and the triple junction at Oklahoma-Texas border are digitized from the isostatic gravity map. The thick blue lines associated with the East Continental rift is digitized from Stark [1997]. RR: Reelfoot rift; NMSZ: New Madrid seismic zone; ETSZ: eastern Tennessee seismic zone; SGT: southern Georgia triplet; OA: Oklahoma Aulacogen.

We use the surface waves extracted from the cross-correlation of ambient noise data to invert for the group velocity structure in eastern North America. Owing to the three dense local and regional seismic networks deployed to monitor the New Madrid Seismic Zone and eastern Tennessee seismic zone and the national Seismic Network, we were able to achieve a group velocity tomography with resolutions as high as 1° by 1° and 2° by 2° for periods of 5 and 15 seconds, respectively. The short period (T=5 sec) group velocity map shows strong correlations with the surface geological units. Many subtle local structures can be clearly identified from the velocity map, including the Ozark uplift, Cincinnati Arch, Nashville Dome and the Blue Ridge province of the Appalachians showing relatively high group velocity. The long period (T=15 sec) group velocity map (Figure 1) shows strong correlations with regional geology. Ancient rift basins are associated with low velocity belts along their rift axes, such as, the Mid-Continent Rift (MCR) system, the Reelfoot rift, the Oklahoma Aulacogen and the Eastern Continent Rift. The triple junction located at the Oklahoma and Texas border, characterized by extreme gravity highs (Figure 1), is associated with low velocities. The low velocities associated with Ouachita orogen can be traced eastward into the southern Appalachian mountains. Prominent high velocity belts along the Appalachian Mountains are associated with the up-thrusted Precambrian rocks. We also find that all major seismic zones in eastern North America, such as the New Madrid and Eastern Tennessee seismic zones, as well as one linear seismic zone extending from southern Appalachian westward to Oklahoma Aulacogen, are approximately located at transition zones separating velocity highs and lows. This observation suggests that those seismic zones may reflect the reactivation of ancient faults associated with continental rift and collision zones. Our results provide unprecedented new views of the eastern North America and they may help Earthscope to motivate scientific goals and define new experiments in this region.

STRAIN PARTITIONING AND FAULT INTERACTION IN THE SAN ANDREAS FAULT PLATE BOUNDARY ZONE: INSIGHTS FROM GEODYNAMIC MODELING

Mian Liu · University of Missouri
Qingsong Li · Lunar and Planetary Institute
Hui Wang · University of Missouri & China Earthquake Administration

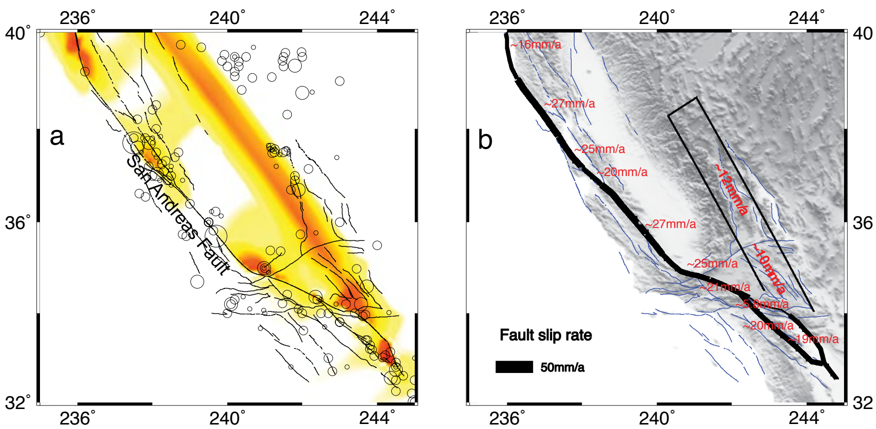

Predicted rate of plastic strain in the crust outside the San Andreas Fault proper. b) predicted long-term slip rate along the San Andreas Fault and the Eastern California Shear Zone.

The San Andreas Fault (SAF) system is the transform boundary between the Pacific and the North American plates, but strain is partitioned among a complex fault system. Up to 25% of the relative plate motion is now accommodated by the Eastern California Shear Zone (ECSZ); along the SAF proper slip rates vary significantly. We have developed a 3D lithospheric dynamic model to explore the causes of strain partitioning and localization, and to simulate long-term fault interaction in the SAF plate boundary zone. The 3D finite element model assumes a visco-elasto-plastic rheology that allows simulation of both long-term fault slip (plastic creep) within the fault zones and plastic deformation outside fault zones. Our results suggest that the geometry of the SAF proper has important impact on slip rate variations along the SAF and strain partitioning in the plate boundary zone. The development of the Big Bend is shown to localize strain along the ECSZ, thus may have contributed to it initiation. Similarly, formation of the restraining bend over the San Bernardino segment of the SAF ~2 Myr ago may have facilitated the initiation of the San Jacinto fault (SJF). Once activated, the SJF tends to enhance strain localization along the ECSZ, while slip in the ECSZ is shown to reduce long-term slip rates on the SAF. These results provide useful insights into long-term fault evolution in the SAF plate boundary zone.

IMAGING THE LAYERED STRUCTURE OF THE EARTH'S CRUST AND MANTLE BENEATH WESTERN US USING CONVERTED WAVES FROM USARRAY AND OTHER BROADBAND DATA SETS

Kelly Liu, Stephen Gao · University of Missouri

Seismic discontinuities reflect abrupt changes in composition, mineralogy, temperature, or mantle fabric as a function of depth. Consequently, studies on the existence, velocity contrast, depth, and sharpness of those discontinuities have played an important role in the understanding of the structure, dynamics, and evolution of various parts of the Earth. The western United States is among the best areas in the world with the highest density in coverage by portable or permanent broadband seismic stations. Unfortunately, prior to the deployment of the USArray stations, the distribution of the stations was very uneven. This has resulted in limited overall resolution and/or the dimension for imaging crustal and mantle discontinuities. In addition, the resulting images over a large region could be dominated by a few small areas with a relatively large number of ray-piercing points. The deployment of the ongoing USArray in the study area has significantly increased the spatial coverage, and therefore has greatly improved our capability to image the layered structure of the Earth's crust and mantle.

We have obtained from the IRIS DMC all the available broadband data from magnitude 5.3 or larger teleseismic (distance 30 - 100 degrees) events recorded prior to December, 2006 by all the permanent and portable stations in the area of 30N-45N latitudes, and 110W-125W longitudes. About 400 stations were found to have usable data that are archived as SEED files at the DMC. The total size of the SEED file is about 50GB. We have developed a set of computer codes to batch-process the large amount of data. The codes window the seismograms based on the IASP91 first arrival time, select seismograms with usable arrivals, compute P- and S-wave ray parameters and add them and other useful parameters in the SAC headers, and sort the seismograms based on event time. We (actually the Sun fire V240 computer and the two RAID systems which drive 6 TB of hard-disks) are in the final stage of finishing the processing of the data sets.

While the comprehensive data sets can be used for many purposes, our current focus is to map the first-order discontinuities (the Moho, 410, 520, and 660 km) from the surface of the Earth to the top of the lower mantle, and to search for possible discontinuities in the lower mantle by stacking P-to-S receiver functions. Results from those investigations and comparison with previous studies will be presented.

INTER-REGION VARIABILITY IN PERSISTENT SCATTERER BEHAVIOR

Rowena Lohman · Jet Propulsion Laboratory

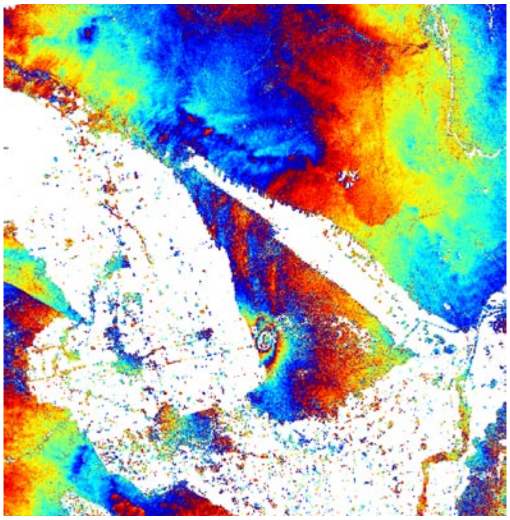

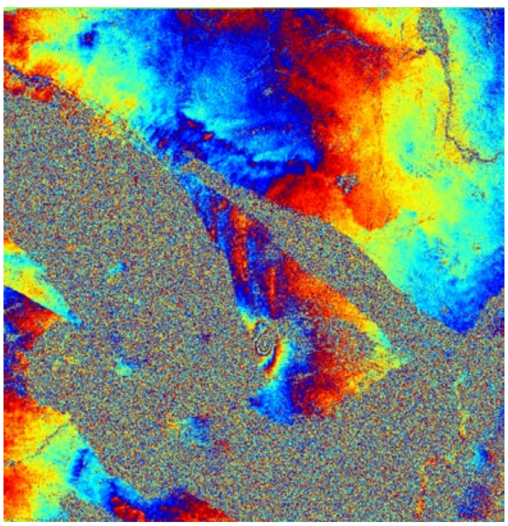

Interferogram with poor scatterers masked, showing coherent phase in otherwise incoherent regions of high agricultural activity.

Persistent scatterer analysis of InSAR data capitalizes on the idea that some sets of pixels will have stable phase behavior even when they are surrounded by regions of water, agriculture or vegetation which have low interferometric coherence. "Good" pixels are ones where the radar return is dominated by a stable structure such as a road, building or rocks. The use of persistent scatterer analysis can extend the use of SAR data to regions where traditional interferometry fails in cases where the persistent scatterers are dense enough and close enough to eachother that the interferometric phase can be unwrapped. Here, we examine both the density and quality of persistent scatterer targets in three areas: The Imperial Valley, CA, the San Francisco Bay area, CA, and the region around New Orleans, and discuss the feasibility of unwrapping these scatterers in each area.

ASSESMENT OF ACOUSTIC AND MAGNETIC PROPERTIES IN CORE SAMPLES FROM THE SAFOD MAIN HOLE: PRELIMINARY RESULTS

Laurent Louis, Philippe Robion, Christian David · Université de Cergy-Pontoise
Teng-fong Wong · SUNY Stony Brook

Two core samples from the SAFOD main hole located respectively at 3063 and 3992 meters measured depth (i.e. along the borehole) have been studied through the measurement of P-wave velocity, magnetic susceptibility, and the estimation of their associated anisotropies.

The first sample is an arkosic sandstone from spot core collected at the bottom of Phase I hole. P-wave velocity results show a slightly planar fabric with a maximum anisotropy of the order of 10-15 %, while the fabric obtained for the magnetic susceptibility is less anisotropic (~2%) and the three eigenvectors are well defined with a slight elongation along the maximum susceptibility vector, K1. No obvious correlation arises from the comparison between elastic and magnetic fabrics and further investigation such as P-wave velocity measurements on water saturated samples and a microstructural analysis under reflected light will follow.

The second section belongs to the spot core sampled at the bottom of Phase II hole and is mostly shaly siltstone. Due to a high tendency to fracturing, samples were cored at a smaller diameter (18 mm) than for the arkosic sandstone (25mm). Results of P-wave velocity measurements show anisotropy of the order of 15-30 % along with a strong attenuation effect of the veins and no 3D reconstruction of the angular velocity variations could be performed. The anisotropy of magnetic susceptibility consists of three well isolated eigenvectors with ~3-4 % anisotropy.

Due to the lack of information concerning the exact orientation of the spot cores structural interpretation could be not be done. In order to reorient the studied samples with respect to geographical coordinates and therefore relate the observed anisotropies to the tectonic setting, we are currently pursuing two kinds of remanent magnetization measurement techniques. Preliminary results obtained from demagnetization under alternative magnetic fields shows that at least two sources of remanent magnetization coexist and none appears as being parallel to the borehole axis.

A MULTIDISCIPLINARY INVESTIGATION OF RIO GRANDE RIFT DEFORMATION

Anthony R. Lowry · Utah State University
Anne F. Sheehan, R. Steven Nerem, Monica Guerra · University of Colorado
Mousumi Roy, Amy Luther · University of New Mexico

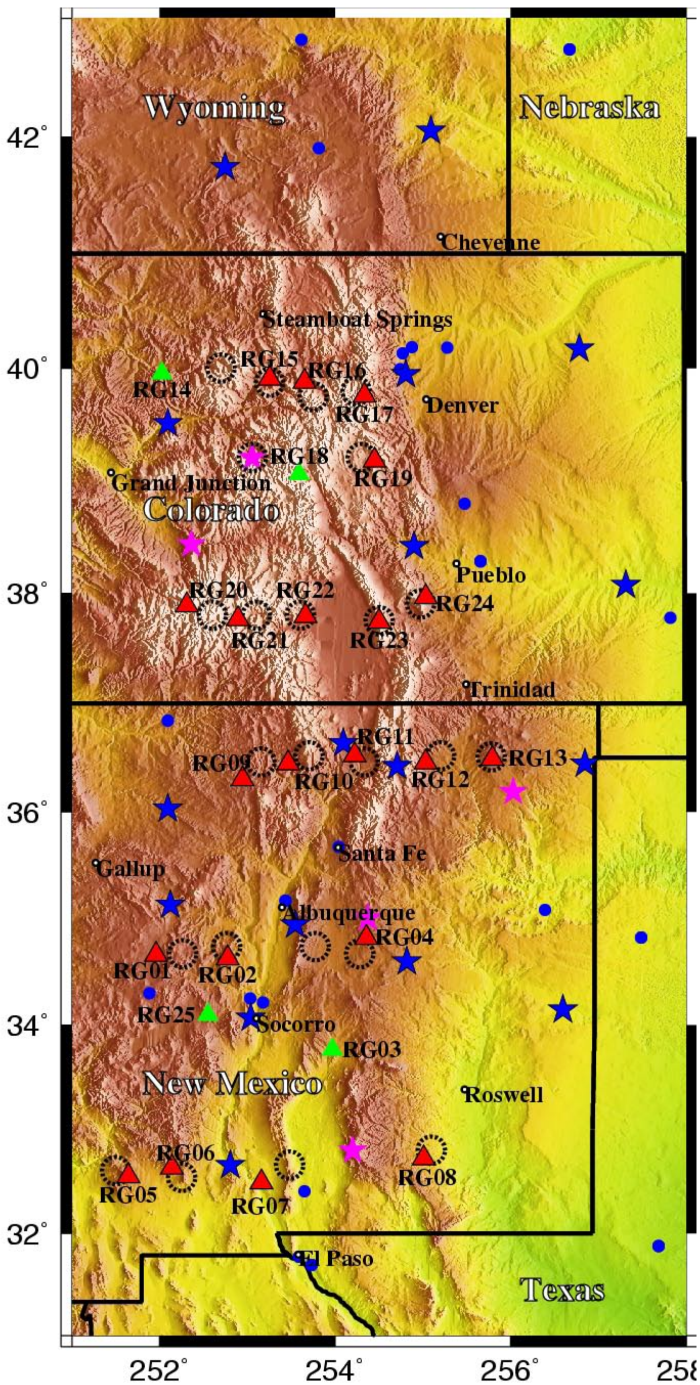

The Rio Grande rift is the easternmost actively deforming province on North America's western margin. The character of rifting changes from north to south, with a single narrow rift valley in Colorado and northern New Mexico grading to a broad â€œbasin and rangeâ€ expression in south-central New Mexico. This expression is not well understood, but may have significant bearing on our understanding of how and why continental lithosphere extends and of earthquake and volcanic hazards in rift zones. A large body of geophysical data make it an ideal laboratory in which to study the roles of lithospheric rheology, plate boundary forces and local buoyancy in active continental rifting. However, existing data are ambiguous about processes, rates and spatial distribution of RGR extension. For example, mantle seismic expression of the rift may be narrow or wide depending on whether one assumes Vp, Vs or Q anomalies as a proxy. Existing geodetic and geological data suggest rates ranging from 0.3 to 5 mm/yr extension, with uncertainties as large as the signal.

Complementary to PBOâ€“EarthScope deployment of coarsely spaced continuous GPS instruments in the RGR region, and with expertise and support provided by UNAVCO, we are installing a focused deployment of 25 quasi-continuous GPS sites in five dense profiles to study the nature of continental rifting. As of February 2007, 21 of the sites are installed and collecting data. Another two are ready for installation as soon as weather permits, and two more are in late stages of reconnaissance with plans to install in spring 2007.

Our current research focuses on improving estimates of atmospheric effects and multipath in GPS positions, to better capture the extremely low signal. In this presentation we will show results of initial data analysis at some of the sites, as well as plans for improving our analysis of tectonically-derived motions. Early efforts will focus on re-analysis of data collected at other regional GPS sites and on identifying nonlinear motions in the GPS time series at all sites. Nonlinear signals may provide evidence of monument instability (particularly if directions and timing are consistent with those expected for unstable hillslopes), and will certainly include mass loading effects which we will model from independent data. However nonlinear deformation may also result from magmatic intrusion. The JPL site at Pietown, New Mexico (PIE1) shows evidence of nonlinearity throughout its 13-year time series. Our calculations suggest the site lies near the sphere of influence of the Soccoro magma body, but the directions of motion would imply another source. Quaternary volcanism is ubiquitous throughout the RGR study area, as is mantle-derived CO2 gas in springs, so we anticipate that understanding the contribution of magmatic intrusion to the total permanent deformation will be vital to understanding the rifting process. In this presentation we will also discuss future plans for geodynamical modeling and preliminary results of our attempts to estimate rheological variations in the regional lithosphere.

SMALL-SCALE VARIATION IN SEISMIC ANISOTROPY ACROSS THE SAN ANDREAS FAULT NEAR PARKFIELD, CALIFORNIA

Lauren R. Mattatall, Matthew J. Fouch · Arizona State University

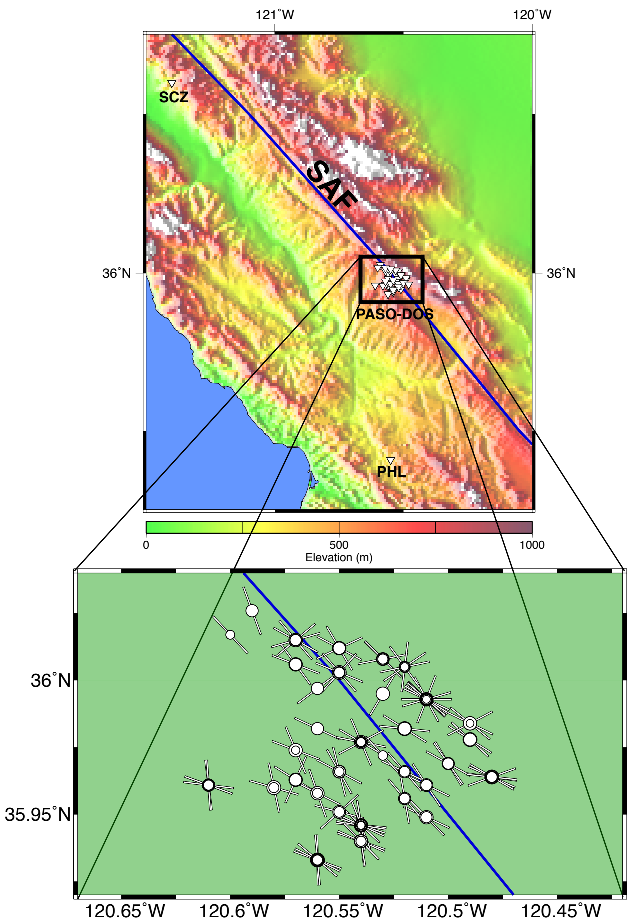

(upper panel) Geographic setting of study region. Blue line delineates San Andreas Fault (SAF). Inverted open triangles denote broadband stations used in this study. (lower panel) Shear wave splitting results across the PASO-DOS broadband seismic array. Fast polarization directions are denoted by white bars; circles are scaled to splitting time and range from 0.7 s to 2.75 s. Blue line denotes local trace of SAF. For individual stations, splitting parameters vary based on backazimuth. For several individual events, splitting parameters exhibit a first-order variation for stations on each side of SAF.

The goal of this study is to determine the extent of variation in seismic anisotropy around a well-studied area of the San Andreas Fault (SAF). To this end, we have surveyed data gathered by a dense broadband seismic array near Parkfield, California. The Parkfield Area Seismic Observatory (PASO), was originally installed as a method of constraining proposed locations of the fault strike for the drilling of the San Andreas Fault Observatory at Depth (SAFOD). The bulk of the data collected is from the second phase of the array called PASO-DOS (Densification of Stations). The array has an approximate aperture of 15 km and is diagonally bisected northwest to southeast by the surface trace of the SAF (Figure 1). The stations recorded seismic activity for approximately one year beginning in October of 2001. We examined the SKS arrival times for events with epicentral distances between 85 and 130 degrees and minimum body wave magnitudes of 5.8. We evaluated seismograms for the fast polarization direction (phi) and splitting time (dt) that most effectively produced linear particle motion of the horizontal components. Resulting splitting times range from 0.7s to 2.75s with a mean splitting time of roughly 2.0s.

Splitting from individual events recorded at the array exhibit strikingly different results across the array (Figure 1). First-order variations in fast polarization directions are evident for stations on opposite sides of the SAF, consistent with a very sharp lateral anisotropic boundary across the fault. Additionally, well-constrained splitting parameters at individual stations are variable for events with differing backazimuths, suggesting complexity in anisotropy with depth across the array. These results suggest that previously assumed 2-layer models of anisotropy are not adequate to explain the fundamental variations in seismic anisotropy near Parkfield. This style of structural complexity is also likely persistent along many other regions of the San Andreas Fault system.

EXPERIMENTAL INVESTIGATION OF MONUMENT STABILITY IN THE NEW MADRID SEISMIC ZONE

G.S. Mattioli, P.E. Jansma · University of Arkansas
J. Davis, R. Smalley · University of Memphis

The 1811-12 NMSZ seismic events are still poorly understood. It was recently reported that strain rates based on GPS observations from the GAMA network are well above background and may be as high as in plate boundary zones (Smalley et al. (2005). In contrast, Calais et al. (2005) argued that the GAMA data are still too uncertain and provide only an upper bound on strain accumulation in the NMSZ, suggesting that strain rate may yet be zero in the NMSZ.

Errors related to monument instability and other unmodeled effects may mask any small tectonic signal. While spatial averaging may reduce the size of both white and random-walk noise, it does not mitigate their relative effects on strain accumulation models. Long-term correlations thus can have a large effect on estimating deformation rates. Because several years may be required to obtain accurate site velocity estimates from GPS time series in areas of small strain such as the NMSZ, a variety of errors with different timescales, whose relative contributions change with time, potentially corrupt the data. Although averaging can minimize white noise, it cannot mitigate time-correlated effects.

Monument behavior is not well constrained for different types from various geologic settings. Because monument motion is likely significant in the NMSZ, which is dominated by unconsolidated sediments of the Lower Mississippi Valley, we have installed two new cGPS sites at existing GAMA sites to analyze experimentally monument stability and noise. Our new sites use SCIGN-type drilled, deep-braced monuments, precision levels, and radomes, but in every other way are identical to GAMA sites ~10 m away. 30 s data have been accumulating for these sites over six months. We will discuss our initial results: 1) to assess quantitatively monument motion in different geological substrates; and 2) to evaluate the suitability of different monument types in low strain environments.

USING GPS DEFORMATION DATA IN UNDERGRADUATE CLASSES AND RESEARCH PROJECTS: STORIES FROM THE FRONT LINES

Glen S. Mattioli · University of Arkansas

We have been involved in using GPS deformation data in undergraduate education for over a decade. Our efforts can be separated into two basic categories: 1) development of curricular materials, such as lectures, labs, and homework exercises, based either on our existing research projects or other published or publicly available data; and 2) supervision of senior undergraduate independent research projects either as part of formal coursework required for completion of a B.S. degree or as part of a summer Research Experience for Undergraduates (REU).

Classroom use of GPS deformation data presents an excellent opportunity to address several pedagogical issues of broad significance within an undergraduate Earth Science curriculum. These include: 1) development of basic statistical analysis of experimental data of all types; 2) understanding the difference between accuracy and precision; 3) instrumental error and cross-calibration; and 4) spatial variability and correlation. We have found that using established data sets with clearly discernable trends works best in the classroom setting and we have successfully developed a one-semester class for senior undergraduate/first year graduate students toward this end. A screening exam, administered both at the beginning and end of the semester, was developed to assess the success of acquisition of basic statistical literacy.

In contrast, use of GPS deformation in undergraduate research is far more difficult. While GPS deformation data are extremely powerful to elucidate neotectonic or neovolcanic processes, the time and effort needed to acquire any scientifically meaningful observations requires archival data in a region of interest to allow design of individual student projects. In 2006, we completed the first year of a NSF-supported REU site in Dominica in which five undergraduates collectively made GPS observations, then analyzed and modeled these data from 23 sites. Individual projects used GPS observations previously collected, in most cases by former cohorts of REU students, during campaigns completed between 2000 and 2004. The implication is that future REU students will gain additional benefit from the work of the predecessors, requiring that careful thought be given to the initial design of individual research projects.

QUATERNARY TECTONISM IN A COLLISION ZONE, NORTHWEST WASHINGTON

Patricia McCrory, Stephen Wolf, William Danforth · U.S. Geological Survey
Steven Intelmann · Olympic Coast National Marine Sanctuary
Ray Weldon · University of Oregon

Kinematic, geodetic, and geologic observations define a region with 6-8 mm/y of north-south contraction between the Columbia River and Vancouver Island. We attribute this contraction to differential forearc-block motion within the Cascadia subduction system where the Oregon Coast Range block is moving northward relative to Vancouver Island. The contraction is accommodated by a combination of distributed uplift in the Olympic Mountains, and faulting along the margins of the Coast Range and Vancouver Island blocks. The tide gauge at Neah Bay, which records one of the highest rates of uplift anywhere along the Cascadia subduction margin, suggests that a significant portion of this north-south contraction occurs between the northern Olympic Peninsula and Vancouver Island.

The northwest-trending Calawah fault, extending from Makah Bay eastward to near Lake Crescent, appears to mark the modern boundary between the Olympic Mountains block and the Vancouver Island block in northwestern Washington. Onshore, the 80+ km-long Calawah fault displaces late Quaternary glacial sediments and geodetic uplift rates increase abruptly across the fault zone. Offshore in Makah Bay, new multibeam, sidescan-sonar, and high-resolution seismic reflection data image a complex, multi-strand fault zone that offsets the seafloor and moves Cape Flattery rocks seaward. Two parallel, northwest-trending fault strands bound a down-dropped block that in turn terminates along a northward-trending anticlinal fold and thrust fault. These data suggest that the Calawah fault zone currently accommodates contraction both by uplift and by seaward translation of rocks north of the forearc-block boundary. Our geologic mapping in the Cape Flattery area indicates that differential block motion is accommodated by a combination of crustal uplift, folding, and left-lateral, strike-slip faulting.

FOCUSSING EARTHSCOPE OUTSIDE THE US - A STUDY OF ANDEAN CRUSTAL THICKNESS

Neil McGlashan, Larry Brown · Cornell University

Although crustal thickness is a critical value for geodynamic models of Andean orogenesis, relatively few measurements exist from local seismic studies. Depth-phase precursors are interpreted as reflections off the underside of the Moho from intermediate depth earthquakes and provide estimates of crustal thickness for the central Andes (16° – 34°S). We have identified such reflected signals (pmP) as precursors to the depth phase pP recorded on pre-EarthScope stations at teleseismic distances (35° to 85°). Although relatively small in amplitude, the pmP phase is often clear even on single seismograms. Less obvious precursor arrivals are enhanced by stacking signals recorded by arrays. This method is most effective for events of Mw>6 and depth>100km and has provided crustal thicknesses estimates which display dynamic variation ranging from 59 to 70 km in southern Peru, from 49 to 80 km across the Puna-Altiplano and from 50 to 60 km above the Pampean flat slab. The irregularity of Moho depth is echoed in the variation of respective reflectance quality throughout the Andes. While many events yield compelling Moho reflections, significant numbers also indicate a complete absence of signal which in turn provides insight into the lithologic nature of the Moho.

Earthscope's USArray is fortuitously located for recording pmP from the Andes. It thus represents a substantial leap in capabilities for mapping, in detail, the morphology and character not only of the Moho in this critical region, but other lithospheric interfaces as well. This potential is illustrated by the analysis of the Mw 6.6 earthquake on 25th August 2006 that was recorded by 235 USArray stations in the western U.S. Preliminary analysis identified over 46 clear reflections that map the Moho variability over an area 20 km2 beneath the northern Puna. Variations in pmP amplitudes seem to be systematic, suggesting significant changes in Moho reflectivity over short distances beneath the Andes. The areal distribution of USArray stations provide means of evaluating interference and focal mechanism effects. As USArray sweeps eastward, it will continue to scan the deep Andean lithosphere over a larger area.

A FOCUSED DRILLING PROGRAM IN THE NEW MADRID SEISMIC ZONE

Jason McKenna · US Army Research & Development Center
Andrew Newman · Georgia Institute of Technology
Seth Stein · Northwestern University
Carol Stein · University of Illinois at Chicago

As the type example of a continental intraplate earthquake zone, the New Madrid area demonstrates how little is understood about the underlying physics of the rifting, and subsequent relaxation/reactivation processes, and hence about the potential hazard. At present we don't know why the earthquakes occur, when and why they started, if and when future large earthquakes will occur, how serious the danger of such earthquakes is, and how society should confront it. A crucial question is whether New Madrid and other seismic zones are hotter and weaker than surrounding regions. If so, they are likely to be long-lived weak zones where intraplate strain release concentrates. Alternatively, if they are not significantly hotter and weaker than their surroundings, strain release and seismicity are likely to be transient phenomena that migrate among many fossil weak zones.

Because large earthquakes here are far rarer than in many other seismic zones, the seismological data we would like to address these hotly debated issues will not be available for hundreds or thousands of years. However, much could be learned by characterizing the thermomechanical structure of New Madrid and other intraplate seismic zones. Doing so would help reconcile the earthquake history - large earthquakes in 1811 and 1812, small earthquakes today, and large earthquakes within the past several thousand years – with geodetic data showing little or no present deformation and geologic data suggesting that the present seismicity is a recent phenomenon.

We propose a program conceptually similar to the San Andreas Fault Observatory at Depth (SAFOD) component of the EarthScope Initiative, to explore the thermo-mechanical state of the crust in and adjacent to New Madrid. This would include (1) using repeated temperature logging and other geophysical logs to better characterize the thermal-hydrologic regime to make more precise heat flow determinations in open hole situations; (2) assessing whether or not in situ heat production estimates of basement derived from spectral gamma ray logs are comparable to measurements made on core in the laboratory, and its implications for the heat flow-heat production relationship in non-tectonized terrains; (3) using acoustic televiewer and full wavefield sonic logs to characterize the orientation of fractures downhole and compare it to the regional surface stress field derived from earthquake focal mechanisms and GPS studies. The program would integrate naturally with ongoing seismological, geodetic, and geological studies.

A 70+ STATION GPS RECORDING OF THE JANUARY, 2007 CASCADIA ETS

Timothy Melbourne, Marcelo Santillan, Meghan Miller · CWU

Of the 35 slow slip events that have been recognized to date with GPS in the Cascadia subduction zone, the coverage of the most recent January 2007 transient is unprecedented and reflects the ongoing geodetic instrumentation of the northern Cascadia forearc. Compared with previous events recorded on a handful of stations, this most recent ETS ruptured through more than 70 instruments from the combined PBO and PANGA arrays and shows measurable deformation on 40 of them. Although at this time final orbits are still pending for last few days of the event, many of its characteristics are already measurable. The event nucleated mid-January to the west of the southern Puget Basin and propagated only northwards: transient deformation appears in the southern Puget Basin for at least 14 days prior to its onset around the Strait of Juan de Fuca. The greatest offsets are also found along a swath beneath the eastern Olympic Mountains and overlying the 30 km depth contour, west of the southern Basin. The largest of these measure 6+-1.8 mm and is directed towards the southwest, characteristic of previous Cascadia events. The total effective moment of the event appears to be Mw=6.6, as estimated by inverting transient offsets for thrust-only slip; this number is also typical of past events in this region. Slip appears to be more concentrated, with best-fitting inversions yielding 4 cm of slip. Qualitatively, this event looks like the northern half of the Feb-March 2003 ETS, which also nucleated in the SW Puget Basin but propagated bidirectionally to the north and south. Due to the number and density of stations that constrain this event, it is possible to estimate time-dependent slip propagation. These will be computed once final orbits become available and presented at the workshop.

(8e6.jpg) - Slip distribution for January 2007 ETS

EARTHSCOPE AND INTEGRATION OF SYNOPTIC DATA: UNDERSTANDING THE STRUCTURE AND EVOLUTION OF A CONTINENT *(Speaker)*

Anne Meltzer · Lehigh University

EarthScope provides an integrating framework for investigating continental evolution, dynamics, and structure using the continental US as a natural laboratory. EarthScope provides new observational facilities to deliver seismic, GPS, strain, and borehole data that, for the first time allows earth scientists to observe plate tectonics in real-time on a continental scale. These new facilities provide synoptic data at an order of magnitude higher resolution than previously available, providing the first continuous, coherent, high-resolution, three-dimensional images of the Earth's interior, and allowing Earth scientists to link deep earth processes and structure to their surface expression on a continental scale. These new facilities will undoubtedly improve our understanding of lithospheric and sublithospheric mantle structure and composition and deformational processes. To maximize the potential for significant advances in our understanding of tectonic processes, observations from these new facilities must be integrated with additional geologic data sets of similar quality and resolution. The integration, manipulation, and analysis of these combined data sets provide significant IT challenges for the earth science community. Data quality control, access, retrieval, integration, and visualization tools need to be developed. Community models have provided a mechanism within the atmospheric and ocean science disciplines for scientists to integrate, analyze, and share data and results within a process oriented framework. Community models can play a similar role in the earth science community.

SUPPORTING EARTHSCOPE FACILITY SITING WITH GIS

Matt Mercurio, Fred Pieper, Bill Schultz, Jean Miller · IAGT

As part of its contribution to the EarthScope project, IAGT provides GIS and mapping support to aid in the selection of candidate sites for Plate Boundary Observatory (PBO) GPS and USArray seismic geophysical instrument construction. This support geospatial data and geographic information system (GIS) software to assist the field siting engineers with the siting process in three key areas: 1) Site Suitability Analysis, 2) GIS tool and data development, and 3) geovisualization products.

Site Suitability Analysis

Suitability analysis refers to a spatial information overlay technique that helps identify the most appropriate locations for specific land uses. As applied to the work of PBO and USArray, this technique allows field personnel to quickly focus their initial site reconnaissance efforts on much smaller areas within the larger target siting buffer zones. This approach is applicable for any instrument siting activity where explicit site characteristics can be identified. For the PBO GPS instrument siting, a number of key variables are used to quantify potential site quality and they include: 1) land ownership, 2) slope, 3) aspect, 4) viable communication availability, 5) access, and 6) bedrock availability. The suitability analysis for the USArray seismic stations adds a step by initially excluding all areas in the siting tolerance buffer that are not viable for seismic station siting due to their high levels of background noise, including criteria for varying distances from roads depending on their size and distance from water features. The end result of the suitability analyses are maps and datasets showing areas that have the highest coincidence of the criteria identified above. These GIS-based site suitability analysis techniques have proven to be extremely valuable to the EarthScope engineers, but the same concepts and approach are directly applicable to any geophysical instrumentation planning, siting, and installation activities.

GIS Tool and Data Development

Various GIS tools and datasets have been developed in support of Earthscope facility siting efforts. The tools that were developed include a web-based viewshed analysis tool, the mapping component for the PBO network state of health map, and a Google Maps based tool for allowing the public suggest locations for future USArray sites. Each of these tools brings GIS map, data and analysis techniques to bear with regards to assisting in facility siting. Providing GIS support to the siting process has also involved the compilation of large amounts of public data (e.g. aerial photos, digital U.S. Geological Survey quad maps, etc), the creation of new datasets and the serving of these datasets to the web. Specifically, the USArray site suitability analysis results are packaged with reference datasets that include layers detailing land ownership, basic infrastructure, aerial photographs, satellite photography, and digital raster graphics. Google Earth is used as a mechanism for serving up to date PBO and USArray network installation progress. The PBO network state of health map uses reference GIS data served via a Web Mapping Service (WMS) for a backdrop to the state of health markers.

Geovisualization Products

Novel and traditional geovisualization products are used extensively in the support of the Earthscope facility siting process. Most recently, several time lapsed animations showing the current and planned progression of the PBO and USArray Transportable Array facility were created to assist in the visualization of the build out. The results of the suitability analyses are presented to field engineers as hard copy map products showing the suitable areas on a variety of backdrops (i.e. aerial photos, land ownership, etc). Combining GIS output with graphic art applications allows for the creation of presentation and press quality graphics to support Earthscope electronic and print media. Large format maps have been used in many ways to communicate network build out status, as general reference for siting principal investigators and to solicit possible site locations from the natural science departments on various college campuses.

PROCESSES OF TERRANE ACCRETION AND MODIFICATION: THE KLAMATH MOUNTAINS OF CASCADIA

Kate Miller · University of Texas at El Paso
Calvin Barnes · Texas Tech University

We have assembled some preliminary thoughts for an integrated program of geological mapping, geo/thermochronology, and seismic investigations of the Klamath Mountains province (KMp) designed to significantly advance our understanding of Mesozoic accretionary processes and Cenozoic modifications that led to the formation of this fundamental tectonic element of the Cascadia suprasubduction zone. The KMp formed by amalgamation and accretion of tectonostratigraphic terranes by successive contractional events over at least 450 m.y. Compared to similar terranes in the Western Sierra Nevada metamorphic belt, KMp terranes are well preserved because they were not affected by emplacement of, and heating by Cretaceous plutons. The province underlies the southern Cascades arc and is traditionally considered a classic example of an orogen in which terranes are successively accreted at the base of crustal section. However, recent geologic and geochronological studies show that, contrary to conventional wisdom: (1) the exposed terranes do not record the entire accretionary history, thereby requiring involvement of unexposed thrust sheets, and (2) some accretionary events may have excised large parts of the pre-existing orogen. It is possible that none of this record would be visible were it not for Neogene doming in the central KMp and as much as 2000 m uplift in the past 2 m.y.

We believe that the current geological knowledge base for the KMp and surrounding regions can form the foundation for building a new 4-D model of terrane accretion and modification through a full integration of new EarthScope results from the refraction, reflection, and passive seismic experiments, geochronology and other geologic data. Specifically: (1) Geologic and geochronologic study could focus on the timing and shear sense of faults to be imaged by seismic experiments, and provide tight age constraints on magmatic, metamorphic, cooling, and exhumation events. (2) Reflection and refraction experiments could identify boundaries between terranes, geometry of faults (including the possibility of out-of-sequence thrusting) and a 3-D image of the Moho from passive array data. Balanced cross-sections produced by integration of surface and seismic data could be the basis for the tectonic interpretation of this region. (3) Zircon systematics on plutons of distinct ages will be used to “remotely sense” changes in the architecture of the crustal section (via ages of inherited zircon) and mantle age (via Hf isotope analysis) through time. (4) Passive seismic results would image mantle features (Moho topography, relic slabs, velocity anomalies related to hydration, thermal anomalies) that might indicate stabilization of lithosphere associated with tectonic (accretionary) events. (5) Combined passive seismic results, analysis of landform development (including geochronology), and regional tectonic reconstructions to evaluate the mechanism(s) responsible for current topography and state of isostatic support could be used to determine to what extent slab geometry, hydration or thermal anomalies may drive surface tectonic processes.

A CONTINENT-WIDE 1-HZ MAP OF LG CODA Q VARIATION ACROSS EURASIA AND ITS RELATION TO LITHOSPHERIC EVOLUTION

Brian Mitchell · Saint Louis University
Goran Ekström · Lamont-Dougherty Earth Observatory
Lianli Cong · Yunnan University

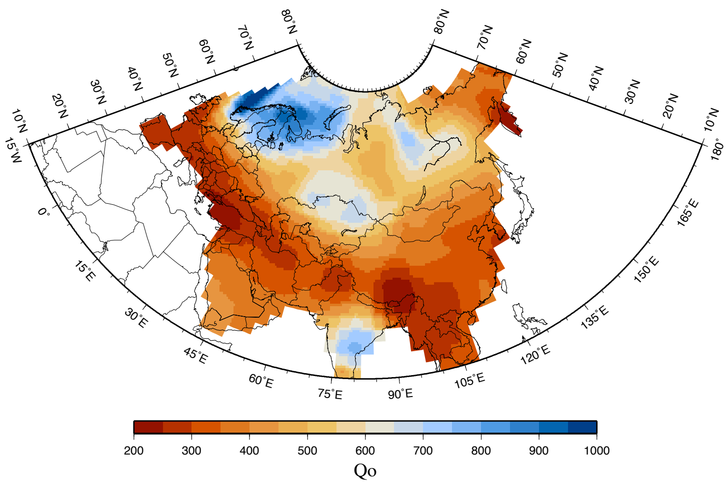

We present new maps of Lg coda Q and its frequency dependence at 1 Hz (Qo and , respectively) that cover virtually all of Eurasia. Our new data set, which nearly quadruples the number of previously available measurements, provides coverage for virtually the entire continent. Qo is relatively high, up to 700 and more, in most cratonic regions but is surprisingly low in the Arabian craton (300-450), the Siberian trap portion of the Siberian platform (~450) and the Deccan trap portion of the Indian platform (450-650). It is generally low throughout the Tethysides orogenic belt but there too it displays substantial regional variations (150-400). All major Qo anomalies, and several relatively minor ones, appear to be related to the tectonic history of the Eurasian lithosphere. The four regions with lowest values approximately coincide with four out of the five most seismically active earthquake concentrations in Eurasia. Observed Eurasian Qo variations are consistent with a previously developed plot of global values in which Qo in any region is directly proportional to the time that has elapsed since the most recent episode of tectonic or orogenic activity there. Our favored explanation for this evolution in Qo values is that it is produced by the dissipation with time of crustal fluids either by loss to the surface or by retrograde metamorphism.

Comparisons of the new Qo map with continent-wide maps of long-period Rayleigh-wave phase velocities, short-period Rayleigh-wave group velocities, upper mantle temperatures, subducted lithosphere and available information on crustal strain lead us to infer that hydrothermally-released fluids in the upper mantle travel to the crust and begin a long process of dissipation that leads to the Qo distribution of that we see today. Some lower than expected values in central and southern Asia suggest that the fluids were produced by some documented, and some yet undiscovered, lithosphere that subducted during the Paleozoic era.

TALC IN SAFOD SERPENTINITE CUTTINGS AND ITS POSSIBLE SIGNIFICANCE FOR FAULT CREEP

Diane Moore, Michael Rymer · U. S. Geological Survey

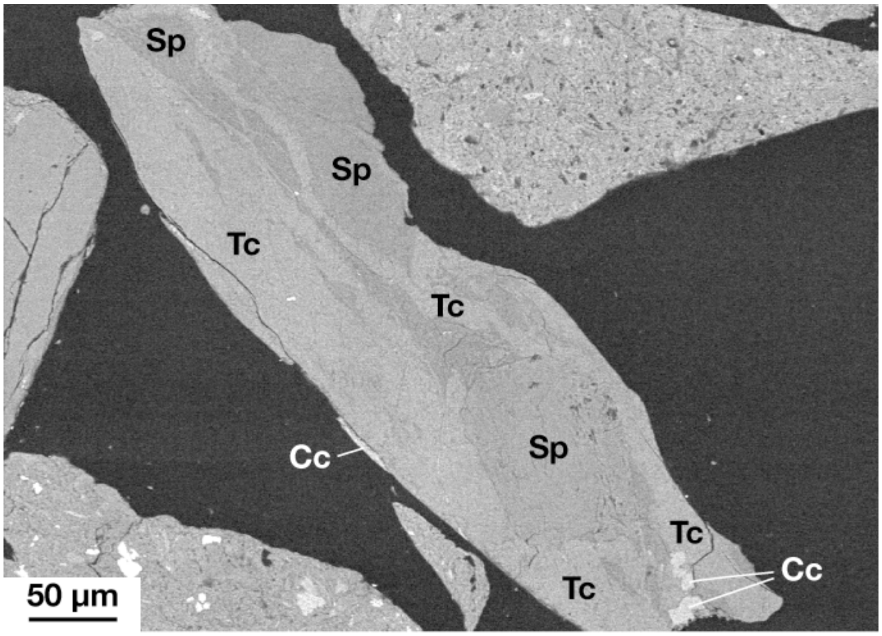

Talc (Tc) in a sheared serpentinite (Sp) grain from 3325-m MD. Minor amounts of calcite (Cc) associated with the talc indicate fluid migration through the sheared rock. Talc commonly appears at the edges of the grains, probably because the serpentinite breaks preferentially along the weaker talc during drilling.

The San Andreas Fault Observatory at Depth (SAFOD) drillsite is located near the southern end of the central creeping section of the San Andreas fault, and a portion of the well casing is actively deforming in response to creep on a fault strand intersected by the drillhole. Minor serpentinite was identified in SAFOD cuttings collected in the interval 3322-3353 m measured depth (MD), at the eastern margin of the zone of active deformation. Serpentinite is commonly invoked to explain both the creep of this section of the fault and the low strength that is indicated by modelling of heat flow data and earthquake focal mechanisms. However, the serpentine minerals themselves are too strong to satisfy the constraints on fault strength, and they also have the potential for unstable slip at some conditions. Talc is a magnesium-rich phyllosilicate that can form as a result of the reaction of serpentinite with silica-saturated hydrothermal fluids. Laboratory values of the frictional strength of talc under hydrothermal conditions are low enough to satisfy the limitationts on shear strength of the fault, and talc is characterized by inherently stable, velocity-strengthening sliding behavior. Localization of shear strain in a talc-rich zone could therefore meet the conditions for creep without the need to invoke other weakening mechanisms such as fluid overpressures. As a first step in testing this possibility, we conducted petrographic examinations of serpentinite grains from the SAFOD cuttings to determine whether or not they contain talc. Work to date has focused on the interval 3325-3341 m MD, where the proportions of serpentinite grains in the cuttings appear to be highest. Talc has been identified in serpentinite grains in all cuttings samples in that interval. Many of the serpentinite grains contain calcite veins, and talc partly replaces serpentine minerals at the vein walls. The hydrothermal fluids from which calcite was deposited provided the silica needed to convert serpentine to talc. Some quartz has been deposited metastably in fractures in the serpentinite, and the quartz is reacting with the serpentine minerals to produce talc. More significantly, talc forms along the foliation in sheared serpentinite grains. The abundance of talc and the proportion of sheared talc-bearing grains are greatest in the 3325-m sample, closest to the actively deforming zone. The veins and talc-bearing shears overprint all other textural features visible in the serpentinite grains, suggesting that talc is currently forming in the fault zone. The actively creeping zone should be one of the main targets of the Phase 3 coring planned for 2007, to determine the extent to which talc-bearing serpentinite may contribute to the creep.

UNDER CONSTRUCTION: WHAT WE'VE LEARNED ABOUT VOLCANO BUILDING FROM THE ONGOING ERUPTION AT MOUNT ST. HELENS *(Speaker)*

Mike Lisowski, Seth Moran, Dan Dzurisin, Jon Major, Larry Mastin, Mike Poland, Greg Waite · U.S. Geological Survey
Weston Thelen · University of Washington

An earthquake swarm on September 23, 2004, heralded the reawakening of Mount St. Helens (MSH) after almost 18 years of quiescence. The subsequent prolonged (2.5 years as of March 2007) eruption has produced a ~90-million-cubic-meter dacite lava dome, along with some very basic volcanological questions including "What caused MSH to start erupting?" and "When is it going to stop?" The question of what started the MSH eruption is to some degree unanswerable, as the real-time instrumentation in place prior to the onset of unrest consisted solely of a short-period seismic network with 13 stations within 20 km of the volcano and a single continuous GPS (CGPS) instrument installed in 1997 at a site 9 km north of the volcano. Seismic unrest rapidly escalated, and within a week it was judged too hazardous for field personnel to install new equipment within 3 km of the volcano. As a result, although seismicity was reasonably well-characterized by the existing seismic network, much of the detailed deformation field associated with the buildup to the eruption was not recorded. However, the CGPS instrument installed in 1997 showed no signs of significant volcano-related deformation from 1997 through September 23, 2004. Radar interferograms spanning 1992-2004 similarly showed no evidence of pre-eruption deformation. Thus it appears that MSH had been poised to erupt for over a decade, perhaps since the last dome-building episode in 1986, and that the 2004-present eruption was not triggered by a significant influx of new magma (Iverson and others (2006)).

Over the subsequent 2.5 years a principal focus of research and monitoring efforts has been to constrain the magmatic processes driving the eruption, as such processes strongly influence the nature and duration of the eruption. One of the remarkable features of the current eruption has been its duration, a feature all the more surprising given that the erupted dacite is cooler, more crystalline, and less gas-rich than that erupted in the relatively short-lived (days-to-weeks) lava-dome-building eruptions that characterized the volcano's behavior in the1980s. Important clues regarding current magmatic processes come from CGPS instruments installed in early October 2004 by the Cascades Volcano Observatory and the Plate Boundary Observatory. Eruption-related motion of CGPS instruments has been relatively subtle but widespread, consisting of inward and downward movements that have exponentially decreased with time, roughly in parallel with an exponentially-decreasing extrusion rate. Geodetic models of the CGPS data are consistent with a vertically-elongate magma chamber with its center at 7-8 km depth and a total volume loss of 15-25 million cubic meters since 2004. The volume discrepancy between modeled magma loss and erupted lava suggests that some of the erupted magma has been replaced by new magma coming from greater depths. However, uncertainties in magma compressibility and wall-rock elasticity make it difficult to determine how much, if any, magma recharge has occurred. Nevertheless, the possibility of recharge suggests that the eruption could continue for years to come.

A MICROSEISMIC VIEW OF THE IMMEDIATE SAFOD TARGET ZONE

Robert M. Nadeau · University of California, Berkeley

Pattern scanning of continuous and triggered waveform data recorded by the borehole High Resolution Seismic Network (HRSN) since August of 2001 reveals that over 100 similar microseismic events ranging in Ml from -1.4 to +2.2 occurred in a tight cluster around the SAFOD primary and secondary targets with dimensions comparable to those of an American football field (long and short dimensions along-strike and in depth, respectively).

Detection criteria for the pattern scanning required waveform similarity with the July 16, 2005 repeat of the primary (SF) target of > 0.60 maximum cross-correlation coefficients at 2 of the 8 scanned channels for a 4 sec pattern window starting just ahead of the P-arrival, effectively doubling the number of real event detections over the NCSN routine processing scheme for this same period.

By virtue of their similar waveforms, processing of these events allows for,

1) automated P- and S- phase picking to subsample precision,
2) quality control and weighting of phase picks based on maximum cross-correlation coefficients and relative signal to pre-event noise levels.
3) identification of data channels with faulty time stamps.
4) delineation of fine scale seismicity structure with cross-correlation aligned double-difference relocations from many constraining events.
5) Robust and automated relative magnitude information based on P- and S-phase spectra-ratios.

The range in magnitudes and tight clustering of the events also allows for advanced relative event techniques (e.g., empirical Green`s function deconvolution) to be applied to study the source properties of the SAFOD target (see poster by Dreger, Nadeau and Morrish) and to investigate the behavior of seismic activity in the immediate SAFOD zone.

All repeats of both SAFOD target sequences were identified with matching parameters well above the minimum required for detection. The numerous other events on the ~ 100 x 50 m fault surface show highly systematic patterns of localized spatio-magnitude clustering indicative of additional sites of characteristic microearthquake activity similar to that of the SAFOD M2 repeating target(s).

DIVERSE GEOPHYSICAL DATA FOR EARTHSCOPE-RELATED SCIENCE AT THE NORTHERN CALIFORNIA EARTHQUAKE DATA CENTER

Douglas Neuhauser, Mario Aranha, Stephane Zuzlewski, Robert Uhrhammer · University of California, Berkeley
Stan Silverman, Fred Klein, Lynn Dietz, Babara Romanowicz · U.S. Geological Survey

The Northern California Earthquake Data Center (NCEDC) has been a leader in providing diverse integrated geophysical data sets to the earth science community. The NCEDC archives and distributes data from surface and borehole seismic sensors, borehole strain meters, geodetic GPS receivers, electric and magnetic field sensors, creep meters, tilt meters, and other related sensors. Data providers include the Berkeley Seismo Lab (BSL), U.S. Geological Survey, EarthScope SAFOD, PBO and USArray programs, and other regional networks.

A number of networks contribute multi-parameter data sets to the NCEDC, and together they provide users with a diverse set of geophysical observations for northern California and beyond. The Berkeley Digital Seismic Network (BDSN) stations include data from surface and/or borehole seismic, GPS, electromagnetic, borehole strain, and pore pressure sensors. The U.S. Geological Survey low frequency geophysical network, operating for over 30 years, has collected multi-parameter creep, strain, tilt, well water level, and other geophysical data at more than 170 sites, with ~ 275 current channels. The BSL Parkfield High Resolution Seismic Network (HRSN) and the BSL/U.S. Geological Survey Hayward Fault Network seismic data compliment the data from SAFOD, PBO boreholes, and other neighboring BDSN and U.S. Geological Survey NCSN surface stations. The NCEDC is an official archive for the SAFOD borehole data and the PBO strain data. In addition to archiving SAFOD event data, the NCEDC maintains a multi-terabyte online buffer of all recent continuous SAFOD timeseries data for researchers interested in examining this unique data set.

The NCEDC can provide virtually all timeseries data in SEED format with the corresponding metadata, and distributes data through a variety of interfaces such as NetDC, BREQ_FAST, EVT_FAST, FISSURES/DHI servers, and STP. Processed level 2 data from PBO strain sites are distributed in an XML format that describe the transformations applied to the data to remove attributes such as data logger offsets and tidal signals. GPS data are available in standard RINEX and raw formats through the GPS Seamless ArChive (GSAC) retailers, FTP and HTTP. Timeseries and metadata from multiple networks and sensors can easily be retrieved in a common and consistent format. NetDC and FISSURES/DHI allow users to easily query and retrieve data from multiple data centers. The NCEDC, a joint project of the BSL and U.S. Geological Survey, is accessible at http://www.ncedc.org.

STRUCTURE AND EVOLUTION OF THE TAGUS ABYSSAL PLAINSTRUCTURE AND EVOLUTION OF THE TAGUS ABYSSAL PLAIN

Maria C. Neves · UALG
Alexandra Afilhado, Luís Matias · CGUL

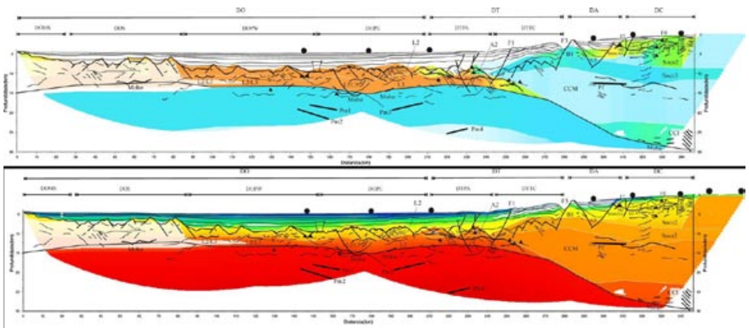

The opening of the North Atlantic Ocean is registered along the Newfoundland and West Iberia margins, perhaps the best studied nonvolcanic margins of the world (e.g. Boillot et al., 1987; Reid, 1994; Reston et al., 1995; Pickup et al., 1996; Dean et al., 2000; Withmarsh et al., 2001; Funk et al., 2003; Hooper et al., 2004; Shillington et al., 2006). Striking differences occur in the structure of this conjugated system. In Newfoundland extended continental crust thins abruptly with few crustal-scale normal faults, while Galicia Bank continental crust is dominated by seaward dipping normal faults and high angle faults that terminate at low angle-surfaces interpreted as detachment faults. The character of the transition zone is also remarkably different, having in Newfoundland margin been interpreted as thinned continental crust emplaced during the late stages of rifting, while in the Galicia Bank and Iberian Abyssal Plain (IAP) it is interpreted as a varying width zone of exhumed continental mantle (ZECM). These contrasts favour asymmetric models of continental breakup and complex transitions from late stage continental rifting to oceanic accretion.

Spatio-temporal variations in the rifting process also appear to exist between the Iberian Abyssal Plain, in the north, and the Tagus Abissal Plain (TAP), in the south of the Iberian margin. A geological transect of the crust and upper mantle structure in the TAP, extending from the un-thinned continental crust in the east to the oceanic crust in the west, has been recently published (Afilhado, 2006). This cross-section is constrained by one deep-penetrating MCS profile - IAM5 (Figure 1), coincident recordings of refractions and wide-angle reflections by OBS's and land stations, 2-D modelling of gravity and magnetic data. The knowledge of the deep structure obtained is comparable to the one already available in the Iberia Abyssal Plain where 2 Legs of the Ocean Drilling Program took place.

Comparing the TAP and IAP crustal structures we find several differences. At the TAP a short (~30 km) segment of transitional crust contrasts to the wide ZECM (~150 km) found at the IAP. Although a large body of exhumed mantle at the ocean-continent transition is hardly supported by the potential dataset, the eastern 35km segment of the TAP is a mass excess segment, bordered by positive magnetic anomalies, in good agreement with an intruded and partly ultramafic transitional crust, as suggested by the seismic data. Furthermore, the lower transitional crust extends from the TAP to the continental slope, while at the northern segment of the margin the ZECM is confined to the abyssal plain.

According to the last exhaustive work on seismic stratigraphy of the region (Mougenot, 1989), the margin suffered a main compressive event during Miocenic times. The deformation that this event produced is clearly identified on IAM5 profile and seams to be concentrated in two main areas, within the short transitional domain and further west near the base of the Tore-Madeira rise.

Other important event that affected this region is the sub-aerial volcanism at M0 times that formed the Madeira Tore Rise and the well known J magnetic anomaly (Tucholke and Ludwig, 1982). The thermo-mechanical effect of such event has not yet been addressed. Thus, both the Miocenic compression and the emplacement of the Tore-Madeira need to be taken into account in order to estimate as accurately as possible the evolution of the geometry of the rifted basin.

To study the thermo-mechanical evolution of the margin we follow the modelling formulation of Behn et al. (2002). We developed a lagrangian visco-plastic finite element program that incorporates strain-rate softening to simulate the rate-dependence of frictional strength observed in the laboratory. In this approach non-linear rheology is simulated by iterative linearization of the effective viscosity. A frictional failure criterion is use to bound the maximum principle shear stress in each element. The time-dependence of the frictional strength is simulated by introducing a strain-rate dependence on the cohesion coefficient. Forcing of the model is implemented through velocity boundary conditions and gravitational body forces. The modelling results are a proxy for the initial pattern of deformation that will form in response to a given set of thermal and rheological conditions. The advantage of this formulation is that it predicts zone of localized deformation (high strain rate) that can be considered analogous to faults. The method has been succefully applied to explain the spatio-temporal evolution of deformation in the North Sea (Cowie et al., 2005). By using these numerical tools we expect to assess the degree of coupling between basement and near surface deformation and determine the thermal conditions and boundary forces that cause zones of strain localization consistent with the fault patterns observed in the TAP transect. A well constrained picture of the evolution of the south segment of the West Iberia margin will also contribute to a better understanding of the North Atlantic rifting process.

ADVANCES IN WEB-BASED VISUALIZATION OF THE STATE-OF-HEALTH OF EARTHSCOPE'S TRANSPORTABLE ARRAY

Robert Newman · Scripps Institution of Oceanography
Kent Lindquist · Lindquist Consulting
Frank Vernon, Geoff Davis, Jennifer Eakins, Luciana Astiz · Scripps Institution of Oceanography

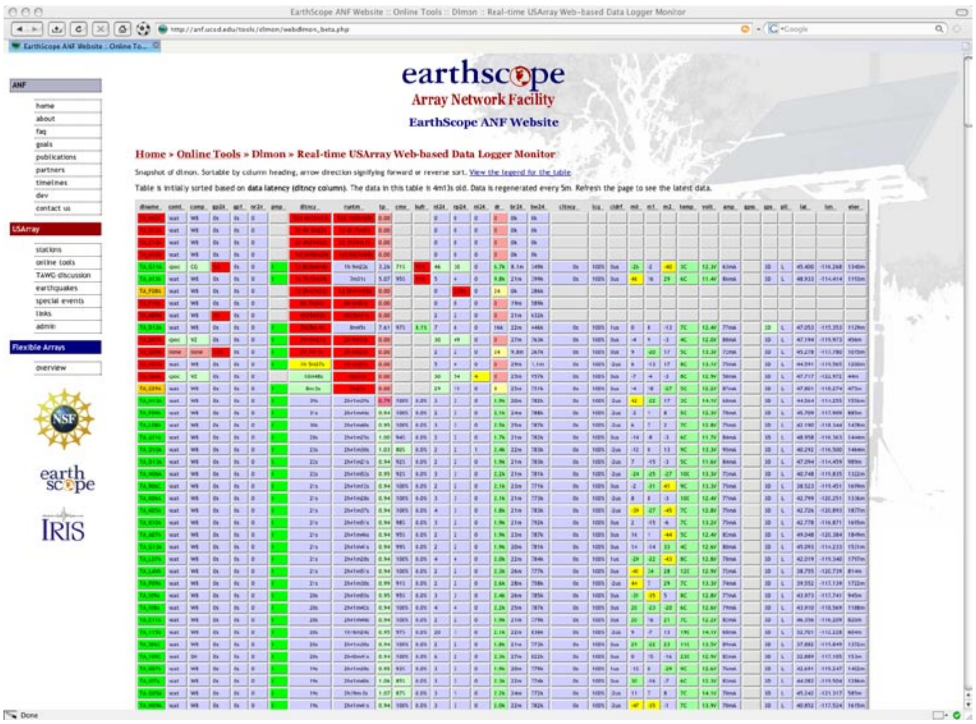

Screen dump of the XML, Javascript and PHP powered web-based datalogger monitor (webdlmon), http://anf.ucsd.edu/tools/dlmon/webdlmon.php

The Earthscope Transportable Array has increased in size over the last three years to over 250 broadband seismic stations. Critical real-time assessment of datalogger state-of-health information and data transfer metadata is fundamental to maintaining a healthy network. Providing this information to analysts, station engineers, administrative staff, researchers and the public is the responsibility of the Array Network Facility (ANF). Various interconnected software packages (including the Antelope Environmental Monitoring System, Round Robin Database Tool, Generic Mapping Tools, MATLAB) and web services (including Nagios and Flickr) build data products in near real-time that are organized and integrated into the ANF website using XML, Javascript, and PHP. These metadata and data products are readily accessible via the world-wide-web at http://anf.ucsd.edu. This poster will highlight recent advances in web-based tool development, including an XML-based Datalogger Monitor (webdlmon) that is integrated with real-time graphing capabilities.

VELOCITY WEAKENING IN PHYLLOSILICATE-BEARING FAULT GOUGES: IS THERE EVIDENCE FOR SIMILAR PROCESSES IN SAFOD SAMPLES?

André Niemeijer · Pennsilvania State University
Chris Spiers · Utrecht University, The Netherlands

Rotary shear experiments, performed on a halite-muscovite fault gouge analogue system, have shown that the presence of phyllosilicates, under conditions favoring the operation of cataclasis and pressure solution in the matrix phase, can have major effects on the frictional behaviour of fault gouges. Our experiments have shown that while 100% halite and 100% muscovite samples exhibit rate-independent frictional/brittle behaviour, the strength of mixtures containing 10-30% muscovite is both normal stress and sliding velocity dependent. At low velocities (<1 micrometer/s), the strength increases with increasing velocity and normal stress, and a strong mylonitic foliation develops. At high velocities (>1 micrometer/s), velocity-weakening frictional behaviour occurs, along with the development of a structureless, cataclastic microstructure. The observed velocity-weakening effect is much larger than typically seen in friction experiments. Micromechanical modelling of the behaviour observed in the velocity weakening (cataclastic) regime indicates that this behaviour can be explained in terms of a granular flow process involving competition between intergranular dilatation and compaction by pressure solution. The predictions of the model agree well with the experimental results. Extension of this model to quartz-mica systems implies that the presence of phyllosilicates can strongly promote (unstable) velocity weakening behaviour at rapid slip rates on natural faults, under mid-crustal conditions. In future, we hope to acquire fault gouge samples from the SAFOD project and to assess, from microstructral studies, whether similar mechanisms may have operated. We also hope to extend our rotary shear experiments to SAFOD material, to compare the frictional behaviour of this material under in-situ conditions with our analogue experiments and microphysical models.

CONSTRAINING SERPENTINITE PRESENCE BENEATH THE CASCADES.

Alex Nikulin, Vadim Levin · Rutgers University
Jeffrey Park · Yale University

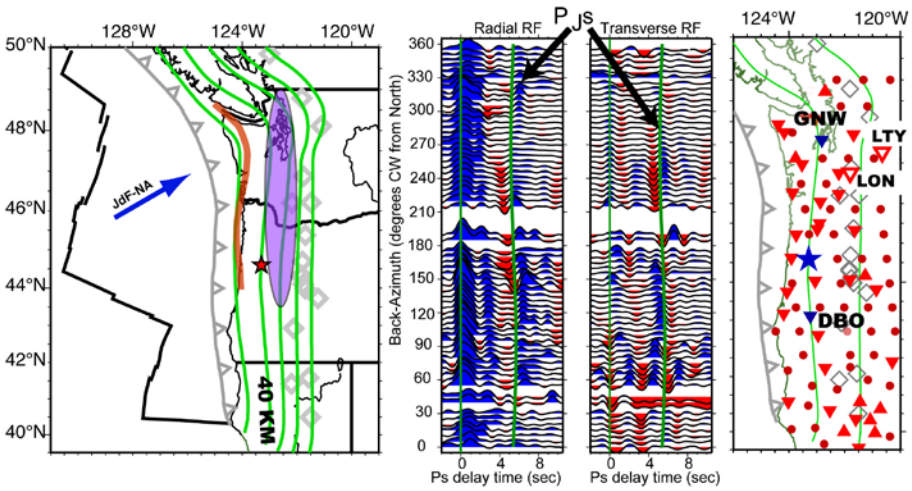

Figure Caption LEFT: A map of the Cascadia subduction zone shows volcanoes (grey diamonds) and contours of the subducting plate (green lines). Also shown are the location of the seismic station COR where the serpentinite layer has been identified (red star), the down-dip extent of the seismogenic zone based on thermal modeling and geodetics (orange line), and the region where the supra-slab mantle wedge is believed to contain significant amounts of serpentinite (purple oval). MIDDLE: Receiver functions computed from 602 earthquakes observed at Corvallis, OR. A straight green line marks the arrival time of the "parent" teleseimic P wave, the curved green line shows expected arrival time of the "daughter" P-to-S converted wave from an interface at 43 km, dipping 15 to the east. A clear two-sided phase seen on both sides of the curved green line is interpreted as evidence for the layer of sheared serpentinite above the Juan de Fuca slab. RIGHT: Existing permanent sites (triangles) for which data are available through IRIS DMC. Sites where we see the signature of the serpentinite layer are in blue, where we do not see are open. Red dots show the transportable array deployment plan as of spring of 2006.

The presence of serpentinite between the tectonic plates of subduction zones has been proposed as an inhibitory mechanism for earthquake rupture. In Cascadia, presence of serpentinite layer was recently proposed beneath Corvallis, Oregon from teleseismic receiver functions. Detection of the serpentinite layer and assessment of its spatial distribution is an important task in understanding regional geodynamics. We use receiver function methodology to analyze seismograms from permanent observatories located along the West coast of the US in Oregon and Washington. Preliminary results allow us to discern differences in subsurface velocity structure between areas potentially affected by serpentinite, and control areas where no serpentinite is thought to be present. In this presentation we show and discuss the results of our preliminary work, a set of receiver function profiles from permanent seismic stations throughout the region. To date, in addition to Corvallis, OR, we observe seismic signature of the serpentinized layer at stations GNW (Green Mountain, WA), and also at station DBO (Dodson Butte, OR). The signature is not obviously present at data-rich seismic stations LON and LTY in Northern Oregon. It is notable that all three sites showing a signature of the proposed serpentinite layer are ~40 km above the surface of the subducting Juan-de-Fuca plate. Sites where we cannot find the signature are further inland, and the slab surface beneath them is deeper.

In the future we will analyze emerging data from the transportable array of the EarthScope that is currently deployed in the region, aiming to map the serpentinite layer in detail.

CONTINUOUS IN-SITU MEASUREMENT OF STRESS-INDUCED TRAVEL TIME VARIATION AT PARKFIELD

Fenglin Niu · Rice University
Paul Silver · DTM, Carnegie Institution of Washington
Tom Daley, Ernest Majer · Lawrence Berkeley National Laboratory

It is well known that seismic velocity is stress dependent, due to the effect of stress on crack density. This dependence constitutes, in principle, a powerful means for studying subsurface transient changes in stress. We have been attempting to measure this stress sensitivity using continuous crosswell travel time measurements. We conducted an experiment at the site of the SAFOD drill hole at Parkfield from October 28, 2005 to January 9, 2006. A specially-designed 18-element piezoelectric source was placed at a depth of ~1 km depth in the SAFOD pilot hole and a three-component clamped accelerometer was deployed at around the same depth in the main hole. We used a commercial Geometrics GEODE data logger to record the data. The data were collected at a sampling rate of 48,000 samples per second. The source was pulsed every 250 ms with a record length of 200 milliseconds, which yields 4 traces per second. The waveforms were automatically stacked for every 100 shots and then further manually stacked another 100 times and filtered with a bandpass filter of 1 to 5 KHz. The signal to noise ratio is around 40 and the uncertainty in the delay-time estimation from stacking of 1-hour records is ~60 ns. Since the travel time (including coda) is 10 ms, we are able to detect velocity changes of order 10-6. Delay times were measured for the S wave and the coda (Figure 1). In general, the delay times of the coda are about twice as large as those of the S wave, which suggests that they are caused by a change in the bulk velocity of the medium, since coda waves travel longer in the media and thus are more sensitive to velocity changes. Variation in delay time is around 3 microseconds and shows a remarkably good negative correlation with the barometric pressure change. We attribute this correlation to stress sensitivity of seismic velocity and the stress sensitivity is estimated to be 3x10-7/Pa. Our results indicate that substantial cracks and/or pore spaces exist even at seismogenic depths and may thus be used to monitor the subsurface stress field.

AFRICAARRAY

Andrew Nyblade, Richard Brazier · Pennsylvania State University
Gerhard Graham · Council for Geoscience, South Africa
Paul Dirks · University of the Witwatersrand, South Africa

AfricaArray is a long-term initiative to promote coupled training and research programs in geophysics for building and maintaining a scientific workforce for Africa's natural resource sector. The main goals of AfricaArray are to: 1) maintain and develop further geophysical training programs in Africa, in response to industry, government and university needs, 2) promote geophysical research in Africa, and establish an Africa-to-Africa research support system, 3) obtain geophysical data, through a network of shared observatories, to study scientific targets of economic and societal interest, as well as fundamental geological processes shaping the African continent. AfricaArray is supported by a public-private partnership consisting of many government organizations in the US and Africa, and mining and oil companies.

AfricaArray has been built on existing programs and expertise within partner institutions and is being implemented in three phases over ten years. During Phase 1 (1/2005 – 12/2007), the educational program at the University of the Witwatersrand is being expanded and improved to provide B.Sc., M.Sc., and Ph.D. degree training in geophysics for students from across Africa. Seismic stations are being installed or upgraded in participating countries to form a network of shared scientific observatories, and technical personnel are being trained to operate and maintain the seismic equipment. Data from the seismic stations are being used for student thesis research projects, and the seismic network is helping to catalyze scientific community building through educational and research collaborations. During subsequent phases (2007-2014), the in-situ education and research program will grow to provide B.Sc., M.Sc. and Ph.D. training for many more African students, the network of shared scientific observatories will be expanded, temporary networks of seismic stations will be installed, sustainable centers of excellence in geophysics will be established at other African universities, additional sensors (i.e., GPS, meteorological) will be installed at the seismic stations.

AfricaArray also has developed a US education program aimed at recruiting students from physics, math, engineering and earth science programs at historically black colleges and universities into graduate programs in geophysics at US universities.

DATA FOR EDUCATORS: BRINGING GPS AND DATA-RICH ACTIVITIES INTO COLLEGE AND SECONDARY EARTH SCIENCE CLASSROOMS

Shelley Olds · UNAVCO
Andrew Newman · Georgia Institute of Technology
Susan Eriksson · UNAVCO

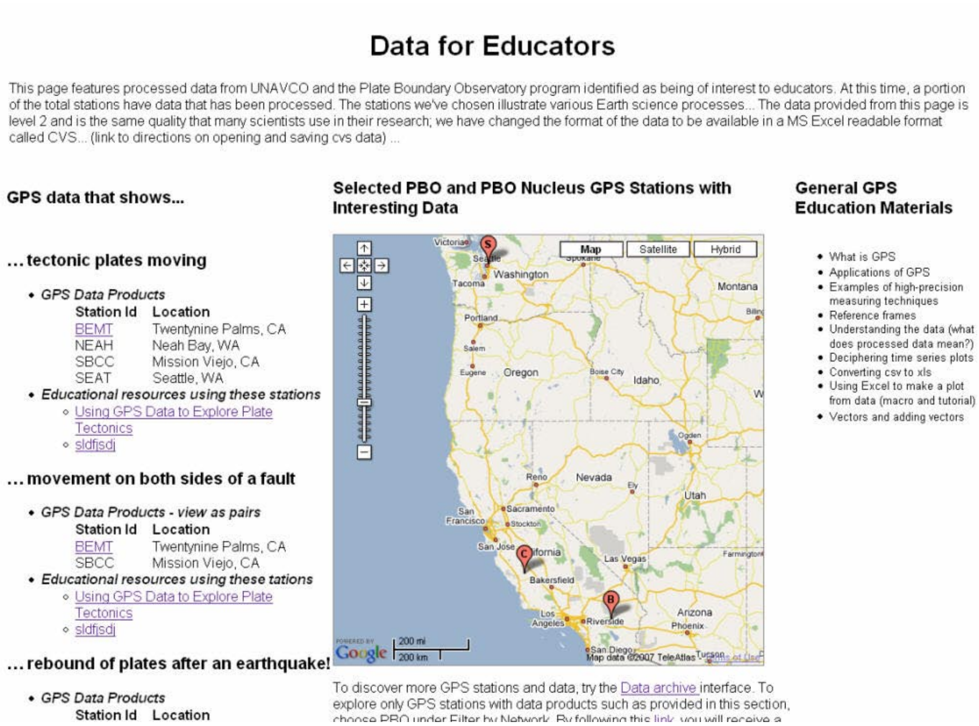

Prototype Data for Educators Website

Over the past three years, the UNAVCO Education and Outreach Program has worked with the community to communicate its mission to promote a broader understanding of Earth science through the scientific methods, data, and results of the unique suite of scientific research of UNAVCO`s community. One of our goals has been to broaden the use of UNAVCO data and products by a wide audience of educational and research users. This past year we have made great strides to accomplish this goal by developing data-rich learning activities targeted to undergraduate and secondary education students in general / introductory Earth science and by creating a website to specifically connect faculty with GPS data.

UNAVCO began the process of creating data-rich learning activities and an educational by soliciting from undergraduate faculty and secondary education teachers their suggestions and analyzing evaluations from workshop participants. On a fundamental level, although most faculty had used hand-held GPS units in their instructional environment, very few were familiar with how high-precision GPS is used to study geo-tectonic processes such as plate motion, volcanic activity, post-earthquake plate deformation, or other phenomena.

The need for students to explore and analyze data has been well documented. Students need real world examples to help develop their abstract thinking skill so they can critically assess data, visualize abstract concepts, and use multiple lines of evidence to evaluate an idea. Because many crustal deformation processes are expressed on Earth's surface over the familiar time scales of days, months, and years, GPS data represent an effective method of illustrating the geomorphic effects of plate tectonics and in essence, allow students to “see” plate tectonics in different temporal and spatial scales. GPS data also provide a means to study events like earthquakes and volcanic eruptions that are influential to humans and our infrastructure.

Coupled with student needs, a broad set of requirements emerged from undergraduate faculty. These depend on the logistical constraints of the teaching environment, the presence of a laboratory component accompanying the course, internet access in lecture halls, teaching load, etc. All faculty want their students to be exposed to data; however, some faculty prefer the data to be in tabular or graphical form (such as time series plots) and other faculty prefer students to have access to the numerical data files to construct their own tables and graphs. The following criteria emerged as being critical: an intuitive interface, data in Excel readable formats, clearly documented data, multiple pathways and previews to data, sub-setting of the data, data that illustrates a geo-tectonic process identified for them, and the ability to use common software tools.

To explore the Data for Educators website, visit: http://www.unavco.org/edu_outreach/data.html

ACCELERATED LOADING RATE ACCOMPANIES CLUSTERED EARTHQUAKE ACTIVITY IN THE EASTERN CALIFORNIA SHEAR ZONE

Michael Oskin, Eitan Shelef, Michael Strane, Emily Gurney · University of North Carolina at Chapel Hill
Lesley Perg · University of Minnesota
Brad Singer · University of Wisconsin

Clustering of major earthquakes over periods of years to decades is observed historically and in paleoseismic records. Seismic hazard forecasts may be improved by identifying a cluster in-progress and its relationship to fault loading processes. We present new late Quaternary fault slip-rates from the Mojave Desert portion of the Eastern California shear zone (ECSZ), where both paleoseismic and historic earthquake clusters are recognized, to test if the interseismic loading rate is transiently elevated during the present cluster of activity. The sum of six fault slip rates that average a few to several tens of earthquakes is 5.9 +/- 1.4 mm/yr. This long-term rate is only half the present-day loading rate of 12 +/- 2 mm/yr across the 60 km-wide shear-zone. This discrepancy began prior to the 1992 Landers earthquake, and its magnitude precludes residual post-seismic deformation following other large historic earthquakes in southern California. These observations support that significantly elevated regional strain accumulation rate may be characteristic of clustered earthquake activity, and that interseismic loading may oscillate between different fault sets within a hierarchal fault system.

PALEOMAGNETIC REORIENTATION OF THE SAFOD BOREHOLE

Josep Pares, Ben van der Pluijm, Anja Schleicher · University of Michigan
Stephen Hickman · U.S. Geological Survey

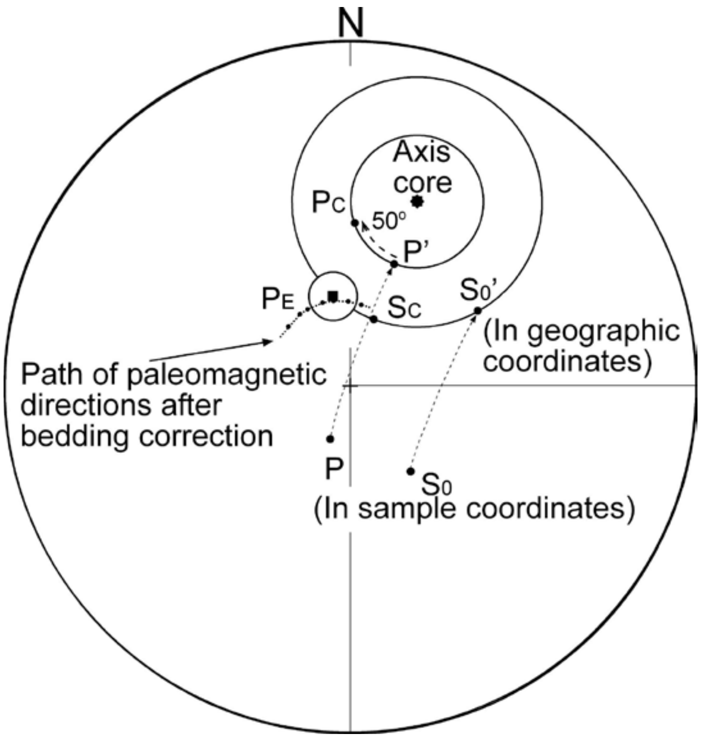

Paleomagentic reorientation of SAFOD core.

A number of physical properties that are being measured in the SAFOD core have a directional nature, including bedding attitude, fracture planes, and permeability. Azimuthal orientation of drill core material is therefore of great importance when examining the directional properties of the sediments and fault rocks. Paleomagnetic core reorientation has been successfully used for a number of years and offers considerable advantages over other reorientation methods. The measurements are made on samples from the cores themselves; unlike methods such as “multishot” orientation or imaging tools, the technique can be applied to recently drilled cores and to stored old cores. The accuracy of paleomagnetic reorientation is often greater than other measurements, especially in disaggregated or highly fractured cores. We present a protocol based on paleomagnetism to determine the azimuth of the main SAFOD whole-core by providing a reference direction in geographic coordinates. Orientation and location of samples for paleomagnetism were taken in relation to a ‘common reference line’. Samples were obtained using two different methods, including a standard 1” diameter drill bit and cutting ~ 8cc cubes with a regular rock saw equipped with a non-magnetic blade. All specimens were processed using standard paleomagnetic techniques at the Paleomagnetism Laboratory of the University of Michigan, including a 3-axis cryogenic magnetometer to measure the remanence. Both thermal and alternating field demagnetization procedures were applied in order to isolate the magnetic components.

In the Salinian granodiorite acquired during Phase 1 drilling, there is strong evidence for drilling induced remanence both at whole-core drilling level and at sub-sampling level. Samples taken from opposing sides of the whole-core produce similar magnetization directions in core coordinates. In addition, the average NRM intensity of these specimens is unusually high, suggesting that a DC field may have induced remanent magnetization in the sample. For these reasons, paleomagnetic core reorientation is probable not reliable in these granodiorite cores.

A second set of samples was obtained from Phase 2 core at a depth between 3991.36 and 3992.58 meters, including siltstones and fine-grained sandstones belonging to the Great Valley sequence that is Upper Cretaceous in age. Progressive thermal demagnetization shows a steady decay of magnetization upon increasing temperature, and samples generally show very little or no viscous overprint at all. Remanent magnetization is reduced to ~10% of its initial value at 490oC. Alternating field demagnetization is equally efficient in revealing the paleomagnetic direction and shows that most intensity is reduced to ~10% by 60 mT. Collectively, these observations are consistent with the presence of magnetite in the sediments. Once the Characteristic Remanent Magnetization directions are obtained, a three-step process is applied to determine the azimuth of the core. First, the magnetization direction (P) and bedding (S0) are both rotated by the core dip angle in its plunge direction. This produces two small circles that contain all the possible locations of P and S0 in geographic coordinates. Although the ‘true’ orientation of P and S0 can in principle lie anywhere within their respective small circles, there will be one particular location where, upon restoring bedding to the horizontal, the measured paleomagnetic direction P’ will coincide with the expected paleomagnetic Cretaceous reference direction, PE. The optimal location of P’ and S0 is found iteratively by restoring S0 to the horizontal and rotating P’ by the same angular distance, until it lies within the error of the reference direction. Regardless of the azimuthal correction obtained for the whole-core, we find that the paleomagnetic inclination obtained matches the expected value for the Upper Cretaceous. After performing this reorientation operation, bedding in these cores matches very closely the attitude of bedding inferred from image logs and measurements of S-wave anisotropy in SAFOD by Boness and Zoback (Geophysics, 2006) . Since compositionally similar siltstones and fine-grained sandstones were encountered all the way across the San Andreas Fault Zone during Stage 2 rotary drilling, we are optimistic that this paleomagnetic core reorientation technique will yield reliable core orientations when we obtain continuous core from directly within and adjacent to the San Andreas Fault during Phase 3.

SEISMIC ANISOTROPY, SUBDUCTION, MANTLE FLOW AND UPLIFT IN THE NORTHERN APENNINES, CENTRAL ITALY

Jeffrey Park · Yale University
Jaroslava Plomerova, Petr Jedlicka · Czech Academy of Science
Simone Salimbeni, Silvia Pondrelli · INGV Bologna
Lucia Margheriti, Francesco Pio Lucente · INGV Rome
Vadim Levin · Rutgers University

The Apennines orogen parallels Africa-Eurasia convergence, so its origin is not a direct consequence of large-scale plate collision. The orogen has been explained by the progressive eastward retreat of a regional-scale subduction zone trapped between two continents. Along the geologically young Apennines orogen in Italy multiple lines of evidence suggest both a westward subduction of the Adriatic lithosphere and an eastward retreat of the subduction zone via slab rollback. Apennines slab rollback has been characterized as an ongoing process or a stalled process, a distinction relevant to seismic hazard in the region. An alternative scenario removes lithosphere beneath the Apennines through detachment and sinking rather than active subduction.

Slab rollback induces the sub-slab mantle material to flow parallel to the subduction zone and deflect near the slab edge. The deformation of upper mantle rocks will align olivine crystals, and cause seismic wavespeed to have directional dependence (anisotropy). The slab-rollback model can be validated by the detection of strong orogen-parallel fast-polarization of shear-wave splitting on the Adriatic side of Italy, and orogen-normal extensional fabric on the Tyrrhenian side. Alternatively, if a lithospheric fragment detaches and sinks, asthenosphere should flow towards the site of detachment (orogen-normal).

Shear-wave splitting estimates from recordings of portable seismographic stations during the RETREAT seismic deployment, in combination with broadband data from the Italian national seismic network, seem to exclude a 2-D sub-lithosphere corner flow, associated with the Apennines slab rollback, as the main source of the inferred anisotropy. Surface waves from the great Sumatra-Andaman earthquakes of 2004 and 2005 that cross Italy south of ~44°N display Love-to-Rayleigh scattered waves (quasi-Love phases) diagnostic of sharp lateral gradients in the anisotropic properties of Earth's upper mantle. Surface waves that traverse Italy further north lack this distinctive phase, documenting a change in the upper mantle fabric that corroborates the shift in the fast polarization of shear wave birefringence. These observations suggest that orogen-parallel asthenospheric extension behind the retreating Apennines slab has limited geographical expression. Comparison with P-wave tomography suggests that the Apennines slab has lost contact with the root of the orogen west of the Bologna-Florence axis. A lateral bend in the slab may be associated with observed transitions in surface lithology, Quaternary uplift style, earthquake frequency and source mechanism, and the deep exhumation of metamorphic rocks such as the Alpi Apuane marbles.

MITIGATING SEISMIC NOISE CAUSED BY ATMOSPHERIC PRESSURE CHANGES WITH COLLOCATED, HIGH-RESOLUTION, BROADBAND BAROMETERS

Jerome Paros · Paroscientific

Local atmospheric pressure fluctuations are significant sources of noise in seismic data. Pressure changes associated with common atmospheric phenomena such as frontal passages, jet-stream passages, boundary-layer convection, and gravity waves can deform the ground that surrounds a seismometer to cause significant horizontal tilt noise. Other atmospheric influences include the gravitational effects of a variable weight of the column of air above the seismometer, vertical ground deformations, and possible buoyancy effects. The reconstruction and elimination, in real time or post facto, of these atmospheric effects requires the monitoring of local pressure changes with collocated high-resolution, broadband barometers. The pressure-induced noise can be deterministically removed from the seismometer, strainmeter, and tiltmeter data to substantially increase the overall performance of an entire sensor network such as EARTHSCOPE. High-resolution barometers can also improve the analysis of the Earth's free oscillations by measuring and correcting for atmospheric effects.

We present and describe a state-of-the-art, high-resolution, broadband barometer and wind-insensitive pressure port that are well suited for the mitigation of seismic noise caused by atmospheric pressure changes. For a sampling period of 10 seconds, this Quartz Resonant Barometer has a resolution better than 0.01 Pa (0.1 microbar). The pressure sensors also feature high accuracy, long-term stability, low power consumption, and inherently digital outputs that are compatible with the data acquisition system used for the EARTHSCOPE seismometers. We also present a preliminary analysis of our collocated barometer and seismometer measurements.

THE EARTHSCOPE PLATE BOUNDARY OBSERVATORY RESPONSE TO THE 2006 AUGUSTINE ALASKAN VOLCANIC ERUPTION.

Benjamin Pauk, Michael Jackson, Karl Feaux, Barrett Friesen, Max Enders, Austin Baldwin, Ally Marzulla, Kelly Fournier · UNAVCO

During September of 2006, UNAVCO installed five permanent Plate Boundary Observatory (PBO) GPS stations on Augustine Volcano, in the lower Cook Inlet of Alaska. The installations were done at the request of the PBO Magmatic Systems committee in response to the January 11, 2006 eruption of Augustine Volcano. Prior to the eruption, PBO installed five permanent GPS stations on Augustine in 2004. The five existing stations on the volcano were instrumental in detecting precursory deformation of the volcano's flanks prior to and during the eruption. During the course of the first explosive phase of the eruption, two existing PBO stations, AV03 and AV05 were subsequently destroyed by separate pyroclastic flows. The existing station AV04 was heavily damaged by a separate pyroclastic flow during the continuous phase of the eruption and was repaired during September as well. Existing stations AV01 and AV02 were not affected or damaged by the eruption and remained operating during the entire eruptive phase and subsequent debris flows. All five new stations, and maintenance on the three remaining existing stations, were completed by PBO field crews with helicopter support provided by Maritime Helicopters. Lack of roads and drivable trails on the remote volcanic island required that all equipment be transported to each site from an established base camp by slinging gear beneath the helicopter and internal loads. Each new and existing station installed on the volcano consists of a standard short braced GPS monument, two solar panels mounted to an inclined structure, and a six foot high Plaschem enclosure with two solar panels mounted to one of the inclined sides. Each Plaschem houses 24 12 volt batteries that power a Trimble NetRS GPS receiver and one or two Intuicom radios and are recharged by the solar panels. Data from each GPS receiver is telemetered directly or through a repeater radio to a base station located in the town of Homer that transmits the data over the internet to the UNAVCO data archive at ftp://data-out.unavco.or/pub/PBO_rinex where it is made freely available to the public.

ARRAY PROCESSING OF TELESEISMIC BODY WAVE PHASES RECORDED BY THE TRANSPORTABLE ARRAY

Gary Pavlis · Indiana University
Frank Vernon · University of California, San Diego

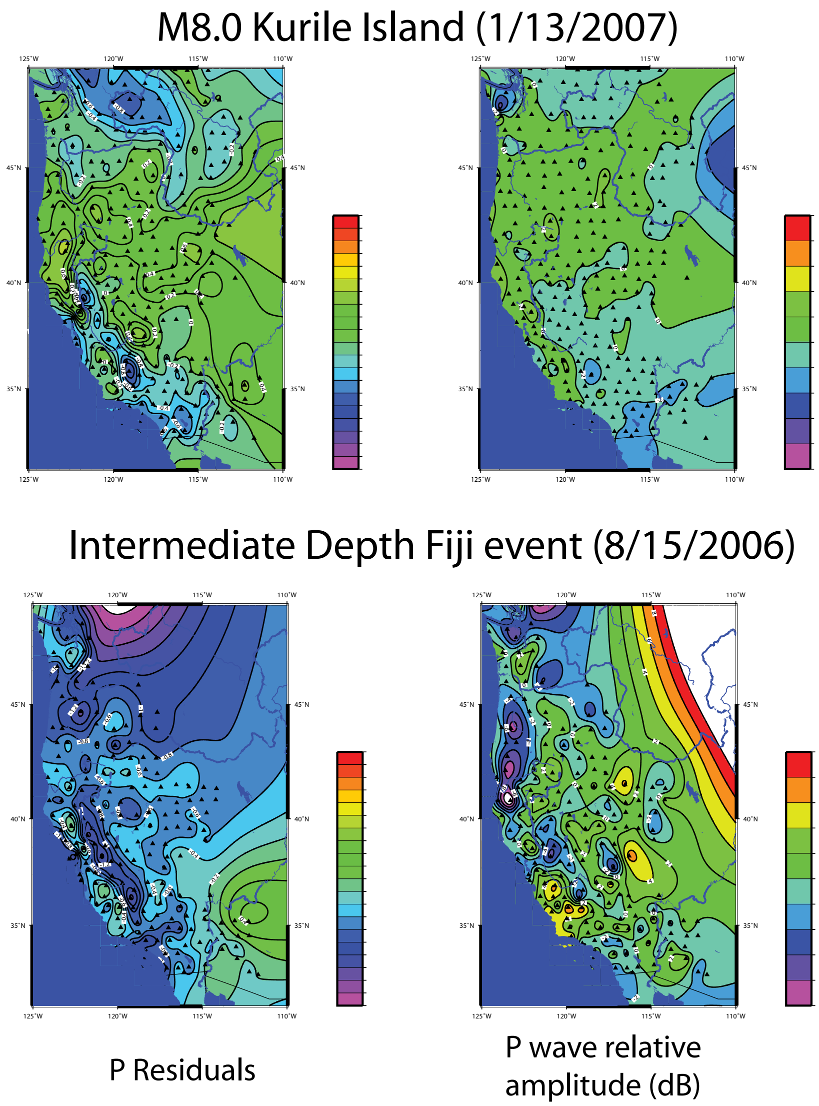

P wave residuals and relative amplitudes for two events recorded by the Transportable Array. Left panels are contour plots of P wave residuals. Right panels are amplitudes for each station relative to the array beam. Top panels shows results for the recent M=8 Kurile Islands earthquake and the bottom panel shows results for an intermediate depth earthquake from near Fiji.

We have begun routine application of a new array processing procedure to body waves recorded by the USArray. Unlike standard slant stack processing used in high frequency arrays this procedure begins by assuming the source is already known. This allows initial alignment of data from a very large aperture array like the USArray to within a few seconds versus several minutes of moveout that is present in the raw data. The core of this new procedure is a novel nonlinear stacking algorithm. The analyst is required to pick an initial trace to use as a starting estimate of the array beam. This trace is used to provide initial alignment of data by cross-correlation with this initial beam estimate. A median stack is then used to provide a robust starting estimate of the array beam. The final beam is computed as a weighted stack with a novel penalty function that automatically downweights data that are not coherent with the array beam. An iterative loop continues to refine the array beam estimate until lags computed by cross-correlation with the array beam do not change. This procedure is found to normally converge in 2 to 5 iterations and is remarkably effective in automatically discarding problem data. The primary outputs of the procedure are an array beam estimate, arrival time residuals, and relative amplitudes at each station relative to the array beam. We have successfully applied this procedure to a number of both P and S body wave phases. We find remarkable coherence of the initial P and S phase in the 30 to 90 degree range routinely used for body wave tomography. Large events commonly show coherence of 0.8 or higher for most of the array. A remarkable advantage of the grid geometry of the Transportable Array is that the results are readily contoured to produce travel time and relative amplitude maps. These readily illuminate first-order tectonic features.

USING IRIS INSTRUMENTS IN AN UNDERGRADUATE GEOPHYSICS COURSE

Gary Pavlis · Indiana University

It has been my experience that teaching basic geophysics to undergraduate geoscience majors is more effective when taught in a hands-on fashion. I have taught a senior-level class in elementary geophysics for a number of years. I focus the class around a series of data collection exercises focused on standard geophysical techniques appropriate for the shallow subsurface including gravity, magnetics, electrical resistivity, electromagnetic, seismic refraction and seismic reflection methods. I aim the course to improve the professional development of these students through several real-life situations that I find help keep the students engaged. Each student is assigned as the PI for one of the class experiments. They are required to meet with me to plan the experiment. During the field work they are responsible for organizing the field crew and making sure all elements of the experiment are properly executed. On completion of the field work they are then required to organize first order data processing and to give an oral class experiment report the week after the end of each experiment. Most experiments require students to write individual reports which are graded to improve writing skills of the students, but more complex experiments have sometimes worked better as group projects. I have also found it useful to enforce very rigid deadlines for report submission to model the real-life deadlines we all face professionally. For the past several years I have borrowed multichannel seismic systems from the IRIS facilities to teach the seismic component of the course. This has been a major benefit to our program as it would be hard to justify owning and maintaining comparable equipment for strictly teaching purposes.

HTDP 2.9: UPDATING HTDP FOR THE 28 SEPTEMBER 2004, M 6.0 PARKFIELD, CA EARTHQUAKE

Christopher Pearson, Richard Snay · National Geodetic Survey

The western part of the United States is constantly deforming due to the boundary between tectonic plates that runs through this region. As a result, accurate surveying in the western US requires a model describing crustal velocities and earthquakes to allow survey measurements to be corrected for differential movement so that surveys conducted at different epochs may be compared. The National Geodetic Survey (NGS) has developed the HTDP (Horizontal time dependent positioning) software that enables its user to make these corrections. This software must be updated periodically to address the displacements associated with each new earthquake.

This paper describes the NGS process for selecting and validating models for earthquakes prior to their inclusion in HTDP, focusing on the Parkfield, California earthquake which occurred on 28 September 2004 and had a magnitude of 6.0. This earthquake is a good test of the process of modeling and correcting for deformation because it occurred on a part of San Andreas fault that is one of the best instrumented locations in the world. While the earthquake was relatively small, it produced displacements of over 0.1 m over a relatively small area across the fault trace. It also produced a mix of co-seismic deformation, that occurs suddenly during an earthquake and post seismic deformation that can accumulate over a period of a few months after the earthquake. Clearly dealing with deformation at these disparate time scales represent a major challenge to developing accurate models of deformation that are required to support modern high accuracy surveying in tectonically active areas like California.

We selected a dislocation model of this earthquake from Johanson et al. (2006) because it was based on a combination of GPS vectors and InSAR, which allows deformation field to be sampled with a higher spatial density than would otherwise be the case. This study also provided separate dislocation models of the co-seismic and post-seismic deformation, which is important because, for this earthquake, the post-seismic deformation is comparable in magnitude to the coseismic deformation. The accumulation of post-seismic deformation was shown to follow an exponential power law with a time constant of 0.087 years, which implies that post-seismic deformation had largely ceased after 3 months. For this reason, we were able to combine the co- and post-seismic dislocation models to produce a single model for the total deformation associated with this earthquake.

GEOEARTHSCOPE: AERIAL AND SATELLITE IMAGERY AND GEOCHRONOLOGY

David Phillips, Mike Jackson, Chuck Meertens · UNAVCO

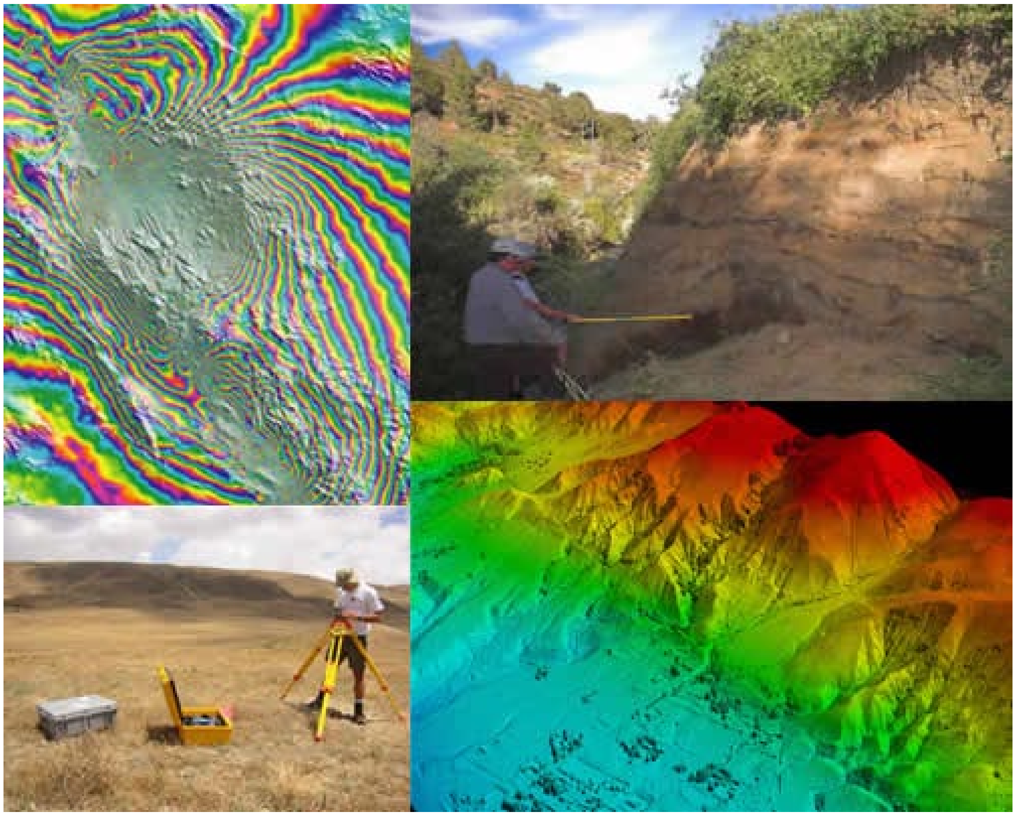

GeoEarthScope: Aerial & Satellite Imagery and Geochronology

GeoEarthScope, a component of the National Science Foundation's EarthScope project, includes the acquisition of aerial and satellite imagery and geochronology to assist with EarthScope instrument siting and to examine the strain field beyond the time scales available from seismology and geodesy. InSAR, LiDAR and Geochronology working groups consisting of community members are providing guidance to UNAVCO and NSF regarding acquisition plans and targets for GeoEarthScope. These working groups have prepared a series of reports outlining their recommendations (these reports are available for download from the EarthScope and UNAVCO websites). A subcommittee of the Plate Boundary Observatory Standing Committee will review the working group reports and recommend an overall acquisition plan that balances the working group recommendations with the resources available. We will present an update on the overall GeoEarthScope acquisition plan as well as updates on current, planned, and recently completed activities including the geochronology request for proposals (RFP); the Death Valley-Fish Lake Valley LiDAR project; the northern California LiDAR project; and the Basin & Range InSAR project.

COMBINATION OF GPS-OBSERVED VERTICAL MOTION WITH ABSOLUTE GRAVITY CHANGES CONSTRAIN THE TIE BETWEEN REFERENCE FRAME ORIGIN AND EARTH CENTER OF MASS

Hans-Peter Plag, William C. Hammond, Corne Kreemer · University of Nevada

It has long been suspected that the Reference Frame Origin (RFO) of the International Terrestrial Reference Frame (ITRF) exhibits a secular trend with respect to the Center of Mass of the whole Earth system (CM). Such a secular trend would cause a global bias of vertical rates with a spherical harmonic degree of two. Estimates for ITRF2000 indicate that locally the uncertainty due to this bias is of the order of 2 mm/yr. This bias hampers the interpretation of vertical rates in terms of geodynamics processes. In particular, the apparent generally upward vertical motion of GPS sites in the Basin and Range with respect to ITRF2000 is contrary to the expectation based on a province extending owing to gravitational collapse.

Extending the theory of Wahr et al. (1995), we have used a global network of absolute gravity measurements collocated with GPS stations to determine the linear secular trend of the RFO with respect to CM that would minimize the discrepancy between absolute gravity and GPS-observed secular trends. The inverted parameters are consistent with theory and the secular trend is of the same order and direction as the difference between ITRF2005 and ITRF2000, potentially indicating that ITRF2005 is better connected to the CM than ITRF2000.

Applying the translation to secular trends determined for a network of North American GPS sites, we discuss the vertical motion of this region. Both in ITRF2005 and in the absolute gravity frame, the vertical trends are on average increased compared to the ITRF2000 trends by approximately 1.0 mm/yr. As a consequence, the general uplift of the Basin and Range province with respect to the CM is confirmed, indicating a gain in gravitational energy in that area.

VERTICAL MOTION OBSERVED WITH GPS: WHAT CAN WE LEARN ABOUT REGIONAL GEOPHYSICAL SIGNALS, EARTH STRUCTURE, AND RHEOLOGY?

Hans-Peter Plag, Corne Kreemer, William C. Hammond, Geoff Blewitt · University of Nevada

Tectonic studies utilizing observations of surface displacements from GPS are based predominantly on observations of horizontal displacements, while vertical displacements mostly provide constraints for loading-related geophysical processes. A main reason for this disjunct use of GPS observations is that, on the one hand, tectonic signals often are larger in the horizontal component while loading signals dominantly are contained in the vertical component. On the other hand, the horizontal components of GPS-determined displacements have a precision about three times that of the vertical component. Considering the growing number of PBO stations with records long enough to determine reliable secular trends, it is worthwhile to ask the question to what extent vertical displacement time series can be used to constrain tectonic processes, Earth structure, and rheology. In order to answer this question, we study the anatomy of time series of vertical displacements determined from regional and local GPS networks in North America and derive the spatio-temporal pattern of vertical crustal motion as seen by these networks.

For GPS, uncertainties in the long-wavelength field of observed vertical motion result partly from instabilities of the global reference frame including a mutual contamination of the horizontal and vertical components due to relative motion of reference frame origin and the center of mass of the Earth system. Surprisingly, the spatial correlation of the time series is found to be determined by constraints on station coordinates used to align the daily solutions to a terrestrial reference frame. The intra-annual to annual part of the temporal spectrum is dominated by semi-annual and annual constituents with high spatial coherency in amplitude and phase over large geographical areas. This spatial coherency shows that GPS picks up geophysical signals at the seasonal time scale. Generally, at interannual periods, the GPS time series of vertical motion show significant nonlinear components potentially contaminating the derived secular velocity field. Nevertheless, the spatial pattern of the secular vertical velocity field displays features potentially related to geophysical processes, including tectonics. A suite of model predictions of surface loading, postseismic tectonic deformations, and postglacial rebound is used to synthesize the predicted vertical motion field and to assess in a regression analysis to what extent the observations constrain Earth model parameters and processes.

DISLOCATION MODELS OF INTERSEISMIC DEFORMATION IN THE WESTERN UNITED STATES

Fred Pollitz, Patricia McCrory, Jerry Svarc, Jessica Murray · U.S. Geological Survey
Doug Wilson · UCSB

The GPS-derived crustal velocity field of the western US is used to construct dislocation models in a viscoelastic medium of interseismic crustal deformation. The interseismic velocity field is constrained by 1052 GPS velocity vectors spanning the ~2500 km-long plate boundary zone adjacent to the San Andreas fault and Cascadia subduction zone and extending ~1000 km into the plate interior. The GPS dataset is compiled from U.S. Geological Survey campaign data, Plate Boundary Observatory data, and the WUSC velocity field of Bennett et al. (1999). In the context of viscoelastic-cycle models of post-earthquake deformation, the interseismic velocity field is modeled with a combination of earthquake sources on about 100 known faults plus broadly distributed deformation. Models that best explain the observed interseismic velocity field include the contributions of viscoelastic relaxation from known faults and broadly distributed faults, as well as lateral variations in depth-averaged rigidity in the elastic upper lithosphere. The role of lateral rigidity variations is enhanced when viscoelastic cycles of major faults are implemented with known fault history rather than in a cycle-averaged sense. Slip rates are inferred on faults along the entire San Andreas fault system, Eastern California Shear Zone, Walker Lane, the Mendocino triple junction, and the Cascadia megathrust. Primary deformation characteristics are captured in and around these zones with small residual velocities.

TRACKING MAGMA ASCENT IN THE 2006 ERUPTION OF AUGUSTINE VOLCANO, ALASKA: THE ROLE OF EARTHSCOPE *(Speaker)*

Stephanie Prejean, Peter Cervelli, Michelle Coombs, John Power · U.S. Geological Survey
Chris Nye · Alaska Division of Geological and Geophysical Surveys
Tom Fournier, Jeff Freymueller, Jessica Larsen, Mariah Tilman · University of Alaska, Fairbanks

Augustine Volcano, 275 km southwest of Anchorage, Alaska, erupted in early 2006 after two decades of quiescence. Augustine was chosen as an EarthScope target because of its frequent eruptive activity (major eruptions in 1964, 1976, and 1986) and high silica composition of its magma (andesites to dacites). At the onset of unrest, Augustine Island had five continuously recording, telemetered GPS receivers operated by the Plate Boundary Observatory (PBO) and one jointly operated by the Alaska Volcano Observatory (AVO). In the summer of 2005, geodetic baselines began lengthening while seismicity and gas emissions increased, giving AVO about six months of warning that an eruption was on the way. In anticipation, AVO installed five additional semi-permanent campaign GPS receivers along with a host of other instruments including broadband seismometers, web cameras, radiometers, ash collectors, etc. During the explosive phase of the eruption, three of the PBO GPS receivers and six seismometers were destroyed.

Geodetic data were a key near real-time indicator of deep magma movement during the eruption, especially because there is seldom any seismicity deeper than 1 km below sea level. Between late November 2005 and the onset of explosive eruption on January 11, 2006, geodetic and petrologic data together suggest that a dike propagated upward from sea-level to the summit. Such direct evidence of the time history of magmatic ascent is unusual for stratovolcanoes. The first episode of explosive activity lasted only seven days. However, the volcano continued inflating, strongly indicating that further activity was likely. During the second explosive phase of January 28 - February 2, the volcano began deflating. Inflation returned on February 10 as magma again accumulated at depth while slowly effusing from the volcano`s summit. Dome building accelerated during the volcano`s final deflation episode, beginning March 1. Augustine stopped deforming and effusing lava by late spring, and the volcano again became quiet.

KINEMATICS AND DYNAMICS OF WESTERN U.S. DEFORMATION

Christine Puskas · University of Utah
Lucy Flesch · Purdue University
Robert Smith · University of Utah

GPS data and fault slip rates are used to characterize regional deformation and kinematics for the western U.S. The dominant deformation pattern is one of intraplate rotation, with velocities rotating from southwest in the Yellowstone-Snake River Plain volcanic field to west in the eastern Basin-Range to northwest in the western Basin-Range and California and northeast in the Columbia Plateau and the Pacific Northwest. GPS velocities increased from east to west from ~2 to 12 mm/yr at the eastern and western Basin-Range boundaries, and to 35 mm/yr at the San Andreas fault. This rotation pattern was modeled with both microplate and continuum formulations, with a comparison between the two types of models. The microplate model was based on tectonic and volcanic history and the locations of active fault zones in the western U.S. This model examined the rotations, internal strain, and relative motions between the microplates. The continuum model allowed distributed deformation rather than requiring motion to be concentrated at microplate boundaries. The deformation data were also used to constrain models of driving forces. Forces contributing to western interior deformation arise primarily from variations in gravitational potential energy due to variations in thickness of the lithosphere (from seismic data) and density variations in the lithosphere/upper mantle (from geoid data). Plate boundary forces from the interaction of North America with the Pacific and Juan de Fuca plates also contribute to regional deformation. The forces are modeled to examine the relative contribution of buoyancy forces from the Yellowstone hotspot to regional western deformation as well as the contributions of lithospheric thickness variations and plate boundary forces. The force models are then combined with the deformation data to estimate effective lithospheric viscosity and compared with the microplate models to ascertain whether changes in effective viscosity correspond to tectonic regions.

ANALYSIS OF THE REELFOOT MAGNETIC ANOMALY AND AGE OF THE REELFOOT THRUST FAULT

Ivan Rabak, Charles Langston, Christine Powell · The University of Memphis

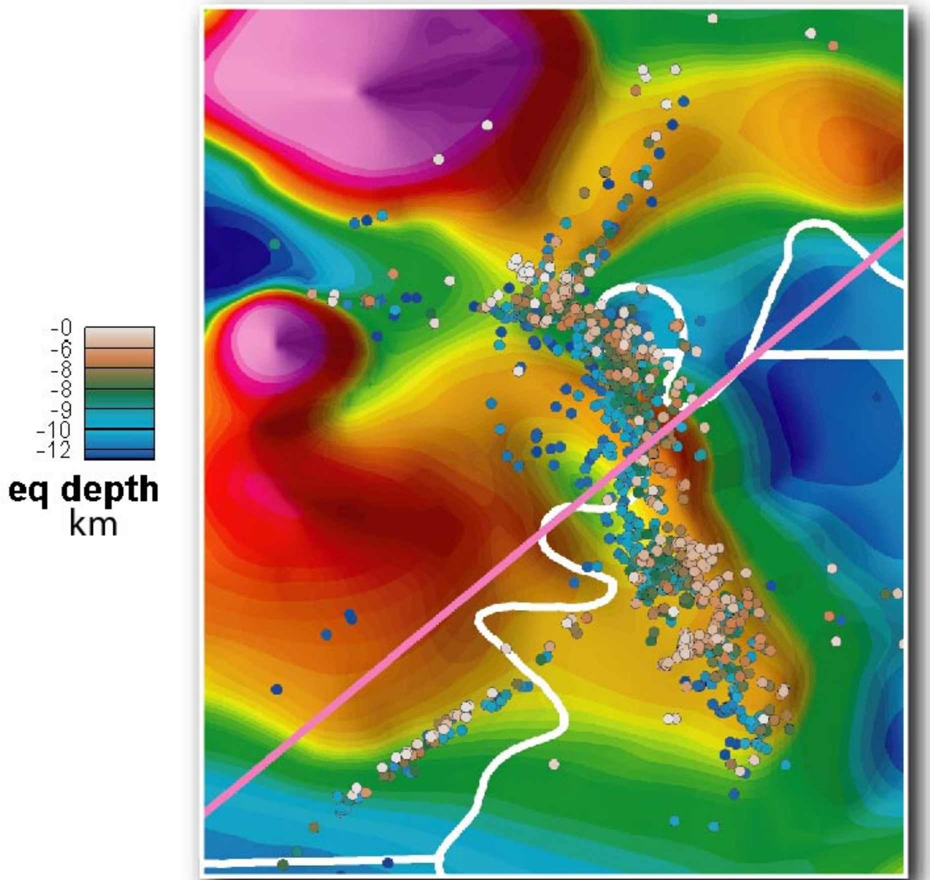

Contemporary NMSZ seismicity relocated using tomography results (P & S arrival times). The thrust earthquakes sit on top of the Reelfoot magnetic anomaly (red - highs, blue - lows). Deeper earthquakes are colored from light brown to blue. The analyzed profile across the anomaly is indicated in pink.

A distinctive magnetic anomaly delimits seismicity associated with the Reelfoot thrust fault and is modeled as an intrusive body with magnetic susceptibility one order of magnitude higher than the susceptibility of the Precambrian basement. The analysis requires that the overlying Paleozoic sediments be vertically offset approximately 2 km at the eastern limit of Reelfoot fault seismicity. This basement uplift corresponds to estimates of erosion of Paleozoic sediments from the top of the Pascola Arch uplift. The available depth-to-basement maps are poorly constrained by borehole and seismic reflection data surrounding the Reelfoot fault but suggest Precambrian basement depths of ~3 km. Most of the present-day seismicity of the New Madrid Seismic Zone (NMSZ), relocated using tomography results, is situated on this fault segment and forms two different-dip fault planes. The association of the anomaly edge, seismicity, and antiformal subcrop and basement structure of the Pascola Arch suggests that the Reelfoot fault is a late Paleozoic thrust fault that was active in the core of the Pascola Arch, with uplift possibly driven by igneous intrusion. This hypothesis can serve as a framework for developing fine scale seismic tomographic experiments for imaging structures within the Paleozoic sediments and crystalline upper crust within the NMSZ.

CONSCIENTIZATION AND MISCONCEPTIONS ROLES IN NATURAL HAZARD PREPAREDNESS: AN EARTHSCOPE PRIORITY GOAL.

Carlos Rios · Oregon State University/Universidad de Antioquia, Colombia
John DeLaughter · EarthScope Education & Outreach Program
Shawn Rowe · Oregon State University
Charley Faria · University of New Hampshire

Natural hazards such as earthquakes/tsunamis (e.g., Sumatra 2004, Indonesia), hurricanes (e.g., Katrina 2005, USA), volcanoes (e.g., Nevado del Ruiz 1985, Colombia), and floods (e.g., Venezuela 1999), can exact a tremendous toll on both lives and property. And yet, most damage from natural hazards can be mitigated or even avoided completely with proper preparedness. Why, then, do so few people take precautions?

A primary method for presenting disaster education is via free-choice learning (Falk & Dierking, 2002), which takes place when an individual opts to engage in a learning activity (e.g., reading about earthquakes, going to a science museum). Because most of the learning we do about things like natural hazards is done on our own free time by our own choice, participation in free-choice learning activities can enhance the conscientization process or the ongoing process of becoming aware of the impacts of self-behaviors (Freire, 1970, 1997, 1998), which contributes to emergency preparedness (Norris et al., 2002).

Over the summer of 2006, as part of the EarthScope Education & Outreach Program efforts, we researched common misconceptions about geosciences, natural hazard preparation styles, and awareness for natural disasters at the entry of some informal learning environments on both the East and West coasts of the United States. Our intent was to see if the level of misconceptions about geosciences concepts might correlate to the level of self-preparedness by using an instrument combining Likert-scale and forced choice items. The results of our research will be presented.

SITE RECONNAISSANCE FOR THE EARTHSCOPE/USARRAY TRANSPORTABLE SEISMIC ARRAY: GEOGRAPHIC INFORMATION SCIENCES & COMMUNITY PARTICIPATION IN OREGON AND WASHINGTON STATES

Carlos Rios · Oregon State University/Universidad de Antioquia, Colombia
Matt Mercurio, Maxwell Ruckdeschel · IAGT
Robert Busby · IRIS
Anne Trehu, Mark Meyers, Paul Anderson, Jan Baur, Mark Bernard, Brian Anderson, Monika Moore, Susan Potter, Barbara Zennaro, Shanon Helbock, Don Lippert, Maxwell Ruckdeschel · Oregon State University

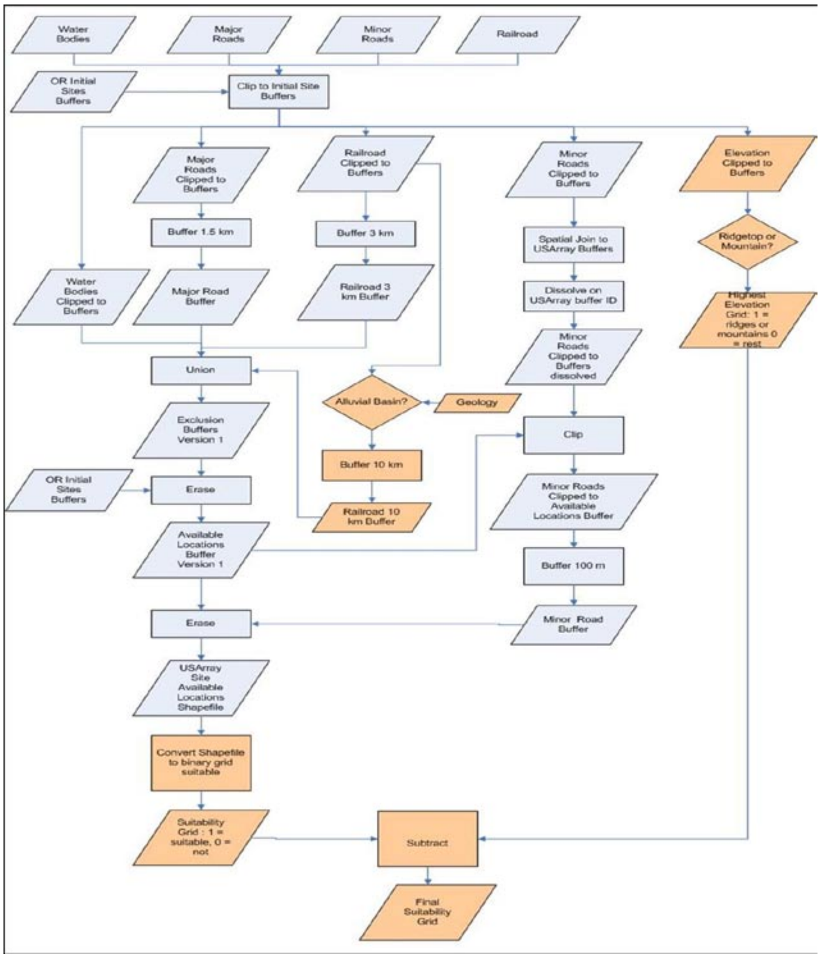

GIS RECONNAISSANCE MODEL

Identification and permitting of sites for seismic stations of EarthScope's USArray Transportable Seismic Array is a very ambitious undertaking. Initial site reconnaissance requires skills to integrate information from a variety of geographic databases as well as an understanding of the regional geology and tectonics and of the objectives of the EarthScope and USArray programs. It thus provides rich opportunities for students in earth sciences and geography to apply and enhance their knowledge. During summer, 2005, Oregon State University participated in site reconnaissance for USArray in Oregon and Washington as part of a USArray-sponsored internship program. The program began with a 3-day workshop attended by authors of this presentation. The workshop included lectures about the scientific objectives of EarthScope, training on procedures to identify sites that meet the requirements of USArray, and a field trip to find a few local sites. Prior to going into the field, GIS tools using databases assembled by OSU, IAGT and IRIS were used to identify locations that met as many requirements as possible:

Appropriate topography and geology,

Adequate distance from cultural noise sources,

Private ownership, and

Digital cell phone coverage.

Lab work was followed by field visits to make contact with landowners and identify specific sites. In rural areas, University extension agents provided a valuable introduction to the local community. The "products" of this project were formal "Reconnaissance Reports" that included contact information, special site considerations and detailed instructions for finding the sites. Site locations were finalized by professional USArray staff. This has proven to be an efficient and cost-effective way to locate a large number of sites while simultaneously providing an exciting practical training opportunity for students, involving a variety of units throughout the university system, and transmitting the excitement of EarthScope/USArray to the public.

AMBIENT NOISE TOMOGRAPHY IN THE WESTERN US USING EARTHSCOPE/USARRAY TRANSPORTABLE ARRAY DATA

Michael Ritzwoller, Morgan Moschetti, Yingjie Yang, Fan-Chi Lin, Gregory Bensen, Anatoli Levshin, Mikail Bramin · University of Colorado at Boulder

Ambient noise tomography and two-plane wave teleseismic tomography are two complementary new methods that, when used jointly, provide unprecedented resolution of the seismic structure of the crust and upper mantle over extended regions. We report on the application of these methods to Transportable Array data obtained over the first 2.5 years of its deployment. Results include group and phase velocity maps for Rayleigh and Love waves from 8 - 35 sec period obtained from ambient noise tomography and Rayleigh wave phase velocity maps from the two-plane wave method from 25 - 150 sec. Simultaneous inversion of these maps together with receiver function data is underway for 3D shear velocities and new images of the seismic structure of the crust and uppermost mantle are beginning to emerge.

RADIAL AND AZIMUTHAL ANISOTROPY IN THE LITHOSPHERE AND ASTHENOSPHERE UNDER NORTH AMERICA FROM LONG PERIOD WAVEFORM INVERSION

Barbara Romanowicz · University of California, Berkeley
Federica Marone · Paul Scherrer Institute, Switzerland

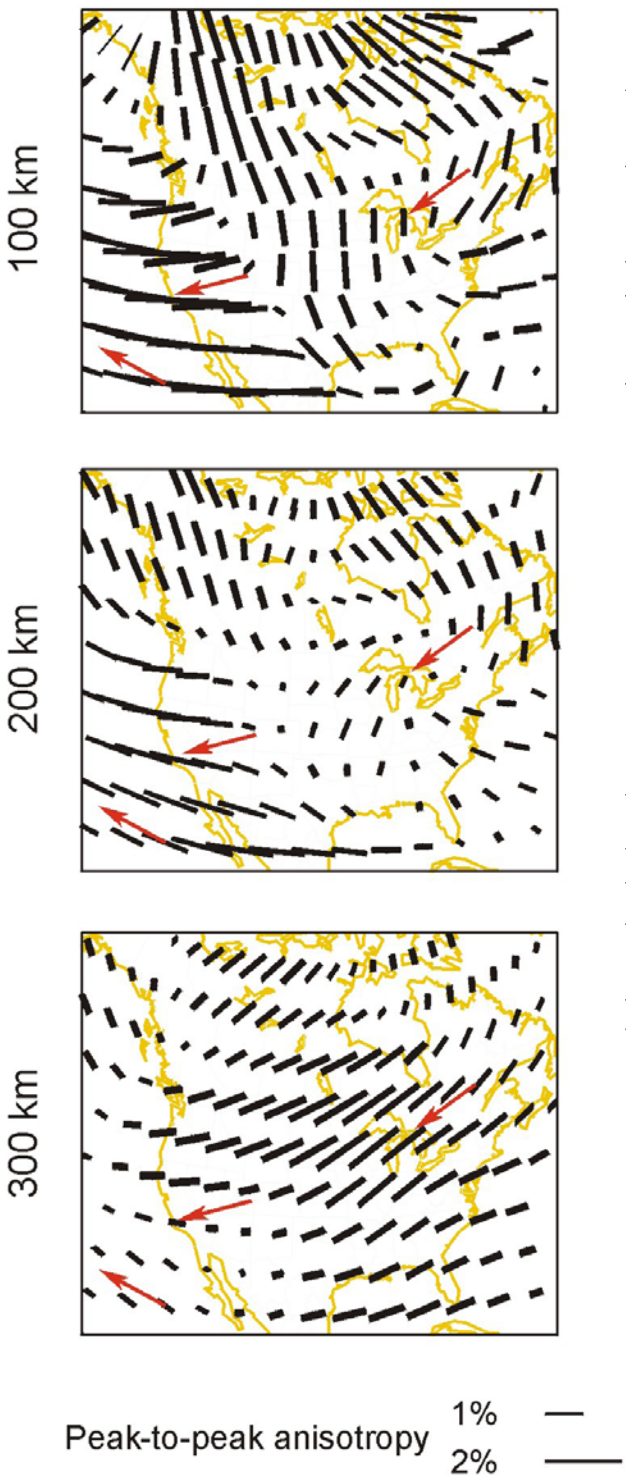

Horizontal slices at three different depths showing azimuthal anisotropy

Seismic anisotropy provides insight into paleo and recent deformation processes and therefore mantle dynamics. Our knowledge of the upper mantle anisotropic structure under North America is based mainly on global tomographic models or SKS splitting studies which lack horizontal and vertical resolution respectively. In particular, the azimuthal anisotropy derived from local SKS splitting measurements and that predicted from surface wave inversions shows a well documented discrepancy especially under continents.

We have developed the tools to construct continental scale tomographic models of the upper mantle from teleseismic long period waveform data, that include both isotropic S-velocity structure as well as radial and azimuthal anisotropy. We present the results of a joint inversion of fundamental and overtone surface waveforms for anisotropic S-velocity structure under the north American continent. The most notable feature of our model is the presence of two layers of anisotropy of varying thickness across the continent, one in the lithosphere and the other in the asthenosphere. Notably, the anisotropy in the asthenosphere exhibits SH>SV velocities, and a fast anisotropic axis direction aligned with the absolute plate motions of the north American plate, at depths greater than 250 km in the central and eastern parts of the continent. West of the Rocky Mountains, the asthenospheric layer is shallower, and the direction of anisotropy is aligned with the absolute motion direction of the Pacific Plate (Figure 1). These results suggest lattice preferred orientation of anisotropic minerals in the present day asthenospheric flow. In the shallower lithospheric layer, on the other hand, the anisotropy appears to hold the record of past tectonic events. When inverting jointly our waveform dataset with constraints from observed SKS splitting measurements over the north American continent, the amplitude of the anisotropy in the asthenospheric layer under the central cratonic regions is increased, and the model provides good fits to both surface wave and SKS splitting data. We believe that previous surface wave based models, under north America as well as other continents, had poor resolution at depths greater than 200km, and strongly underestimated the strength of the anisotropy at large depths under cratons, resulting in the observed discrepancy with SKS splitting observations. Higher lateral resolution will be achieved progressively with the accumulation of high quality data from the USArray backbone and TA data.

TESTING THE CONSTANCY OF TERTIARY AND QUATERNARY DEFORMATION RATES ACROSS THE SIERRA NEVADA FRONTAL FAULT ZONE USING CRN GEOCHRONOLOGY AND PALEOMAGNETIC DATA

Dylan H. Rood, Robert C. Finkel · Lawrence Livermore National Laboratory
Douglas W. Burbank · University of California, Santa Barbara

It is commonly unknown how to relate geodetic and geologic rates of deformation, although it is frequently assumed that the short-term rates can be extrapolated to long time scales in a meaningful way. Despite its widespread usage, the "steady rate" assumption remains largely untested. Similarly, the assumption that nearly all significant deformation occurs on faults remains unverified. Thus, our goal is to document rates of both focused (on-fault) and distributed (off-fault) deformation at multiple timescales, which will enable us to (1) test the constancy of fault slip rates and (2) quantify off-fault strain.

We focus on the Sierra Nevada Frontal Fault Zone (SNFFZ) in the central eastern Sierra Nevada, California, where deformed strain markers record a spectrum of deformation rates and styles. Both elastic (via fault displacement) and inelastic (via both vertical-axis block rotation and folding) strain can be quantified. Our study compares Tertiary and Quaternary deformation in the Sonora Pass, Bridgeport Basin, and Bodie Hills regions along the SNFFZ. Rates and styles of deformation have been derived from: (1) geologic and geomorphic mapping, (2) paleomagnetic sampling of Tertiary volcanic rocks, (3) differential GPS and total-station surveys of faulted landforms, and (4) detailed chronological studies of Quaternary glacial and alluvial deposits using in-situ cosmogenic radionuclide (CRN) exposure dating techniques. These data enable us to define mean deformation rates, and also, by utilizing markers of different ages, to define changes in deformation rates through time. Using these methods, long-term deformation histories have been constructed for (1) block rotation rates in the Bodie Hills and (2) fault slip rates in the Sonora Pass region.

SEISMIC VELOCITY STRUCTURE OF THE PACIFIC NORTHWEST FROM SEISMIC TOMOGRAPHY AND FORWARD MODELING OF RELATIVE DELAY TIMES

Jeffrey B. Roth, Matthew J. Fouch · Arizona State University
The HLP Seismic Working Group

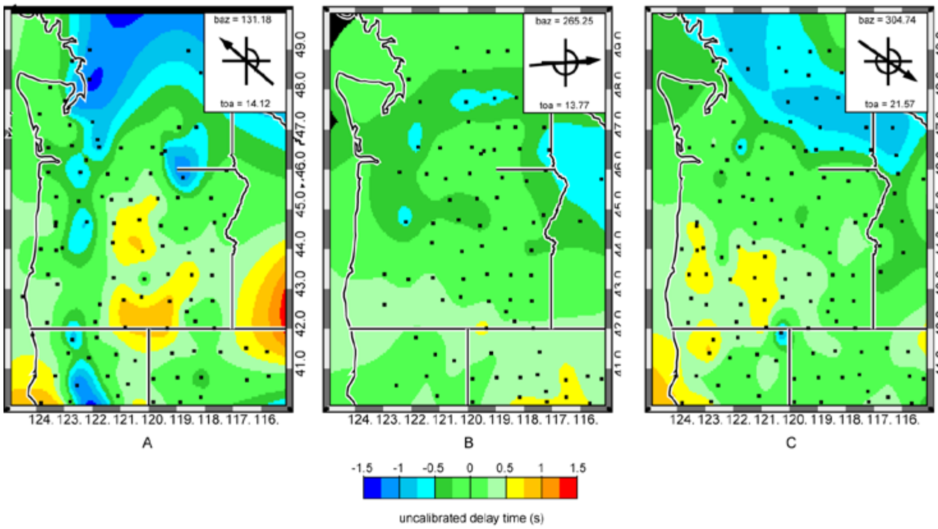

P-wave relative delay times for three events recorded at USArray stations in the Pacific Northwest. Black squares represent seismic stations. toa = take of angle, and is measured from vertical; baz = backazimuth. Colors represent magnitudes of relative delay times: cool colors indicate relatively early arrivals; warm colors indicate relatively late arrivals. Plot A is for an event with a southeastern backazimuth. Plot B is for an event with a western backazimuth. Plot C is for an event with a northwestern backazimuth.

We are utilizing data from a variety of datasets to constrain seismic velocity structure beneath the Pacific Northwest. In order to provide bounds on the seismic structure of the subducting Juan de Fuca (JdF) plate, we utilized data from the Cascadia array (a linear, E-W trending, broadband seismic array extending from the coast 300 km inland). We employed a multi-channel cross correlation technique to accurately determine relative delay times for 66 regional and teleseismic P-wave events, resulting in 1899 individual measurements. The raw relative delay times were corrected for elevation and for moveout assuming the IASP91 velocity model. We then developed suites of seismic wavespeed forward models and predicted delay times for each model to explain the patterns in the data. Using 9 variable parameters, we evaluated 3762 seismic wavespeed models. Because tradeoffs exist between many of the model parameters evaluated, we developed a series of grid searches to examine these tradeoffs and provide improved limits on the model space. We performed a total of 225 grid searches using 3402 models. Models which reproduce the data well are ones in which the slab dips shallowly (~10 deg) from the trench to a depth of ~80 km, just west of the Cascade Range. Below this region, the slab dips more steeply at ~50 deg to a depth of ~250 km. This model is consistent with studies that suggest that the slab is shallower to the north and becomes steeper towards the south near the Mendocino transform. The necessity of a steeply dipping end of the Juan de Fuca slab in our models provides an important constraint on the tectonic history of the region. For instance, a steepening slab may be the result of slab rollback and foundering after detachment from the Farallon slab at ~45 Ma. Many workers have argued for a mantle plume source for the voluminous volcanism in the area. In order for a deep seated plume to exist in this region, the subducted portion of the JdF plate would have to be steeply dipping and/or of shallow depth extent in order to not interfere with the plume conduit. Therefore, while our results do not require the presence of a plume in the region, they are also not inconsistent with such a phenomenon.

To provide 3D constraints on the structure of the region, we are currently utilizing the unprecedented amount of data afforded by broadband stations of the USArray Transportable Array, regional networks, and temporary stations of the High Lava Plains Broadband Seismic Experiment. To date, we have made over 2700 relative delay time measurements from 33 teleseismic events recorded at USArray stations between 40 – 50 deg N latitude, and 115 – 125 deg W longitude, covering all of Oregon and Washington, as well as parts of western Idaho, northern California and northwest Nevada. Delay times exhibit peak-to-peak variations of ~3.0 sec and reveal the following features: 1) Events from southeastern backazimuths (Figure 1A) illuminate a region of relatively high seismic wavespeeds in a narrow band parallel, and interior to, the Oregon coast. This feature is more subtle, and in many cases nonexistent in events from western backazimuths (Figure 1B). We infer this feature to be the result of the subducting JdF plate, consistent with our results from the Cascadia array. 2) Events from southeastern backazimuths (Figure 1A) also illuminate a large region of relatively low seismic wavespeeds that extend N-S across central Oregon, likely the result of mantle wedge structure and/or heterogeneous crust in the High Lava Plains. 3) Events from western backazimuths (Figure 1C) exhibit less heterogeneity in delay times, on average. In addition to this dataset, we will be adding data from the High Lava Plains experiment, which will add 170 seismometers in two transects across central Oregon. Once complete, we will perform a full suite of linear and nonlinear inversions to the dataset.

NON-VOLCANIC TREMOR DRIVEN BY LARGE TRANSIENT SHEAR STRESSES

Justin Rubinstein, John Vidale, Paul Bodin, Ken Creager, Steve Malone · University of Washington
Joan Gomberg · U.S. Geological Survey

Tremor, i.e., non-impulsive seismic radiation, has long been observed around volcanoes [Konstantinou and Schlindwein, 2002] and more recently around subduction zones [Obara, 2002], but the mechanical details remain unresolved. Here, we show that during the strongest shaking near Vancouver Island, Canada, in the Mw7.8 2002 Denali, Alaska earthquake, bursts of tremor radiated from the Cascadia subduction zone. The Love waves triggered most of these bursts, which are similar to non-volcanic tremor in that they have no clear onset, an extended duration, and a high-frequency spectrum depleted compared to earthquakes. The tremor was triggered when the Love wave displacement, building stresses of about a half bar, moved southwest (the direction of slip of the overriding plate on the megathrust) and shut off when the surface was displaced northwest. Our observations suggest that tremor is caused by driven slip on the subduction interface, in our case, effectively a plastic rheological response to the driving stress, and show tremor can be induced by shear stress nearly instantaneously as well as having the previously documented sensitivity to dilatational stress.

INTEGRATING CONTROLLED-SOURCE AND PASSIVE SEISMIC DATASETS

Eva-Maria Rumpfhuber · University of Texas at El Paso/University of Oklahoma
Randy Keller · University of Oklahoma
Aaron Velasco · University of Texas at El Paso

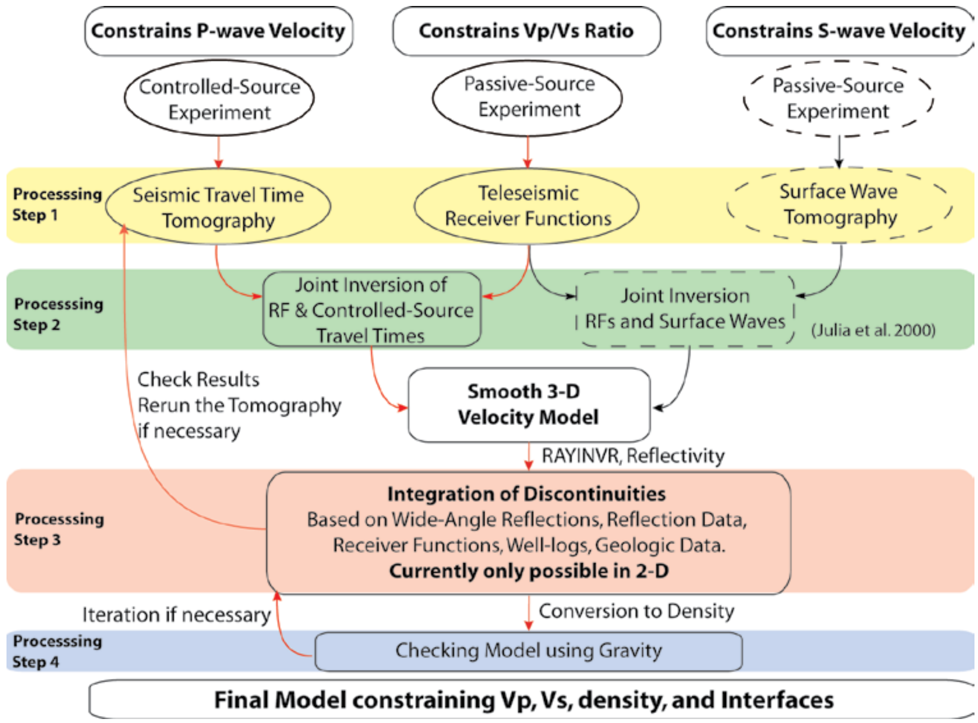

EarthScope enables geoscientists to address fundamental questions about continental structure, dynamics and evolution by its multidisciplinary nature. In general, models derived from the analysis of individual geological and geophysical datasets indicate the complexity of the Earth's structure and the processes at work. However, all too often these models have discrepancies, mainly due to contrasts in resolution and parameters they target. Thus, it is essential to incorporate geophysical and geological datasets and techniques to produce one consistent earth model and to further understand the Earth's dynamics. We focus on developing a formal integration approach using continental scale controlled-source experiments (CS) and passive source experiments (PS) in overlapping regions. CS experiments provide the highest resolution for a number of geophysical properties (Vp, Vs, etc.), as well as interfaces and transition zones, but generally can only cover specific regions in detail. PS experiments collect large quantities of data from three-component broadband stations, such as the USArray component of EarthScope, but usually with sparse station coverage. We explore formal integration schemes for the combination of controlled-source seismic data and receiver functions on a lithospheric scale. Our initial attempt stems from a tomography approach using interfaces partly constrained by receiver functions, and we are also investigating ray-tracing as basis for the integration. We use datasets from recent field experiments, and build a framework for adding additional data to the integration scheme.

INSAR OBSERVATIONS OF CREEP ON THE CENTRAL SAN ANDREAS FAULT

Isabelle Ryder, Roland Burgmann · University of California, Berkeley

While the San Andreas Fault is locked along most of its length, the 170 km-long section between San Juan Bautista and Parkfield undergoes creep. Measurements from creepmeters, alignment arrays and GPS over the last 25 years have shown that rates of creep reach 25-30 mm per year in the central portion, tapering off towards the locked segments at either end. Though useful, these measurements have been spatially isolated and intermittent in time. We present preliminary new InSAR observations of creep across the fault. The new dataset covers a period of time from 1992 to 2004, and has superior spatial coverage than previous data. From multiple ERS-1 and ERS-2 interferograms processed using ROI_PAC, we produce a stack which gives the spatial distribution of creep rate up to about 50 km either side of the fault. A combination of descending and ascending scenes enables resolution of vertical and horizontal components of motion. The InSAR rate maps are also supplemented by campaign GPS data obtained by the University of California, Berkeley network in this area.

ICE MASS CHANGES AND EARTHQUAKE HAZARD IN SOUTHERN ALASKA

Jeanne Sauber · NASA GSFC
Natasha Ruppert · Alaska Earthquake Information Center

Across southern Alaska the northwest directed subduction of the Pacific plate, Vp = 53 mm/yr is accompanied by accretion of the Yakutat terrane to continental Alaska (Vaccr = 33-44 mm/yr). This has led to high tectonic strain rates and dramatic topographic relief of more than 5000 meters within 15 km of the Gulf of Alaska coast. The glaciers of this area are extensive and many of them have undergone significant advances and retreats of kilometers to tens of kilometers on time scales ranging from decades to thousands of years. The repeat times of great earthquakes in this region are hundreds of years. Since large ice mass fluctuations occur directly above a proposed shallow main thrust zone associated with subduction of the Pacific-Yakutat plate beneath continental Alaska, the region between the Malaspina and Bering Glaciers is an excellent test site for evaluating the influence of ice mass changes on earthquake hazard Earlier we concluded that the largest contribution to ongoing crustal deformation and earthquake occurrence is strain accumulation due to plate convergence; we hypothesized, however, that the cumulative ice mass changes over the last 100+ years were large enough that they would promote thrust earthquakes [Sauber et al., 1995, 2000; Sauber and Molnia, 2004]. Here we use promote to mean that the incremental stresses on favorably oriented faults due to ice mass changes would bring them closer to failure. This is quantified by estimating the change in the fault stability margin (dFSM, Wu and Hasegawa, 1996), the distance between the Coulomb failure envelope and the outer Mohr circle. Our earlier results suggested that a cumulative decrease in FSM due to glacial wastage between 1899 (Yakataga earthquake, MW = 8.1) and 1979 in the region of the St. Elias earthquake (MS =7.2) was up to 1-2 MPa. A fair criticism of this analysis was whether ice mass changes had a testable influence on earthquake occurrence. To evaluate the possible influence of ice mass changes on earthquake occurrence requires an accurate knowledge of the ice mass changes as a function of time and a seismic catalog with a constant detection threshold over a representative seismic history. The changes in glacial extent and ice elevation are well-documented in the last 20 years by numerous studies [Sauber et al., 1995, 2000, Sauber and Molnia, 2004 and references therein; Arendt et al., 2002; Muskett et al., 2003, 2007; Lingle and Echelmeyer, 2005]. In this study, we calculated the incremental displacements and stresses and the change in FSM between 1988 and 2006 for alternate ice mass change scenarios. From analysis of the Alaska Earthquake Information Center (AEIC) catalog we have established a constant seismic detection threshold of M = 2.4 for the 1988 to 2006 time period in the study area. Aftershocks from the 1979 St. Elias earthquake (MS =7.2) were determined to bias the earlier decade. Analysis of the seismic data by AEIC included identification of glacial earthquakes in the catalog. As anticipated, we did not observe a seasonal change in the frequency of tectonic earthquakes; however, like Greenland, the glacial earthquakes showed a seasonal dependence. Although we found a localized increase in the number of tectonic earthquakes and seismic rate associated with ice thinning (as predicted, the converse scenario as well) the number of events in the test areas are small and this association may not be statistically significant.

WAVEFIELD MIGRATION OF EARTHSCOPE USARRAY DATA APPLIED TO PRECURSORS OF SS TO IMAGE UPPER MANTLE DISCONTINUITY STRUCTURE

Nicholas Schmerr · School of Earth and Space Exploration, Arizona State University
Christine Thomas · Department of Earth and Ocean Sciences, University of Liverpool
Edward Garnero · School of Earth and Space Exploration, Arizona State University

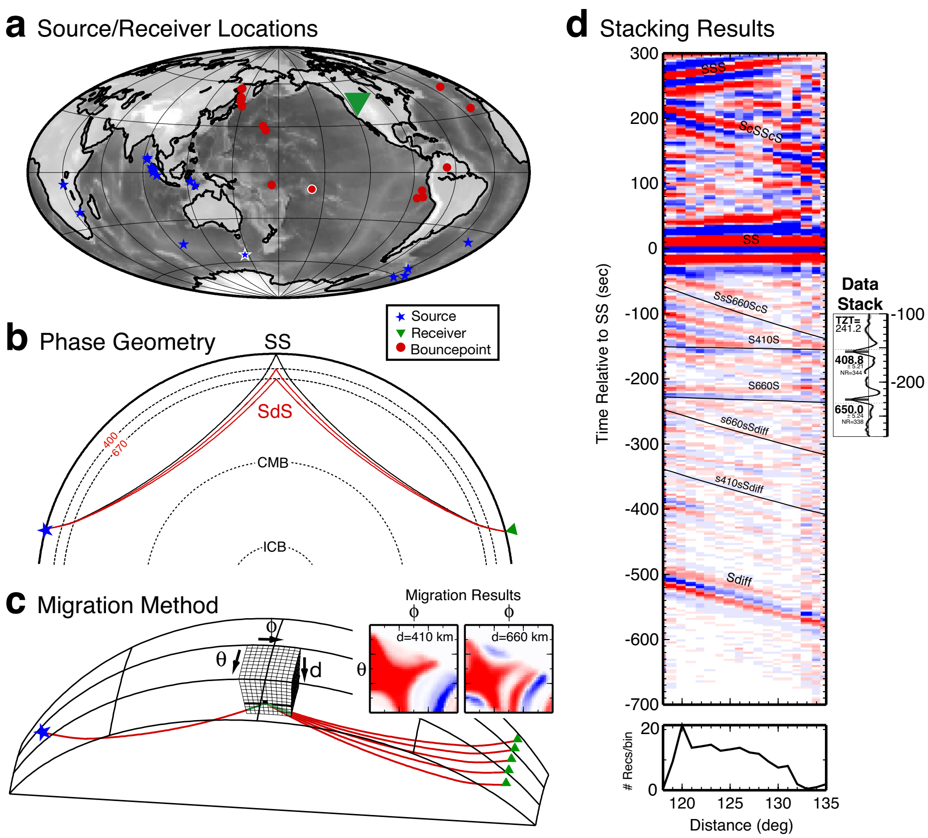

a) Events recorded at USArray that satisfy our epicentral distance, magnitude, and source depth criteria. b) Phase geometry for SS (black) and the precursors (red). c) Migration parameterization; the bounce point region is divided into 5km x 5km blocks in latitude, longitude, and depth. Energy recorded at the receivers in the array is then migrated to theoretical reflectors near the bouncepoint. This is done for each node in the migration grid, producing a map of reflected energy over lateral space and depth (see inset). d) One degree bin epicentral distance stacks for an event occurring at 54.96 degrees S and 145.40 degrees E (see a, highlighted in white) on 2007-01-30 04:54:48.060 at 10 km depth (Mw=6.8). Shown to the right are stacks of all data for each precursor; the depth (km), number of records in each stack, and relative error are given next to each reflector. The gray shading represents the 95% confidence bound from bootstrap resampling.

Precursors to the seismic phase SS are useful for retrieval of depth, amplitude, and topography of upper mantle discontinuities, particularly the 410- and 660-km phase boundaries. The depth and sharpness of the discontinuities are sensitive to both mantle temperature and composition, and regions of thermal and/or chemical heterogeneity produces topography on these boundaries. Seismic mapping of this topography provides an important constraint on the thermal and compositional state of the mantle.

Previous efforts employing the SS precursors nearly always required stacking of many hundreds or thousands of records to bring the typically low amplitude precursors out above the noise level. High-quality broadband data recorded by the EarthScope USArray Seismic Network, however, allows for unprecedented resolution of Earth structure with the SS precursors, which are in some cases are detectable in individual non-stacked seismograms.

In this study, we apply a seismic migration approach to the precursor wavefield, and show that depths of discontinuities in the depth range of 150-800 km can be well determined, and compare the accuracy to the traditional stacking methods. Migration, which is used frequently in exploration seismology, has the advantage to also detect out-of-plane reflections and focuses precursor energy at the true reflection point.

To achieve this, we utilize the transverse component of motion of data with epicentral distances of 100-165 degrees, source depths < 33 km to avoid interference with depth phases, and source magnitudes (Mw) ? 6.5 to ensure excitation of sufficient seismic energy. We also investigate several deep events (hypocenters > 450 km depth) for precursory arrivals to further reduce uncertainties/ambiguities owing to interference with the depth phases of the precursor waveforms.

We present discontinuity structure from several different regions, including the central Pacific, northern Japan, and central South America. Preliminary results from traditional stacking indicate a transition zone thickness of 242 km underneath sampled regions of the central Pacific, and thickened transition zone beneath our bouncepoints near subduction at Japan and South America. Migration of the datasets for each region will allow us to detect high-relief topography on the discontinuity boundaries, as well as additional horizons. Such structures are likely related to significant thermal and/or compositional heterogeneity at the discontinuities, or possibly further phase changes within the mantle.

SYNSEIS: A COMPUTATIONAL ENVIRONMENT FOR SYNTHETIC SEISMOGRAM SIMULATIONS

Dogan Seber · University of California, San Diego
Cindy Santini · Digital Mud Studio
Choonhan Youn, Tim Kaiser · University of California, San Diego

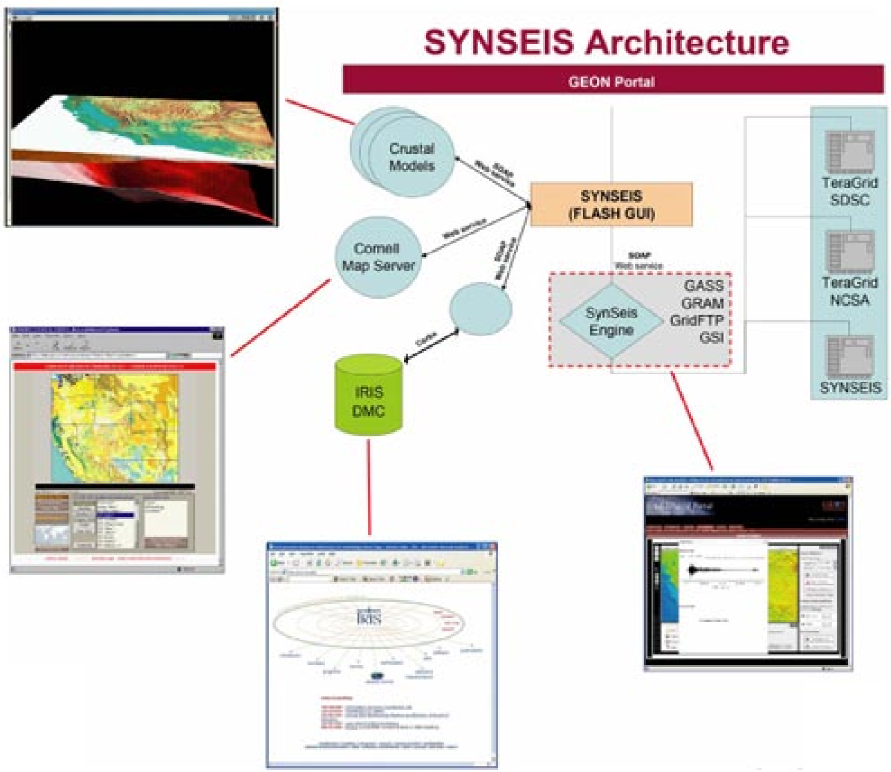

Simplified architecture of SYNSEIS and its service components

The Synthetic Seismogram Generation Tool (SYNSEIS) has been developed to help researchers compute 2D/3D regional seismic waveforms based on a well-tested, finite difference code, E3D, developed by the Lawrence Livermore National Laboratory. SYNSEIS has been developed as a Grid-based application which provides the capability to access distributed data and computational resources, creating a powerful but easy to use modeling tool that is accessible via the Web.

An interactive user interface with mapping tools and event, station, and waveform extraction mechanisms allows users to seamlessly access station and seismic waveform data from the data archives of the IRIS Data Management Center. Users can interactively set their region of interest, access seismic event and station locations, and extract waveforms on-the-fly for any selected event-station pair, and then compute synthetic seismograms. The SYNSEIS job monitoring and job archiving tools maintain the metadata and provenance for each run, such as the parameter settings for the run, and provide tracking of different job runs. This metadata can be exported in XML format thereby enabling researchers to share run outputs as well as job parameters. Outputs from the simulation runs are stored in the user's myGEON space. The SYNSEIS tool is one of the Science Gateways to the TeraGrid. This means simulation requests submitted using the tools can be executed directly on one of the supercomputer systems in the TeraGrid. This is done by utilizing a GEON "community user account" in the TeraGrid. GEON users who are interested in utilizing the TeraGrid capability are required to acquire a GEON Grid Certificate. Thus, the SYNSEIS Science Gateway provides Web-based supercomputing while eliminating the need for individual users to obtain supercomputer accounts, receive CPU allocation, and develop and optimize codes for each supercomputer platform.

While the system currently utilizes a fixed 3-D crustal model across the US, the goal is to incorporate more such models when they become available. The entire application is built using a service-based architecture. SYNSEIS is designed for use in day-to-day research, in particular for projects like EarthScope where scientists may be interested in understanding the crustal structure by accessing data from hundreds of stations everyday and processing them in a timely fashion.

SLOW-SLIP AND TRIGGERED EARTHQUAKES ON KILAUEA VOLCANO, WITH IMPLICATIONS FOR SLOW-SLIP AND TREMOR IN SUBDUCTION ZONES

Paul Segall · Stanford
Shin-ichi Miyazaki · ERI, University of Tokyo
Allan Rubin · Princeton
Emily Desmarais, David Shelley · Stanford

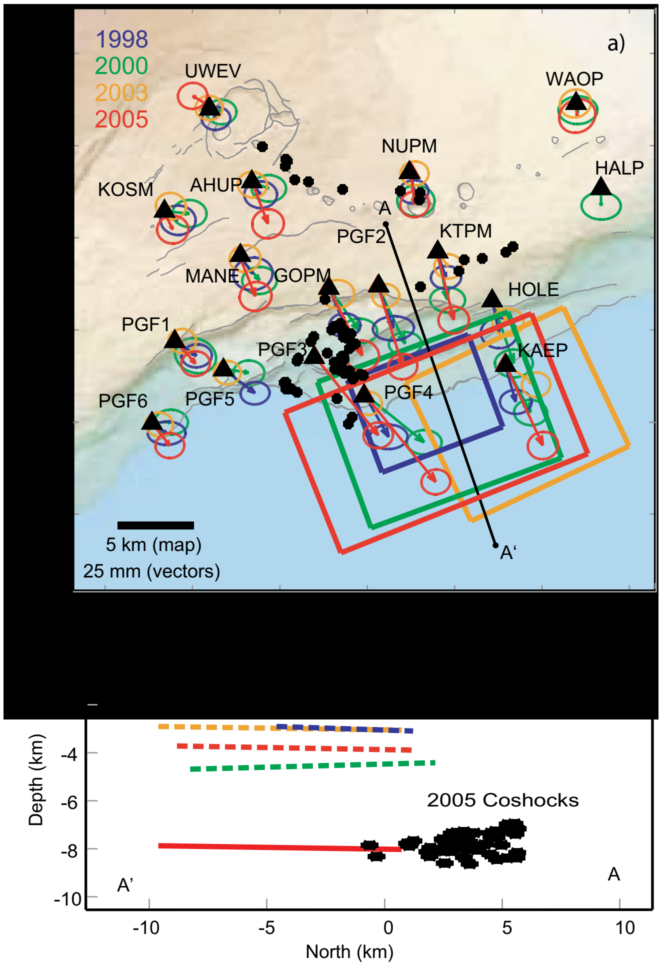

Displacements and inferred slip zones for four silent slip events on Kilaeua volcano. a), Vectors indicate displacements determined as the difference between mean position before and after the event. Ellipses represent 95% confidence intervals. Rectangles show surface projections of best-fitting dislocations. Asterisks represent earthquakes during the 2.2 days of the slow slip event beginning 00h UTC Jan 26, 2005. b), Cross-section. Dashed lines represent dislocations from inversion of GPS-derived displacements only. The solid red line indicates the 2005 event with depth constrained by micro-seismicity.

Slow-slip events on Kilauea volcano displace the south flank seaward ~1 cm over 1-2 days. Four events are clear in GPS data in 1998, 2000, 2003, and 2005, although smaller events may have occurred. Depths of slow events are difficult to constrain based on surface deformation measurements. Kilauea slow events are associated with swarms of small quakes. In 2005, the swarm follows the onset of GPS displacement, making the quakes “coshocks” and aftershocks of the otherwise silent earthquakes. The temporal evolution of the quakes is consistent with stressing caused by slip, implying that the quakes are triggered. The focal depths of 7–8 km, constrain the slow slip to be at comparable depths, since they must fall in zones of positive Coulomb stress change. Triggered quakes are similarly located in other slow events, in areas of background seismicity, suggesting that their locations are controlled by structural or material heterogeneity. We have been unable to confirm non-volcanic tremor associated with the Kilauea slow events, although the network has not been well suited to detection.

Recent work on tremor, low frequency quakes, and slow slip in Japan suggests that the tremor occurs as shear slip on the plate interface. Slow events appear to be located in regions that are transitional between velocity weakening and strengthening friction. Two mechanisms for generating slow slip will be discussed. In the first, a velocity weakening region is sufficiently large to nucleate transient slip, but too small to support dynamic slip. Low effective normal stress and near velocity-neutral friction favors larger transient slip regions. In the second, velocity-weakening regions, sufficiently large to slip dynamically, are separated by velocity strengthening barriers. Dynamic rupture of the weakening regions radiates high frequency seismic waves, while the rate of propagation of the slow slip is controlled by the rate at which slip can traverse the velocity strengthening barriers.

EARTHSCOPE ENGAGES AMERICAN INDIAN STAKEHOLDERS IN ARIZONA

Steven Semken · Arizona State University, School of Earth and Space Exploration
Peterson Zah, Jaynie Parrish · Arizona State University, Office for American Indian Affairs
Matthew Fouch, Edward Garnero · Arizona State University, School of Earth and Space Exploration
Rena Martin · Dinetahdoo Cultural Resource Management
Donald Lippert · USArray

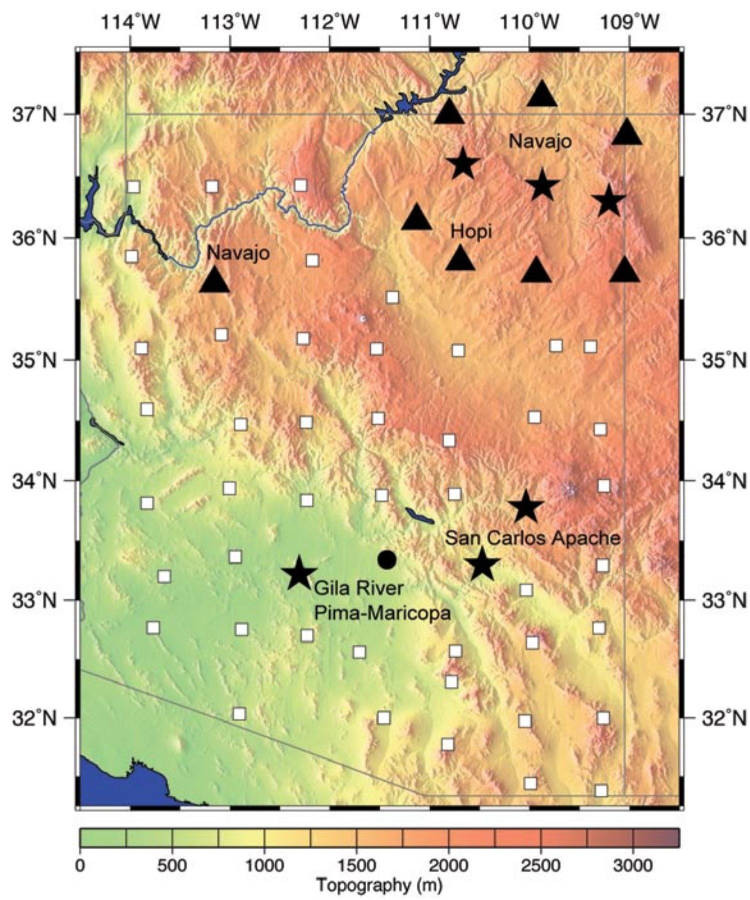

Location map of USArray (Transportable Array or Bigfoot) sites in Arizona. Black symbols indicate sites on or adjoining American Indian lands: Stars indicate K-14 school hosts, Triangles indicate other American Indian sites, Circle indicates a school outside Tribal jurisdiction. White squares indicate other USArray sites.

EarthScope is taking up residence in Arizona, where planned deployments place USArray and Plate Boundary Observatory stations on or near the lands of seven different American Indian nations. In concert with the research, the EarthScope education and outreach (E&O) plan calls for direct affiliations with Native stakeholders and school systems. For the past eighteen months we have been collaborating with American Indian communities in Arizona to facilitate USArray deployment and EarthScope E&O activities in a culturally appropriate manner. The collaboration began with a fall 2005 workshop at Arizona State University (Native American Perspectives and Preferences Bearing on EarthScope Deployments in the Southwest, NAPP-ES) for decision-makers and experts in cultural resources and education from the nations that would be affected. The workshop embodied a successful cross-cultural exchange: EarthScope researchers provided Tribal representatives with an introduction to the scientific and educational components of the project, while the American Indian participants shared critical information on relevant cultural and jurisdictional issues. These included sacredness of lands, the significance of ancestral homelands, multi-agency clearance procedures, and best approaches to community-based outreach. Outcomes of the NAPP-ES workshop, including direct connections established with five American Indian nations, guided a successful siting and permitting plan for USArray in Arizona carried out in 2006 and early 2007. The program has also initiated E&O partnerships with six K-14 schools on the Navajo, San Carlos Apache, and Gila River Pima-Maricopa Nations. Results and findings of this two-year project will be offered to inform subsequent EarthScope deployment and E&O activities across American Indian nations in the Rocky Mountain and Northern Plains regions.

THE MECHANICS OF EPISODIC TREMOR AND SLIP

David Shelly, Gregory C. Beroza · Stanford University
Satoshi Ide, Takahiko Uchide · University of Tokyo

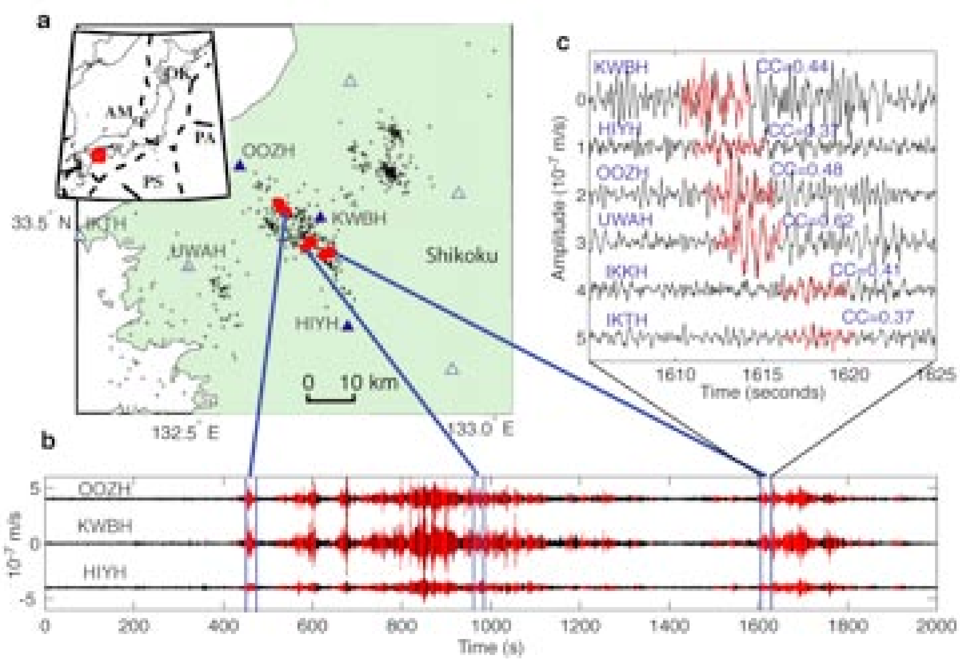

Figure 1 | Detection of low-frequency earthquake swarm forming tremor. a, Map view of westernmost Shikoku showing areas active (red circles) during three windows of tremor from part b. Small black crosses show the locations of template events used in this study. Blue triangles show station locations; filled triangles indicate stations with waveforms plotted in part b. Inset at upper left shows the tectonics of the region, with the red box indicating the area shown in the main figure. PA, Pacific plate; PS, Philippine Sea plate; AM, Amur plate; OK, Okhotsk plate. b, North-component waveforms during a tremor sequence for three Hi-net stations starting September 2, 2005 at 19:00, bandpass filtered between 1 and 8 Hz. Portions plotted in red indicate times with a detected event similar to a template event. Blue lines point to the source region of tremor for each time window shown, according to what template events are active during this time. c, Example of waveforms at the time of a detection. Continuous tremor waveforms are shown in black and template event waveforms in red for five Hi-net stations (north component). Waveforms are bandpass filtered between 1 and 8 Hz. Amplitudes of the template event waveforms are scaled to match the continuous data. The correlation coefficient (CC) for each trace is also given.

Non-volcanic tremor is a weak, extended duration seismic signal observed episodically on some major faults, often in conjunction with slow slip events. The coupled phenomenon has been termed “episodic tremor and slip.” Although the generation mechanism of tremor and its exact relationship to slow slip has been a recent subject of controversy, new results may begin to provide a clearer understanding of this phenomenon. We find that tremor beneath Shikoku, Japan can be explained as a swarm of small, low frequency earthquakes (LFEs) [Shelly et al., 2007]. Precise relocation places these LFEs on the subduction interface, immediately down-dip of the locked portion of the plate boundary [Shelly et al., 2006]. In order to determine the mechanism by which tremor is generated, we analyze stacked LFE waveforms and compare them with the waveforms of nearby earthquakes of known mechanism within the subducting Philippine Sea Plate. Both P-wave first-motion focal mechanism and the S-wave moment tensor analysis indicates that LFEs are generated by shear slip on a low-angle thrust fault dipping to the northwest [Ide et al., 2007a]. We conclude that LFEs, and hence deep non-volcanic tremor, are generated directly by shear slip on the plate boundary, and thus represent a seismic signature of the accompanying slow slip events (SSEs). SSEs that accompany tremor have durations of up to weeks. They have been observed in Japan using borehole accelerometers and in Cascadia using GPS. Recently discovered very low frequency earthquakes (VLFs) with characteristic durations of 10s of seconds have been demonstrated to occur as shear slip in the same location as LFEs and SSEs, but with a longer time constant [Ito et al., 2007]. Taken together, tremor, LFEs, VLFs, and SSEs define a spectrum of slow shear-slip events on the plate boundary that span 8 orders of magnitude in moment and duration [Ide et al., 2007b].

GPS CONTRIBUTION TO NEW MADRID SEISMIC ZONE HAZARD ESTIMATION

Robert Smalley · CERI/Univ. Memphis

Continued study of the New Madrid seismic zone further deepens the enigma of the worlds most active intraplate seismic zone. Paleoseismic studies show there were three to four previous events and they may have also been clusters. Newer estimations of the magnitudes of the 1811-1812 sequence events suggests they are smaller than initially proposed, which lessens the energy needed to be stored in the crust by two to three orders of magnitude. Studies of earthquake recurrence show that the most likely places for future earthquakes, even away from plate boundaries, is near the locations of previous earthquakes. Application of GPS technology to the problem of understanding New Madrid seismic zone earthquakes has not yet produced a definitive determination of a strain field. Both more time and denser continuous GPS measurements are needed before strong results from GPS can significantly change seismic hazard estimates obtained by non-GPS studies.

VELOCITY STRUCTURE OF THE LAS VEGAS VALLEY, NEVADA

Catherine Snelson, Sandra Saldana, Shelley Zaragoza, John Karr · Geoscience Department, University of Nevada Las Vegas

The Las Vegas Valley sits atop a deep basin that has been shown to amplify energy from strong ground motion. As a result, a series of seismic refraction experiments have been conducted in order to better characterize the Las Vegas basin for seismic hazards. The basin is located within the central Basin and Range, and is characterized by local strike-slip fault zones (in-active) and a series of normal faults (active). Several of these normal faults within the Valley have been identified as potential sources of future seismic activity with the potential are capable of producing M 6 to 7 earthquakes within the highly populated Valley. In addition, within a 150-km radius of the Valley are several regional strike-slip fault zones, including the Furnace Creek fault zone, that have the potential for generating large magnitude earthquakes that could pose a significant seismic threat to the Valley. A series of seismic refraction and reflection profiles have been acquired to better image the geometry of the basin, locating active faults at depth and to better understand potential focusing effects of the basin. The results from these various experiments have provided us with a new view into the sub-surface of the Las Vegas Valley. We have produced a 3-D P-wave velocity model across much of the Valley that imaged faults at depth. In addition, these data have shown the basin to have a two-tier structure with a consolidated Tertiary basin below an unconsolidated Quaternary basin. The velocities range from 2.5 to 4.5 km/s within the basin. The 4.5 km/s contour indicates the base of the basin where velocities increase to 6 km/s to the base of the model (9 km depth). From these data, we have acquired high-resolution seismic data across several key faults as well as suspected new faults. These new data are being used to attempt to understand the extent of the faulting and timing. Future work entails acquiring new crustal data to understand the regional tectonic picture for Southern Nevada and how it relates to the active tectonics in the Las Vegas Valley. All of these data are being integrated into a model with current geotechnical and geologic data to interpret the Las Vegas Valley for seismic hazard potential and understand the current tectonic regime.

WHAT HAVE WE LEARNED ABOUT FAULTS AND EARTHQUAKES? USING A VIEW FROM SAFOD TO INCREASE UNDERSTANDING OF FAULT BEHAVIOR *(Speaker)*

John Solum · Sam Houston State University, Department of Geography and Geology

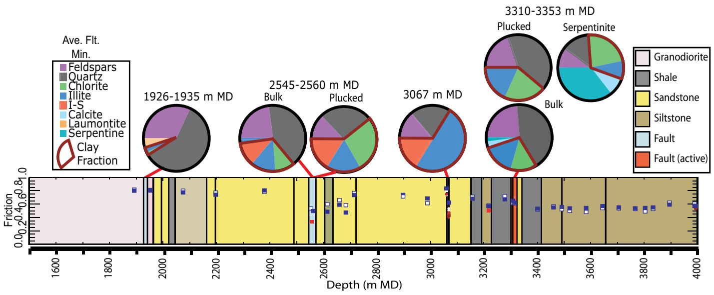

Lithologies, fault rock mineral assemblages, and coefficients of friction for samples from the SAFOD main hole. The actively creeping strand of the San Andreas Fault is shown in red.

In order to understand the behavior of active strands of large faults like the San Andreas at SAFOD it is necessary to understand the behavior of micron to millimeter-scale slip surfaces as well as kilometer-scale fault systems. Several of the faults penetrated during drilling of SAFOD are characterized by thin shear zones, but the formation of the neoformed mineral assemblages within those shear zones is controlled in part by larger, fault system-scale, structures and interactions.

One indication that thin shear zones are important at SAFOD comes from the occurrence of serpentine in the hole. Serpentine (lizardite and chrysotile) is present in <2 wt % in cuttings collected near the region of the main hole where casing is actively deforming due to fault creep at ~3.3 km measured depth (MD). The low abundance of serpentine in the cuttings suggests that if serpentine is rheologically important at SAFOD then it occurs as very thin veins. The spatial distribution of serpentine will be resolved during Phase III coring in the summer of 2007.

Some faults penetrated during drilling contain fault rocks that are characterized by very thin slip surfaces (~10`s of microns) composed of neoformed mixed-layer smectitic clays (Schleicher et al., 2006 GRL; Solum et al., 2006 GRL). The weakness of smectites, montmorillonite in particular, has been proposed as a mechanism to explain the weakness of the San Andreas Fault, at least at shallow crustal levels (<~3 km). The heat flow and stress orientation constraints on the coefficient of friction, mu, of the San Andreas fault are ~0.1-0.2. Plucked grains of fault rocks from these zones exhibit mu as low as 0.3-0.35 for a fault at 2.5 km MD, and 0.4-0.49 for the active fault at 3.3 km MD (Tebme et al., 2006 GRL; Morrow et al., 2006 AGU presentation). Talc has also been observed in cuttings from ~3.3 km MD, which is significant since talc is weak (mu ~0.1-0.15) and persists to deeper crustal levels than montmorillonite (Moore and Rymer, this volume). These results suggest that the weakness of the San Andreas is due in part to the growth of weak phases. It is therefore critical to understand the processes that control the formation of these phases. Since neomineralization requires fluid activity it becomes necessary to characterize fault-related fluids.

The relationship between fault strength and fluid pressure has been recognized for decades, and widespread neomineralization in fault zones from SAFOD suggests significant fluid activity (although not necessarily elevated fluid pressure, which has yet to be observed in fault zones at that location). Neomineralization promoted by fluid activity is important, however variations in fluid chemistry can also change the behavior of existing minerals. The strength and rate dependence of montmorillonite is strongly influenced by brine chemistry (Lockner et al., 2006 AGU presentation). For example montmorillonite in fresh water exhibits ? of ~ 0.1 and ~0.2 in KCl brine. The addition of brine also reduces a-b from ~ 0 in fresh water to ~-0.0008. This means that changing pore fluid chemistry can dramatically change fault behavior. If the fluid reservoirs tapped by a fault system change over time, then that may be enough by itself to dramatically change fault behavior.

Stable isotopic analyses of carbonate grains plucked from cuttings suggest that fault zones in the deeper portion of the main hole are tapping a fluid reservoir that is much less common in protolith (Kirschner et al., this volume). This suggests that as individual faults in the SAFOD area grew they became interconnected, which indicates that the plumbing system of large fault systems may be dynamic. The distribution of alteration minerals in SAFOD (laumontite, chlorite, illite, and illite-smectite) can be used to infer paleo fluid reservoirs. For example, while the modern San Andreas Fault at SAFOD is a barrier to fluid flow (Wiersberg and Erzinger, 2007 Geochemistry, Geophysics, and Geosystems), the similarity of some aspects of chlorite mineralization on either side of the active fault at 3.3 km MD indicates that it was not always a barrier to cross-fault fluid flow. When it became a barrier to fluid flow, faults on the southwestern side of the fault that had presumably been in communication with fluid reservoirs on the northeastern side of the fault lost contact with those reservoirs, resulting in a change in pore fluid chemistry. Since several significant faults were crossed during drilling it therefore becomes critical to constrain the historical relationship of those faults to the active strands of the San Andreas in order to understand the evolution of those active strands.

The mineral assemblages discussed herein and their implications for fault behavior are not unique to SAFOD. For example, the influence of smectitic clays on the behavior of faults in accretionary prisms has been an area of active research. The tentative generalizations that can be made are: 1) the permeability structure of a fault can influence neighboring faults; 2) fault zone mineral assemblages , and therefore physical properties, are evolving; 3) very thin coatings of neoformed minerals on slip surfaces may be rheologically important; 4) fluid chemistry can effect the frictional properties of some fault zones.

PROBING CONTINENTAL LITHOSPHERE USING WAVEFORMS

Teh-RU Song, Don Helmberger · Caltech

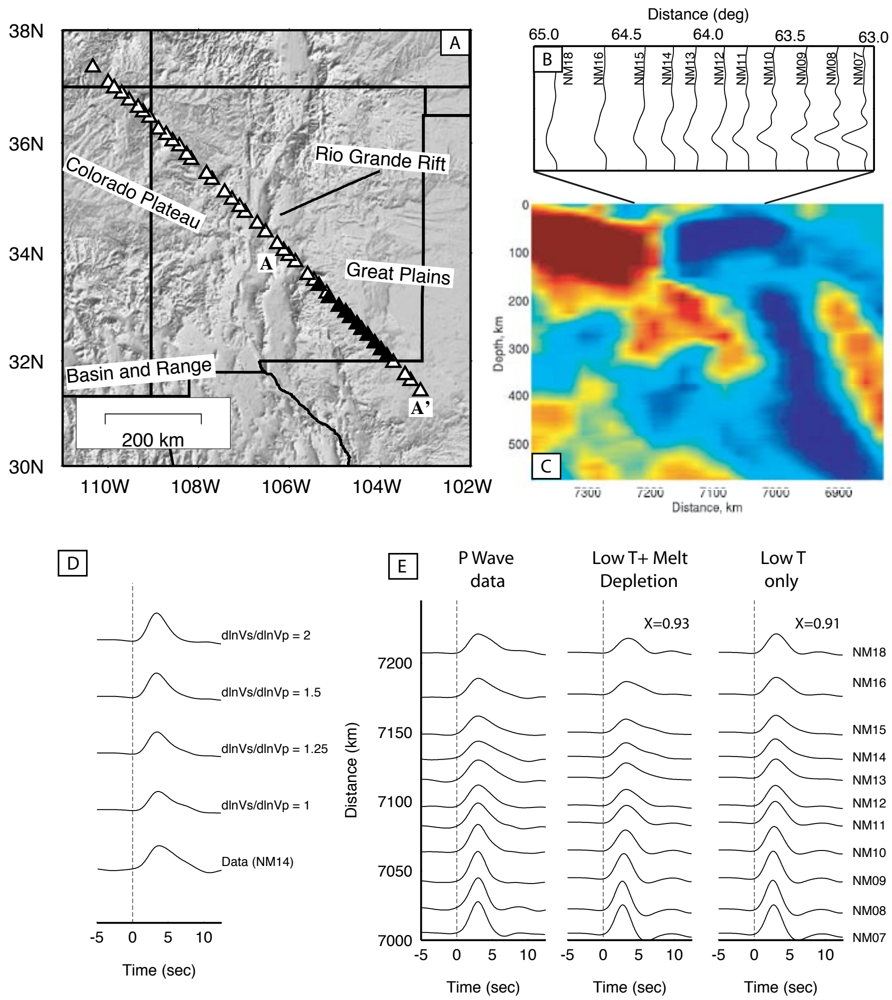

Travel time tomography has been extensively conducted to invert velocity structures of the Earth's mantle at both regional and global scales. Recent dense instrumentation at regional scale provides excellent opportunities to study detail tectonic features such as slabs, mobile belts and rift zones. Tomographic analysis along the La Ristra Transect (Fig. 1A) (Gao et al., 2004) is an excellent example of using a dense linear array to resolve lithospheric heterogeneities. However, finite difference synthetics of such a model do not reproduce the waveform distortions as observed in broadband waveform data (Fig. 1B), which directly sample a SE dipping, slab-like structure underneath the western edge of the Great Plain (Fig. 1C). In addition to travel time anomalies, Song and Helmberger (2006) demonstrated how to use S waveforms and their amplitude patterns to further constrain the magnitude of the anomalous structure. Their preferred model suggests the slab-like structure is about 4% fast, 120 km thick and dipping 70-75 degree to the SE to about a depth of 600 km. We adopt the preferred S wave model from Song and Helmberger(2006), and scale it to the P wave model using a suite of scaling factors dlnVs/dlnVp. We find the scaling factor about 1.25 fits the P waves amplitude patterns best, although waveform fits indicate an even lower SF value of about 1 (Fig. 1D). In short, the P waveform distortion is as profound as the S waveform and temperature alone is not able to explain the data (Fig. 1E). To explain the P waveform data, Monte Carlo and bootstrap approaches are performed to include compositional effect along with temperature. We find the most probable model to explain the data is a temperature anomaly of about $-$400 K with additions of olivine (11%), orthopyroxene (12%) and losses of clinopyroxene (-14%), garnet (-9%) relative to the adjoining mantle asthenosphere beneath the Rio Grande Rift (Fig. 1E). This sesimic anomaly, probably continental lithosphere, is cold and is as depleted as the Archean continental lithosphere. It was likely formed in the Proterozoic age but destabilized during the Cenozoic rifting of the Rio Grande Rift.

P AND S WAVEFORM DISTORTIONS REVEAL A DEPLETED, DESTABILIZED CONTINENTAL LITHOSPHERE NEAR THE RIO GRANDE RIFT

Teh-RU Song, Don Helmberger · Caltech

Travel time tomography has been extensively conducted to invert velocity structures of the Earth's mantle at both regional and global scales. Recent dense instrumentation at regional scale provides excellent opportunities to study detail tectonic features such as slabs, mobile belts and rift zones. Tomographic analysis along the La Ristra Transect (Fig. 1A) (Gao et al., 2004) is an excellent example of using a dense linear array to resolve lithospheric heterogeneities. However, finite difference synthetics of such a model do not reproduce the waveform distortions as observed in broadband waveform data (Fig. 1B), which directly sample a SE dipping, slab-like structure underneath the western edge of the Great Plain (Fig. 1C). In addition to travel time anomalies, Song and Helmberger (2006) demonstrated how to use S waveforms and their amplitude patterns to further constrain the magnitude of the anomalous structure. Their preferred model suggests the slab-like structure is about 4% fast, 120 km thick and dipping 70-75 degree to the SE to about a depth of 600 km. We adopt the preferred S wave model from Song and Helmberger (2006), and scale it to the P wave model using a suite of scaling factors dlnVs/dlnVp. We find the scaling factor about 1.25 fits the P waves amplitude patterns best, although waveform fits indicate an even lower SF value of about 1 (Fig. 1D). In short, the P waveform distortion is as profound as the S waveform and temperature alone is not able to explain the data (Fig. 1E). To explain the P waveform data, Monte Carlo and bootstrap approaches are performed to include compositional effect along with temperature. We find the most probable model to explain the data is a temperature anomaly of about $-$400 K with additions of olivine (11%), orthopyroxene (12%) and losses of clinopyroxene (-14%), garnet (-9%) relative to the adjoining mantle asthenosphere beneath the Rio Grande Rift (Fig. 1E). This sesimic anomaly, probably continental lithosphere, is cold and is as depleted as the Archean continental lithosphere. It was likely formed in the Proterozoic age but destabilized during the Cenozoic rifting of the Rio Grande Rift.

CONSTRAINING YELLOWSTONE MAGMATIC PROCESSES ALONG THE EASTERN SNAKE RIVER PLAIN VIA AMBIENT NOISE AND TELESEISMIC RAYLEIGH WAVE DISPERSION INVERSION

Josh Stachnik, Ken Dueker, Derek Schutt · University of Wyoming

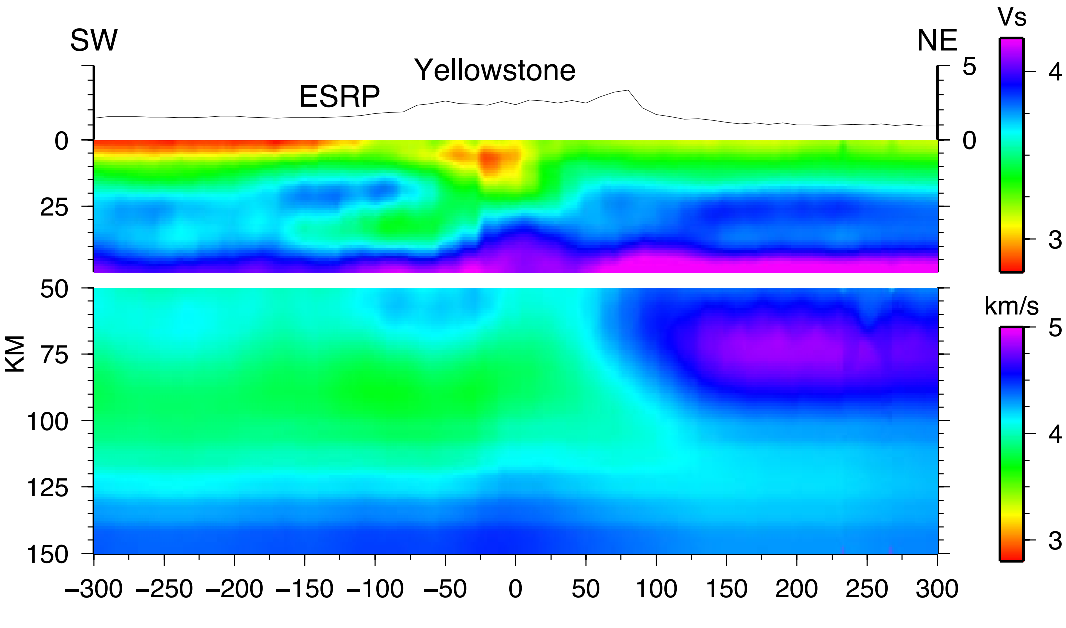

Cross section showing shear wave velocity variations along the eastern Snake River Plain via joint inversion of Rayleigh wave dispersion data from ambient noise group velocities and ballistic wave phase velocities. High shear wave velocity at 15-25 km depth below ESRP represents mid-crustal sill. Note different color velocity scales for crust (upper 50 km) and mantle (below 50 km).

The prominent feature of the Yellowstone hotspot track is the time-transgressive sequence of rhyolitic calderas that fill the 80 km wide structural downwarp associated with the eastern Snake River Plain (ESRP). The caldera eruptive products are estimated to be 2-3 km thick with a <1 km lid of late stage basalts. Three processes are used to explain the ESRP downwarp: 1) densification of the mid-crust due to emplacement of mantle derived basalts 2) differential extension between the ESRP and its margins 3) outward directed flow of the ESRP lower crust forced by the load associated with mid-crustal densification. Several lines of evidence support the existence of a dense ESRP mid-crust. Petrologic analysis suggests that the caldera eruption magmas are fractionated from mid-crustal basalt intrusions with minor amounts of crustal melting and assimilation. Given the estimated extrusive volcanic volumes, petrologic constraints suggest that a 17-37 km thick layer of mantle derived basalt has been added to the ESRP crust. Flexural modeling to match observed tilt indicators about the ESRP suggests that a 10-20 km thick layer with a 3-4% density increase is required. Remarkable is that a new synoptic scale crustal thickness map shows no significant crustal thickness gradient between the ESRP and its margins: circumstantial evidence for outward directed lower crustal flow. Seismic constraints with respect to the volume and excess density of the mid-crustal sill remain relatively poor. Two seismic refraction lines from 1978 modeled a 10-15 km thick high velocity body in the ESRP mid-crust. Imaging using converted P to S waves from PASSCAL experiments are consistent with this model, but do not constrain the volume of the mid-crustal 'sill'. To provide new constraints on the the ESRP mid-crust, dispersion measurements between 5-30 s are measured from the diffusive wavefield (ambient noise) recorded by the 75 station Yellowstone-Billings-NSN arrays. A joint inversion of Rayleigh wave ballistic-wave phase velocity dispersion measurements and diffusive wave group velocity dispersion measurements reveals a high velocity body at 10-25 km depth. Remarkable is that this mid-crustal high velocity layer deepens down the hotspot track. This would be consistent with the observed systematic structural subsidence down the ESRP. Additionally, a 3.3 km/s low velocity lower crust is resolved beneath the ESRP that extends about 100 km to either side of the ESRP downwarp. This finding of very low velocity lower crust beyond the margins of the ESRP is consistent with the lateral advection of the hot lower crust beneath the ESRP via lower crustal flow. Beneath the Yellowstone Caldera low shear wave velocities (2.8 to 3.1 km/s) are resolved above 12 km with normal lower crust velocities suggesting that magma is not being ponded (staged) in the lower crust Overall, our new images are consistent with previous results, but provide improved constraints on crustal structure.

NEW MADRID: A COLD, DYING FAULT?

Seth Stein · Northwestern University
Andrew Newman · Georgia Institute of Technology
Jason McKenna · U.S. Army Engineer Research & Development Center
Carol Stein · University of Illinois at Chicago

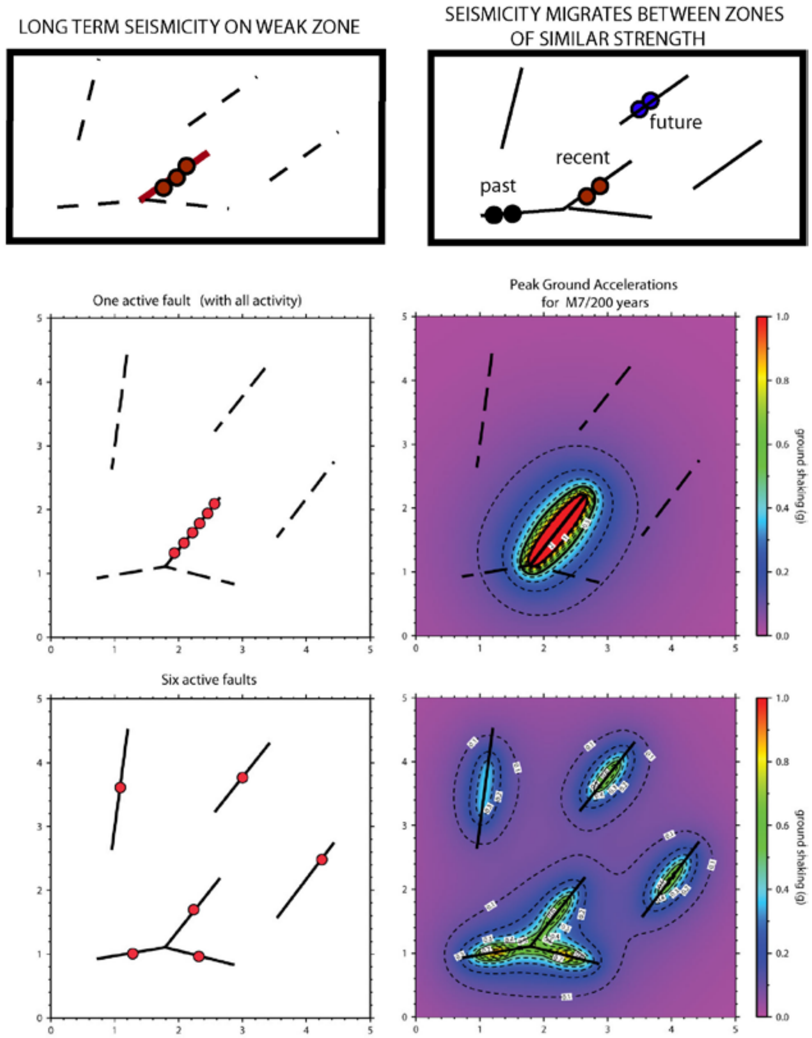

A fundamental question about continental intraplate earthquakes is why they are where they are. For example, why are the New Madrid Seismic Zone (NMSZ) earthquakes concentrated on the Reelfoot Rift, when the continent contains many fossil structures that would seem equally likely candidates for concentrated seismicity? A key to answering this question is understanding the thermo-mechanical structure of the seismic zone. If it is hotter and thus weaker than surrounding regions, the weak lower crust and mantle concentrate stress and seismicity in the upper crust. A weak zone that recently relaxed has been proposed as a mechanism by which strains can be released faster than they are observed to accunulate by geodesy (Kenner and Segall, 2000). Alternatively, if it is not significantly hotter and weaker than its surroundings, the seismicity is likely to be a transient phenomenon that migrates among many similar fossil weak zones. These different models have important implications for the mechanics of the seismic zone, stress evolution after and between large earthquakes, and seismic hazard assessment.

The sparse heat flow data in the New Madrid area can be interpreted as supporting either hypothesis. There is a possible small elevation of heat flow in the area compared to its surroundings, depending on the New Madrid and regional averages chosen. The inferred high heat flow has been interpreted (Liu and Zoback, 1997) as indicating that the crust and upper mantle are significantly hotter and thus significantly weaker than surrounding areas of the central and eastern U.S. However, reanalysis of the heat flow indicates that the anomaly is either absent or much smaller (3 rather than 15 mW/m**2) than assumed in that analysis, leading to much (90%) smaller temperature anomalies and essentially the same lithospheric strength. Moreover, if a small heat flow anomaly exists, it may result from groundwater flow in the rift's fractured upper crust, rather than higher temperatures. The latter interpretation seems more consistent with studies that find low seismic velocities only in parts of the seismic zone and at shallow depths. Hence although the question cannot be resolved without additional heat flow data, we find no compelling case for assuming that the NMSZ is significantly hotter and weaker than its surroundings.This result is consistent with the migrating seismicity model and the further possibility that the NMSZ is shutting down, suggested by the small or nill motion observed geodetically. In this model the present seismicity are aftershocks of the large earthquakes of 1811 and 1812, and such large earthquakes will not recur there for a very long time. Hence the seismic hazard should be viewed as diffuse rather than concentrated near the 1811-12 rupture.

USING SPACE GEODETIC DATA TO TEACH ABOUT TECTONICS, EARTHQUAKES, AND HAZARDS

Seth Stein · Northwestern University

GPS SITES DEMONSTRATE PLATE ROTATION

Stein & Sella, 2002

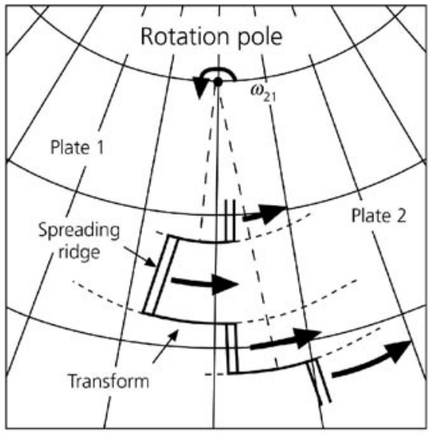

Stein & Wysession, 2003

GPS SITES DEMONSTRATE POST-GLACIAL REBOUND

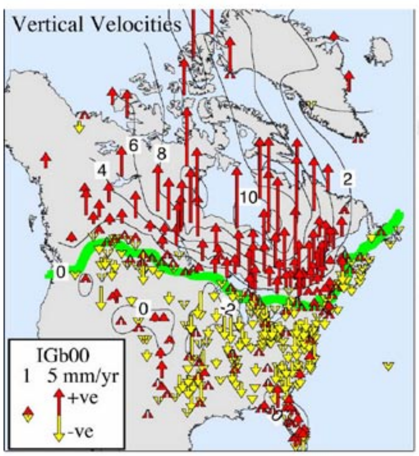

Sella et al., 2007

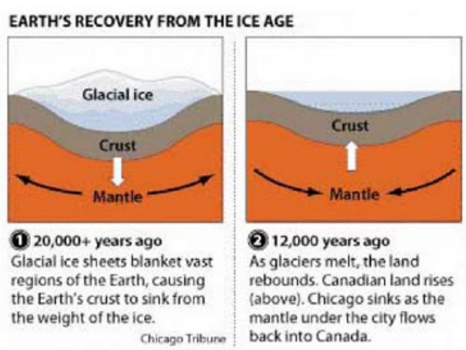

Space geodetic data, especially GPS data, are valuable in teaching about various topics in tectonics, seismology, and earthquake and volcano hazards. Many ideas about these topics are hard for students to understand because they are derived via inferences that can be unintuitive from data that appear complicated such as magnetic anomalies, topography, structures, etc. In contrast, although geodetic site velocities are derived from a complicated technology, the velocities themselves are easy to understand. The velocities also indicate motions over the past few years, and are thus easier to visualize than data indicating motions over much longer time periods. In particular, plate motions and motions within plate boundary zones are beautifully shown by space geodetic data, making the resulting structures and topography easier to understand. Similarly, GPS data clearly indicate the abstract-sounding idea of a plate rotating rigidly about an Euler pole. They also show the nature and extent of intraplate deformation, especially that due to postglacial rebound. The idea of earthquakes resulting from the seismic cycle - elastic rebound - is illustrated nicely by GPS data showing deformation accumulating that will be released in future earthquakes along the San Andreas, Cascadia, and other plate boundaries. Conversely, the lack of significant motion in the New Madrid seismic zone suggests that the recent series of large earthquakes is ending. Space geodesy is also useful in discussing volcanic dynamics and hazard mitigation.

Space geodetic data are useful in classes ranging to elementary to advanced. The velocity plots work for all levels, because they can be presented descriptively at an introductory level and more mathematically at a higher level. In addition to “what we are learning”, it is also useful to discuss “how we find out,” by describing the technology at various levels. In discussing the technology it is interesting to explain underlying concepts, such as the similarity between GPS positioning and earthquake location, the resulting need for precise clocks, and the use of interferometry. For example, it is fun to explain how interferometric methods like those used to study plate motions, earthquakes, and volcanos are used in seismic travel time studies and were used by Michelson and Morley more than 100 years ago to lay the foundations of the theory of relativity.

Using space geodetic data in teaching faces several challenges. One is to strike the balance - which depends on the class level - between presenting the results as magic and presenting too much detail. Another is to move beyond “gee-wiz” via problems appropriate for the class. The last - but most satisfying - is picking examples that are appropriate for the classes` specific goals from the steady stream of new results that are becoming available, often on the WWW. Fortunately, it is hard to go wrong!

HELIUM ISOTOPE MEASUREMENTS ON MATRIX FLUIDS FROM THE SAFOD DRILLCORE

Martin Stute, Gisela Winckler, Peter Schlosser · Lamont-Doherty Earth Observatory, Columbia University
Thomas Torgersen · University of Connecticut

Helium isotope ratios have been measured on matrix fluids from the SAFOD main hole at ~3060, 3432, and 3990m measured depth in September 2004, July 2005, and August 2005, respectively. The first set of samples is located on the American Plate, the second very close to the fault, and the third on the Pacific Plate. Samples were collected as 2.54cm diameter subcores drilled into the ends if the core barrels, or from the core catcher and drillcore fragments within <2hr after core recovery. The samples were placed into ultra high vacuum stainless steel containers, flushed with ultra high purity nitrogen and immediately evacuated. Since sample collection began in September 2004, noble gas concentrations have been measured between 2 and 5 times. When stored at room temperature, is appears that it can take up to 2 years until most of the gas (>99%) has been released. Samples collected more recently (2005, 3990m depth) were stored at 120C to speed up the release, but an additional measurement is needed to determine the rate.

Helium isotope ratios expressed relative to air are remarkably consistent, R/Ra = 0.37±0.01(n=4, 1 standard deviation), 0.71±0.02(n=2), 0.96±0.01 (n=6) for the samples from 3060m, 3432m, and 3990m, respectively. There is no indication of contamination by atmospheric Helium, except for the 4th or 5th measurement of the same sample, when He concentrations approach the detection limit of the instrument. The exact origin of the two samples from 3432m is uncertain, because they consisted of small fragments that might stem from a shallower depth. The isotope ratios indicate mantle He components of up to ~10%. The isotope ratio at 3060 (R/Ra=0.37) is consistent with those measured on fluid samples collected in the open hole at the same depth (R/Ra=0.33 to 0.36, Kennedy et al.). Measured isotope ratios are also consistent with data obtained from gases extracted from drilling mud at the surface (Wiersberg et al., 2006).

4He concentrations are still preliminary, However, for the samples from 3060m depth, the ratio of the total recovered 4He to water ranges from 3.6-7.8x10-5 ccSTP4He/gwater (n=4), again consistent with the water sample collected in the open hole (4-6x10-5 ccSTP4He/gwater, Kennedy et al.). The consistency among matrix fluid samples collected at the same location and the comparison with open hole fluids suggest that matrix fluids collected from core material are representative of fracture-filling fluids and represent a viable means for fluid collection when flow tests are restricted by limited permeability and/or drilling schedules.

Our preliminary results show promise for constraining the long-term dynamics of fluids in the San Andreas Fault, but further study is necessary.

MAPPING THE PV-PPV BOUNDARY BENEATH CENTRAL AMERICA

Daoyuan Sun, Don Helmberger · California Institute of Technology

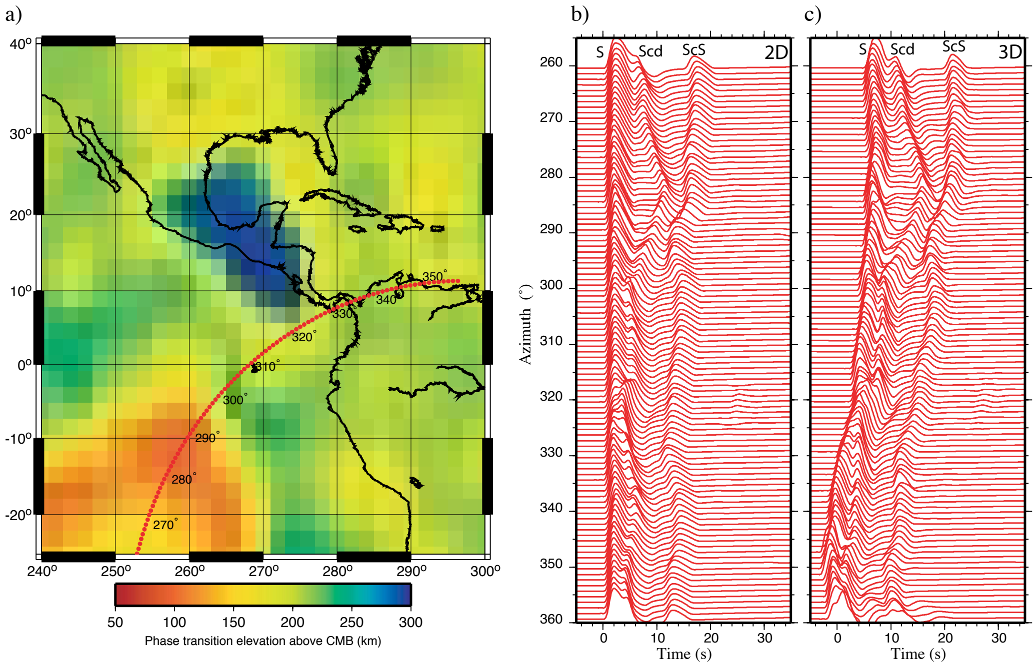

A lower mantle S-wave triplication with a Scd branch occurring between S amd ScS appears to be explained by a recently discovered Perovskite (PV) to Post-Perovskite (PPV) phase-change. It is predicted to have a positive Clapeyron slope ( ) between 5 to 13 MPa/K with a small S-velocity jump (1.5 to 4%) and an even smaller 1 to 2% jump in P-velocity. Seismic observations indicate that Scd arrives earlier and stronger beneath fast regions (circum-Pacific) than slow regions (super plumes) indicating a positive . However, it proves difficult to separate effects produced by downwelling (slab debris) from upwelling (plumes) in refining the actual physical properties. Here we model dense record sections collected from USArray and existing PASSCAL data to isolate effects produced by lower mantle structure as evidenced by P and S tomographic models, to better define the seismic phase-change properties beneath Central America. We find that the PV-PPV velocity jump is twice as strong beneath slow regions as fast regions requiring distinct reference heights indicative of changing chemistry. Moreover, the edges of the supposed buckled slabs deliminated by both P and S-waves display very rapid changes in phase-boundary heights producing Scd multipathing. These features can explain the unstable nature of this phase with easy detection to no detection commonly observed. The fine structure at the base of the mantle beneath these edges contains particularly strong reflections indicative of local ultralow velocity zones, which is predicted by some dynamic models.

ASSESSING SEISMIC SLIP FRACTIONS AT SUBDUCTION ZONES

Laura Swafford, Seth Stein · Northwestern University

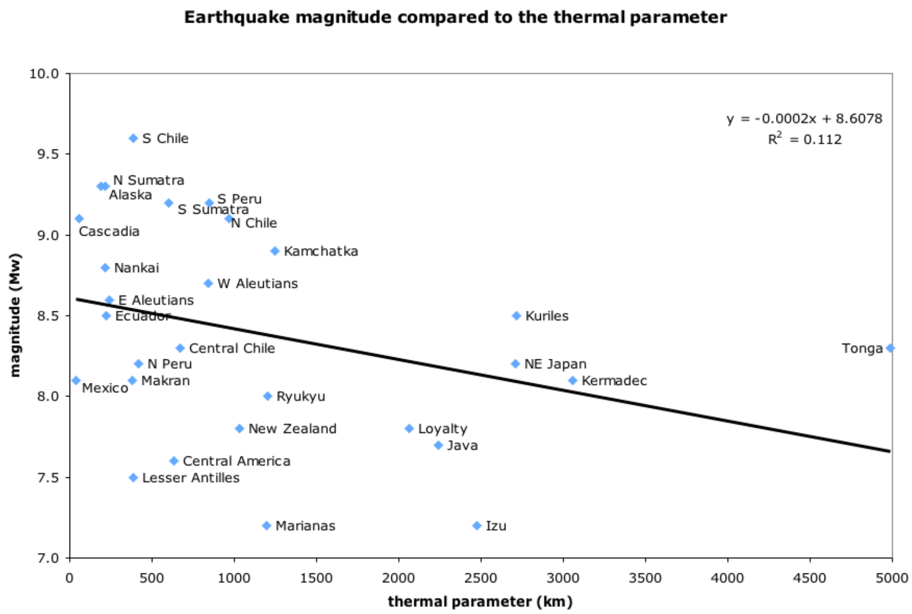

The graph compares the earthquake magnitude of great interplate thrust earthquakes to the thermal parameter, which is the product of the vertical descent rate and the lithospheric age. Each data point is labeled with the subduction zone arc that it occurred in. There is no correlation between the magnitude and thermal parameter, which may be at least partly caused by the off set between young lithosphere subducting quickly and old lithosphere subducting slowly.

A key goal of the Plate Boundary Observatory is to advance understanding of how great trench earthquakes are generated at convergent plate boundaries. An important new insight, which has emerged from studies following the great 2004 Sumatra earthquake, is the consequences of variability in rupture mode at trench segments. It is increasingly clear that sometimes a large region slips in large earthquakes, whereas in other intervals slip divides into smaller events. Such combinations of multi-segment and single-segment rupture appear to be the reason why previously accepted differences between subduction zones, such as some trench segments but not others being prone to great earthquakes due to convergence rate and age, now appear to fail. This variability poses a major challenge in assessing what fraction of the convergent plate motion is released seismically in large earthquakes. Assessing this seismic slip fraction has long been challenging because all possible approaches have limitations. GPS data show the fraction of locked slip at present, but this may not represent the long term average. The instrumental seismic record can be used to predict the recurrence of large earthquakes from the rate of smaller ones, but this estimate may be biased if large earthquakes are characteristic or uncharacteristic - more or less frequent than predicted by the rate of smaller ones. Additional data is provided by historic seismic records. To understand how different data types can be compared and combined, we are comparing seismic slip fractions predicted in different ways. We focus on the North America-Pacific (Alaska and Aleutians) and North America-Juan de Fuca (Cascadia) convergent boundaries, with complementary data from others.

DETECTING SEISMOGENIC STRESS EVOLUTION AND CONSTRAINING FAULT-ZONE RHEOLOGY IN SAN ANDREAS FAULT, FOLLOWING THE 2004 PARKFIELD EARTHQUAKE

Taka'aki Taira · University of Utah
Paul Silver · Carnegie Institution of Washington
Fenglin Niu · Rice University
Robert Nadeau · University of California, Berkeley, Berkeley Seismological Laboratory

We investigate temporal changes in seismic scatterer properties at seismogenic depth attributed to the 2004 M 6 Parkfield earthquake, making use of the SAFOD repeating-earthquake target sequences, as well as nearby similar-earthquake aftershock clusters. We use a two-step process: (i) observing temporal variations in the decorrelation index reflecting changes in the scattered wavefield of repeating-earthquake sequences and (ii) estimating the spatial distribution of these time-dependent scatterers by using a larger-aperture similar-earthquake source array. We focus on three scattered phases (X1, X2, and X3) exhibiting clear time dependence, using pairs of earthquakes that span or follow the 2004 Parkfield earthquake. For these scattered phases, the temporal variation is confined to a time interval from the occurrence of the mainshock to 4 months after. The locations of these scatterers are found to be on the fault and beneath Middle Mountain with a depth range of 11 km to 17 km (Figure 1). The shallowest and most prominent scatterer is located near a region of predicted increased Coulomb stress as well as significant post-seismic slip following the 2004 Parkfield earthquake, and a large M=5 aftershock. The other two deeper ones are also in regions of increased Coulomb stress. We show that the square root of decorrelation index is expected to be proportional to the level of stress in the fault zone. Under this interpretation it is possible to constrain fault-zone rheology by comparing the time dependence of the decorrelation index with geodetic or seismic measures of strain rate, assuming a power-law rheology between stress and strain rate characterized by exponent n. Such a comparison yields n = 2.65 with the standard deviation of 0.25 (Figure 2). This value is more consistent with ductile behavior, rather than frictional sliding, at the bottom of the seismogenic zone.

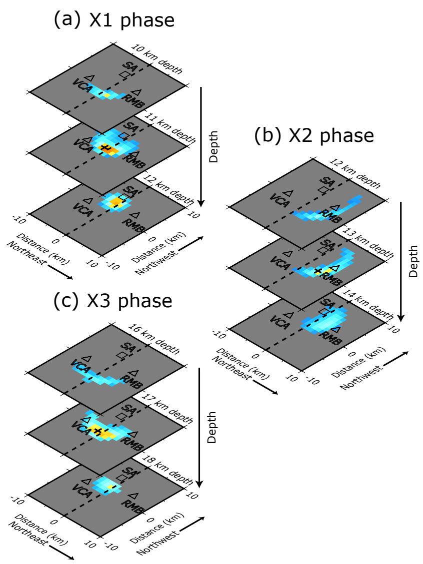

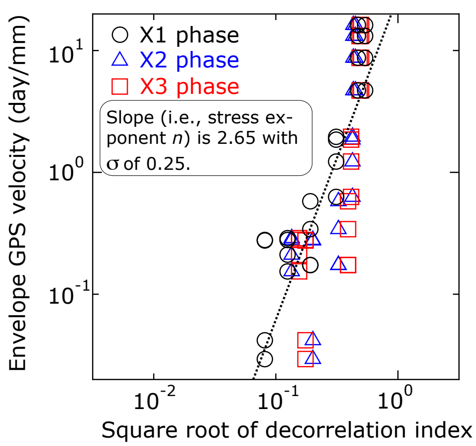

Figure 1: Depth slices of the 95 per cent confidence regions (shown by colored region) for the location probability density determined by combining semblance values and travel times of scattered phases. Warm colors indicate high probability density values. Crosses are maximum points of the location probability density. Each 95 per cent confidence region extends approximately 2 km from its maximum point in vertical. Dashed lines are the projected surface trace of San Andreas Fault. The coordinate center is the 1966 Parkfield earthquake near Middle Mountain. Squares and triangles denote the source array and borehole stations used to locate time-dependent scatterers.

Figure 2: Comparison of the square root of decorrelation index with surface strain rate inferred from GPS velocities. We used two horizontal GPS velocities observed at stations POMM and PKDB, which are close to the locations of time-dependent scatterers.

PRELIMINARY GEOMORPHIC AND STRUCTURAL OBSERVATIONS ALONG THE CENTRAL SEGMENT OF THE GARLOCK FAULT; WHY DOES THE GARLOCK DEFY SLIP RATE PREDICTIONS?

Michael Taylor, J. Douglas Walker, Zachary Casey, Eugene Szymanski, Justin Fairchild, Bethia Hall, Jacqueline Grunau, William Scriven, David Lobue · University of Kansas

We present new geomorphic mapping and structural observations conducted along the central segment of the ENE striking left-slip Garlock fault, where fault motion is currently dominated by fault parallel strike-slip displacement. The varied tectonic history for the Garlock implies that its slip rate likely spans a significant range temporally, and suggests that the Garlock is a good example for studying transient loading processes. The ENE striking left-slip Garlock fault initiated as an intracontinental transform fault separating the extending Basin and Range, and Death Valley regions from the more stable Mojave block. The Garlock fault remained active during later NW-SE directed dextral transtensional deformation connecting the developing plate margin in the Gulf of California in the south, with the Walker Lane belt to the north. Such a complex tectonic history implies that the fault slip rate history should vary, and should attain a maximum rate during Basin and Range extension (ca. 15 to 10 Ma). The fault slip rate during the last 10 Ma should be lower, but currently the Garlock can defy precise predictions, because of the uncertainties on how and when changes in tectonic styles occurred.

BUILDING A CONTINENT: THE SCIENTIFIC MOTIVATION BEHIND A COAST-TO COAST GEOSWATH *(Speaker)*

Basil Tikoff · University of Wisconsin, Madison

GeoSwath is a new geologic initiative that focuses on the construction, stabilization and modification of the North American continent (Building a Continent). One particular GeoSwath was chosen at a national workshop, which agreed on the intellectual merit, scientific necessity and nature and role of a coast-to-coast swath in EarthScope science. The GeoSwath was divided into seven focus regions across the conterminous U.S. and an eighth xenolith topic, which collectively constitute a seamless continent-scale geologic experiment. The initiative was conceived as way to achieve the promise of the EarthScope initiative as a transformative program for the Earth Sciences, integrating geological, geochronological, geochemical, and geophysical perspectives. To date, however, this integration has been elusive, because the geological disciplines that provide both the ground-truthing and the time component operate at spatial scales that are small relative to many seismic experiments. Yet, integration of the geological perspective is essential to the success of EarthScope science.

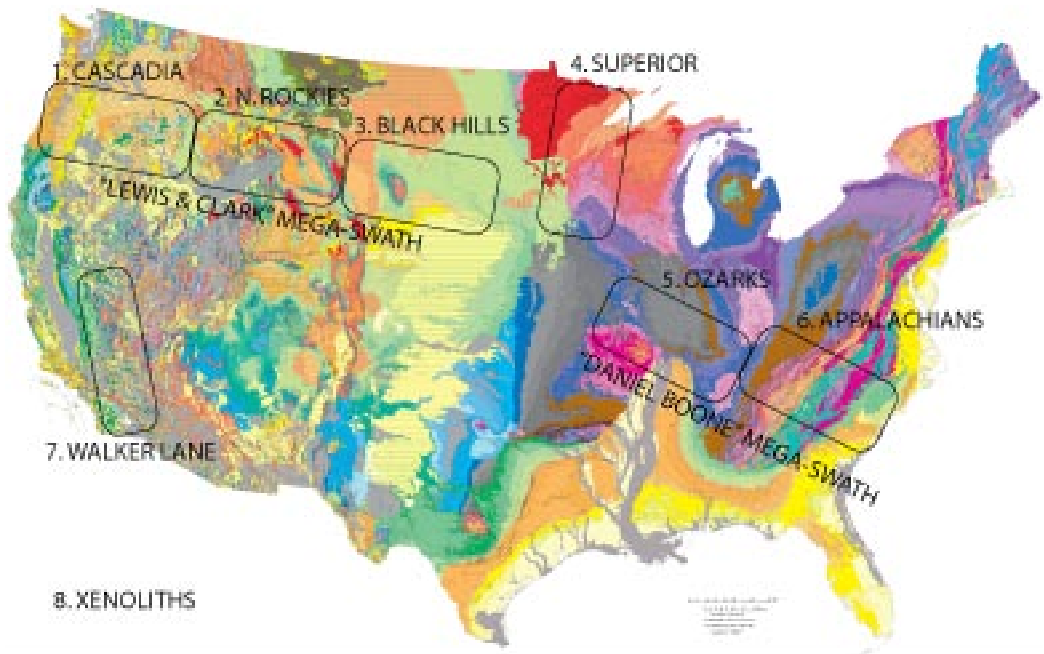

Geological map of the conterminous United States from King & Beikman (1974) and Schruben et al. (1994).

This talk will primarily address the scientific motivation and opportunities for the selected GeoSwath. Studies within each target area will best address fundamental geological questions about the assembly and evolution of the continental lithosphere through time. The specific areas are, from west to east: 1) Cascadia; 2) Northern Rockies; 3) Black Hills/Great Plains; 4) Superior; 5) Mid-continent; 6) Appalachian; and 7) Walker Lane. The areas represent all types of tectonic boundaries (collisional, transpressional, strike-slip, transtensional, extensional) at different times in Earth History (Archean, Proterozoic, Paleozoic, Mesozoic, active). The studies will allow us to investigate clearly articulated questions (e.g., How was the Archean tectosphere modified during mid-continent rift extension?), but also allow us to investigate questions about which the current paucity of data does not let us formulate specific predictions (e.g., What is the geodynamic role of the ~1.4 Ga felsic igneous event in the mid-continent?). Each area will allow integrated teams of geoscientists to focus on the fundamental tectonic processes related to the building of North America that are best studied within each target area, related to lithospheric and whole-earth plate tectonic processes.

Study of these regions should proceed in an intensified fashion, in concert with planned USArray steps (BigFoot array). Specifically, this stage of investigation would entail map-scale densified arrays of passive source seismic receivers (LittleFoot array), with associated active-source seismic studies and complementary geophysics in conjunction with geologic-based synthesis.

In conclusion, integration of the geological perspective in EarthScope has the potential to deliver on the promise of this initiative and chart the course for future integrative efforts and experiments in the Earth Sciences.

USARRAY DATA AND QUALITY CONTROL AT THE IRIS DMC

Chad Trabant, Mary Templeton, Gillian Sharer, Peggy Johnson · IRIS

The IRIS Data Management Center (DMC) is the primary access point for all raw USArray data and most of the low-level data products. Currently over 3 terabytes of USArray data is available and the volume is increasing with 4 gigabytes being archived daily and stations still being installed. These data are quickly becoming a significant and unique multi-scale dataset. The DMC also manages seismic data from the PBO and SAFOD components of EarthScope. All of the raw SEED format time-series data is managed with other SEED data at the DMC, and is therefore available via all DMC access methods, including real-time data feeds. In addition to functioning as the perpetual archive and access point, the DMC performs quality control on all USArray data as it arrives at the data center. This quality control effort is divided into two parts: automated and manual processing. Automated QC is applied to all USArray, PBO and SAFOD data arriving at the DMC in real-time using the QUACK software framework. All QUACK generated results are available through the IRIS DMC`s web site via a flexible query interface allowing customized requests. Analysts at the DMC review these automated QC results while also performing routine, manual review of all USArray data. The manual review of data is primarily performed using a modified version of PQLX, which itself is an extension of the PASSCAL "quick look" program. This review software integrates many time-series analysis and diagnostic methods including PSD/PDF creation. The current status of EarthScope data at the IRIS DMC, including station lists, maps and detailed information is available on the DMC`s website at http://www.iris.edu/earthscope/.

ASSESSMENT OF STATION PERFORMANCE: NOISE LEVELS AT BDSN, TA AND NC

Robert Uhrhammer, Margaret Hellweg, Barbara Romanowicz, Peter Lombard · University of California Berkeley

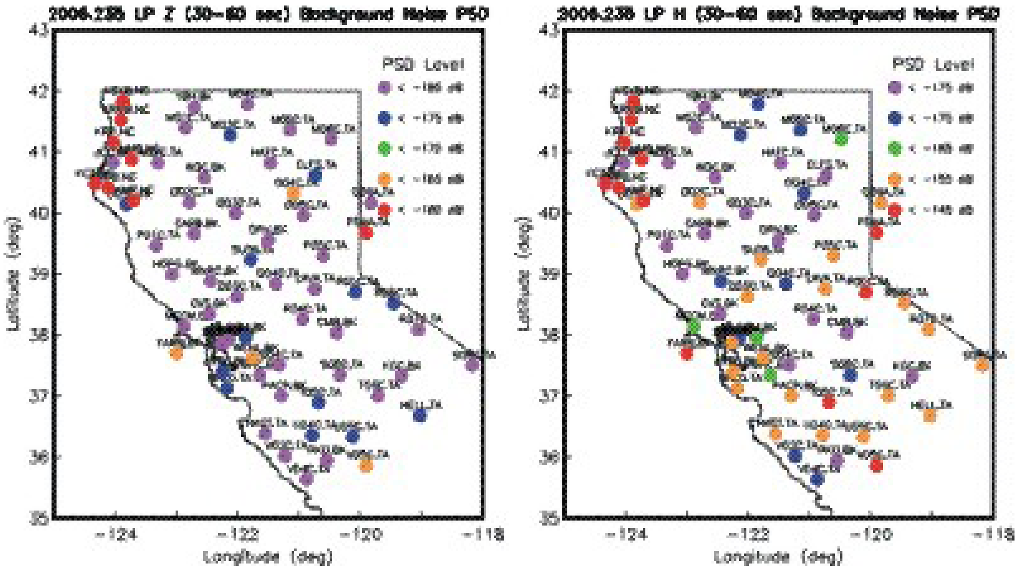

Figure 1: Station noise assessment for BK, NC and TA stations in northern California in the period band 30 - 60 s. Data were taken from day 2006.235. Horizontal components were assessed together.

We have been using data from USArray stations installed in Northern California, as they become available, in routine processing for earthquake monitoring. At the same time, we have been reviewing their performance to assess whether to keep them as the Berkeley Digital Seismic Network (BDSN) grows. Probability density functions (PDF) of power spectral densities (PSD) provide an exhaustive view of noise and signals on a given component of the network. They must be looked at individually, however, for each component. We have developed several tools to provide network-wide overviews of the noise characteristics of each station. The first tool is an automated weekly characterization of the seismic noise level recorded by each broadband seismometer through the estimation of the PSD of the ground motion. This provides an objective measure of background seismic noise characteristics over a wide range of frequencies. When used routinely, the PSD algorithm also provides an objective measure of seasonal and secular variation in the noise characteristics and aids in the early diagnoses of instrumental problems. The PSD estimation algorithm developed at the BSL for characterizing the background seismic noise generates a bargraph output which compares broadband stations by components over the course of the year. Station noise maps (see Figure 1) allow a comparison of noise in specific bands (30-60 s and 1 - 5 Hz) by station location. The PSD is estimated from the quietest part of the day, and for vertical and horizontal components separately. The overall noisiest stations at long periods (30 - 60 s) are the CREST stations along the northern California coast. These stations are equipped with low-sensitivity seismometers and are often situated on hilltops, as they are telemetry nodes. All other stations (BK, NC, TA) are relatively quiet at long periods for the vertical component, except FARB.BK, on the Farallon Islands, WENL.BK in the Wente Winery, O04C.TA and V05C.TA. For the horizontal components, noise levels are generally higher, except for the BK stations located far from the influences of civilization and in or on hard bedrock. We present other aspects of station noise in the poster.

SWELLING CLAYS AND SHALLOW FAULT BEHAVIOR: MICROSTRUCTURAL AND MICROCHEMICAL RESULTS FROM THE SAN ANDREAS FAULT OBSERVATORY AT DEPTH (SAFOD)

Ben van der Pluijm · Univ Michigan
Laurence Warr · CNRS-Strasbourg
Sara Tourscher · Univ Michigan
Anja Schleicher · Univ Michigan/Univ Wurzburg

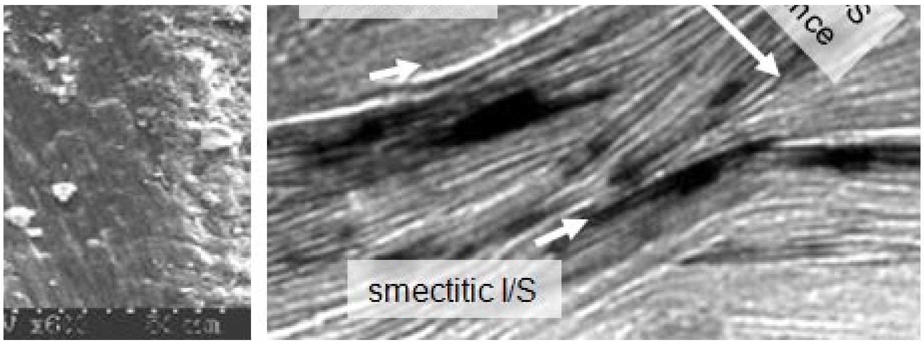

SEM and TEM images of smectitic slickenfibres in “Main Fault” samples (3436m) from SAFOD.

Swelling clays are common in shallow fault rocks, but their properties and the role these minerals play in influencing the mechanical and hydrological behavior of active fault systems is poorly understood and may, in fact, be underappreciated. Based on new mineralogical (XRD, TEM) and chemical (ICP-OES) analytical data, hydrated clays in faulted, clay-rich rock samples of SAFOD mudrocks were studied for their mineralogic characteristics, mass transfer, hydration behavior, and fabric and textural relationships. Several clay mineral phases are present in the matrix and on fracture surfaces at 3067 (“Shallow Fault”) and 3436 m (“Main Fault”) depths, which is a segment of recent creep and faulting. The samples contain detrital grains of chlorite and biotite, along with a range of authigenic illite, illite-smectite, chlorite, chlorite-smectite and smectite phases; the dominant authigenic clay minerals are illite and chlorite. The illite, 20-30 nm in thickness, is mainly of a 1Md polytype. The illite in the shallower part constitutes ~75% of the illite-smectite mixed-layer particles, with a long-range ordering ($R \geq 3$). The illite at greater depths shows less ordering and a higher proportion of smectite in the mixed-layer particles. These authigenic mineral phases were likely formed during the movement of aqueous fluids along permeable fractures and veins by dissolution-precipitation reactions, and partly at the expense of larger (~150 nm thick), deformed detrital packets. Differential thermal analysis (DTA) and heat flow results from a whole rock mudstone indicate a loss of ~6% of total volatiles (~2% interlayer water, ~4% crystalline water), the latter would occur during the dehydroxylation of clays (at 400-600°C). Based on textural observations the timing of authigenic mineral growth in the matrix assemblages is mostly coeval with mineralization along polished fractures and grain boundaries that are common in these samples. Hand-plucked fracture grains are notably smectite-rich and show high element mobility and mass transfer, indicating circulation of low temperature fluids of varying composition and extensive dissolution of detrital components. The alignment and widespread occurrence of these coating along microscopic displacement surfaces indicate a direct relationship between slip and mineral formation. The physical properties of these coatings, therefore, will significantly affect the fault behavior at these shallow depths.

Our current observations permit the following conclusions:

- Neomineralized smectite in matrix and especially on fracture and grain surfaces is present in all fault rocks, while most common in the Main Fault segment. These microstructures may be representative of fault creep and support a lower shear strength.
- Dissolution and precipitation reflect high fluid flow and element mobility in both faults.
- High interlayer water (2-3WL) in smectite is characteristic of fracture and grain surfaces of both Shallow and Main Fault rocks, which further supports a low frictional strength.
- Displacement surfaces and veins with 2-3WL smectite are more common in the Main Fault, where the target earthquakes occur, than in the Shallow Fault; this likely reflects greater deformation in Main Fault rocks.

ERUPTION DYNAMICS AT MOUNT ST. HELENS IMAGED FROM INVERSION OF BROADBAND SEISMIC WAVEFORMS: INTERACTION OF THE SHALLOW MAGMATIC AND HYDROTHERMAL SYSTEMS

G P Waite, B A Chouet, P B Dawson · U.S. Geological Survey

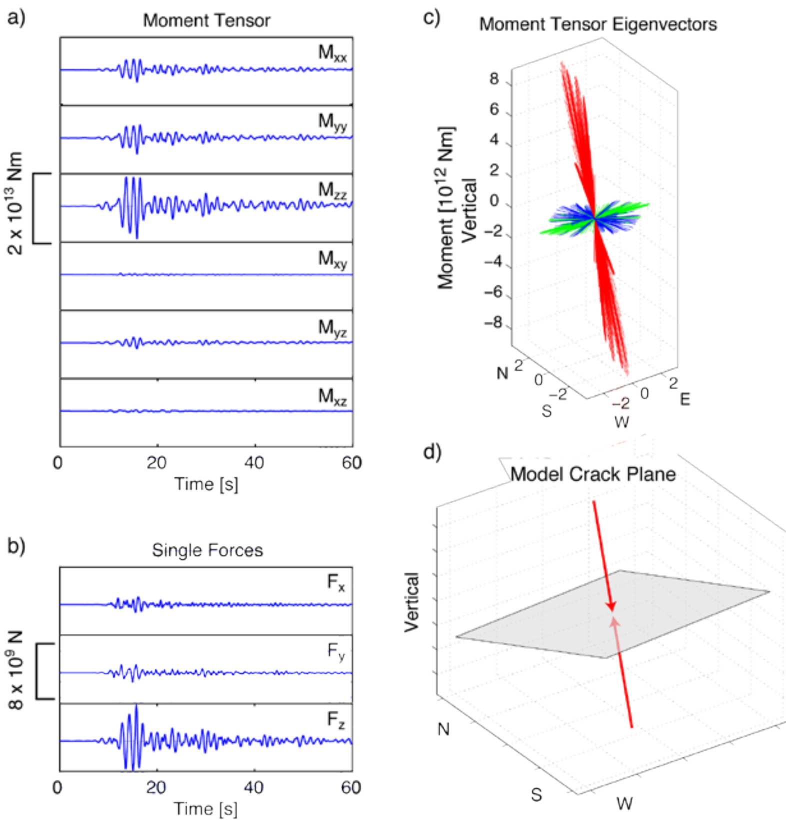

Summary of the LP source model. On the left are the source time functions of the (a) moment tensor components and (b) single forces for an LP earthquake recorded during July 2005. The moment tensor is dominantly volumetric, and the single forces are dominated by a large vertical force. The ratios of the moment tensor eigenvalues are approximately 3:1:1, values consistent with a steam-filled crack. The eigenvectors (plotted in c: red, blue and green are the eigenvectors corresponding with the maximum, intermediate, and minimum eigenvalues, respectively) give the orientation of such a crack, shown conceptually as a plane dipping NNW (d). Given a rigidity μ=20 GPa, we can estimate maximum ΔV for the resonating crack from the eigenvalues as 300 m3. Assuming a crack width and length of 120 m, the maximum crack expansion (or dilation) is 2 cm.

The current eruption at Mount St. Helens is characterized by dome building and by small, shallow, repetitive, long-period (LP) earthquakes that have been termed "drumbeats". Waveform cross-correlation reveals remarkable similarity for a majority of the LP events over periods of several weeks. Stacked spectra of these events display multiple peaks between 0.5 and 2 Hz that are common to most stations. The similarity of waveforms from different LP events reflects the repetitive action of a non-destructive source. Very-long-period (VLP) events commonly accompany the LP events, but are too weak to be detected clearly by more than the two closest stations. We model the source mechanisms of LP and VLP events in the 0.25 - 2 Hz and 0.025 - 0.125 Hz bands, respectively, using data recorded in July 2005 with a temporary broadband network. The source mechanism of the LP events includes both a volumetric and a vertical single-force component. The volumetric component points to the resonance of a steam-filled crack that dips gently NNW and is located directly beneath the active part of the new dome, within 100 m of the post-1980 eruption crater floor. Because dilatational first motions were observed on all of the stations, this resonance must initiate as the collapse of the crack, which is consistent with gas venting. The single-force is attributed to the vertical movement of the overlying dome. The VLP source, which also includes volumetric and single-force components, is 100-200 m deeper than and located NNW of the LP source, at the SW edge of the 1980-1986 lava dome. The volumetric component points to the compression and expansion of a shallow, magma-filled sill, which is subparallel to the hydrothermal crack imaged at the LP source, coupled with a smaller component of expansion and compression of a dike. The VLP single-force components reflect mass advection within the sill-dike system. The location, geometry and timing of the inferred crack sources for the VLP and LP events suggest they are caused by perturbations of a crack system which links the magmatic conduit and shallow water-saturated region of the volcano.

ALMOST THERE: STATUS OF THE SOUTHERN CALIFORNIA REGION OF THE PLATE BOUNDARY OBSERVATORY

Christian Walls, Edward Arnitz, Shawn Lawrence, Scott Bick, Ryan Bierma, Karl Feaux, Mike Jackson · UNAVCO

Of the 852 total PBO GPS stations, 207 proposed sites are distributed throughout the Southern California region. Currently the production status is: 140 stations built (57 short braced monuments, 83 deep drilled braced monuments), 157 permits signed, 203 permits submitted and 207 station reconnaissance reports. Production goals to date are on schedule and slightly under budget. The balance of 67 stations (37 short braced monuments and 30 deep drilled braced monuments) will be built over the next 1.5 years from Long Valley to the Mexico border in order of priority as recommended by the PBO Transform, Extension and Magmatic working groups.

Throughout the reconnaissance phase the PBO Southern California region has used GIS databases, stereo aerial photography, updated fault maps, shaded relief imagery, peer reviewed publications, InSAR imagery and unpublished propriety data to locate the most geologically stable sites that meet the target science goals. Permit turnaround times have ranged from 1 day with private landowners to well over a year with federal agencies. Approximately half of the "high risk" sites on federal property have been permitted with the balance of permits expected to be secured in 2007. The timeline for construction of sites has ranged from 6 hours in ideal conditions to 5 days due to extensive site modification, equipment failure or at remote long carry-in locations.

In the past 3.5 years the PBO Southern California region conducted responses to three earthquakes; the M6.5 San Simeon earthquake, the M6.0 Parkfield earthquake, and the M5.6 Anza earthquake. For each event, PBO began a response within hours and developed reconnaissance, prioritization, relocation, and deployment plans at the request of the PBO Transform Site Selection Working Group. The San Simeon event initiated the beginning of the PBO GPS station construction phase when 5 stations (P295, P526, P067, P576, P278) were located, permitted, and built within 38 days of the earthquake. For the September 28th, 2004, Parkfield earthquake, the PBO Transform Site Selection Working Group elevated the priority of two planned GPS stations (P539 and P532) sited to the south of the earthquake epicenter. Reconnaissance for five sites in Parkfield began the day following the earthquake and two permits were secured within three days of the earthquake. Materials and equipment for construction were brought along with the response team and within 4 days the first monument (P539) was installed. Following the June 12 M5.6 Anza earthquake, the first station (P484) was located, permitted, and built within 4 days and the second station (P479) within 12 days. The Plate Boundary Observatory remains ready for the rapid deployment of permanent GPS units following large earthquakes to capture postseismic transients and any long-term viscoelastic-response.

THE CENTRAL UNITED STATES SEISMIC OBSERVATORY

Zhenming Wang, Edward Woolery · University of Kentucky

Drilling a deep borehole into bedrock is completed in the New Madrid Seismic Zone. The final depth of the completed hole is 1,950 ft (595 m). The depth to bedrock (hard) is 1,920 ft (585 m). The suspension, E-logs, and deviation log were successfully performed for the hole. This is the first phase of the Central United States Seismic Observatory (CUSSO) led by the University of Kentucky through a partnership of federal, state, and private organizations. CUSSO will be one of three existing “deep” vertical accelerometer observatories on earth, and the only one to exist in a seismically active intraplate setting. CUSSO will be used to evaluate the soil transfer function of the unlithified post-Paleozoic sediments at a site near the center of the New Madrid Seismic Zone. In addition to constraining existing and future site response models in the region, CUSSO will serve as a calibration site for regional seismic and strong-motion stations in the New Madrid Seismic Zone. The thick Mississippi embayment soil/sediment deposits are expected to produce significant influence on seismic wave propagation. Recordings from the existing University of Kentucky vertical strong-motion arrays indicate substantial influence of soil/sediment deposits on seismic waves. Significant technical contributions to earthquake seismology and engineering include: 1) the effect of deep soil conditions on seismic waves and strong ground motions, 2) dynamic soil properties in the New Madrid Seismic Zone, 3) evaluation of current analytical models for deep soil sites, 4) lateral propagation effects and spatial variation in seismic waves and ground motions.

AIR-GUN AS AN ONSHORE SEISMIC SOURCE?

Baoshan Wang · Institute of Geophysics, China Earthquake Administration
Huawei Zhou · Geosciences Department, University of Houston
Hongkui Ge, Yong Chen · Institute of Geophysics, China Earthquake Administration

Air-gun as a highly repeatable and easily controllable seismic source has long been used for offshore seismic surveys, but rarely used onshore. Several important questions exist about the possibility of using air-gun as an onshore seismic source in lakes, such as the effects of air-gun explosion on dams and on the fresh water fish. To shade some light on these questions, we conducted an air-gun experiment in a reservoir, which is located NE of Beijing, China, where a densely distributed permanent seismic network is available.

The source of our experiment was composed of 4 air-guns, each with volume 1500 cubic inches. The air-guns were hung on a 4x6-meter metal frame. The air-gun array is submerged 9 meters into the water, where the water depth is 18 meters. To find out the effect of air-gun on the dam of the reservoir, the array source was fired in two different positions, about 80 and 1500 meters away from the dam, respectively. The experiment was repeated for 4 days, and on each day the air-gun was fired at night continuously in the second position with interval about 2 minutes from 23:00 to 04:00 of the next day. Totally about 500 shots were fired throughout the experiment, the shot times were recorded with a precision higher than ms.

In addition to the densely distributed permanent seismic stations, a 180-km-long profile of 103 portable short period seismometers was deployed northwards from the experimental site.

The energy released by one excitation is estimated to be 6.68 x 10^6 J, which roughly corresponds to a 3 kg TNT explosion. The acceleration of the dam was measured when the air-gun was fired. When the air-gun is fired 80 meters away from the dam, the maximum acceleration of the dam is about 17 gal, which is far less than the shock strength of the dam. And when the source is 1.5 km away from the dam, the vibration is within the ambient noise level.

The seismic signal of single excitation can be detected by portable stations with offset around 100 km. And after massive stacking, clear waveform can be identified for all portable stations and permanent stations within 220 km as well. And signal to noise ratio recorded by remote stations is equivalent to the wave excited by a 1000-kg dynamite explosion. Clearly, air-gun can be used as a onshore seismic source to illuminate the under ground structure of an area as large as 100,000 km^2.

S-WAVE VELOCITY STRUCTURE OF THE HIGH LAVA PLAINS, OREGON, FROM RAYLEIGH-WAVE DISPERSION INVERSION

Linda Warren · University of Arizona
David James · Carnegie Institution of Washington
Arthur Snoke · Virginia Tech

The High Lava Plains (HLP) “hotspot” track is a prominent volcanic lineament that trends SE-NW from the southeast corner of Oregon in the northern Great Basin to Newberry volcano in the eastern Cascades. The HLP volcanism is a rough mirror image both temporally and geographically of the Snake River Plain (SRP) - Yellowstone track to the east. Unlike the SRP, however, HLP volcanism remains an enigma, apparently unrelated to motion of the North American plate. Moreover, many of the tectonic or physiographic features that characterize the SRP volcanic province are not mimicked in HLP terrane. While the recently initiated HLP Seismic Experiment will ultimately consist of a dense array of about 170 broadband stations for high-resolution imaging of the mantle beneath the HLP and adjacent terranes, the preliminary analysis reported here is based on a relatively sparse array (the 16 stations of the current HLP deployment, as well as nearby stations from USArray, the USNSN, and the Berkeley network), and is intended to highlight regional contrasts in uppermost mantle structure. We image the upper-mantle velocity structure beneath the High Lava Plains and adjacent tectonic provinces by analyzing fundamental-mode Rayleigh-wave phase velocities regionalized along a series of two-station propagation paths for which both stations are in the study region. The resulting dispersion curves, which typically give robust results over the period range 16-128 seconds, cross the region along several different azimuths and allow relatively localized velocity anomalies to be isolated and quantified. Throughout the region, uppermost mantle velocities are low (~4.2 km/s). Directly beneath the HLP, the shear velocity decreases at about 50 km depth and remains below 4.1 km/s down to ~100 km depth, as shown in the figure of dispersion data (symbols) from 155 station pairs for six events following NW-SE-trending paths. The line in the left panel is produced by a linearized least-squares inversion using a modified Tectonic North America (TNA) starting model. As shown in the figure, such velocities are slow relative to TNA, suggesting high uppermost mantle temperatures and at least a small degree of partial melting.

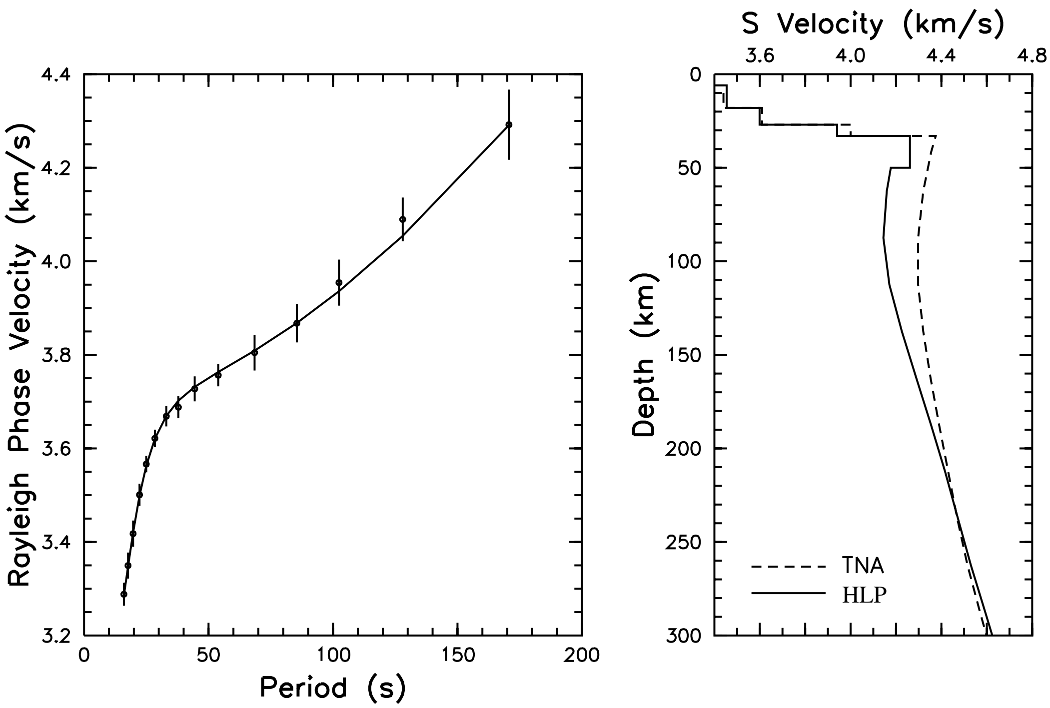

TREMOR

Aaron Wech, Kenneth Creager · University of Washington

Small-aperture Earthscope array data from the Olympic Peninsula region of the Cascadia subduction zone reveal uncharacteristic stability both in surface motion polarization and in the linearity of tremor signals. During the September 2005 episodic tremor and slip event, the tremor source was observed to migrate directly beneath the array, during which time, in the tremor frequency band (1—6 Hz), the measured ground motion became highly linear and dominantly horizontal, stabilizing to an azimuth of 57 degrees. This observed horizontal polarization of tremor energy beneath the array can be explained by S-wave polarizations produced by the relative plate motion of the subducting Juan de Fuca plate, suggesting that tremor is the direct result of fault slip along the plate boundary or a series of vertically stratified faults accommodating the slow slip over a range of depths.

SUPERSTITION HILLS FAULT CREEP EVENT ON OCT.3 2006

Meng Wei, David Sandwell · Scripps Instition of Oceanography

Following many years of surface slip at less than 1.5 mm/yr, the Superstition Hills fault slipped more than 27 mm in October 2006. No triggering mechanism has been proved and no related earthquakes were detected. The creep length is at least 11.64 km from field observation. InSAR and GPS data from PBO project has been processed to observe the surface deformation. We will analysis the data and understand the variations in creep along the fault but more important the displacement away from the fault can be used to estimate the depth extent of creep.

SHEAR-WAVE SPLITTING IN THE GREAT BASIN

John D. West, Matthew J. Fouch · Arizona State University

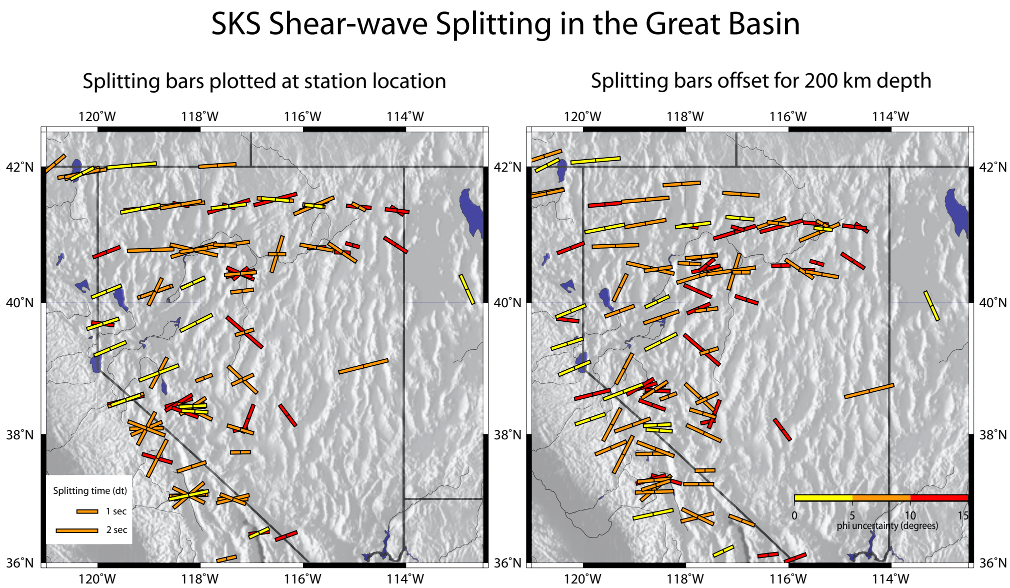

SKS shear-wave splitting results for the Great Basin. Bar length is proportional to splitting time, bar direction is along the fast splitting axis, and bars are color-coded to represent uncertainty in splitting direction. (Left panel) Splitting parameters centered on the recording station location. (Right panel) Splitting parameters plotted along each event backazimuth at a piercing depth of 200 km.

One of the goals of the EarthScope program is to investigate the processes and mechanisms responsible for continental tectonics. Within that framework, we are investigating the role that mantle forces play in widespread crustal extension in the Great Basin region of western North America. Shear-wave splitting analysis to measure seismic anisotropy is widely used to infer strain conditions and recent history in the upper mantle, and is an important method in our research. We are analyzing shear-wave splitting in SKS-phase seismic data from EarthScope/USArray stations in the Great Basin region of the western United States with the goal of better understanding the underlying forces and structure of the crust and upper mantle and the causes of extension in the region.

Across the region, we determined 106 well-constrained shear-wave splitting measurements. While there is considerable variance in fast-axis direction, our average fast-axis azimuth is 83 degrees indicative of the general east-west trend. Splitting intensities, as measured by the delay in time (dt) between the fast axis (radial) signal and the slower axis (transverse) signal, varied in our measurements between approximately 0.6 sec and 2.4 sec with an average of 1.5 seconds. In the northern portion of the Great Basin, fast polarization directions are predominantly east-west, with some less-well constrained results showing that splitting directions dip southward as we move east. Results from the central and southern Great Basin show a somewhat more complex pattern, although data is still sparse due to the fairly recent installation of USArray Transportable Array (TA) stations in the region. Most data from this area also show a general east-west trend, but are more widely variable than in the northern portion of the region.

The predominant east-west direction of fast splitting axis, especially in the northern portion of the Great Basin, agrees well with the direction of extension indicating that surface and upper mantle processes in the area may be linked. In the northeast portion of Nevada we see little evidence for the sharp rotation to the northwest-southeast that has been previously reported. Surface wave phase velocities from TA stations (Beghein et. al., this meeting) show a suggestion of approximately E-W azimuthal anisotropy at around 100 km depth, consistent with our results.

In the central portion of the Great Basin our data shows considerable complexity, with large variations in both fast direction and splitting time. Where the Great Basin transitions to the Sierra Nevada in the southwestern portion of the region, we observe backazimuthal dependence in fast directions. These results suggest complex upper mantle structure in this region, which will be further elucidated once USArray EarthScope stations in the region have recorded additional data.

HEAT FLOW MEASUREMENTS ACROSS THE SAN ANDREAS FAULT NEAR PARKFIELD, CALIFORNIA – PRELIMINARY RESULTS FROM SAFOD

Colin Williams, Frederick Grubb, S. Peter Galanis, Jr. · U.S. Geological Survey

We have acquired new temperature and thermal conductivity measurements from the San Andreas Fault Observatory at Depth (SAFOD), a scientific borehole that crosses the active trace of the San Andreas fault (SAF) at a depth of approximately 2700 m, in order investigate the variation in conductive heat flow in the vicinity of the fault. We have used these measurements to determine heat flow at a series of depths in the SAFOD borehole along its course across the SAF from approximately 1400 m west of the SAF to a point approximately 300 m east of the SAF. The heat flow values range from 85 to 98 mW m-2, with an average of approximately 90 mW m-2. This average is consistent with other measurements in the vicinity. Observed variations in heat flow in the SAFOD hole are not consistent with significant frictional heating on the fault and most likely reflect the combined effects of local thermal refraction and uncertainties in thermal conductivity measurements on cuttings from the heterogeneous sediments bounding the west side of the SAF. Thermal conductivity measurements on core that will be recovered in the summer of 2007 will reduce these uncertainties and clarify the true spatial variability of conductive heat flow. A modest reduction in the geothermal gradient is observed in a 200-m-wide zone corresponding to the active trace of the SAF. The available data indicate that this change in gradient may be a purely conductive feature reflecting a corresponding change in thermal conductivity, although further monitoring and more detailed thermal properties measurements are needed to rule out the possibility of transient cooling due to fluid flow. In the larger scale, the consistency of heat flow measurements across the transition from sub-hydrostatic pore pressure in the Salinian block west of the SAF to greater than hydrostatic pore pressure in the Franciscan block east of the SAF indicates that regional-scale fluid flow does not affect the conductive thermal regime beyond the resolution of the measurements.

LONG-BASE STRAINMETERS IN THE PBO: EARLY RESULTS

Frank Wyatt, Duncan Agnew · IGPP/Scripps/UCSD

The PBO included funding for five long-base laser strainmeters, three of which are now in operation. The first was at Durmid Hill (DHL2), very close to the southern termination of the San Andreas Fault; this instrument, 405 m long, was installed at right angles to an existing 524-m instrument (DHL1) that has operated at this site since 1994, under U.S. Geological Survey/NEHRP sponsorship. The next two instruments (SCS1 and SCS2) were also installed in the Salton Trough; they are more distant from the San Andreas fault (23 km rather than only 2 km at DHL), but much closer to the San Jacinto fault zone (17 km from the main trace, though there is significant seismicity within 10 km). The instrument pair at SCS is a NS instrument 490 m long and an EW instrument 405 m long. All these instruments are on the surface, but anchored to depths of 20 m using an optical-fiber anchor. Digital data are downloaded daily and provided in several forms through the PBO Strainmeter Data Center. The DHL2 instrument began operation on June 1, 2005, and the two SCS instruments on October 1, 2006, basically on schedule. These three instruments, like earlier versions, have given records of strain that cover the full range from seismic waves through tides and longer-period changes, including, at DHL2, secular strain accumulation (the SCS records are still too short to evaluate fully, but indicate low rates of strain). This is true even though the sites are not on ”hard” rock: DHL2 is on Pleistocene sediments, and SCS1 and SCS2 on a layer of Holocene lacustrine clay overlying Pleistocene sediments. The use of deep anchoring is crucial to getting these good results. The tides recorded on these sensors agree reasonably well with theoretical tides for the same locations, though with systematic differences that reflect the distortion of the strain field by geological inhomogeneities. All three instruments show a response to pressure that is larger than what we have seen on earlier installations, and whose source is not yet clear. These instruments have not yet detected any strain fluctuations, whether aseismic or coincident with local earthquake clusters. At this time a third pair of instruments is planned for the Cholame area, south of Parkfield, in a region that shows aseismic tremor. A site has been located and permitted, and we expect construction to begin in May 2007 and be completed one year later.

HIGH-RESOLUTION 3-D SHEAR VELOCITY MODEL OF THE CRUST AND UPPER MANTLE BENEATH W. US: SURFACE WAVE TOMOGRAPHY COMBINING AMBIENT SEISMIC NOISE AND TELESEISMIC DATAA:

Yingjie Yang · University of Colorado at Boulder
Donald Forsyth · Brown University
Michael Ritzwoller, Morgan Moschetti · University of Colorado at Boulder

Short-period surface wave dispersion measurements are extremely hard to obtain from teleseismic events due to scattering and attenuation. Ambient seismic noise is rich in short-period surface waves from which the Rayleigh wave Green function between pairs of stations can be extracted by cross-correlating long noise sequences. Tomography based on surface wave dispersion obtained from the estimated Green functions has been shown to produce high-resolution, short-period (6-30 s) surface wave dispersion maps that principally image crustal geological units (e.g., southern California: Shapiro et al., 2006; Europe: Yang et al., 2007).

In this study, we measure phase velocity dispersion curves from the ambient noise cross-correlations to obtain phase velocity maps at periods from 6 to 30 sec using data from the Transportable Array Component of USArray. A two-plane-wave tomography method including finite-frequency effects was employed to obtain phase velocity maps at complementary periods from 25 to 150 sec using teleseismic events. We compare phase velocity maps at overlapped periods from the two methods, and find phase velocities are similar for both methods. The combined phase velocity data set from 6 to 150 sec is used to invert for high-resolution 3-D Vs structure from the surface to ~200 km depth beneath the western USA. The new 3-D Vs model can be used to interpret regional tectonics, model seismic wave propagation, and improve earthquake location.

TESTING THE FIVE SIMPLEST UPPER MANTLE ANISOTROPIC VELOCITY PARAMETERIZATIONS USING TELESEISMIC S AND SKS DATA FROM THE BILLINGS, MONTANA PASSCAL ARRAY

Huaiyu Yuan, Ken Dueker, Derek Schutt · Univ. of Wyoming

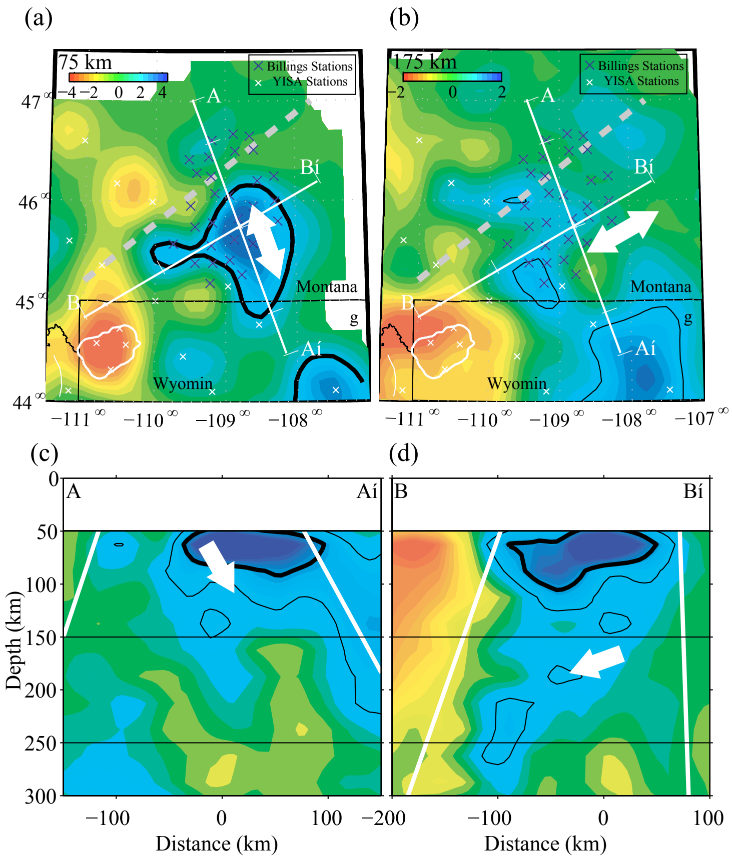

Figure 1. Correlation of our best model P5 and P-wave tomographic results of Yuan and Dueker [2005]. (a) Map views at the 75 km. The percent P-wave velocity perturbation is color-coded. The thick black lines contour the 2% velocity perturbation. The white contour denotes the Yellowstone Caldera. Gray dash line approximates the location of the Madison Mylonite zone. Thick blacks contours the 2% velocity purturbation. The two-head white arrow shows the strike of the FVA in the top layer. Two profiles shown in (c) and (d) are labeled as A-Aí and B-Bí. (b) Map view at 175 km. Thin blacks contours the 1% velocity perturbation. (c) Profile view along A-Aí. The white arrow shows the FVA dip in the top layer. Two thick white straight lines show approximately the extent of the SKS and S ray paths. (d) Profile view along B-Bí. The white arrow shows the FVA dip in the bottom layer.

The five simplest parameterizations of upper mantle anisotropy are tested and ranked by the F-test to determine model significance. These five hexagonal symmetry anisotropy models are: a single layer with a horizontal fast velocity axis (FVA), a single layer with a dipping FVA, two layers with a horizontal FVA, two layers with one dipping and one flat FVA, and two layers with dipping FVA. These five velocity models are fit to data from a 30 broad-band station array that operated around Billings, Montana for ten months. This array recorded fifteen high quality direct S and SKS arrivals whose recordings across the array are stacked to provide accurate waveforms and error estimates to model. Source normalization is accomplished using the cross-convolution technique. The stack traces are fit to the five anisotropic model parameterizations using the Neighborhood Algorithm to map the posteriori model probability density (PPD) volume. The F-test shows that the two models which do not permit a dipping FVA can be rejected at >91% confidence. The best model is a two layer dipping FVA parameterization, albeit the two layer model with one flat and one dipping FVA can only be rejected at 68% confidence. The 2-D marginal PPD for most of our models are compact and show little model parameter correlation. The best model (Figure 1) has an upper layer with a N13°W FVA strike and a 47° FVA dip and a lower layer with a N65°E FVA strike and a 12° dip down to the southwest. The N13°W FVA strike of the upper (lithospheric) layer is broadly consistent with the FVA strike found by several other studies [Currie, et al., 2004 ; Fox and Sheehan, 2005; Marone and Romanowicz, 2006], and is readily interpreted as fossil fabric in the lithosphere. The bottom (asthenospheric) layer FVA strike is parallel to North American absolute plate motion and the dip is opposite of that predicted for a quiescent asthenosphere [Bokelmann, 2002]. Comparison of the PPD modeling of a SKS-only dataset with respect to the full-dataset PPD shows that the direct S waves improve resolution of the anisotropic model parameters.

A MECHANICAL MODEL OF THE LARGE-DEFORMATION 2005 SIERRA NEGRA VOLCANO ERUPTION DERIVED FROM INSAR MEASUREMENTS

Sang-Ho Yun, Paul Segall, Howard Zebker · Stanford University

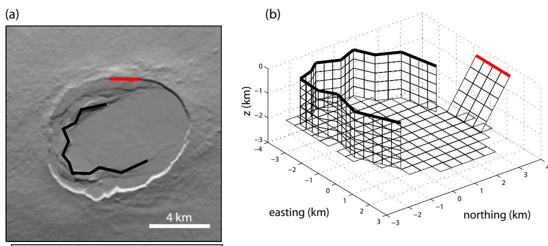

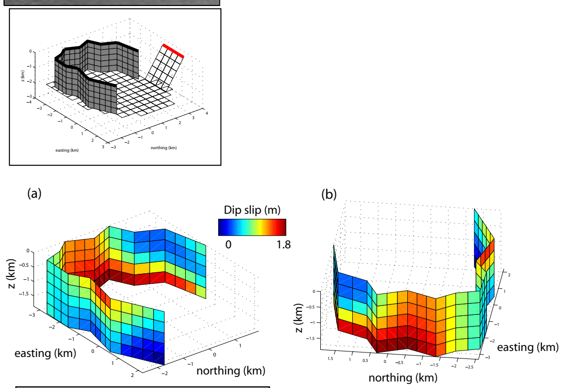

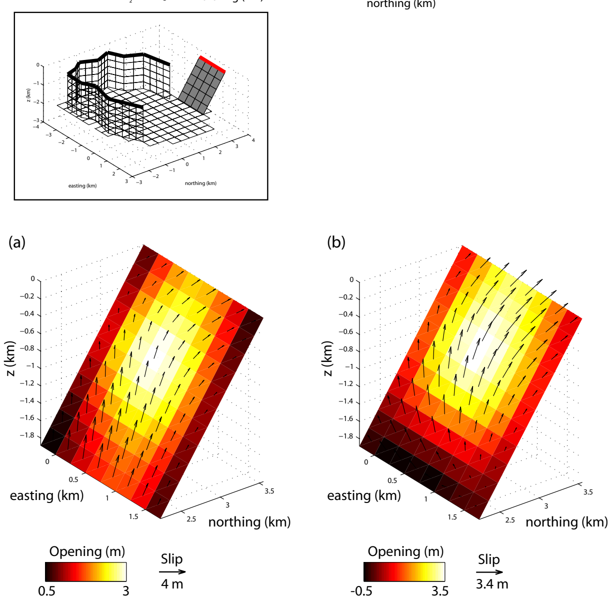

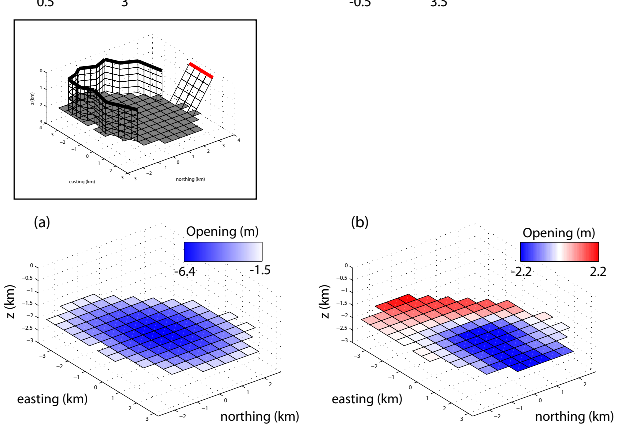

Sierra Negra volcano erupted from October 22 to October 30 in 2005. During the 9 days of the eruption, the center of Sierra Negra's caldera subsided about 5.4 meters. Three hours prior to the onset of the eruption, an earthquake (Mw 5.4) occurred, somewhere near the caldera. We analyze here a pair of interferometric synthetic aperture radar (InSAR) images from ascending and descending orbits of Envisat satelite that temporally span the eruption. The interferograms plus the azimuth offset image from the ascending pair are used to model the euption. The data display several different events overlapped in time and space; pre-eruptive deformation, trapdoor faulting, dike intrusion and eruption, co-eruptive subsidence, and post-eruptive uplift. The pre- and post-eruptive uplift is modeled using the InSAR data plus GPS observations. The faulting, dike intrusion, and subsidence are modeled using a mixture of kinematic and uniform pressure boundary conditions. We estimate that the pre- and post-eruptive pressurization rate of a sill-like magma body are 29 MPa/year (23 days average) and 79 MPa/year (21 days average) respectively. The seismic moment of the trapdoor faulting is $4.35 times 10^{24}$ dyne-cm, equivalent to Mw 5.7. This suggests that a substatial amount of slip must have happened aseismically. The co-eruptive uniform depressurization of the sill-like magma body was about -33 MPa, and the average thickness of the dike opening was about 2 m. We find significant interaction between the trapdoor faulting and the sill; When the faulting occurred, the sill underwent a sudden stress perturbation, which caused an uneven opening and closing of the sill accompanied by horizontal magma transport. This effect combined with the co-eruptive uniform depressurization provides an opening/closing map with about -8.8 m of maximum sill closing. The total volume decrease at sill was 0.13 km^3, which roughly matches the erupted volume.

Figure 1. Sierra Negra Volcano and model space. (a) Map view of the surface constraint, where eruption fissure is indicated with a red line and the the fault trace on the surface, drawn in black, goes along the C-shaped sinuous ridge. (b) 3-D perspective view of the model geometry, where fault (Figure 2), dike (Figure 3), and sill (Figure 4) are shown.

Figure 2. Best-fit fault model estimated simultaneously with dike and sill models, (a) with the same view as in the inset, and (b) when the model is rotated 130 degrees counterclock-wise. The inset shows the location of the fault.

Figure 3. Best-fit dike models estimated simultaneously with fault and sill models, (a) when displacements of dike and sill are not coupled and (b) they are coupled. The inset shows the location of the dike.

Figure 4. (a) Best-fit uniformly depressurized sill model, and (b) best-fit kinematic sill model (opening), which is the effet of interaction of sill with faulting and dike intrusion.

INTERFEROGRAM FORMATION IN THE PRESENCE OF LARGE DEFORMATION

Sang-Ho Yun, Howard Zebker, Paul Segall · Stanford University
Andy Hooper · University of Iceland
Michael Poland · U.S. Geological Survey

Sierra Negra volcano erupted from October 22 to October 30 in 2005. During the 9 days of eruption, the center of Sierra Negra's caldera subsided at least 4 meters. Three hours prior to the onset of the eruption, an earthquake (Mw 5.4) occurred, near the caldera. Because of the large and complex phase gradient due to the huge subsidence and the earthquake, it is difficult to form an interferogram inside the caldera that spans the eruption. The deformation is so large and spatially variable that the approximations used in existing InSAR software (ROI, ROI_PAC, DORIS, GAMMA) cannot properly coregister SAR image pairs spanning the eruption. We have developed here a two-step algorithm that can form intra-caldera interferograms from these data. The first step involves a "rubber-sheeting" SAR image coregistration. In the second step we use range offset estimates to mitigate the steep phase gradient. Using this new algorithm, we retrieve an interferogram with the best coverage to date inside the caldera of Sierra Negra.

ROTATIONAL MANTLE FLOW BENEATH THE WESTERN US

George Zandt · University of Arizona
Gene Humphreys · University of Oregon

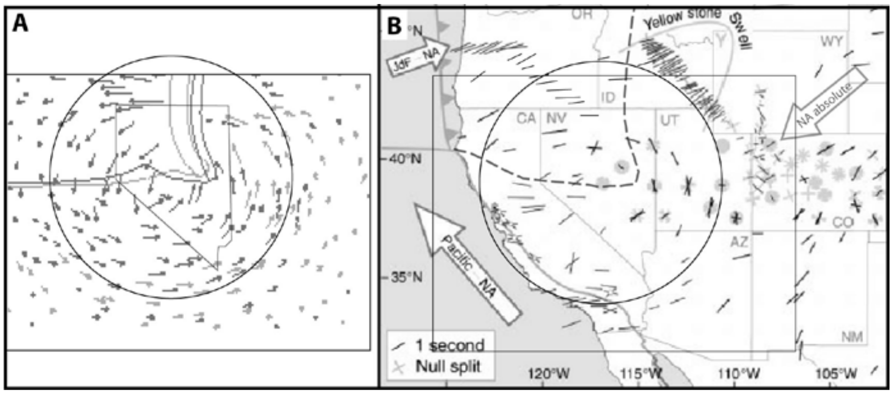

Figure 1. A. Flow pattern observed in laboratory fluid dynamical experiments of lithospheric subduction. Slab retreat results in a rotational mantle flow around the lateral slab edge (from Schellart, JGR, 2004). Outline of Nevada and circle added to aid comparison with observations. B. Observed SKS-splitting fast directions for the western US (modified from Schutt & Humphreys, Geology, 2001; and Xue & Allen, EPSL, 2006). Circle centered on central Nevada encloses area of rotational pattern of fast directions around a central null region. Dashed line outlines southern and eastern edges of the Gorda-Juan de Fuca plate to a depth of ~350 km based on kinematic plate reconstructions and seismic imaging (Bijwaard et al., JGR, 1998).

The circular pattern of anisotropic fast-axis orientations of split SKS arrivals observed in the western US can not be attributed reasonably to either preexisting lithospheric fabric or to asthenospheric strain related to global-scale plate motions (Becker et al., EPSL, 2006). A plume origin for this pattern accounts more successfully for the anisotropy field (Savage & Sheehan, JGR, 2000), but little evidence exists for an active plume beneath central Nevada. We suggest that mantle flow around the edge of the sinking Gorda-Juan de Fuca slab is responsible for creating the observed anisotropy pattern. Seismic images and kinematic reconstructions of Gorda-Juan de Fuca plate subduction have the southern edge of this plate extending from the Mendocino triple junction to beneath central Nevada and beyond, and flow models of narrow subducted slabs produce a strong toroidal flow field around the edge of the slab, consistent with the observed pattern of anisotropy (Fig. 1). An absence of obvious correlation between inferred mantle flow and tectonic stress indicators suggests that sub-lithospheric horizontal mantle flow is mechanically decoupled from the lithosphere, but nonetheless the rotational upwelling of asthenosphere from beneath the oceanic plate can influence surface uplift and magmatism.

SEISMIC IMAGING OF VELOCITY CONTRAST ALONG THE SAN ANDREAS FAULT SYSTEM WITH FAULT ZONE HEAD WAVES GENERATED BY REPEATING EARTHQUAKES

Peng Zhao, Zhigang Peng · Georgia Tech

Major plate boundary faults such as the San Andreas fault often juxtapose blocks with different elastic properties. A sharp material contrast is expected to refract seismic energy along the interface. Fault zone head waves (FZHWs) are generated by slip along the material interface and recorded by near-fault stations on the slower block as emergent first arriving waves with opposite polarity from that of the following direct P waves [Ben-Zion and Malin, 1991; McGuire and Ben-Zion, 2005]. Since FZHWs spend most of their times propagating along the fault interface, waveform analysis based on such phases provides high-resolution information of fault zone structure at seismogenic depth.

We systematically investigate seismic velocity contrast along the central Calaveras fault using waveforms of repeating earthquakes in the aftershock zone of the 1984 M6.2 Morgan Hill, California, earthquake. The analysis employs a total of 353 repeating earthquakes clusters identified from 7857 microearthquakes in relocated catalog of Schaff et al. [2002], with at least five events in each cluster. We align the direct P waves with that of the last trace and stack the resulting waveforms. Clear FZHW signals are found at station CCO, which is located about 3 km southwest of the surface trace of the Calaveras fault. Next, we align the peaks or troughs of the stacked direct P waves for all clusters assuming right-lateral slip focal mechanisms. Initial arrival times of FZHWs are picked manually and compared with nearby clusters. Clear moveout of FZHWs is shown for both along strike and down dip directions. We estimate the velocity contrast at seismogenic depth based on the slope of differential arrival times between FZHWs and direct P arrivals [Ben-Zion and Malin, 1991; McGuire and Ben-Zion, 2005]. The velocity contrast across the Calaveras is ~ 7% and ~15% to the northwest and southeast of the station CCO, respectively. This is compatible with the geological condition on the southwest side of the fault, which is characterized by deformed marine sediment [Manaker et al., 2005] with relatively low P wave velocity compared with northeast of the surface trace. Moreover, the FZHWs are more complicated for the ray paths propagating along the fault to the southeast of the station CCO, which is consistent with a shape change of surface trace of the Calaveras fault and diffuse distribution of seismicity at depth [Schaff et al., 2002].

Our next step is to apply the analysis technique to the Parkfield section of the San Andreas fault near SAFOD. Many repeating microearthquakes recorded by dense near fault instruments in this region provide us exciting opportunity to conduct high resolution imaging of fault zone structures at seismogenic depth. Updated results will be presented in the meeting.

SEISMIC IMAGING OF SOUTHERN CALIFORNIAN CRUST USING DEFORMABLE-LAYER TOMOGRAPHY AND PRESTACK DEPTH MIGRATION: INNOVATIVE APPLICATIONS FOR EARTHSCOPE/USARRAY PROJECTS

Hua-wei Zhou, Michael Thornton, Li Li, Chris Gantela, Tom Bjorklund · University of Houston

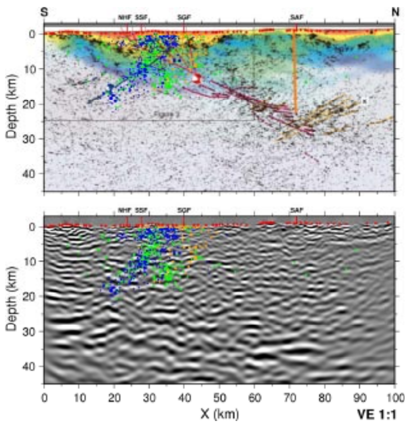

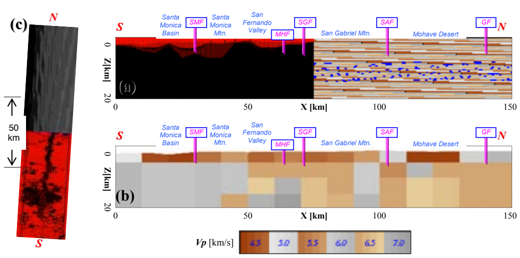

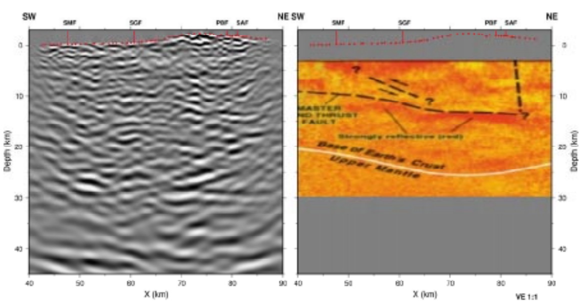

Fig. 1 Comparison between cross sections of: (a) deformable-layer tomography and (b) cell tomography along 1999 LARSE II profile. These tomography models were based on the same P-wave arrivals from local earthquakes and the LARSE II profile. Faults (pink) are: Sierra Madre (SMF), Mission Hills (MHF), San Gabriel (SGF), San Andreas (SAF), and Garlock (GF). (c) Map showing earthquakes (purple crosses), stations (green triangles), LARSE II shots (red circles) and LARSE receivers (black triangles).

Fig. 2 Comparison between (Left) prestack depth migration (Thornton and Zhou, 2007) and (Right) stacked image with interpretations (Henyey et al., 1999) of 1994 LARSE I profile. Red dots along the surface denote LARSE II shots. Faults are: Sierra Madre (SMF), San Gabriel (SGF), and San Andreas (SAF).

Fig. 3 Comparison between (Upper) stacked image with interpretations and tomographic velocities in color (Fuis et al., 2003) and (Lower) prestack depth migration (Thornton and Zhou, 2007) of 1999 LARSE II profile. Red dots along the surface denote LARSE II shots, other color dots are earthquake foci. Faults are: Northridge Hills (NNF), Santa Susana (SSF), San Gabriel (SGF), and San Andreas (SAF).

To better understand the crustal structure and geodynamics of southern California, we are applying new subsurface imaging methods to map the regional 3D crustal velocity structure and major reflection events across the San Andres fault system. The data for this study include earthquake readings compiled by the Southern California Earthquake Center (SCEC) and seismic reflection records from the Los Angeles Regional Seismic Experiment (LARSE). We are using deformable-layer tomography to directly map the geometry of P-wave and S-wave velocity discontinuities in the crust and uppermost mantle, which are constrained by independently-derived crustal thickness variations. We have also applied an advanced wave equation prestack depth migration technology to develop new reflection images for the LARSE profiles.

The preliminary results from this analysis indicate that deformable-layer tomography produces sharper vertical resolution of velocity discontinuities and realistic representations of lens-shaped geologic features such as the edges of basins and lithologic pinchouts, which cannot be achieved by fixed-in-space mesh grids with conventional tomography. Compared to previously published analyses of LARSE data, the LARSE reflection images from this study indicate that prestack depth migration can better treat lateral velocity variations in the shallow crust and improve the resolution of reflection events. Our results suggest that prestack depth imaging is much better than simple CMP stack techniques to process 2D seismic data in the presence of high noise level, strong lateral velocity heterogeneity and crooked survey geometry. The innovative seismic imaging techniques from this study are directly applicable to EarthScope/USArray projects planned to study the structure of the crust and mantle.